National Library
of Canada

Acquisitions and
Bibliographic Services Branch

395 Wellington Street
Ottawa, Ontario
K1A 0N4

Bibliothèque nationale
du Canada

Direction des acquisitions et
des services bibliographiques

395, rue Wellington
Ottawa (Ontario)
K1A 0N4

Your file Votre référence

Our file Notre référence

NOTICE

The quality of this microform is heavily dependent upon the quality of the original thesis submitted for microfilming. Every effort has been made to ensure the highest quality of reproduction possible.

If pages are missing, contact the university which granted the degree.

Some pages may have indistinct print especially if the original pages were typed with a poor typewriter ribbon or if the university sent us an inferior photocopy.

Reproduction in full or in part of this microform is governed by the Canadian Copyright Act, R.S.C. 1970, c. C-30, and subsequent amendments.

AVIS

La qualité de cette microforme dépend grandement de la qualité de la thèse soumise au microfilmage. Nous avons tout fait pour assurer une qualité supérieure de reproduction.

S'il manque des pages, veuillez communiquer avec l'université qui a conféré le grade.

La qualité d'impression de certaines pages peut laisser à désirer, surtout si les pages originales ont été dactylographiées à l'aide d'un ruban usé ou si l'université nous a fait parvenir une photocopie de qualité inférieure.

La reproduction, même partielle, de cette microforme est soumise à la Loi canadienne sur le droit d'auteur, SRC 1970, c. C-30, et ses amendements subséquents.

Canada

UNIVERSITY OF ALBERTA

STRUCTURAL AND TECTONIC EVOLUTION OF THE TESLIN TECTONIC ZONE, YUKON: A DOUBLY-VERGENT TRANSPRESSIVE SHEAR ZONE

BY

© ROBERT ALLAN STEVENS

A thesis submitted to the Faculty of Graduate Studies and Research in partial fulfillment of the requirements for the degree of DOCTOR OF PHILOSOPHY

DEPARTMENT OF GEOLOGY

Edmonton, Alberta
SPRING 1994

National Library
of Canada

Acquisitions and
Bibliographic Services Branch

395 Wellington Street
Ottawa, Ontario
K1A 0N4

Bibliothèque nationale
du Canada

Direction des acquisitions et
des services bibliographiques

395, rue Wellington
Ottawa (Ontario)
K1A 0N4

Your file Votre référence

Our file Notre référence

The author has granted an irrevocable non-exclusive licence allowing the National Library of Canada to reproduce, loan, distribute or sell copies of his/her thesis by any means and in any form or format, making this thesis available to interested persons.

L'auteur a accordé une licence irrévocable et non exclusive permettant à la Bibliothèque nationale du Canada de reproduire, prêter, distribuer ou vendre des copies de sa thèse de quelque manière et sous quelque forme que ce soit pour mettre des exemplaires de cette thèse à la disposition des personnes intéressées.

The author retains ownership of the copyright in his/her thesis. Neither the thesis nor substantial extracts from it may be printed or otherwise reproduced without his/her permission.

L'auteur conserve la propriété du droit d'auteur qui protège sa thèse. Ni la thèse ni des extraits substantiels de celle-ci ne doivent être imprimés ou autrement reproduits sans son autorisation.

ISBN 0-612-11382-5

Canada

UNIVERSITY OF ALBERTA

RELEASE FORM

NAME OF AUTHOR: Robert Allan Stevens

TITLE OF THESIS: Structural and Tectonic Evolution of the Teslin Tectonic Zone, Yukon: A Doubly-Vergent Transpressive Shear Zone

DEGREE: Doctor of Philosophy

YEAR THIS DEGREE GRANTED: Spring 1994

Permission is hereby granted to the University of Alberta Library to reproduce single copies of this thesis and to lend or sell copies for private, scholarly or scientific research purposes only.

The author reserves all other publication and other rights in association with the copyright in the thesis, and except as hereinbefore provided neither the thesis nor any substantial portion thereof may be printed or otherwise reproduced in any material form whatever without the author's prior written permission.

1 Glenbrook Place
Nepean, Ontario
K2G 0V4

April 15, 1994

UNIVERSITY OF ALBERTA

FACULTY OF GRADUATE STUDIES AND RESEARCH

The undersigned certify that they have read, and recommend to the Faculty of Graduate Studies and Research for acceptance, a thesis entitled STRUCTURAL AND TECTONIC EVOLUTION OF THE TESLIN SUTURE ZONE, YUKON: A CRUSTAL-SCALE, DOUBLY-VERGING, HETERGENEOUS TRANSPRESSIVE SHEAR ZONE submitted by ROBERT ALLAN STEVENS in partial fulfillment of the requirments for the degree of DOCTOR OF PHILOSOPHY.

Philippe Erdmer

Dr. P. Erdmer

H. Baadsgaard

Dr. H. Baadsgaard

Thomas Chacko

Dr. T. Chacko

H.A.K. Charlesworth

Dr. H.A.K. Charlesworth

M E Evans

Dr. M.E. Evans

APR 14 1994

Robert Thompson

Dr. R.I. Thompson

Philippe Erdmer
Department of Geology
University of Alberta
Edmonton, AB
T6G 2E3

To whom it may concern:

I, Philippe Erdmer, give Robert Stevens permission to use a version of the following papers and abstracts, for which I am co-author, in his thesis.

> Stevens, R.A., and Erdmer, P., submitted February 1994. Characteristics of ductile transpression and an example from the Teslin suture zone, northern Canadian Cordillera. Journal of Structural Geology.
>
> Stevens, R.A., and Erdmer, P., submitted March 1994. Tectonic evolution of the Teslin suture zone, Yukon; subduction, ductile transpression, thrusting and development of a two-sided orogen. Geology.
>
> Stevens, R.A., and Erdmer, P. 1993. Geology and structure of the Teslin suture zone and related rocks in parts of Laberge, Quiet Lake, and Teslin map areas, Yukon Territory: In Current Research, Part A, Geological Survey of Canada, Paper 93-1A, pp.11-20.
>
> Stevens, R.A., and Erdmer, P. 1992. Structure and tectonic history of the Teslin suture zone, southwestern Yukon Territory: subduction, transpression and formation of a positive flower structure. Presented at the annual meeting of the Canadian Tectonics Group, Nordegg, AB, October 23-25.
>
> Stevens, R.A., and Erdmer, P. 1992. Regional geology, structure and tectonics of the Teslin suture zone in northwest Teslin map area, Yukon. Presented at the combined meeting of the 18th annual Cordilleran Tectonics Workshop and the southern Cordilleran Lithoprobe transect workshop, University of Alberta, Edmonton, AB, March 6-8.
>
> Stevens, R.A., and Erdmer, P. 1993. Tectonic evolution of the Teslin suture zone, south-central Yukon Territory: subduction, transpression and extrusion. Presented at the Geological Association of Canada/Mineralogical Association of Canada annual meeting, Edmonton, Alberta, May 17-19, vol. 18, p.A100.

Philippe Erdmer　　　　5 April 1994

Philippe Erdmer　　　　Date

James K. Mortensen
Department of Geological Sciences
University of British Columbia
6339 Stores Road, Vancouver, B.C.
V6T 1Z4

To whom it may concern:

I, James Mortensen, give Robert Stevens permission to use a version of the following paper, for which I am co-author, in his thesis.

> Stevens, R.A., Mortensen, J.K., and Hunt, P.A. 1993. U-Pb and ^{40}Ar-^{39}Ar geochronology of plutonic rocks from the Teslin suture zone, Yukon Territory. In: Radiogenic Age and Isotopic Studies: Report 7; Geological Survey of Canada, Paper 93-2, p. 83-90.

Jan 26/94

James K. Mortensen Date

Patricia A. Hunt
Geological Survey of Canada
601 Booth St.
Ottawa, ON
K1A 0E8

To whom it may concern:

I, Patricia Hunt, give Robert Stevens permission to use a version of the following paper, for which I am co-author, in his thesis.

> Stevens, R.A., Mortensen, J.K., and Hunt, P.A. 1993. U-Pb and ^{40}Ar-^{39}Ar geochronology of plutonic rocks from the Teslin suture zone, Yukon Territory. In: Radiogenic Age and Isotopic Studies: Report 7; Geological Survey of Canada, Paper 93-2, p. 83-90.

Patricia A. Hunt

Jan 26/94
Date

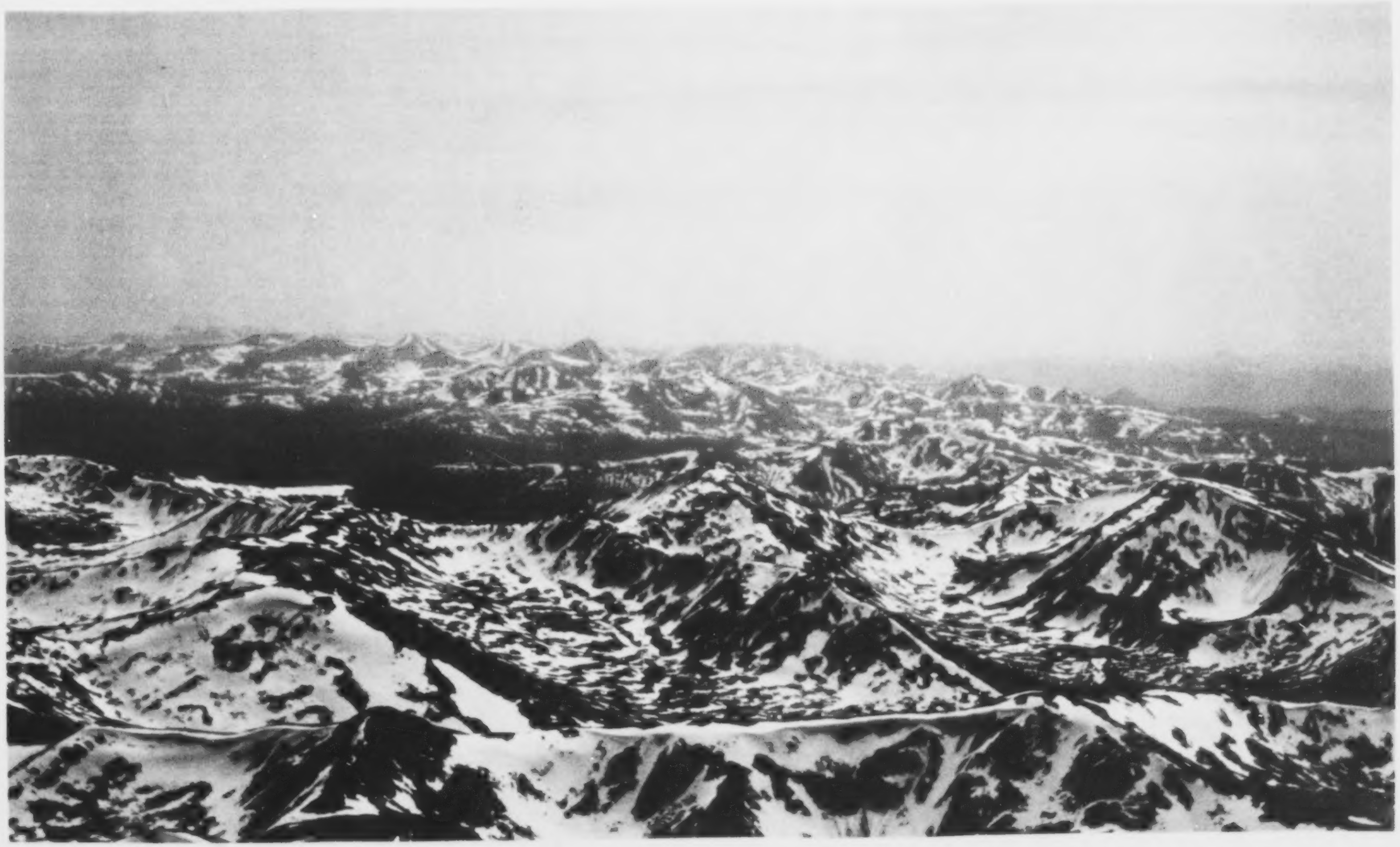

View of the Teslin tectonic zone in the southern Big Salmon Range of the Pelly Mountains. The view is to the south with the Teslin River valley trending southeast in the back right of the photograph.

ABSTRACT

The Teslin tectonic zone (formally the Teslin suture zone) of southern Yukon, consists of a variety of S-, L-S, and L-tectonics derived from sedimentary, volcanic and plutonic rocks. Local preservation of primary depositional and intrusive relationships and Early Mississippian U-Pb zircon dates from metaplutonic rocks, are combined with regional correlation of lithotectonic assemblages to show that the Teslin tectonic zone is part of a regionally extensive continental terrane formed by mid-Mississippian time. Evaluation of metamorphic petrology, amphibole chemistry, and garnet-based geothermobarometry from this study and a re-evaluation of P-T data from previous studies, reveal that the tectonites generally underwent a "medium-pressure", greenschist to amphibolite facies metamorphism at 450-650°C.

Rocks of the Teslin tectonic zone underwent at least two deformation phases; an earlier penetrative phase that produced the wide range of S-, L-S, and L-tectonites, and a later, weaker folding phase accompanied by development of an axial planar cleavage. The Teslin tectonic zone can be subdivided into more than 25 structural domains, each with distinct fabric orientations, shear-sense and/or structural style. Northeast- or southwest-dipping foliation, variable lineation orientations, and normal, reverse and strike-slip shear are characteristic in the different domains. These strain features preserve a doubly-vergent transpressive shear zone interpreted to have formed at the root of a crustal-scale "flower structure".

A tectonic model is proposed that includes the following elements: 1) formation of the continental Nisutlin terrane (including rocks that now comprise the Teslin tectonic zone) by the mid-Mississippian; 2) Permian to Early Triassic? west-dipping subduction of the Slide Mountain Ocean crust beneath the Nisutlin terrane; 3) Middle Triassic? to Early Jurassic transpressive shearing and formation of a doubly-vergent shear zone; 4) Early to Middle Jurassic, regional northeast- and southwest-vergent thrusting; 5) Middle Jurassic to Late

Cretaceous foreland thrust and fold belt development which transported the Teslin tectonic zone eastward as a coherent package over a basal decollement; and 6) Mid-Cretaceous dextral strike-slip faulting which truncated the western margin of the tectonic zone and transported it northward.

ACKNOWLEDGEMENTS

Dr. Philippe Erdmer suggested this project and introduced me to the geology of the Canadian Cordillera. His assistance and support provided me with the right environment for undertaking and successfully completing this thesis. His encouragement and guidance are gratefully acknowledged. Dr. Steve Gordey provided thoughtful and important help with both the field work and with suggestions on how to approach or undertake various scientific problems. Through employment with the Geological Survey of Canada, Steve also gave me the opportunity to map other parts of southern Yukon, which helped to broaden my knowledge of the geology of the Yukon. Dr. Jim Mortensen assisted with isotopic dating for this study which helped to improve the project. Numerous discussions with Jim throughout this thesis were invaluable to my understanding of the geology of the Yukon. Steve Johnston, Heather Plint, and participants in the 1993 NUNA conference are thanked for lively discussions. Murray Rydman in 1990, Andy Turnbull in 1991, and Gord Stretch in 1992 provided untiring assistance and friendship while in the field.

The geochronology section of the Geological Survey of Canada, under Dr. R.R. Parrish provided the isotopic data. Pat Hunt was very helpful with all aspects of completing the isotopic study. The Geological Survey of Canada is also acknowledged for publishing several Current Research reports and one Open File on this project.

The members of my supervisory committee, Dr. H. Baadsgaard, Dr. H.A.K. Charlesworth, and Dr. T. Chacko are thanked for guidance during this project. Paul Wagner provided important assistance with the microprobe and Don Resultay prepared several hundred excellent thin sections. Discussions with many fellow graduate students, in particular Chris Holmden, Agnes Koffeyberg, Jochen Mezger, Dinu Pana and Gerrard Zaluski made graduate student life more interesting.

Barb Henderson provided unending support throughout this project. She constantly suggested better ways of approaching a problem and was always patient when I started rambling about Cordilleran geology. My parents, Joanne and Phil, my brother and sister, Dave and Lynn and Barb's family always provided me with strong family support, which is sincerely appreciated.

Field work was supported by joint EMR/NSERC research agreements and NSERC operating grants to P. Erdmer and by Northern Scientific Training Program Grants from the Department of Indian Affairs and Northern Development, grants from the Canadian Circumpolar Institute of the University of Alberta, and a grant from the Geological Society of America awarded to the author. An NSERC Post Graduate Scholarship, and several University of Alberta scholarships gave me the financial freedom to complete this project. Logistical support provided by the Department of Indian Affairs and Northern Development (Whitehorse) and the Geological Survey of Canada are greatly appreciated.

TABLE OF CONTENTS

CHAPTER 1 - INTRODUCTION 1
REFERENCES 6
CHAPTER 2 - GEOLOGY, GEOLOGICAL CORRELATIONS AND METAMORHPISM IN THE TESLIN TECTONIC ZONE, SOUTH-CENTRAL YUKON TERRITORY 8
INTRODUCTION 9
GEOLOGY OF THE TESLIN TECTONIC ZONE 12
Background 12
Teslin Tectonic Zone Units 14
Siliceous Schist and Quartzite (Proterozoic(?) to Early-Mississippian) 14
Graphitic Phyllite (Proterozoic(?) to Mississippian) . . . 15
Meta-Tonalite to Quartz-Diorite (Early Mississippian) . . 16
Metagabbro and Greenstone (Paleozoic and/or Mesozoic) 16
Hornblende/Sillimanite Pelitic Schist and Gneiss (Proterozoic? and/or Paleozoic) 17
Minor Teslin Tectonic Zone Units (Paleozoic and/or Mesozoic) 17
Massive Plutonic Units (Mesozoic) 18
Regional Correlations and Interpretations 18
METAMORPHIC EVOLUTION OF THE TESLIN TECTONIC ZONE . 21
Background 21
Mineral Assemblages 22
Thermobarometry 22
Amphibole Chemistry and Metamorphic Grade 23
Garnet-Based Thermobarometry 28
Evaluation of Garnet Thermobarometry 30

Discussion 31

TECTONIC IMPLICATIONS 34

CONCLUSIONS 35

REFERENCES 36

CHAPTER 3 - U-Pb AND ^{40}Ar-^{39}Ar GEOCHRONOLOGY OF PLUTONIC ROCKS FROM THE TESLIN TECTONIC ZONE, YUKON TERRITORY 44

INTRODUCTION 45

REGIONAL GEOLOGY 45

ANALYTICAL METHODS 48

U-Pb RESULTS 49

Deformed Meta-Tonalite to Quartz-Diorite 49

Massive Tonalite to Quartz-Diorite 52

^{40}Ar-^{39}Ar RESULTS 53

DISCUSSION 54

REFERENCES 57

CHAPTER 4 - CHARACTERISTICS OF DUCTILE TRANSPRESSION AND AN EXAMPLE FROM THE TESLIN TECTONIC ZONE, NORTHERN CANADIAN CORDILLERA 61

INTRODUCTION 62

THE CHARACTERISTICS OF DUCTILE TRANSPRESSION 62

General 62

Extrusion and Boundary Conditions 64

Foliation and Lineation 65

Shear Sense 66

REGIMES OF DUCTILE TRANSPRESSION 67

Homogeneous and Heterogeneous Transpression 67

Strike-slip and Thrust Transpression 68

Examples 68

THE TESLIN TECTONIC ZONE, YUKON; A CRUSTAL-SCALE

HETEROGENEOUS THRUST-TRANSPRESSIVE SHEAR ZONE . . 69
  Geological Setting and Previous Work . . . 69
  Structural Characteristics . . . 73
  Structural Domains . . . 84
  Comparison with Other Parts of the Teslin Tectonic Zone . . . 92
DISCUSSION . . . 94
REFERENCES . . . 101
CHAPTER 5 - TECTONIC EVOLUTION OF THE TESLIN TECTONIC ZONE, YUKON; SUBDUCTION, DUCTILE TRANSPRESSION, THRUSTING AND DEVELOPMENT OF A DOUBLY-VERGENT OROGEN . . . 108
INTRODUCTION . . . 109
TERRANE DIVISIONS . . . 110
GEOLOGY OF THE TESLIN TECTONIC ZONE . . . 111
TECTONIC EVOLUTION . . . 113
  Early Permian . . . 113
  Permian to Early Triassic? . . . 115
  Middle Triassic? to Early Jurassic . . . 115
  Early to Middle Jurassic . . . 116
  Middle Jurassic to Late Cretaceous . . . 117
  Early to Mid-Cretaceous . . . 118
TESTS OF THE MODEL . . . 119
REFERENCES . . . 121
CHAPTER 6 -CONCLUSIONS . . . 127
REFERENCES . . . 130
APPENDIX 1 - THE TESLIN SUTURE ZONE IN NORTHWEST TESLIN MAP AREA, YUKON: PUBLISHED IN GEOLOGICAL SURVEY OF CANADA PAPER 91-1A . . . 131
APPENDIX 2 - REGIONAL GEOLOGY, FABRIC AND STRUCTURE OF THE TESLIN SUTURE ZONE IN NORTHWEST TESLIN MAP AREA, YUKON TERRITORY: PUBLISHED IN GEOLOGICAL SURVEY

ZONE AND RELATED ROCKS IN PARTS OF LABERGE, QUIET LAKE, AND TESLIN MAP AREAS, YUKON TERRITORY: PUBLISHED IN GEOLOGICAL SURVEY OF CANADA PAPER 93-1A 149

APPENDIX 4 - ABSTRACTS OF PRESENTATIONS GIVEN ON THE TESLIN TECTONIC ZONE DURING Ph.D. STUDY 160

APPENDIX 5 - SUMMARY OF BIOTITE, MUSCOVITE, GARNET, PLAGIOCLASE, AND AMPHIBOLE MICROPROBE ANALYSES 179

APPENDIX 6 - STATION LOCATIONS AND STRUCTURAL DATA 209

APPENDIX 7 - GEOLOGY OF THE TESLIN SUTURE ZONE IN PARTS OF LABERGE (105E/1), QUIET LAKE (105F/4) AND TESLIN (105/C11, 13, 14) MAP AREAS, YUKON TERRITORY . . . . POCKET

LIST OF TABLES

TABLE 2-1: Microprobe analyses of garnet and plagioclase samples 24

TABLE 2-2: Microprobe analyses of biotite and muscovite samples 25

TABLE 2-3: Microprobe analyses of amphibole samples 26

TABLE 2-4: P-T estimates on rocks of the Teslin tectonic zone 29

TABLE 3-1: U-Pb zircon and titanite analytical data 50

TABLE 3-2: ^{40}Ar-^{39}Ar age data 55

TABLE 4-1: Structural characteristics of transect CC' 90

LIST OF FIGURES

FIGURE 2-1: Terrane map of the Yukon 10
FIGURE 2-2: Geology map of the study area with location of P-T samples . . 13
FIGURE 2-3: Lithotectonic assemblage correlation diagram 19
FIGURE 2-4: Amphibole chemistry of selected samples 27
FIGURE 2-5: P-T diagram for rocks of the Teslin tectonic zone 32
FIGURE 3-1: Simplified geology map of the study area with age data. 46
FIGURE 3-2: U-Pb concordia diagram 51
FIGURE 4-1: Characteristics and regimes of ductile transpression 63
FIGURE 4-2: Terrane map of the Yukon 70
FIGURE 4-3: Simplified geology map of the study area with structural data. . 72
FIGURE 4-4: Strip maps and equal-area plots for transects A and B 87
FIGURE 4-5: Strip map and equal-area plots for transect C 88
FIGURE 4-6: Fabric orientations and shear-sense in transects A, B, and C . 91
FIGURE 4-7: Changes in stratigraphy are not due to folding; an example . . 93
FIGURE 4-8: Average fabric orientations in the Teslin tectonic zone 95
FIGURE 4-9: Structural model for the Teslin tectonic zone 96
FIGURE 4-10: Foliation orientations in the Carmacks map area 99
FIGURE 5-1: Terrane map of the northern Cordillera 112
FIGURE 5-2: Tectonic evolution model for the Teslin tectonic zone 114

LIST OF PLATES

PLATE 4-1: Well developed L-S tectonites from the Teslin tectonic zone 75

PLATE 4-2: Examples of shear-sense indicators found in the study area 77

PLATE 4-3: An example of the degree of developement of strain partitioning 79

PLATE 4-4: Examples of the crenulations that dominate the folding phase 81

PLATE 4-5: Examples of hand-specimen-scale folds that occur locally 83

PLATE 4-6: An example of the spaced cleavage that occurs locally 85

PLATE 4-7: Examples of strain microfabrics preserved in most rocks 86

CHAPTER 1 - INTRODUCTION

The Teslin tectonic zone is defined as the 10-20 km wide and more than 200 km long zone of steeply-dipping ductilely deformed tectonites that forms the southern extension of the Yukon-Tanana terrane. The name "Teslin tectonic zone" is introduced in, and used throughout this study and replaces the name "Teslin suture zone" introduced by Tempelman-Kluit (1979) and used by Erdmer (1985), Erdmer and Helmstaedt (1983), Hansen (1987, 1989, 1992a, 1992b), Hansen et al. (1989, 1991), Stevens (1991, 1992), Stevens and Erdmer (1993), and others. The results of this study suggest that amalgamation of most rock units that comprise the Teslin tectonic zone did not occur during "suturing" of allochthonous terranes of the Intermontane Belt to the North American margin as suggested by Tempelman-Kluit (1979). Rather, the units were amalgamated prior to accretion of these terranes and subsequently underwent intraterrane deformation. Therefore the term "suture zone" may be a misnomer and a term independent of genetic interpretation is required. The more general term "Teslin tectonic zone" which is independent of current or potential future interpretations is therefore applied to this belt of tectonized rocks.

The Teslin tectonic zone which is positioned between autochthonous strata of the North American miogeocline and Cordilleran accreted and suspect terranes, is a key tectonic element of the northern Canadian Cordillera. Tempelman-Kluit (1979) first recognized the Teslin tectonic zone and introduced an important tectonic model for southern Yukon. In Tempelman-Kluit's (1979) interpretation the Teslin tectonic zone was part of a subduction complex formed outboard of the North American margin in the early Mesozoic. Subsequent collision of the overlying arc-terrane with North America resulted in obduction of the subduction complex onto North American strata, and the Teslin tectonic zone was interpreted to preserve the root zone to the obducted package of rocks. This model was refined by Erdmer and Helmstaedt (1983) and Erdmer (1985) with the documentation of eclogite in the Teslin tectonic zone and the recognition that rocks of the zone record a wide range of strains and P-T conditions interpreted to reflect nearly all levels of a zone of subduction and collision. Subsequently, the importance of subduction-zone processes was emphasized by Hansen (1987, 1989, 1992a, 1992b), and Hansen et al. (1989, 1991). In Hansen's (1992a, 1992b) interpretation the Teslin tectonic zone preserves widespread high P/T metamorphic conditions that record backflow, margin-parallel flow, and downflow within a west-dipping B-type Permo-Triassic subduction complex.

The primary reason for undertaking this study was to test the above models for the geological evolution of the Teslin tectonic zone in an area outside of those previously studied.

Prior to this study, work on the Teslin tectonic zone was confined to the eastern Laberge and western Quiet Lake map areas (Fig. 2-1) and consisted of 1:250 000 scale regional mapping and localized structural mapping. The geology north and south of these areas was poorly known and could not be used to test the above models. In addition, examination of the data from the earlier studies, particulary the work of Hansen (1987, 1989), suggested that other interpretations were possible. Therefore this study was undertaken to overcome these limitations by documenting, in detail, the geology of the Teslin tectonic zone in southern Laberge and Quiet Lake map areas, and northwestern Teslin map area. Specifically, this study documents the rock types in the Teslin tectonic zone, their age, their structural and metamorphic characteristics and their tectonic significance.

During the 1990, 1991, and 1992 field seasons, parts of five 1:50 000 scale map areas were mapped to established the geological framework of the Teslin tectonic zone in the study area. In addition, three detailed structural transects at approximately 1:10 000 scale were mapped in 1991 and 1992. Structural measurements and rock samples collected during the mapping were used in subsequent metamorphic, geochronologic and structural studies.

The key characteristics of the rock units exposed in the study area, and their contact relationships are outlined in chapter 2. In addition, the geology of the study area is placed in a regional context by correlating the rock units from this study with those in the Yukon-Tanana terrane of southern Yukon as described by Tempelman-Kluit (1979), Hansen et al. (1991) and Mortensen (1992). More thorough descriptions of the geology in the study area can be found in appendices 1, 2, and 3, and the geology of the entire project area is presented on 1:50 000 scale maps in appendix 7.

The metamorphic character of the Teslin tectonic zone is also described in chapter 2, where petrology combined with garnet-based geothermobarometry and amphibole chemistry are used to establish the nature of metamorphism in the study area. The results of these studies and a re-evaluation of previous metamorphic studies by Hansen (1987, 1992b) are combined to summarize our current knowledge of metamorphism in the Teslin tectonic zone.

The timing of metamorphism and deformation in the Teslin tectonic zone, and the age of rocks that took part in this tectonism are constrained, in this study, by U-Pb and ^{40}Ar-^{39}Ar dating. The results of these analyses are reported in chapter 3. A U-Pb age on deformed plutonic rocks provides a maximum age of deformation, and the age of a cross-cutting undeformed plutonic body provides a minimum age. In addition, ^{40}Ar-^{39}Ar ages on hornblende and biotite are used to help establish the uplift and cooling age of Teslin tectonic zone rocks.

Structural measurements from field mapping, particularly along the three detailed transects, reveal that the Teslin tectonic zone can be subdivided into a number of different domains, each with distinct fabric orientations, structural style or shear-sense. The strain characteristics and kinematics of these domains and the structural features of the Teslin tectonic zone as a whole are reported on in chapter 4.

Also in chapter 4, the characteristics of ductile transpression are reviewed and summarized into a general model for crustal-scale transpression. Extrusion, boundary conditions, the characteristics of foliation and lineation, shear-sense, and ties to brittle transpression are considered. Ductile transpressive zones are also subdivided, on the basis of field characteristics, into four types that identify the transpressive deformation regime under which a zone was formed. These subdivisions are applied to the Teslin tectonic zone in order to characterize its structural evolution.

A tectonic model for the Teslin tectonic zone from Permian to mid-Cretaceous time is outlined in chapter 5. This model summarizes the important conclusions of this study by incorporating the results of geological mapping with age data, metamorphic analyses and structural investigations. It is a new model that departs from traditional interpretations and which incorporates the data from this study, with existing local and regional geological data. Finally, the main conclusions of the study are summarized in Chapter 6.

REFERRENCES

Erdmer, P. 1985. An examination of the cataclastic fabrics and structures of parts of Nisutlin, Anvil and Simpson allochthonons, central Yukon: test of the arc-continent collision model. Journal of Structural Geology, **7**: 57-72.

Erdmer, P., and Helmstaedt, H. 1983. Eclogite from central Yukon: a record of subduction at the western margin of ancient North America. Canadian Journal of Earth Sciences, **20**: 1389-1408.

Hansen, V.L. 1987. Structural, metamorphic, and geochronologic evolution of the Teslin suture zone, Yukon: evidence from Mesozoic oblique convergence outboard of the northern Canadian Cordillera. Ph.D. thesis, University of California, Los Angeles, California.

Hansen, V.L. 1989. Structural and kinematic evolution of the Teslin suture zone, Yukon: record of an ancient transpressional margin. Journal of Structural Geology, **11**: 717-733.

Hansen, V.L. 1992a. Backflow and margin-parallel shear within an ancient subduction complex. Geology, **20**: 71-74.

Hansen, V.L. 1992b. P-T evolution of the Teslin suture zone and Cassiar tectonites, Yukon, Canada: evidence for A- and B-type subduction. Journal of Metamorphic Geology, **10**: 239-263.

Hansen, V.L., Mortensen, J.K., and Armstrong, R.L. 1989. U-Pb, Rb-Sr, and K-Ar isotopic constraints for ductile deformation and related metamorphism in the Teslin suture zone, Yukon-Tanana terrane, south-central Yukon. Canadian Journal of Earth Sciences, **26**: 2224-2235.

Hansen, V.L., Heizler, M.T., and Harrison, T.M. 1991. Mesozoic thermal evolution of the Yukon-Tanana composite terrane: new evidence from ^{40}Ar/^{39}Ar data. Tectonics, **10**: 51-76.

Mortensen, J.K. 1992. Pre-mid-Mesozoic tectonic evolution of the Yukon-Tanana terrane, Yukon and Alaska. Tectonics, **11**: 836-853.

Stevens, R.A. 1991. The Teslin suture zone in northwest Teslin map area, Yukon. In Current research, part A. Geological Survey of Canada, Paper 91-1A, pp. 271-277. See appendix 1

Stevens, R.A. 1992. Regional geology, fabric, and structure of the Teslin suture zone in northwest Teslin map area, Yukon Territory. In Current research, part A. Geological Survey of Canada, Paper 92-1A, pp. 287-295. See appendix 2

Stevens, R.A., and Erdmer., P. 1993. Geology and structure of the Teslin suture zone and related rocks in parts of Laberge, Quiet Lake, and Teslin map areas, Yukon Territory. In Current research, part A. Geological Survey of Canada, Paper 93-1A, pp. 11-20. See appendix 3

Tempelman-Kluit, D.J. 1979. Transported cataclasite, ophiolite and granodiorite in Yukon: evidence of arc-continent collision. Geological Survey of Canada, Paper 79-14.

CHAPTER 2 - GEOLOGY, GEOLOGICAL CORRELATIONS, AND METAMORPHISM IN THE TESLIN TECTONIC ZONE, SOUTH-CENTRAL YUKON TERRITORY*

*A version of this chapter has been submitted for publication. Stevens, 1993. Canadian Journal of Earth Sciences.

INTRODUCTION

The Yukon-Tanana terrane of southern Yukon and east-central Alaska consists of variably metamorphosed and ductilely deformed sedimentary and igneous rocks (Monger and Berg 1987; Jones et al. 1987). It occupies a central position between the ancient continental North American margin to the north and east and the allochthonous terranes of the Intermontane and Coast Belts to the south and west (Fig. 2-1). The Yukon-Tanana terrane as defined by Monger and Berg (1987) and Jones et al. (1987) is a composite terrane that has been divided into several sub-terranes (Churkin et al. 1982; Aleinikoff et al. 1987; Wheeler et al. 1991; Hansen et al. 1991). In Yukon, Wheeler et al. (1991) divide the Yukon-Tanana terrane into the Pelly Gneiss and the Nisling, Slide Mountain, and Kootenay terranes, and Hansen et al. (1991) divide it into a lower plate peraluminous orthogneiss/host metasedimentary rock assemblage and an upper plate consisting of the Nisutlin and Teslin-Taylor Mountain terranes. Although sub-division of the Yukon-Tanana terrane in Yukon appears to be warranted, there is no general agreement on where the divisions should take place, on the names that should be applied, or on the tectonic significance of the divisions. The extent of the Yukon-Tanana terrane as shown on Fig. 2-1 is essentially that of Monger and Berg (1987) with modification in southern Yukon (Gordey and Stevens, 1994).

The Teslin tectonic zone (formerly the Teslin suture zone) (Fig. 2-1) is the southern extension of the Yukon-Tanana terrane in south-central Yukon, and lies between deformed autochthonous North American rocks of the Omineca Belt to the east and accreted terranes of the Intermontane Belt to the west. It includes steeply-dipping S-, L-S and L-tectonites derived from sedimentary, volcanic and plutonic rocks metamorphosed under greenschist to amphibolite facies conditions (Hansen et al. 1989; Stevens 1991, 1992; Read et al. 1991; Stevens and Erdmer 1993).

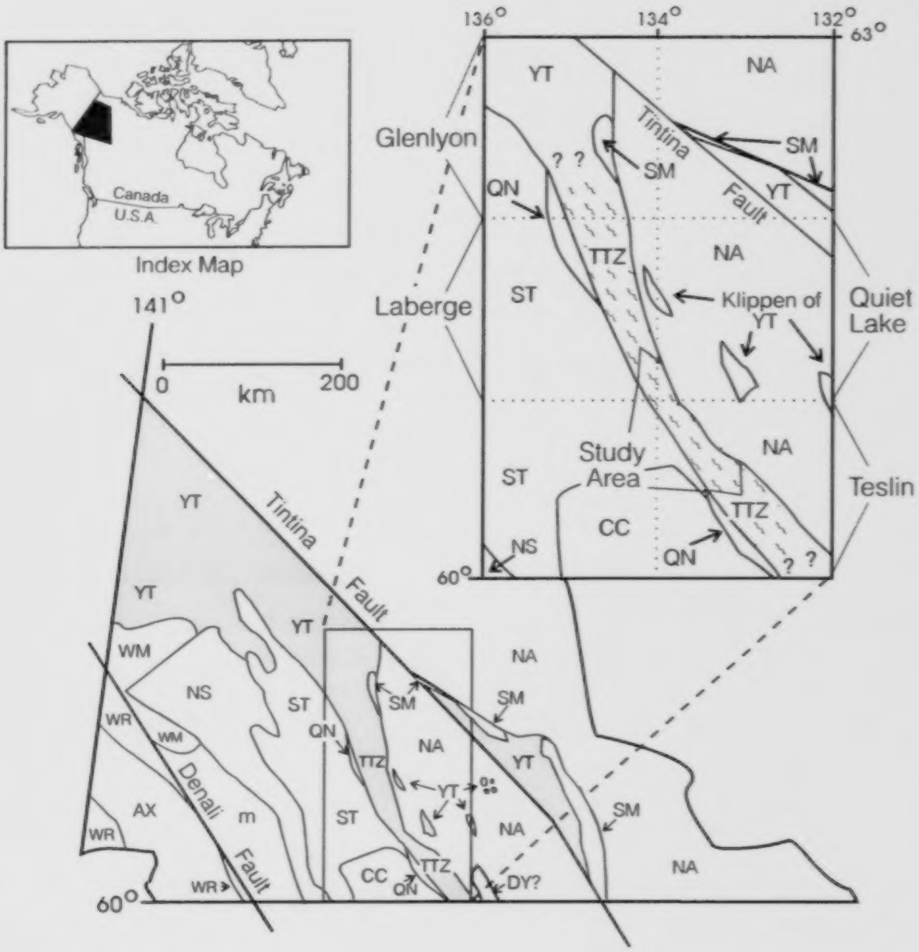
Index Map
Canada
U.S.A.
141°
0
km
200
YT
Tintina
Fault
YT
YT
WM
NS
ST
WR
WM
Denali
Fault
AX
m
WR
WR
60°
QN
TTZ
SM
NA
SM
YT
YT
ST
CC
QN
TTZ
DY?
NA
SM
NA
136°
134°
132°
63°
60°
YT
NA
Tintina
Fault
SM
SM
YT
? ?
QN
TTZ
NA
ST
Klippen of YT
NA
ST
CC
QN
TTZ
? ?
NS
Glenlyon
Laberge
Quiet Lake
Study Area
Teslin

Figure 2-1: Terrane map of the Yukon, highlighting the Yukon-Tanana terrane and the Teslin tectonic zone on the main map and the location of this study on the inset map. Names on the inset map refer to 1:250 000 scale map areas. Terranes are: NA = North America, SM = Slide Mountain, YT = Yukon Tanana, TTZ = Teslin tectonic zone, NS = Nisling, DY = Dorsey, QN = Quesnellia, CC = Cache Creek, ST = Stikinia, WM = Windy McKinley, m = undivided metamorphics, AX = Alexander, WR = Wrangellia, (modified from Monger and Berg 1987; Wheeler and McFeely 1991; Gordey and Stevens 1994).

One of the current models for the formation of the Teslin tectonic zone proposes that its rocks are the product of deformation within the deep-seated portion of a west-dipping Permo-Triassic subduction complex west of ancient North America (Hansen et al. 1989). The rocks were subsequently uplifted and thrust eastward as a coherent sheet onto North American strata in the Early Jurassic as a result of collision of an arc terrane with the North American margin (Tempelman-Kluit 1979; Hansen et al. 1991; Hansen 1992a). The Teslin tectonic zone is interpreted to represent the root zone of these obducted rocks, and flat-lying klippen of Teslin tectonic zone related rock resting on North American strata to the east are remnants of the once continuous sheet (Tempelman-Kluit 1979).

The model described above was based primarily on data from the Laberge map area (Fig. 2-1). Prior to this study, the geology of the Teslin tectonic zone outside of the Laberge map area was poorly known. Therefore, a geological and structural study of the Teslin tectonic zone was undertaken in the southern Laberge and Quiet Lake map areas and the northern half of the Teslin map area (Fig. 2-1), to test that model (Stevens 1991, 1992; Stevens and Erdmer 1993).

In this paper, the geology of the Teslin tectonic zone is outlined and compared to the geology of the Yukon-Tanana terrane elsewhere in southern Yukon. Correlations suggest that prior to mid-Mississippian time, many rock assemblages in the Teslin tectonic zone and Yukon-Tanana terrane shared a common history and formed part of a regionally extensive continental crustal terrane. The results of new metamorphic pressure-temperature studies and a re-evaluation of P-T studies by Hansen (1987, 1992b) are presented. The P-T data suggest that rocks of the Teslin tectonic zone record P-T conditions consistent with medium-pressure regional metamorphism rather than with subduction zone metamorphic conditions.

GEOLOGY OF THE TESLIN TECTONIC ZONE

Background

The Teslin tectonic zone forms part of the Yukon-Tanana terrane. It was originally defined on a structural basis by Tempelman-Kluit (1979) as "a northwest trending zone of steeply dipping cataclastic rocks 15 km wide [that] separates the Omineca and Intermontane belts". The Teslin tectonic zone extends southwards from the southern Glenlyon map area (Little Salmon Lake area) through the Laberge map area to at least the Canol Road in the Teslin map area (Fig. 2-1) (Tempelman-Kluit 1979; Stevens and Erdmer 1993). The northern and southern limits of the Teslin tectonic zone are undefined. The western margin is marked by the Big Salmon Fault in the Laberge map area (Tempelman-Kluit 1984) and by an un-named fault in the Teslin map area (Fig. 2-2) (Gordey 1991; Gordey and Stevens 1994). The eastern margin of the Teslin tectonic zone is the D'Abbadie Fault in the Quiet Lake map area (Hansen et al. 1989), and an un-named thrust fault in the Teslin map area (Gordey and Stevens 1994).

The Teslin tectonic zone was originally divided into three ductilely-deformed lithotectonic assemblages; the Nisutlin, Anvil and Simpson allochthonous assemblages (Tempelman-Kluit 1977, 1979, 1984). The Nisutlin allochthonous assemblage, interpreted to be sheared trench melange, consists of muscovite-bearing siliceous schist and quartzite, graphitic phyllite and minor interleaved marble and metavolcanic rock (Tempelman-Kluit 1979; Hansen et al. 1989). The Anvil allochthonous assemblage, interpreted to be a dismembered slice of oceanic crust, includes sheared and metamorphosed mafic volcanic rocks, gabbro and ultramafic rocks. The Simpson allochthonous assemblage, interpreted as the plutonic root of a dismembered island arc, consists of a variety of sheared felsic to intermediate granitoids (Tempelman-Kluit 1979). Tempelman-Kluit (1979) also included slices of graphitic phyllite in the Teslin tectonic zone that he interpreted to be part of the autochthonous outer shelf of

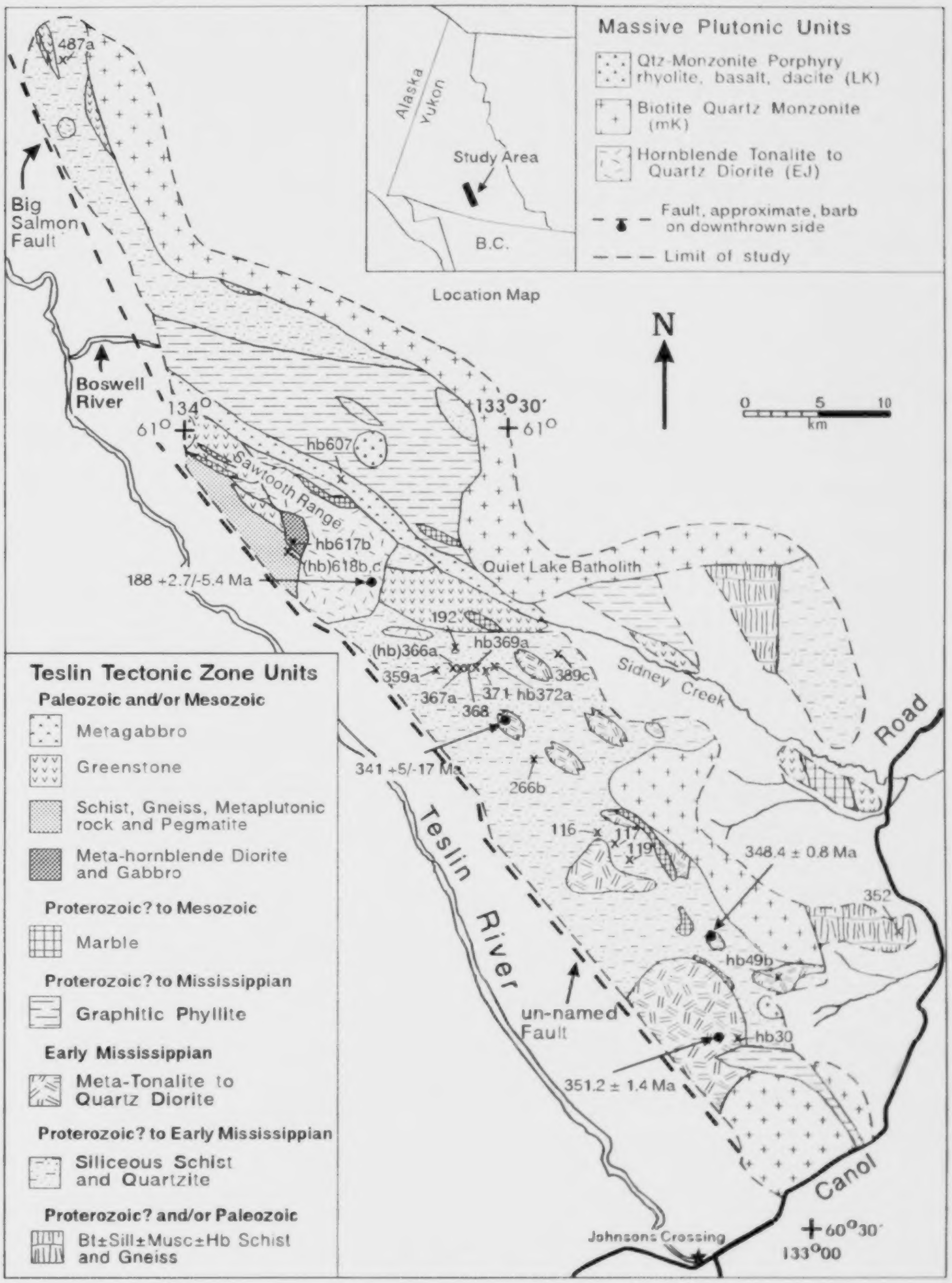
Massive Plutonic Units
Qtz-Monzonite Porphyry rhyolite, basalt, dacite (LK)
Biotite Quartz Monzonite (mK)
Hornblende Tonalite to Quartz Diorite (EJ)
Fault, approximate, barb on downthrown side
Limit of study
Alaska
Yukon
Study Area
B.C.
Location Map
N
0
5
10
km
487a
Big Salmon Fault
Boswell River
134°
61°
133°30′
61°
hb607
Sawtooth Range
hb617b
(hb)618b,c
188 +2.7/-5.4 Ma
Quiet Lake Batholith
192
hb369a
(hb)366a
359a
389c
367a
371
hb372a
368
Sidney Creek
341 +5/-17 Ma
266b
116
117
119
348.4 ± 0.8 Ma
352
hb49b
hb30
351.2 ± 1.4 Ma
Teslin River
un-named Fault
Road
Canol
Johnsons Crossing
60°30′
133°00
Teslin Tectonic Zone Units
Paleozoic and/or Mesozoic
Metagabbro
Greenstone
Schist, Gneiss, Metaplutonic rock and Pegmatite
Meta-hornblende Diorite and Gabbro
Proterozoic? to Mesozoic
Marble
Proterozoic? to Mississippian
Graphitic Phyllite
Early Mississippian
Meta-Tonalite to Quartz Diorite
Proterozoic? to Early Mississippian
Siliceous Schist and Quartzite
Proterozoic? and/or Paleozoic
Bt±Sill±Musc±Hb Schist and Gneiss

Figure 2-2: Simplified geology map of the study area (modified from Stevens 1994). Sample numbers refer to Table 2-4. The prefix hb- with a sample number indicates that amphiboles were analyzed and used in evaluating metamorphic grade. Ages are from Stevens et al. (1993) and are U-Pb zircon dates.

ancient North America (Nasina facies).

A simplified geology map of the study area is presented in Fig. 2-2. Recent 1:50 000 scale geology maps are available for the region (Stevens 1994) as are geological progress reports (Stevens 1991, 1992; Stevens and Erdmer 1993). Rock assemblages are grouped into Teslin tectonic zone units and massive plutonic units (Fig. 2-2). Rocks of the Teslin tectonic zone units display penetrative ductile deformation fabrics and most are interpreted to be part of the Yukon-Tanana terrane. At least two phases of deformation affected rocks of these units; an early penetrative ductile deformation produced the tectonites, and later folding produced widespread crenulation of the earlier fabrics (Stevens and Erdmer 1993). Massive plutonic units are undeformed plutonic rocks that post-date penetrative deformation in the zone and intrude Teslin tectonic zone units.

Where exposed, most contacts between rocks of the Teslin tectonic zone units are fabric parallel, tectonized and lack primary depositional or intrusive characteristics. However, in places primary depositional and intrusive contacts are preserved. These contacts are discussed along with the rock descriptions below.

Teslin Tectonic Zone units

Siliceous Schist and Quartzite (Proterozoic(?) to Early-Mississippian)

As much as 50% of the study area is underlain by a heterogeneous, semi-pelitic assemblage of schist and quartzite. The main rock types are quartz-muscovite±chlorite schist and muscovite-chlorite quartzite with mylonitic to protomylonitic fabrics. Locally epidote, feldspar, biotite, garnet and amphibole are present in these rocks. Minor rock types include calcareous schist, graphitic phyllite and marble. North of the Boswell River (Fig. 2-2) compositional layering, which is interpreted to reflect primary bedding, can be traced for several kilometres along strike, however, in most places it is discontinuous. Tectonic lenses of Early Mississippian meta-tonalite to quartz-diorite are locally abundant, particularly adjacent to plutons of these rocks (Stevens et al. 1993). In addition, an apophysis of meta-tonalite to quartz-diorite was seen to cut rocks of this unit and lenses of siliceous schist were found included in the margins of weakly deformed meta-tonalite to quartz-diorite bodies. These features indicate that a primary intrusive contact existed between the meta-plutonic rock and rocks of the schist and quartzite unit. Therefore these metasedimentary rocks have a pre-Early Mississippian depositional age.

This unit is interpreted to represent a passive continental margin assemblage and is the stratigraphically oldest assemblage known in the area. It is correlated, based on rock type, with the Nisutlin allochthonous assemblage of Tempelman-Kluit (1979), the Nisutlin terrane of Hansen et al. (1991) and the "middle unit" of Mortensen (1992).

Graphitic Phyllite (Proterozoic(?) to Mississippian)

Sheared, fissile, rusty red to black, fine-grained graphite-muscovite phyllite characterizes this assemblage. Minor rock types include calcareous phyllite, marble, muscovite-chlorite schist and quartzite. North of the Boswell River rocks of the graphitic phyllite and siliceous schist and quartzite units are in contact (Fig. 2-2). As the contact is approached from the north, graphite increases in abundance in siliceous and calcareous schist of the schist and quartzite unit. The contact zone, up to 100 m wide, is marked by an increasing abundance of graphitic phyllite bands within siliceous schist. These are not structural lenses of phyllite in the schist, rather they are gradational bands. South of the contact graphitic phyllite is the dominant rock type with minor interbanded siliceous schist. These relationships are interpreted to indicate a pre-deformation depositional link between the two units (Stevens and Erdmer 1993). In addition, north of the contact, within the siliceous schist and quartzite unit, compositional layering with a strike length of at least five kilometres can be traced northwards to the Quiet Lake Batholith. This layering which is parallel to the contact is also interpreted to reflect primary depositional layering and indicates that stratigraphy (modified by metamorphism and deformation) is preserved both at, and north of the contact. A primary intrusive relationship is inferred between an Early Mississippian meta-tonalite to quartz-diorite body and this unit (Fig. 2-2) (Stevens 1991), suggesting that its depositional age may be pre-Early Mississippian.

This unit is correlated, on the basis of rock type, with the autochthonous Nasina Formation of Tempelman-Kluit (1979, 1984), the Cassiar continental margin of Hansen et al. (1991) and the "middle unit" of Mortensen (1992).

Meta-Tonalite to Quartz-Diorite (Early Mississippian)

Massive to mylonitic, metamorphosed, hornblende- and biotite-bearing tonalite to quartz-diorite characterizes this unit. It is intrusive into the siliceous schist and quartzite and graphitic phyllite units (see above). U-Pb dating of zircons from three different exposures indicate Early Mississippian crystallization ages with a minor Precambrian inherited component (Fig. 2-2) (Stevens et al. 1993). Similar rocks elsewhere in the Yukon-Tanana terrane give crystallization ages ranging from Late Devonian to Early Mississippian (Mortensen 1992).

This unit is correlated, on the basis of age and rock type, with the Simpson allochthonous assemblage of Tempelman-Kluit (1979), the Simpson Range Plutonic Suite of Mortensen and Jilson (1985), the I-type orthogneiss of the Teslin-Taylor Mountain terrane of Hansen et al. (1991) and the hornblende-bearing Devono-Mississippian plutons of Mortensen (1992).

Metagabbro and Greenstone (Paleozoic and/or Mesozoic)

White and green, massive to mylonitic metagabbro, and medium to dark green, massive to mylonitic greenstone, including mafic schist and bands of marble, characterize this unit. The greenstone is thought to be derived from basaltic to andesitic flows and tuffs deposited in shallow water near small carbonate reefs. Interleaving of the greenstone and metagabbro along their contact suggests that they are genetically related (Stevens and Erdmer 1993).

This unit is correlated, on the basis of rock type, with the Anvil allochthonous assemblage of Tempelman-Kluit (1979) and the Teslin-Taylor Mountain terrane of Hansen et al. (1991). Alternatively, it may be correlative with the "middle unit" of Mortensen (1992). The "middle unit" contains rocks of similar composition that are also in contact with carbonaceous/graphitic metasedimentary rocks. In this interpretation rocks of this unit would have been deposited during the Late Devonian to Mississippian and would likely be in stratigraphic contact with rocks of the graphitic phyllite unit to the north (see Mortensen 1992).

Hornblende/Sillimanite Pelitic Schist and Gneiss (Proterozoic(?) and/or Paleozoic)

Brownish-grey to red, recrystallized biotite±muscovite±hornblende± sillimanite schist, gneiss and quartzite cut by and including dykes and sills of massive pegmatite and quartz-monzonite characterize this unit. Many of the dykes and sills are lithologically identical to rock of the Quiet Lake Batholith and other mid-Cretaceous quartz-monzonite plutons in the study area (Fig. 2-2). These dykes and sills are unique to the unit, as no other unit is intruded by similar dykes or sills, even when they are in direct contact with the Quiet Lake Batholith or other mid-Cretaceous plutons.

This assemblage is of uncertain tectonic affinity as it has no apparent correlative assemblage in the Yukon-Tanana terrane of southern Yukon. However, it is similar to unit Ꝑn+ (injection migmatite) of Tempelman-Kluit (1977). Unit Ꝑn+ is interpreted by Tempelman-Kluit (1977) to be autochthonous North American rocks presumably metamorphosed during intrusion of mid-Cretaceous plutonic rocks.

Minor Teslin Tectonic Zone Units (Paleozoic and/or Mesozoic)

Two additional units are exposed in the Sawtooth range; an extremely variable unit consisting of felsic to mafic schist and gneiss, quartzite, metaplutonic rock and pegmatite, and sheared meta-hornblende diorite to gabbro (Stevens and Erdmer 1993).

Massive Plutonic Units (Mesozoic)

A large body of medium-grained hornblende granodiorite to quartz-diorite, locally varying to coarse-grained hornblendite and pyroxene hornblendite, crops out in the Sawtooth Range. Local evidence of flow banding and local compositional heterogeneity are characteristic. U-Pb dating of zircons gave an Early Jurassic crystallization age for this pluton (Stevens et al. 1993). This unit is interpreted to be part of a suite of massive and strongly differentiated plutons, ranging from 212 to 185 Ma in age, that intrude the Yukon-Tanana terrane, Nisling and Stikinia terranes (Mortensen 1992).

A number of bodies of biotite quartz-monzonite, including the Quiet Lake Batholith, are exposed in the map area. Rocks similar to these occur throughout south-central Yukon; they consistently yield mid-Cretaceous ages and comprise the Cassiar Plutonic Suite of Woodsworth et al. (1991)

Black basalt and reddish dacite of the upper Cretaceous Open Creek Volcanic suite and quartz-monzonite and rhyolite porphyries of the Late Cretaceous Red Mountain porphyry molybdenum deposit occur in the Sawtooth Range (Stevens 1994; Brown and Kahlert 1986).

Regional Correlations and Interpretations

The rock units from this study are correlated on the basis of rock type with assemblages described by Tempelman-Kluit (1979) (Fig. 2-3a), Hansen et al. (1991) (Fig. 2-3b) and Mortensen (1992) (Fig. 2-3c).

In this study most of the area is underlain by four units of probable pre-mid Mississippian age. Contact relationships and isotopic ages of meta-plutonic rocks suggest the following structural-stratigraphic sequence. A lower siliceous schist and quartzite grades upwards into graphitic phyllite. The schist unit and presumably the base of the phyllite are intruded by Early Mississippian plutonic

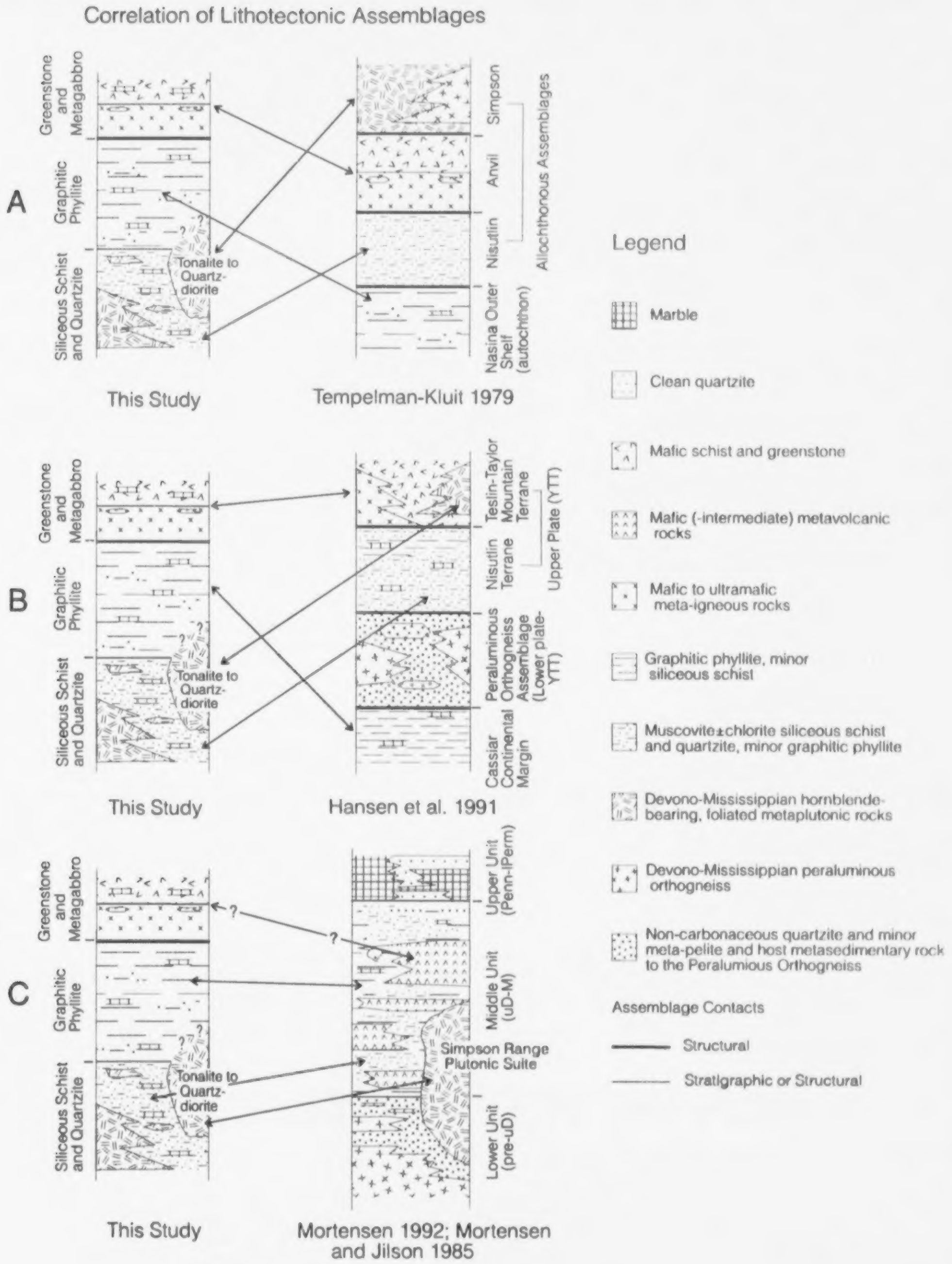
Correlation of Lithotectonic Assemblages
A
Greenstone and Metagabbro
Graphitic Phyllite
Siliceous Schist and Quartzite
Tonalite to Quartz-diorite
Simpson
Anvil
Nisutlin
Allochthonous Assemblages
Nasina Outer Shelf (autochthon)
This Study
Tempelman-Kluit 1979
B
Greenstone and Metagabbro
Graphitic Phyllite
Siliceous Schist and Quartzite
Tonalite to Quartz-diorite
Teslin-Taylor Mountain Terrane
Nisutlin Terrane
Upper Plate (YTT)
Peraluminous Orthogneiss Assemblage (Lower plate-YTT)
Cassiar Continental Margin
This Study
Hansen et al. 1991
C
Greenstone and Metagabbro
Graphitic Phyllite
Siliceous Schist and Quartzite
Tonalite to Quartz-diorite
?
Upper Unit (Penn-lPerm)
Middle Unit (uD-M)
Simpson Range Plutonic Suite
Lower Unit (pre-uD)
This Study
Mortensen 1992; Mortensen and Jilson 1985
Legend
Marble
Clean quartzite
Mafic schist and greenstone
Mafic (-intermediate) metavolcanic rocks
Mafic to ultramafic meta-igneous rocks
Graphitic phyllite, minor siliceous schist
Muscovite±chlorite siliceous schist and quartzite, minor graphitic phyllite
Devono-Mississippian hornblende-bearing, foliated metaplutonic rocks
Devono-Mississippian peraluminous orthogneiss
Non-carbonaceous quartzite and minor meta-pelite and host metasedimentary rock to the Peralumious Orthogneiss
Assemblage Contacts
Structural
Stratigraphic or Structural

Figure 2-3: Lithotectonic assemblage correlation diagram which compares the geology from this study with that of; (a) Tempelman-Kluit (1979), (b) Hansen et al. (1991), and (c) Mortensen (1992) and Mortensen and Jilson (1985). Correlations are based on similarity of lithologic assemblages. The best correlations are made between this study and Mortensen (1992).

rocks, and the phyllite unit is in structural and possibly stratigraphic contact with the metagabbro and greenstone unit. All of these units, with the possible exception of the metagabbro and greenstone, have continental crust characteristics and are interpreted to represent part of a continental crustal terrane formed by the mid-Mississippian. This is an important new interpretation. Previously, rocks of the Teslin tectonic zone were interpreted to have been amalgamated together in a Permo-Triassic subduction complex (Tempelman-Kluit 1979; Hansen 1992a).

An interpretation similar to that described above has been advanced by Mortensen (1992) for the upper Devonian to Mississippian evolution of the Yukon-Tanana terrane northeast of the Tintina Fault (Fig. 2-3c). In addition, rock types from this study can be readily correlated with rock assemblages in other parts of the Yukon-Tanana terrane of southern Yukon (Figs. 2-3a, 2-3b). This is interpreted to indicate that rocks of the Yukon-Tanana terrane in southern Yukon shared a similar history until at least the mid-Mississippian and that the Yukon-Tanana terrane represents a regionally extensive continental crustal terrane.

The structural stacking order proposed by Tempelman-Kluit (1979) for the Yukon-Tanana terrane of southern Yukon is not seen in the area of this study (Fig. 2-3a). Also, some of the lithotectonic terms used by Tempelman-Kluit (1979) (Fig. 2-3a) cannot by supported in this study. It is suggested here, and by Mortensen and Jilson (1985), that use of the term Simpson allochthonous assemblage be abandoned as the rocks correlated with this assemblage do not form a distinct allochthonous assemblage. Also, correlation of graphitic phyllite in the Teslin tectonic zone or Yukon-Tanana terrane with autochthonous North American rocks (Nasina Formation of Tempelman-Kluit 1984) should be avoided. In this study graphitic phyllite is interpreted to be part of the Yukon-Tanana terrane and may be unrelated to North American strata. The Nisutlin allochthonous assemblage as described by Tempelman-Kluit (1979) closely resembles and is considered to be correlative to the siliceous schist and quartzite unit. It is also considered appropriate to include rocks of the graphitic phyllite unit into the Nisutlin allochthonous assemblage, as they are interpreted to be in stratigraphic continuity with the siliceous schist and quartzite unit. Rocks of the metagabbro and greenstone unit are similar to the Anvil allochthonous assemblage described by Tempelman-Kluit (1979, 1984).

Most of the rock units from this study correlate with the upper plate Nisutlin and Teslin-Taylor Mountain terranes of Hansen et al. (1991) (Fig. 2-3b). Rocks of the siliceous schist and quartzite unit correspond with the lithologic description of the Nisutlin terrane and the metagabbro and greenstone unit with the Teslin-Taylor Mountain terrane. However, correlation of graphitic phyllite in the Teslin tectonic zone with rock of the Cassiar margin, as shown by Hansen et al. (1991) (Fig. 2-3b), should be treated with caution. In this study, graphitic phyllite is interpreted to be in stratigraphic continuity with rocks of the siliceous schist and quartzite unit and to be part of the Yukon-Tanana terrane. The interpretation by Hansen et al. (1989) that graphitic phyllite in the Teslin tectonic zone is part of the Nisutlin allocthonous assemblage is more consistent with the results of this study. Rock of the Early Mississippian meta-tonalite to quartz-diorite unit is correlated with the Mississippian I-type orthogneiss of the Teslin-Taylor Mountain of Hansen et al. (1991). However, in the area under study, Early Mississippian meta-tonalite intrudes metasedimentary rocks correlated with the Nisutlin terrane rather than with the Teslin-Tayor Mountain terrane.

METAMORPHIC EVOLUTION OF THE TESLIN TECTONIC ZONE

Background

Rocks of the Teslin tectonic zone and Yukon-Tanana terrane generally record metamorphism under greenschist to amphibolite facies conditions (Tempelman-Kluit 1979; Mortensen and Jilson 1985; Stevens 1992; Hansen 1992b), with eclogite conditions preserved in localized slices (Erdmer and Helmstaedt 1983, Erdmer 1987, 1992). The presence of eclogite originally led to the suggestion that rocks of the Teslin tectonic zone record deformation and metamorphism within a west-dipping subduction complex (Tempelman-Kluit 1979; Erdmer 1985; Hansen 1989, 1992a, 1992b). Hansen (1992b) suggested that in addition to the eclogite blocks, Teslin tectonic zone rocks "record widespread high-P/T metamorphic conditions consistent with subduction zone dynamothermal metamorphism".

In this section the results of new metamorphic P/T studies on rocks from the Teslin tectonic zone and re-evaluation of existing metamorphic P-T data are presented. Most of the metamorphic data are consistent with a medium-pressure regional metamorphic environment. Subduction-zone metamorphism is not required to explain most of the P-T data.

Mineral Assemblages

The main syn-kinematic metamorphic minerals are: quartz, plagioclase, chlorite, muscovite, biotite, carbonate, actinolite, epidote, hornblende, garnet and sillimanite. They define the penetrative planar and linear fabrics. Some recrystallization of muscovite and quartz occurred during later folding. Retrograde metamorphism is not widespread, and is predominantly reflected by the chloritization of biotite and garnet. Post-deformational growth of metamorphic minerals occurred locally and may be related to heating by Cretaceous quartz-monzonite plutons. However, clear evidence of contact metamorphism is not apparent adjacent to these plutons (Stevens 1992).

Thermobarometry

The locations of samples used for thermobarometry are shown on Fig. 2-2. All samples are ductilely deformed S- or L-S tectonites. The minerals analyzed form part of the penetrative planar and/or linear fabric. Semi-quantitative evaluation of metamorphic pressure is examined with reference to the composition of amphibole. Quantitative pressure and temperature estimates are constrained by the garnet-biotite, garnet-muscovite and garnet-hornblende exchange thermometers and the garnet-muscovite-plagioclase-biotite and garnet-hornblende-plagioclase net-transfer equilibria barometers.

Mineral compositions were determined using wavelength dispersive analysis on the University of Alberta's ARL-SEMQ microprobe. Natural silicate standards and samples were analyzed with a sample current of 12 nA, an accelerating voltage of 15 keV and a beam diameter of 1-10 μm. Data were reduced using the Bence-Albee correction. The Fe^{3+}/Fe^{2+} ratio and the site occupance of Na in amphiboles were calculated following Laird and Albee (1981a). Most results are for an average of 4 or more analyses on 2 or more grains. Tables 2-1, 2-2, and 2-3 and appendix 5 present the results of microprobe analysis.

Spot analyses across garnet grains revealed a weak prograde, core to rim, zoning pattern ($X_{Mn/Mn+Mg+Fe+Ca}$ decreases from ≈ 0.100 in the core to ≈ 0.025 along the rim) and no retrograde zoning. Most garnet analyses represent points within 20-30 μm of the rim. Zoning was not found in other minerals.

Amphibole Chemistry and Metamorphic Grade

Laird and Albee (1981b) plotted chemical components of metamorphic amphiboles and found a correlation between metamorphic grade and the site chemistry of the amphiboles. Amphiboles from a variety of metamorphic grades and from mafic schist with the common assemblage amphibole+chlorite+epidote +plagioclase+quartz+Ti phase were considered.

Amphiboles from 8 samples located throughout the study area (Fig. 2-2) were analyzed and the results are plotted on Fig. 2-4. Amphiboles plot dominantly in the Dalradian (medium-pressure) field. Most also lie in the Sanbagawa and Franciscan (high-pressure) field and at least one third fall into the Abukuma (low-pressure) field. Data on Figs. 2-4b and 2-4c lie about a line with a slope of one which is consistent with medium-pressure metamorphism (Laird and Albee 1981b).

Hansen (1992b) used similar plots to interpret the metamorphic grade of

Table 2-1. Microprobe analyses of selected garnet and plagioclase samples

	Garnet						Plagioclase				
Station	RS90-117	RS91-352	RS91-367a	RS91-368	RS92-487a	RS92-618b	RS90-117	RS91-352	RS91-266b	RS91-618b	RS92-618c
SiO_2	37.23	36.73	37.52	37.37	37.50	37.79	67.64	58.42	68.64	57.58	62.39
TiO_2	0.06	0.02	0.22	0.16	0.06	0.14	0.00	0.00	0.00	0.00	0.00
Al_2O_2	21.27	21.35	20.75	21.38	22.28	22.40	20.06	27.25	20.57	25.75	22.85
FeO	27.74	29.42	30.83	30.00	34.53	27.66	0.06	0.21	0.09	0.05	0.14
MnO	3.05	8.23	0.99	0.63	0.13	1.81	0.00	0.00	0.00	0.00	0.00
MgO	0.99	2.07	1.61	1.51	2.04	2.48	0.04	0.03	0.02	0.04	0.04
CaO	9.38	1.85	6.83	9.03	6.03	10.04	0.08	8.36	0.21	8.32	4.58
K_2O	0.00	0.00	0.00	0.00	0.00	0.00	0.08	0.08	0.08	0.06	0.07
Na_2O	0.00	0.00	0.00	0.00	0.00	0.00	10.39	6.20	10.38	6.85	9.05
Total	99.73	99.66	100.00	100.0	102.57	102.30	98.62	100.55	99.98	98.64	99.11
Si	2.99	2.94	3.01	2.98	2.94	2.93	2.99	2.59	2.98	2.61	2.79
Ti	0.00	0.00	0.01	0.01	0.00	0.01	0.00	0.00	0.00	0.00	0.00
Al	2.01	2.04	1.96	2.00	1.80	2.05	1.04	1.43	1.05	1.37	1.20
Fe	1.86	2.00	2.06	2.01	2.27	1.79	0.00	0.01	0.00	0.00	0.01
Mn	0.21	0.57	0.07	0.04	0.01	0.12	0.00	0.00	0.00	0.00	0.00
Mg	0.12	0.25	0.19	0.18	0.24	0.29	0.00	0.00	0.00	0.00	0.00
Ca	0.81	0.16	0.70	0.77	0.51	0.84	0.00	0.40	0.01	0.40	0.22
K	0.00	0.00	0.00	0.00	0.00	0.00	0.00	0.00	0.00	0.00	0.00
Na	0.00	0.00	0.00	0.00	0.00	0.00	0.89	0.53	0.87	0.60	0.78
O	12.00	12.00	12.00	12.00	12.00	12.00	8.00	8.00	8.00	8.00	8.00
Xalm	0.62	0.67	0.68	0.67	0.75	0.59					
Xpy	0.04	0.08	0.06	0.06	0.08	0.10					
Xgr	0.27	0.05	0.23	0.26	0.17	0.28					
An							0.00	0.42	0.01	0.40	0.22
Ab							0.99	0.57	0.98	0.60	0.78

Table 2-2: Microprobe analyses of selected biotite and muscovite samples

	Biotite					Muscovite					
Station	RS90-117	RS91-352	RS91-367a	RS91-368	RS92-618b	RS90-117	RS91-352	RS91-367a	RS91-368	RS92-487a	RS92-618b
SiO_2	35.75	34.44	35.65	37.13	35.86	49.45	45.92	49.13	48.03	48.52	48.97
TiO_2	1.64	2.27	1.77	1.52	1.74	0.24	0.51	0.38	0.50	0.41	0.16
Al_2O_3	15.35	18.56	17.34	17.38	18.86	27.82	34.82	28.84	26.47	30.95	29.94
FeO	20.08	20.84	20.74	19.86	17.86	3.32	1.98	2.26	2.76	2.10	3.06
MnO	0.29	0.26	0.17	0.20	0.09	0.03	0.02	0.01	0.01	0.01	0.03
MgO	10.23	8.37	8.19	9.39	11.11	2.35	0.58	2.56	2.52	2.13	2.13
CaO	0.06	0.00	0.01	0.00	0.00	0.00	0.00	0.00	0.01	0.00	0.00
K_2O	9.22	9.01	9.44	7.15	9.22	10.40	10.46	10.39	8.57	9.95	9.92
Na_2O	0.15	0.33	0.15	2.62	0.01	0.52	0.92	0.62	2.30	0.93	0.83
Total	92.79	94.16	93.42	95.16	94.11	94.13	95.20	94.19	92.85	95.05	95.04
Si	5.64	5.36	5.58	5.66	5.48	6.72	6.15	6.64	6.61	6.48	6.57
Ti	0.19	0.27	0.21	0.17	0.20	0.02	0.05	0.03	0.05	0.04	0.03
Al	2.85	3.40	3.20	3.12	3.26	4.46	5.50	4.59	4.56	4.88	4.74
Fe	2.65	2.71	2.72	2.53	2.28	0.38	0.22	0.26	0.32	0.23	0.33
Mn	0.04	0.00	0.02	0.03	0.01	0.00	0.00	0.00	0.00	0.00	0.00
Mg	2.40	1.94	1.91	2.14	2.53	0.48	0.12	0.52	0.52	0.43	0.41
Ca	0.01	0.00	0.00	0.00	0.00	0.00	0.00	0.00	0.00	0.00	0.00
K	1.85	1.86	1.88	1.85	1.80	1.80	1.79	1.79	1.79	1.70	1.70
Na	0.04	0.10	0.05	0.05	0.03	0.14	0.24	0.16	0.19	0.24	0.22
O	22.00	22.00	22.00	22.00	22.00	22.00	22.00	22.00	22.00	22.00	22.00
Xann	0.46	0.47	0.48	0.45	0.40						
Xphl	0.42	0.34	0.34	0.38	0.44						
FeCel						0.05	0.03	0.02	0.04	0.04	0.07
MgCel						0.06	0.02	0.05	0.07	0.07	0.09

Table 2-3. Microprobe analyses of selected amphibole samples

Sample	RS91-369a	RS91-372a	RS90-49b	RS92-607	RS92-618c
SiO_2	47.85	49.05	47.41	43.17	41.32
TiO_2	0.22	0.29	0.20	1.07	0.27
Al_2O_3	9.66	8.42	8.21	10.97	15.54
FeO	14.67	13.03	14.59	17.43	19.77
MnO	0.20	0.36	0.30	0.21	0.31
MgO	12.33	14.18	13.66	11.17	7.26
CaO	10.44	10.36	11.21	11.46	10.76
Na_2O	2.24	1.76	1.34	2.44	2.01
K_2O	0.47	0.39	0.11	0.84	0.58
TOTAL	98.08	97.84	97.03	98.76	97.82
	Recalculated after Laird and Albee (1981b)				
Si	6.89	6.97	6.84	6.36	6.14
Al(IV)	1.11	1.03	1.16	1.64	1.86
Al(VI)	0.54	0.38	0.24	0.26	0.86
Ti	0.02	0.03	0.02	0.12	0.03
Fe(3+)	0.59	0.89	1.01	0.68	0.82
Fe(2+)	1.18	0.66	0.75	1.47	1.64
Mn	0.02	0.04	0.04	0.03	0.04
Mg	2.65	3.00	2.94	2.45	1.61
Ca	1.61	1.58	1.73	1.81	1.71
Na(M4)	0.39	0.42	0.27	0.19	0.29
Na(A)	0.24	0.06	0.11	0.50	0.29
K	0.09	0.07	0.02	0.16	0.11

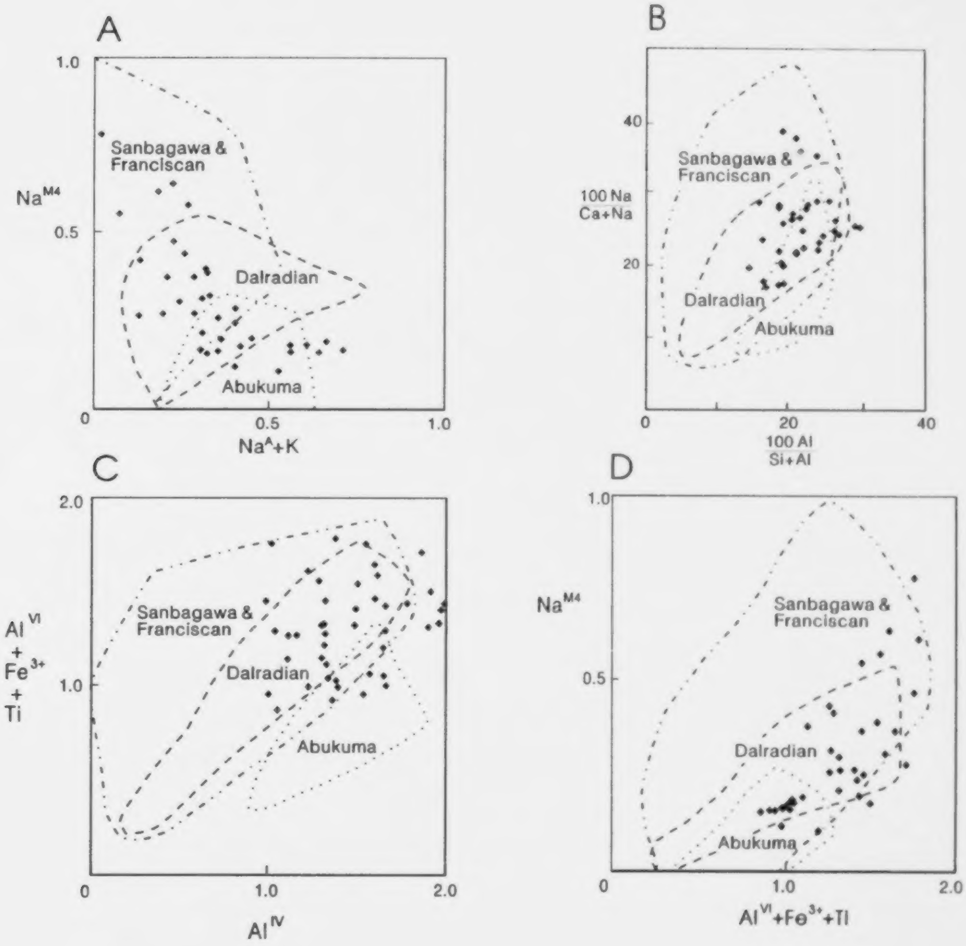

Figure 2-4: Amphibole chemistry for selected samples from this study. The data fall chiefly in the Dalradian medium-pressure metamorphic field. See Fig. 2-2 for sample locations. For each sample four points are shown and each point represents the average analysis of a single grain.

amphiboles from the Teslin tectonic zone in the Laberge area. There, amphiboles were interpreted to plot chiefly in the Sanbagawa and Franciscan field suggesting that Teslin tectonic zone metamorphism is consistent with a subduction zone environment (Hansen 1992b). However much of the data also plot in the Dalradian (medium-pressure) field and many in the Abukuma (low-pressure) field. Data on plots of Na/Na+Ca vs. Al/Al+Si and $Al^{vi}+Fe^{3+}+Ti$ vs. Al^{iv} lie roughly about a line with a slope of one which is consistent with medium-pressure metamorphism (Laird and Albee 1981b). Thus, much of the data from Hansen (1992b) are also consistent with medium-pressure metamorphism.

Garnet-Based Thermobarometry

Table 2-4 summarizes the results of garnet thermobarometry in this study and from Hansen (1987, 1992b). Pressure and temperature estimates were obtained using: 1) the garnet-biotite thermometer of Ferry and Spear (1978), and the garnet-muscovite thermometer of Hynes and Forest (1988) both with the correction of Hodges and Spear (1982) for the non-ideal behaviour of garnet along the pyrope-grossular binary; 2) the garnet-biotite-muscovite-plagioclase barometer of Ghent and Stout (1981) for rocks from this study and after Hodges and Crowley (1985) for the data from Hansen (1987, 1992b); 3) the thermodynamic data of Berman (1988, 1990) and the computer program TWEEQU (Berman 1991) which uses the solution model of Berman (1990) for garnet, McMullin et al. (1991) for biotite, Chatterjee and Froese (1975) for muscovite and Fuhrman and Lindsley (1988) for plagioclase; and 4) the garnet-hornblende thermometer of Graham and Powell (1984) and the garnet-hornblende-plagioclase-quartz barometer of Kohn and Spear (1990). Pressure and temperature results are estimated to have a minimum error of ±1.0-1.5 kbar and ±50°C.

Temperature estimates on rocks from this study range from 427 to 634°C (Table 2-4) and cluster between 450 and 550°C. The highest temperatures were obtained using the garnet-biotite thermometer and the program TWEEQU

Table 2-4: P-T estimates on Yukon-Tanana terrane rocks of the Teslin tectonic zone from this study and from Hansen (1987, 1992b)

Sample #	Source	T(°C)^a Gr-Bt	T(°C)^b Gr-Mu	T(°C)^c Gr-Hb	T(°C)^d Gr-Bt	P(kbar)^d Gr-Pl-Mu-Bt	P(kbar)^e Gr-Pl-Mu-Bt	P(kbar)^f Gr-Pl-Mu-Bt	P(kbar)^g Gr-Pl-Hb	P(kbar)^h GRIPS
RS90-116	1	482			491					
RS90-117	1	443	449		454					
RS90-119	1	438	427		442					
RS90-192	1	566	485		581					
RS91-266b	1	501	476		510					
RS91-352	1	576	593		576	2.7	2.8			
RS91-359a	1		521							
RS91-366a	1	494			510					
RS91-367a	1	581	434		589					
RS91-368	1	530	454		542					
RS91-371	1		451							
RS91-389c	1		521							
RS92-487a	1		445							
RS92-618b	1	622	522		628	8.75	7.35			
RS92-618c	1			634					10.4-10.7	
LV-184	2,3	598		530-600						
LV-189	3	570								
LV-192A	2,3			610-650						
LV-197AB	2	574								
LV-193F	2,3			580-650						
TW-245	3	600-								
TW-263	2,3	610		575-660					8.2-8.8	
TW-261-1	2,4	651			658	9.2		9.9		10.9
TW-263D	2,4	631-65			652-676	8.8-11.7		8.8-9.9		10.7-11.1
TW-245	2	594								
DW-315B	2,4	436-54			433-545	5.3-7.0		5.6-7.4		9.1-12.3
DW-315D	3	390-71								
DW-321	2,4	583-72			590-722	6.5-12.6		7.1-12.7		10.8-14.8
DW-325	2,4	673-74			674-750	9.3-17.0		9.8-15.5		8.5-10.3
DW-294	3			625						
DW-290	3			625-700					10.8	
DW-296	3			660-670						
DW-291-1	3,4	719		715	715	15.8		17		
DW-324	2	625								
DW-282	2	511								

NOTES: The sources of data are: 1 = this study, 2 = Hansen 1987, 3 = Hansen 1992b, 4 = recalculation of the data from Hansen (1987, 1992b) with the program TWEEQU (Berman 1991). When pressure estimates are absent, 7.5 kbars is used in this study and 10 kbars for the data from Hansen (1987, 1992b).

[a] Garnet-biotite (Ferry and Spear 1978) with garnet correction of Hodges and Spear (1982)

[b] Garnet-muscovite (Hynes and Forest 1988) with garnet correction of Hodges and Spear (1982)

[c] Garnet-hornblende (Graham and Powell 1984)

[d] Garnet-plagioclase-muscovite-biotite (Berman 1991)

[e] Garnet-plagioclase-muscovite-biotite (Ghent and Stout 1981)

[f] Garnet-plagioclase-muscovite-biotite (after Hodges and Crowley 1985)

[g] Garnet-plagioclase-hornblende (Kohn and Spear 1990)

[h] Garnet-rutile-ilmenite-plagioclase (Bohlen and Liotta 1986)

(Berman 1991) and the lowest using the garnet-muscovite thermometer (Hynes and Forest 1988). One half of the garnet-muscovite temperatures are also 50-150°C lower than garnet-biotite values on the same sample. Local recrystallization of muscovite during the second deformation phase (folding) may be responsible for these variations. Muscovite also has a wide range of compositions within a single grain or thin section suggesting some degree of disequilibrium. Temperature estimates using the garnet-muscovite thermometer should therefore be interpreted with caution.

Large parts of the study area were probably metamorphosed at temperatures lower than those reported above. Most temperature estimates are from garnet-bearing rocks of the siliceous schist and quartzite unit; elsewhere in this unit, rocks of similar composition (or even more pelitic) lack garnet and consequently are thought to lie below the garnet-isograd. This interpretation is supported by the temperature estimates in garnet-bearing samples, as many fall just above the garnet isograd (450-500°C).

Pressure estimates were difficult to obtain because most samples contain relatively pure albite ($<An_5$) or variable plagioclase compositions, probably reflecting the peristerite gap. Only two sample locations yielded plagioclase with a consistent composition greater than An_{10}.

Sample RS91-352 is a sillimanite-bearing pelitic rock that gave a pressure estimate of 2.7-2.8 kbar at ~575°C. This sample comes from the hornblende/sillimanite pelitic schist and gneiss unit that is of uncertain tectonic affinity and may be a metamorphosed part of the pre-Mesozoic North American margin (see earlier discussion). The significance of this pressure estimate with respect to the pressures of metamorphism of Yukon-Tanana terrane rocks in the Teslin tectonic zone is unclear. Samples RS92-618b,c gave pressure estimates of 7.35-8.75 kbar and 10.4-10.7 kbar respectively at ~625°C.

Evaluation of Garnet Thermobarometry

One of the principal criteria of thermobarometry is that all mineral phases used for P-T estimates should be in equilibrium (Spear 1989). A simple test of equilibrium is to determine whether pressure and temperature estimates using a single calibration are consistent over a small outcrop area (Spear 1989).

In this study, multiple samples were not analyzed within a single outcrop. However, garnet-biotite temperature estimates on samples a few kilometres apart give results that are within error (for example, samples RS90-192, RS91-366a, -367a, and -368 and samples RS90-116, -117 and -118; Fig. 2-2). Garnet-muscovite estimates are also within error but should be interpreted with caution due to compositional variations in muscovite (see earlier discussion).

Temperature estimates from Hansen (1987, 1992b) are consistent within a given sample or local area, except for samples DW-315D and DW-321 which give temperature estimates that vary by more that 100°C (Table 2-4). Pressure estimates from Hansen (1987, 1992b) are within error in some samples but vary greatly in others. In particular, samples DW-321 and DW-325 have pressure estimates that span at least 5.5 kbar using a single barometer. This is interpreted as a strong indication that disequilibrium exists. Sample DW-315B gave pressure estimates that are within error for a single barometer. However, the combined results from the two barometers used on this sample give pressures that vary from 5.3 to 12.3 kbar (Table 2-4) (Hansen 1987). This suggests that the mineral phases are not in equilibrium.

In conclusion, almost all temperature estimates and many of the pressure estimates from this study and from Hansen (1987, 1992b) appear to come from equilibrium assemblages. However, some samples are likely in disequilibrium and are regarded as unreliable and not considered further.

Discussion

The position in P-T space of Yukon-Tanana terrane rocks from the Teslin tectonic zone for which both reliable pressure and temperature estimates are available and the location of P-T estimates for eclogites from the Yukon-Tanana terrane in Yukon (Erdmer 1987) are shown on Fig. 2-5.

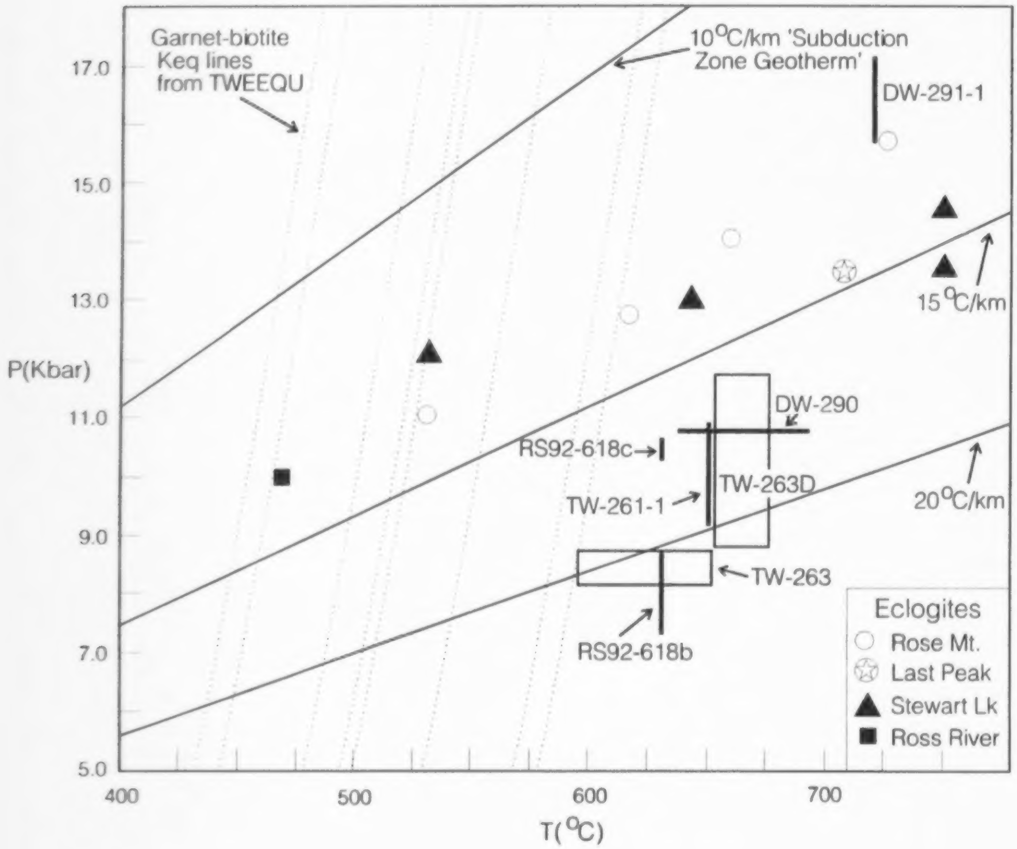

Figure 2-5: Pressure-Temperature diagram showing 1) the position in P-T space of Yukon-Tanana terrane rocks from the Teslin tectonic zone for which both reliable pressure and temperature estimates are available; 2) the location of P-T estimates for eclogites from the Yukon-Tanana terrane in Yukon (Erdmer 1987); 3) garnet-biotite Keq lines (temperature estimates) from the program TWEEQU (Berman 1991) for rocks from this study (dotted lines); and 4) the location of the 10°C/km, 15°C/km and 20°C/km geothermal gradients calculated assuming a bulk crustal density of 2.80 g/cm^3.

Subduction-zone metamorphism has affected some rocks of the Teslin tectonic zone and Yukon-Tanana terrane, as recorded by blueschist and group-C eclogite (Erdmer and Helmstaedt 1983; Erdmer 1987, 1992). However, the extent to which subduction zone metamorphism is preserved in Teslin tectonic zone remains unclear. Hansen (1992b) suggested that there is widespread preservation of these conditions, but the metamorphic data presented here does not support this interpretation.

Examination of the pressure estimates obtained from Teslin tectonic zone rocks show that except for DW-291-1 all samples cluster around 8.5-11.0 kbar @625-675°C (Fig. 2-5). This cluster is at distinctly lower pressures than those from Yukon-Tanana terrane eclogites at similar temperatures (Fig. 2-5). These pressure estimates, although on the high side, are also within the range of pressures estimated for rocks from regionally metamorphosed medium-pressure terranes not associated with blueschist or eclogite (southeastern Vermont, Laird and Albee 1981b, Kohn and Spear 1990; Dalradian, Baker 1985, Watkin 1985; northern British Columbia, Evenchick 1988). In addition, most of the amphibole chemistry from this study and from Hansen (1992b) indicates that metamorphism was of a medium-pressure type (see earlier discussion). Therefore, except for DW-291-1, all of the garnet-based pressure estimates on Teslin tectonic zone rocks are consistent with medium-pressure regional metamorphic conditions. It is interpreted that most rocks of the Teslin tectonic zone record medium-pressure, regional metamorphism, at greenschist to amphibolite facies conditions, which overprinted an earlier subduction-zone metamorphsim. Caution, however, should be exercised when using the garnet-based pressure estimates from this study and from Hansen (1987, 1992b) to evaluate the metamorphic conditions in the Teslin tectonic zone as a whole. Only three small areas are represented by the pressure estimates. The first includes the Last Peak eclogite occurrence (Erdmer and Helmstaedt 1983) and within four kilometres, samples TW-263, -263D, and -261-1 (Hansen 1987). The second, less than one kilometre wide, includes samples DW-290 and DW-291-1, and the last, less than 50 meters wide includes samples RS92-618b and RS92-618c.

Most temperature estimates on rocks from this study (K_{eq} lines; Fig. 2-5) are 100-200°C lower than the temperature estimates on samples for which pressures have been calculated (Fig. 2-5). Much of the study area has probably been metamorphosed at even lower temperatures than the ones reported here (see earlier discussion). Therefore, the pressure to temperature relationships shown on Fig. 2-5 may not be representative of the study area. Temperature estimates on Teslin tectonic zone rocks in the northern half of the Laberge map area average 100-200°C higher than those from the southern half of the Laberge map area and from the Teslin map area (Hansen 1987, 1992b; this study). This suggests that different metamorphic levels are exposed along the strike of the Teslin tectonic zone and that the P-T relationships shown on Fig. 2-5 may be most representative of the northern Laberge map area, rather than the Teslin tectonic zone as a whole.

TECTONIC IMPLICATIONS

This study has revealed that primary intrusive and depositional contacts are preserved between rock assemblages of the Teslin tectonic zone. These relationships indicate that most of the rocks underlying the study area were joined together (depositionally or intrusively) by the mid-Mississippian. Thus, the notion that rocks in the Teslin tectonic zone were amalgamated together during Permo-Triassic subduction (Hansen 1992a) needs to be modified. Clearly, deformation and tectonic remobilization has affected most rock assemblages in the Teslin tectonic zone since the mid-Mississippian and new assemblages may have been added during this deformation. However, the results of this study indicate that most assemblages (>80% of the deformed rock in the study area) were together before any late Paleozoic or early Mesozoic deformation.

The P-T data from this study and re-evaluation of the data from Hansen (1987, 1992b) show that available metamorphic data do not require the interpretation that widespread subduction-zone metamorphism is characteristic in the Teslin tectonic zone. It is interpreted, in this study, that most rocks of the Teslin tectonic zone record medium-pressure, regional metamorphism, at greenschist to amphibolite facies conditions, which overprinted earlier subduction-zone metamorphism. Eclogite occurrences support this interpretation, as they occur in small structural lenses that are often clearly overprinted by amphibolite to greenschist facies metamorphism (Erdmer 1987, 1992). In addition, blueschist and eclogite in the Yukon-Tanana terrane preserve Permian cooling ages (Erdmer and Armstrong 1988; Wanless et al. 1978), compared to widespread Late Triassic-Early Jurassic cooling ages on schists from the Yukon-Tanana terrane and Teslin tectonic zone (Hansen et al. 1991, Stevens et al. 1982; Stevens et al. 1993).

CONCLUSIONS

This paper outlines the geology and metamorphism in a part of the Teslin tectonic zone and arrives at two principle conclusions; 1) that the Teslin tectonic zone and the Yukon-Tanana terrane of southern Yukon are part of a regionally extensive continental crustal terrane that had formed by the mid-Mississippian, and 2) that rocks of the Teslin tectonic zone generally reflect medium-pressure regional metamorphic conditions which mostly overprinted the record of an earlier subduction-zone metamorphism.

These conclusions provide important new constraints on future models for the tectonic evolution of the Teslin tectonic zone. In particular the interpretation that rocks in the Teslin tectonic zone were amalgamated together in a Permo-Triassic subduction zone and that they preserve widespread subduction zone metamorphic conditions needs to be re-evaluated.

REFERENCES

Aleinikoff, J.N., Dusel-Bacon, C., Foster, H.L., and Nokleberg, W.J. 1987. Lead isotopic fingerprinting of tectonostratigraphic terranes, east-central Alaska. Canadian Journal of Earth Sciences, **24**: 2089-2098.

Baker, A.J. 1985. Pressures and temperatures of metamorphism in the eastern Dalradian. Journal of the Geological Society of London, **142**: 137-148.

Berman, R.G. 1988. Internally-consistent thermodynamic data for stoichiometric minerals in the system Na_2O-K_2O-CaO-MgO-FeO-Fe_2O_3-Al_2O_3-SiO_2-TiO_2-H_2O-CO_2. Journal of Petrology, **29**: 445-522.

Berman, R.G. 1990. Mixing properties of Ca-Mg-Fe-Mn garnets. American Mineralogist, **75**: 328-344.

Berman, R.G. 1991. Thermobarometry using multiequilibrium calculations: a new technique with petrologic applications. Canadian Mineralogist, **29**: 833-855.

Bohlen, S.R., and Liotta, J.J. 1986. A barometer for garnet amphibolites and garnet granulites. Journal of Petrology, **27**: 1025-1034.

Brown, P., and Kahlert, B. 1986. Geology and mineralization of the Red Mountain porphyry molybdenum deposit south-central Yukon. *In* Mineral Deposits of the Northern Canadian Cordillera. *Edited by* J.A. Morin. Canadian Institute of Mining and Metallurgy, Special Volume 37, pp. 288-297.

Chatterjee, N.D., and Froese, E.F. 1975. A thermodynamic study of the pseudobinary join muscovite-paragonite in the system $KAlSi_3O_8$-$NaAlSi_3O_8$-Al_2O_3-SiO_2-H_2O. American Mineralogist, **60**: 985-993.

Churkin, M., Jr., Foster, H.L., Chapman, R.M., and Weber, F.R. 1982. Terranes and suture zones in east-central Alaska. Journal of Geophysical Research, **87**: 3178-3730.

Erdmer, P. 1985. An examination of the cataclastic fabrics and structures of parts of Nisutlin, Anvil and Simpson allochthons, central Yukon: test of the arc-continent collision model. Journal of Structural Geology, **7**: 57-72.

Erdmer, P. 1987. Blueschist and eclogite in mylonitic allochthons, Ross River and Watson Lake areas, southeastern Yukon. Canadian Journal of Earth Sciences, **24**: 1439-1449.

Erdmer, P. 1992. Eclogitic rocks in the St. Cyr klippe, Yukon, and their tectonic significance. Canadian Journal of Earth Sciences, **29**: 1296-1304.

Erdmer, P., and Armstrong. R.L. 1988. Permo-Triassic isotopic dates for blueschist, Ross River area, Yukon. *In* Yukon Geology vol. 2. Exploration and Geological Services Division, Yukon, Indian and Northern Affairs Canada, pp. 33-36.

Erdmer, P., and Helmstaedt, H. 1983. Eclogite from central Yukon: a record of subduction at the western margin of ancient North America. Canadian Journal of Earth Sciences, **20**: 1389-1408.

Evenchick, C.A. 1988. Stratigraphy, metamorphism, structure, and their tectonic implications in the Sifton and Deserters Ranges, Cassiar and northern Rocky Mountains, northern British Columbia. Geological Survey of

Canada, Bulletin 376.

Ferry, J.M., and Spear, F.S. 1978. Experimental Calibration of the Partitioning of Fe and Mg between biotite and garnet. Contributions to Mineralogy and Petrology, **66**: 113-117.

Fuhrman, M.L., and Lindsley, D.H. 1988. Ternary-feldspar modelling and thermometry. American Mineralogist, **73**: 201-216.

Ghent, E.D., and Stout, M.Z. 1981. Geobarometry and geothermometry of plagioclase-biotite-garnet-muscovite assemblages. Contributions to Mineralogy and Petrology, **76**: 92-97.

Gordey, S.P. 1991. Teslin map area, a new geological mapping project in Southern Yukon. *In* Current research, part A. Geological Survey of Canada, Paper 91-1A, pp. 171-178.

Gordey, S.P., and Stevens, R.A. 1994. Tectonic framework of southern Yukon in the Teslin region. *In* Current research, 1994-A, Geological Survey of Canada, pp. 11-18.

Graham, C.M., and Powell, R.P. 1984. A garnet-hornblende geothermometer: Calibration, testing and application to the Pelona Schist, southern California. Journal of Metamorphic Geology, **2**: 13-31.

Hansen, V.L. 1987. Structural, metamorphic, and geochronologic evolution of the Teslin suture zone, Yukon: evidence from Mesozoic oblique convergence outboard of the northern Canadian Cordillera. Ph.D. thesis, University of California, Los Angeles, California.

Hansen, V.L. 1989. Structural and kinematic evolution of the Teslin suture zone, Yukon: record of an ancient transpressional margin. Journal of Structural Geology, **11**: 717-733.

Hansen, V.L. 1992a. Backflow and margin-parallel shear within an ancient subduction complex. Geology, **20**: 71-74.

Hansen, V.L. 1992b. P-T evolution of the Teslin suture zone and Cassiar tectonites, Yukon, Canada: evidence for A- and B-type subduction. Journal of Metamorphic Geology, **10**: 239-263.

Hansen, V.L., Heizler, M.T., and Harrison, T.M. 1991. Mesozoic thermal evolution of the Yukon-Tanana composite terrane: new evidence from $^{40}Ar/^{39}Ar$ data. Tectonics, **10**: 51-76.

Hansen, V.L., Mortensen, J.K., and Armstrong, R.L. 1989. U-Pb, Rb-Sr, and K-Ar isotopic constraints for ductile deformation and related metamorphism in the Teslin suture zone, Yukon-Tanana terrane, south-central Yukon. Canadian Journal of Earth Sciences, **26**: 2224-2235.

Hodges, K.V., and Crowley, P.D. 1985. Error estimation and empirical geothermobarometry for pelitic systems. American Mineralogist, **70**: 702-709.

Hodges, K.V., and Spear, F.S. 1982. Geothermometry, geobarometry and the Al_2SiO_5 triple point at Mt. Moosilauke, New Hampshire. American Mineralogist, **67**: 1118-1134.

Hynes, A., and Forest, R.C. 1988. Empirical garnet-muscovite geothermometry in low-grade metapelites, Selwyn Range (Canadian Rockies). Journal of

Metamorphic Geology, **6**: 297-309.

Jones, D.L., Silberling, N.J., Coney, P.J., and Plafker, G. 1987. Lithotectonic terrane map of Alaska (west of the 141st Meridian). United States Geological Survey Miscellaneous Field Studies Map MF-1874-A, scale, 1:2 500 000.

Kohn, M.J., and Spear, F.S. 1990. Two new geobarometers for garnet amphibolites, with applications to southeastern Vermont. American Mineralogist, **75**: 89-96.

Laird, J., and Albee, A.L. 1981a. High-pressure metamorphism in mafic schist from northern Vermont. American Journal of Science, **281**: 97-126.

Laird, J., and Albee, A.L. 1981b. Pressure, temperature, and time indicators in mafic schist: their application to reconstructing the polymetamorphic history of Vermont. American Journal of Science, **281**: 127-175.

McMullin, D., Berman, R.G., and Greenwood, H.J. 1991. Calibration of the SGAM thermobarometer for pelitic rocks using data from phase equilibrium experiments and natural assemblages. Canadian Mineralogist, **29**: 889-908.

Monger, J.W.H., and Berg, H.C. 1987. Lithotectonic terrane map of western Canada and southeastern Alaska. United States Geological Survey Miscellaneous Field Studies Map MF-1874-B, scale 1:2 500 000.

Mortensen, J.K. 1992. Pre-mid-Mesozoic tectonic evolution of the Yukon-Tanana terrane, Yukon and Alaska. Tectonics, **11**: 836-853.

Mortensen, J.K., and Jilson, G.A. 1985. Evolution of the Yukon-Tanana terrane: evidence from southeastern Yukon Territory. Geology, **13**: 806-810.

Read, P.B., Woodsworth, G.J., Greenwood, H.J., Ghent, E.D., and Evenchick, C.A. 1991. Metamorphic map of the Canadian Cordillera. Geological Survey of Canada, Map 1714A, scale 1:2 000 000.

Spear, F.S. 1989. Petrologic determination of metamorphic pressure-temperature-time paths. *In* Metamorphic Pressure-Temperature-Time Paths. *Edited by* F.S. Spear and S.M. Peacock. American Geophysical Union Short Course in Geology, v. 7, pp. 1-55.

Stevens, R.A. 1991. The Teslin suture zone in northwest Teslin map area, Yukon. *In* Current research, part A. Geological Survey of Canada, Paper 91-1A, pp. 271-277. *See appendix 1*

Stevens, R.A. 1992. Regional geology, fabric, and structure of the Teslin suture zone in northwest Teslin map area, Yukon Territory. *In* Current research, part A. Geological Survey of Canada, Paper 92-1A, pp. 287-295. *See appendix 2*

Stevens, R.A. 1994. Geology of the Teslin suture zone in parts of Laberge (105E/1), Quiet Lake (105F/4) and Teslin (105C/11, 13, 14) map areas, Yukon Territory. Geological Survey of Canada, Open File 2768. *See appendix 6*

Stevens, R.A., and Erdmer., P. 1993. Geology and structure of the Teslin suture zone and related rocks in parts of Laberge, Quiet Lake, and Teslin map areas, Yukon Territory. *In* Current research, part A. Geological Survey of Canada, Paper 93-1A, pp. 11-20. *See appendix 3*

Stevens, R.A., Mortensen, J.K., and Hunt, P. A. 1993. U-Pb and ^{40}Ar-^{39}Ar geochronology of plutonic rocks from the Teslin suture zone, Yukon Territory. *In* Radiogenic age and isotopic studies, report 7. Geological Survey of Canada Paper 93-2, pp. 83-90. *See chapter 3*

Stevens, R.D., Delabio, R.N., and Lachance, G.R. 1982. Age determinations and geological studies, K-Ar isotopic ages, report 15. Geological Survey of Canada, Paper 81-2, pp. 19-21.

Tempelman-Kluit, D.J. 1977. Quiet Lake (105F) and Finlayson Lake (105G) map areas, Yukon. Geological Survey of Canada, Open File 486.

Tempelman-Kluit, D.J. 1979. Transported cataclasite, ophiolite and granodiorite in Yukon: evidence of arc-continent collision. Geological Survey of Canada, Paper 79-14.

Tempelman-Kluit, D.J. 1984. Geology, Laberge (105E) and Carmacks (115I), Yukon Territory. Geological Survey of Canada, Open File 1101.

Watkin, K.P. 1985. Geothermometry and geobarometry of inverted metamorphic zones in the W central Scottish Dalradian. Journal of the Geological Society of London, **142**: 157-165.

Wanless, R.K., Stevens, R.D., Lachance, G.R., and Delabio, R.N. 1978. Age determinations and geological studies, K-Ar isotopic ages, report 13. Geological Survey of Canada, Paper 77-2, p. 60.

Wheeler, J.O., and McFeely, P., (comp.). 1991. Tectonic assemblage map of the Canadian Cordilleran and adjacent parts of the United States of America. Geological Survey of Canada, Map 1712A, scale 1:2 000 000.

Wheeler, J.O., Brookfield, A.J., Gabrielse, H., Monger, J.W.H., Tipper, H.W., and Woodsworth, G.J., (comp.). 1991. Terrane map of the Canadian Cordillera. Geological Survey of Canada, Map 1713A, scale 1:2 000 000.

Woodsworth, G.J., Anderson, R.G, and Armstrong, R.L. 1991. Plutonic Regimes, Chapter 15. *in* Geology of the Cordilleran Orogen in Canada. *Edited by* H. Gabrielse and C.J. Yorath. Geological Survey of Canada, Geology of Canada, no. 4, p. 491-531.

CHAPTER 3 - U-Pb AND ^{40}Ar-^{39}Ar GEOCHRONOLOGY OF PLUTONIC ROCKS FROM THE TESLIN TECTONIC ZONE, YUKON TERRITORY*

---

*A version of this chapter has been published. Stevens, R.A., Mortensen, J.K., and Hunt, P.A. 1993. *In* Radiogenic Age and Isotopic Studies: Report 7; Geological Survey of Canada, Paper 93-2, pp. 83-90.

INTRODUCTION

The Teslin tectonic zone in south-central Yukon (Fig. 2-1), is part of the Yukon-Tanana terrane of Monger and Berg (1987) or the Nisutlin terrane of Wheeler et al. (1991). It lies between rocks originally deposited along the western edge of the North American craton to the east and allochthonous rocks of the Intermontane Belt to the west (Fig. 2-1). The Teslin tectonic zone consists of steeply dipping S-, L-S, and L-tectonites derived from sedimentary, volcanic and plutonic rocks metamorphosed and deformed under greenschist to amphibolite facies conditions (Hansen et al. 1989; Stevens and Erdmer 1993a; Tempelman-Kluit 1979).

An isotopic dating study was undertaken in part of the Teslin tectonic zone (Fig. 3-1) in order to help constrain: 1) the protolith ages of rocks that took part in Teslin tectonic zone deformation, and 2) the timing of deformation and uplift of these rocks. To these ends, three bodies of deformed metaplutonic rock were dated using U-Pb methods on zircon and titanite in order to constrain the crystallization age of these bodies and to place a minimum age of deposition for rocks that they intrude. A massive pluton was also dated using U-Pb and ^{40}Ar-^{39}Ar methods, in order to place a local minimum age on deformation and to constrain the cooling/uplift history of this body.

REGIONAL GEOLOGY

The Teslin tectonic zone was defined on a structural basis by Tempelman-Kluit (1979) as "a northwest trending zone of steeply dipping cataclastic rocks 15 km wide [that] separates the Omineca and Intermontane Belts". The Teslin tectonic zone extends from southern Glenlyon map area south through Laberge map area to at least the Canol Road in Teslin map area (Fig. 2-1) (Tempelman-Kluit 1979; Stevens and Erdmer 1993a).

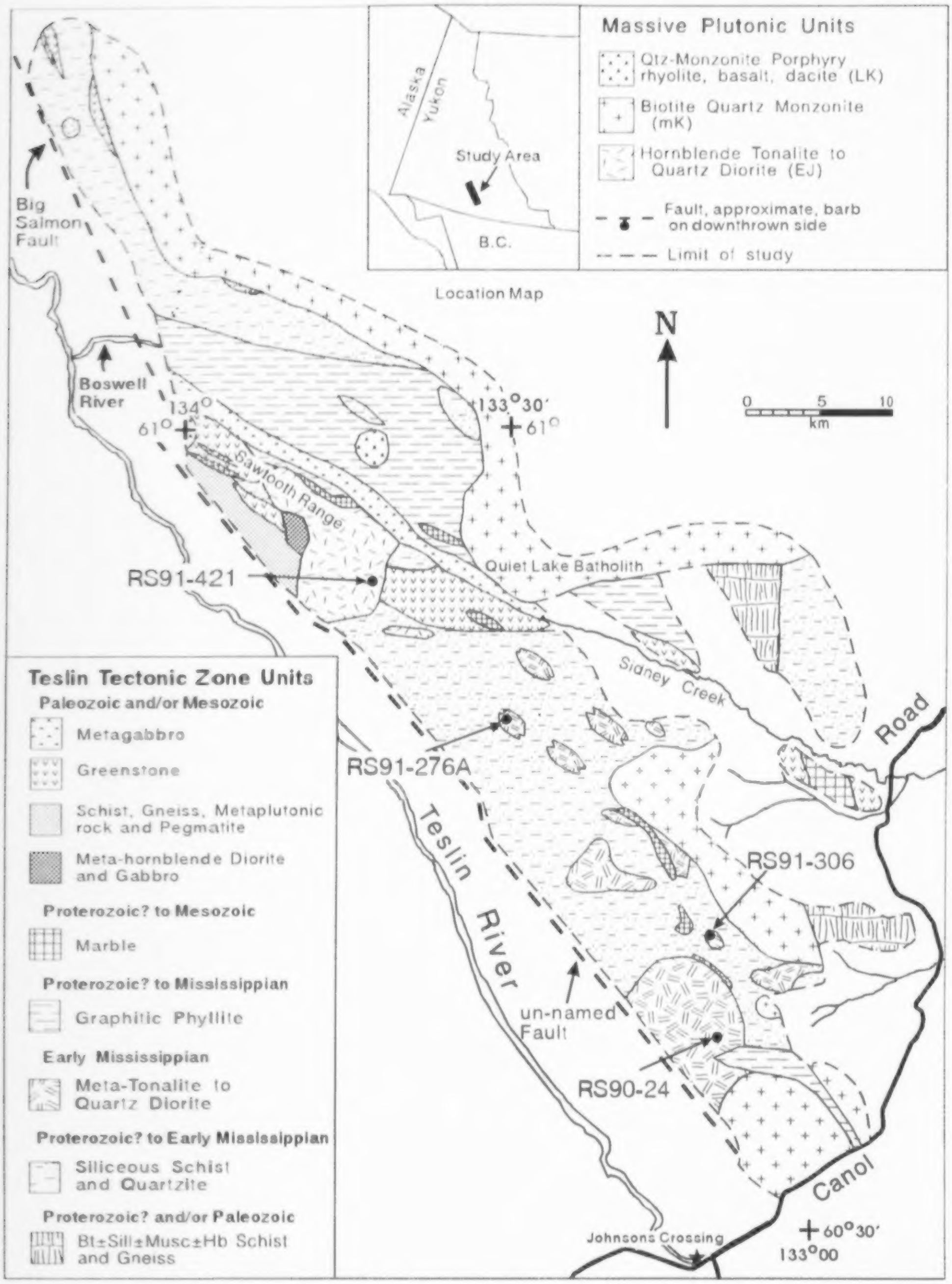
Massive Plutonic Units
Qtz-Monzonite Porphyry rhyolite, basalt, dacite (LK)
Biotite Quartz Monzonite (mK)
Hornblende Tonalite to Quartz Diorite (EJ)
Fault, approximate, barb on downthrown side
Limit of study
Alaska
Yukon
Study Area
B.C.
Location Map
N
0
5
10
km
Big Salmon Fault
Boswell River
134°
61°
133°30′
61°
Sawtooth Range
Quiet Lake Batholith
RS91-421
Sidney Creek
Road
RS91-276A
Teslin River
RS91-306
un-named Fault
RS90-24
Canol
Johnsons Crossing
60°30′
133°00
Teslin Tectonic Zone Units
Paleozoic and/or Mesozoic
Metagabbro
Greenstone
Schist, Gneiss, Metaplutonic rock and Pegmatite
Meta-hornblende Diorite and Gabbro
Proterozoic? to Mesozoic
Marble
Proterozoic? to Mississippian
Graphitic Phyllite
Early Mississippian
Meta-Tonalite to Quartz Diorite
Proterozoic? to Early Mississippian
Siliceous Schist and Quartzite
Proterozoic? and/or Paleozoic
Bt±Sill±Musc±Hb Schist and Gneiss

Figure 3-1: Simplified geology map of the study area showing the location and sample numbers of rocks dated in this study (modified from Stevens 1994). RS90-24 and RS91-306, -276A are from deformed meta-tonalite to quartz-diorite bodies, and RS91-421 is from a massive hornblende-bearing tonalite to quartz-diorite pluton.

A simplified geology map of the study area is shown in Fig. 3-1. Recent 1:50 000 scale geology maps are available for the region (Stevens 1994) as are geological progress reports (Stevens 1991, 1992; Stevens and Erdmer, 1993a). Rock assemblages are grouped into Teslin tectonic zone units and massive plutonic units (Fig. 3-1). Rocks of the Teslin tectonic zone units display penetrative ductile deformation fabrics and most are considered to be part of the Yukon-Tanana terrane (or Nisutlin terrane). Massive plutonic units are undeformed plutonic rocks that post-date penetrative deformation in the zone and intrude Teslin tectonic zone units.

Most of the area is underlain by four Teslin tectonic zone units, which together characterize the Yukon-Tanana terrane in the study area. They are; 1) a siliceous schist and quartzite unit consisting predominantly of protomylonitic to mylonitic quartz-muscovite±chlorite±epidote±biotite±garnet schist, quartzite and minor calcareous schist, marble and graphitic phyllite, 2) a graphitic phyllite unit dominated by sheared, fissile, rusty-red to black graphite-muscovite phyllite with minor marble, siliceous schist and quartzite, 3) a massive to mylonitic, metamorphosed, hornblende- and biotite-bearing meta-tonalite to quartz-diorite unit, and 4) a metagabbro and greenstone unit dominated by white and green, massive to mylonitic metagabbro and medium to dark green, massive to mylonitic greenstone (Fig. 3-1) (Stevens 1992; Stevens and Erdmer 1993a).

The meta-tonalite to quartz-diorite unit is interpreted to be in an original intrusive relationship with both the siliceous schist and quartzite unit and the graphitic phyllite unit (Stevens 1991, 1992). Three bodies of the meta-tonalite to quartz-diorite unit were dated in this study.

Of the three unfoliated plutonic suites (massive plutonic units) exposed in the map area (Fig. 3-1), the age of the quartz-monzonite porphyry unit and the biotite quartz-monzonite unit are inferred to be middle Cretaceous by previous studies (Brown and Kahlert 1986; Wheeler and McFeely 1991). Prior to this study the age of the hornblende tonalite to quartz-diorite unit was thought to range from the Late Triassic to Early Jurassic on the basis of regional correlations (Mortensen 1992). A large body of this unit, exposed in the Sawtooth Range (Fig. 3-1) was dated in order better constrain the crystallization age of this unit, and thus obtain a local minimum age of deformation for the rocks that it intrudes.

Previous studies in the Teslin tectonic zone suggest that rocks were deformed within the deep-seated portion of a west-dipping Permo-Triassic subduction complex outboard of North America, and were subsequently thrust eastward as a coherent sheet onto North American strata in the Early to Middle Jurassic (Hansen 1992a; Hansen et al. 1991; Tempelman-Kluit 1979). This interpretation has been challenged by Stevens and Erdmer (1993b) who suggest that subduction zone deformation in Permian time was followed by development of a crustal-scale transpressive shear zone and formation of a two-sided orogen. In this model tectonic zone rocks were thrust eastward and westward out of the zone during the Early to Middle Jurassic (Stevens and Erdmer 1993b). Both of these models are based, in part, on the presence of eclogite and blueschist in the Teslin tectonic zone and Yukon-Tanana terrane of southern Yukon that give Middle Permian to Early Triassic K-Ar, and Rb-Sr muscovite ages (Wanless et al. 1978; Erdmer and Armstrong 1988), and by widespread Early to Middle Jurassic cooling ages on schist from the Teslin tectonic zone and Yukon-Tanana terrane (Stevens et al. 1982; Hansen et al. 1991; Hunt and Roddick 1992, 1993).

ANALYTICAL METHODS

Zircon, biotite and hornblende were separated from 8-12 kg samples using conventional Wilfley table, heavy liquids, and magnetic separation techniques. All zircon fractions were abraded prior to analysis. Techniques for U-Pb dating of zircon are summarized by Parrish et al. (1987) and for titanite by Parrish et al. (1992). Techniques for ^{40}Ar-^{39}Ar dating are described by Hunt and Roddick (1993).

U-Pb RESULTS

Deformed Meta-Tonalite to Quartz-Diorite

Samples from three bodies of deformed meta-tonalite to quartz-diorite were chosen for U-Pb zircon dating (RS90-24; RS91-306, -276A; Fig. 3-1). All samples are medium grained, mesocratic, weakly to strongly foliated, metamorphosed, hornblende±biotite±chlorite-bearing tonalite to quartz-diorite. Sample RS90-24 was collected from a large pluton in the southern part of the map area. Samples RS91-306, -276A are from smaller bodies that are structurally interleaved with metasedimentary rocks of the siliceous schist and quartzite unit (Fig. 3-1).

U-Pb analytical data are given in Table 3-1 and are shown on conventional U-Pb concordia plots (Figs. 3-2a, 3-2b, 3-2c). Zircons recovered from these samples are mostly euhedral, equant to slightly elongate, colourless to rarely light orange and clear to partially cloudy. Clear, colourless, rod- and bubble-shaped inclusions are present in some grains.

Three fractions of zircon from sample RS90-24 were analyzed (Table 3-1). The analyses overlap at the 2σ level, and give a weighted ^{207}Pb/^{206}Pb age of 351.2 ± 1.4 Ma (Fig. 3-2a), which is considered to be the best estimate for the crystallization age of the rock. In view of the very small amount of total common Pb in the analyses, the discordance cannot reflect an incorrect assumed composition for the initial common Pb in the fractions. The possibility that a minor inherited zircon component was present in some or all of the three fractions cannot be precluded; however it is considered highly unlikely that a fortuitous combination of inheritance and postcrystallization Pb-loss would give such similar isotopic compositions in the three fractions. If an inherited component was present in the zircons, the actual crystallization age would probably not be significantly younger that the youngest ^{206}Pb/^{238}U age of the three fractions (347.9 ± 0.6 Ma). An age of 351.2 ±1.4 Ma is therefore assigned to the unit.

Fraction^1	Wt μg^a	U ppm	Pb* ppm	$^{206}Pb^b$ / ^{204}Pb	Pb^c pg	$^{208}Pb^d$ (%)	$^{206}Pb^d$ / ^{238}U	$^{207}Pb^d$ / ^{235}U	Corr.^{e} Coeff.	$^{207}Pb^d$ / ^{206}Pb	$^{207}Pb/^{206}Pb$ Age(Ma)
Sample RS90-24, deformed tonalite to quartz diorite, (60°38.00'N; 133°17.18'W)											
A: N2,+105,s	174	200	11	13079	9	9.6	0.05549±.09%	0.4098±.10%	0.9484	0.05356±.03%	352.5±1.5
B: N3,+105,e	124	180	10	12606	6	10.4	0.05545±.08%	0.4090±.10%	0.9405	0.05350±.03%	350.0±1.6
C: N3,+105,s	139	206	11	9899	10	9.4	0.05547±.08%	0.4094±.10%	0.9469	0.05352±.03%	351.1±1.5
F: Titanite	1185	454	26	531	3579	9.4	0.05689±.21%	0.42011±.39%	0.7212	0.05356±.28%	352.6±12.6
G: Titanite	645	413	23	995	947	9.5	0.05519±.13%	0.40785±.23%	0.759	0.05360±.15%	354.1±6.8
Sample RS91-306, deformed tonalite to quartz diorite, (60°41.23'N; 133°17.15'W)											
A: N2,+74,s	208	355	20	3436	76	11.3	0.05592±.09%	0.4170±.12%	0.8619	0.05409±.06%	374.7±2.7
C: N2,+105,s	324	322	18	838	444	11.0	0.05549±.13%	0.4088±.24%	0.6979	0.05342±.18%	346.8±8.0
D: N1,+74,s	79	417	24	12282	9	11.1	0.05566±.09%	0.4116±.10%	0.9285	0.05364±.04%	356.1±1.7
Sample RS91-276A, deformed tonalite to quartz diorite, (60°48.01'N; 133°28.00'W)											
A: N5,+74,s	100	523	30	2101	88	11.1	0.056098±.10%	0.41952±.14%	0.8432	0.05424±.08%	381.0±3.4
B: N5,+74,s	55	487	28	4643	20	11.4	0.055816±.09%	0.41470±.11%	0.853	0.05389±.06%	366.3±2.7
C: N2,+74,s	110	590	34	10395	22	11.4	0.056194±.09%	0.42035±.10%	0.9224	0.05425±.04%	381.6±1.8
D: N2,-74,s	69	721	41	2575	67	11.7	0.054997±.10%	0.40730±.12%	0.809	0.05371±.07%	359.0±3.3
Sample RS91-421, massive tonalite to quartz diorite, (60°55.08'N; 133°45.31'W)											
A: N3,+105,e	194	221	7	163	595	10.6	0.03170±.35%	0.2260±1.1%	0.6976	0.05171±.91%	272.4±41.7
C: N3,+74,e	177	264	8	619	150	9.9	0.03005±.13%	0.2090±.30%	0.6339	0.05044±.24%	215.2±11.0
D: N3,+74,s	127	147	5	76	658	11.9	0.03183±.88%	0.2389±2.6%	0.6958	0.05443±2.1%	388.8±94.2
E: N2,+74,s	181	171	6	77	1102	11.7	0.03316±.88%	0.2512±2.6%	0.6964	0.05494±2.1%	409.7±92.2
F: Titanite	685	52	3	64	1503	51.0	0.03042±1.1%	0.2071±4.0%	0.6945	0.04938±3.4%	165.9±150
G: Titanite	1236	59	3	43	5661	51.1	0.03009±2.2%	0.1938±7.4%	0.6946	0.04670±6.1%	33.7±271

Errors are 1 std. error of mean in % except $^{207}Pb/^{206}Pb$ age errors which are $\pm 2\sigma$ in million years.

Pb* = radiogenic Pb

[1] N1,2,3,5 non-magnetic at 1,2,3 or 5 degree side tilt on Frantz isodynamic separator;
sizes (+74, +105) are the size of zircons in microns; e, elongate grains; s, stubby to equant grains.

[a] Sample weight error of ± 0.001 mg in concentration uncertainty

[b] Corrected for fractionation and spike Pb

[c] Total common Pb in analysis in picograms

[d] Corrected for blank Pb and U, and common Pb

[e] Correlation Coefficient of errors in $^{206}Pb/^{238}U$ and $^{207}Pb/^{235}U$.

Table 3-1: U-Pb zircon and titanite analytical data

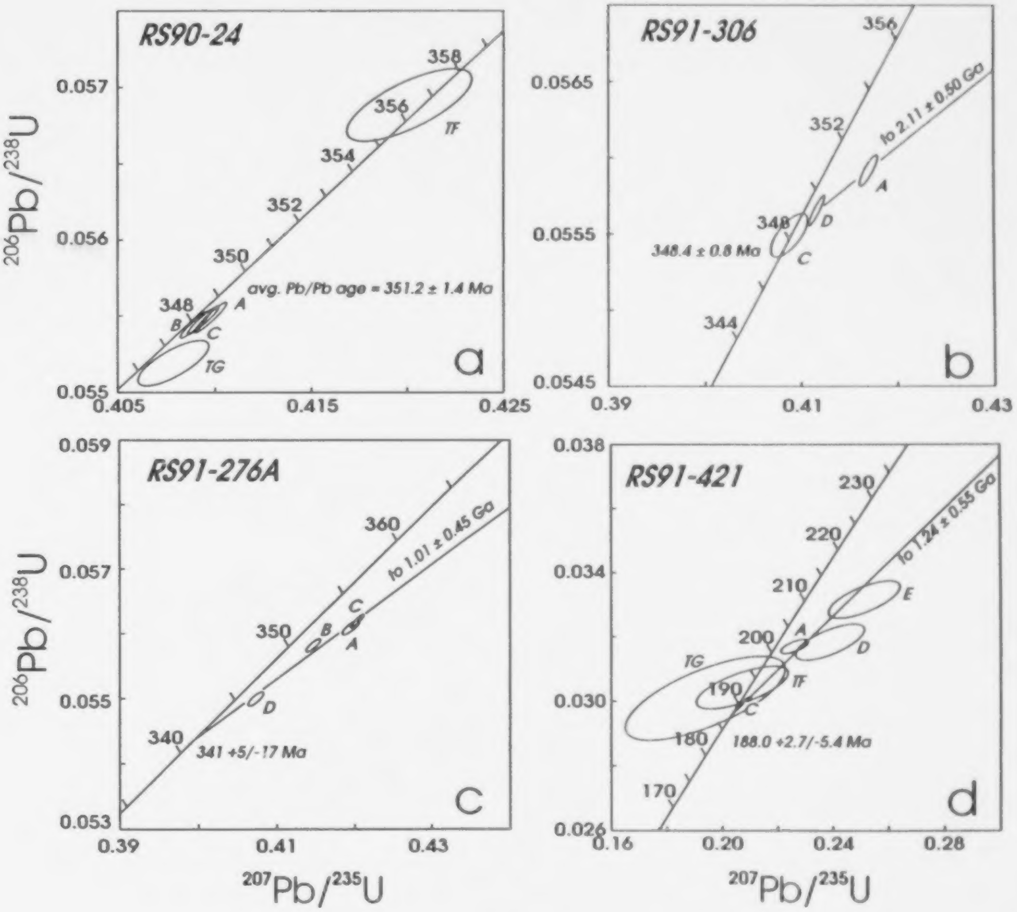

Figure 3-2: U-Pb concordia plots for samples RS90-24, RS91-276a, -306, and -421. Errors are at the 2σ level.

Two fractions of titanite were also analyzed from this sample. Both give relatively imprecise analyses, with an average $^{207}Pb/^{206}Pb$ age of 353.4 ± 9.7 Ma. One of these fractions (TG) appears to have lost Pb, whereas the other fraction (TF) falls slightly above concordia, possible reflecting incomplete dissolution of the sample. The good agreement between the average $^{207}Pb/^{206}Pb$ age of the titanites and that of the three zircon fractions, however, support the assigned age of 351.2 Ma for the unit.

Three fractions of zircon were analyzed from sample RS91-306. One fraction is concordant with a $^{206}Pb/^{238}U$ age of 348.1 ± 0.6 Ma. Two other fractions plot to the right of concordia (Fig. 3-2b), and give $^{207}Pb/^{206}Pb$ ages up to 375 Ma. The data array indicates the presence of an older inherited zircon component in fractions A and D, presumably as "cryptic" cores that could not be distinguished visually. A regression line through the three analyses (MSWD = 0.1) gives lower and upper intercept ages of 348.4 ± 0.8 Ma and 2.11 ± 0.50 Ga, respectively. The lower intercept age is identical to the $^{206}Pb/^{238}U$ age of fraction C, and is taken as the best estimate of the crystallization age of the unit. The upper intercept age indicates an Early Proterozoic average age for the inherited zircon component.

Analyses of four fractions of zircon from the third sample of the meta-tonalite to quartz-diorite plutonic suite (sample RS91-276A) are all discordant (Fig. 3-2c) and define a roughly linear array (MSWD = 10.8) with relatively poorly constrained lower and upper intercept ages of 341+5/-17 Ma and 1.01 ± 0.45 Ga, respectively. The data array indicates the presence of an inherited zircon component in all of the fractions, with an average age of about 1 Ga. The calculated lower intercept age is interpreted as a minimum crystallization age of the unit. The crystallization age is unlikely to be significantly older that the $^{207}Pb/^{206}Pb$ age of the most concordant analysis (D) at 359 Ma.

Massive Tonalite to Quartz-Diorite

A sample from one body of massive, unsheared tonalite to quartz-diorite was chosen for U-Pb zircon dating (RS91-421; Fig. 3-1). The pluton consists mainly of fresh, white and green, fine to medium equant grained, hornblende-bearing tonalite to quartz-diorite. Locally, especially along its northeastern margin, the rock varies to coarse grained hornblendite and pyroxene hornblendite. Local indications of flow banding are also present.

Zircons recovered from this sample range from euhedral, equant, colourless to slightly orange grains to elongate (length:width, ≈4:1), euhedral, clear and colourless grains. Rod- and bubble-shaped clear to rarely opaque inclusions are common in the zircons.

Four fractions of zircon from the sample are discordant (Fig. 3-2d) and define a roughly linear array (MSWD = 3.4) with lower and upper intercept ages of 188.0 +2.7/-5.4 Ma and 1.24 ± 0.45 Ga. The lower intercept age is a minimum crystallization age for the rock, and the age is unlikely to be significantly older than the $^{207}Pb/^{206}Pb$ age of the most concordant fraction (215 Ma). Two fractions of igneous titanite were also analyzed from the sample, and both gave concordant results (Fig. 3-2d). The most precise of these has a $^{206}Pb/^{238}U$ age of 193.2 ± 4 Ma. Since this unit has not been metamorphosed, the titanite ages reflect cooling of the pluton through the closure temperature of the U-Pb system in titanite (~600°C; Heaman and Parrish 1991), and thus should be very close to the actual emplacement age of the body.

^{40}Ar-^{39}Ar RESULTS

Biotite and hornblende from sample RS91-421 were separated for ^{40}Ar-^{39}Ar dating. The analytical data are reported in Hunt and Roddick (1993), and are summarized in Table 3-2. The two ages (179 ± 2 Ma for biotite; 182 ± 2 Ma for hornblende) are the same within analytical uncertainty. The data, together with the U-Pb data described above, indicate a moderate cooling from emplacement temperatures at 193.2 Ma to the closure temperature of hornblende (~500°C), followed by rapid cooling through the closure temperature of biotite (~300°C; Harrison et al. 1985).

DISCUSSION

Late Devonian to early Mississippian, foliated, hornblende-bearing, intermediate meta-plutonic rocks are common in the Yukon-Tanana terrane (Mortensen 1992; Gareau and Mortensen 1993). The three bodies of deformed meta-tonalite to quartz-diorite from this study that give Early Mississippian U-Pb zircon ages are interpreted to be part of this plutonic suite. A primary intrusive relationship interpreted to exist between these Early Mississippian plutonic rocks and rocks of the siliceous schist and quartzite unit and the graphitic phyllite unit provides a minimum depositional age for the two metasedimentary units. This indicates that by the end of the Mississippian most of the rocks exposed in the study area were stitched together.

An Early Jurassic crystallization age for the massive tonalite to quartz-diorite pluton places a local minimum age of deformation on rocks of the Teslin tectonic zone. ^{40}Ar-^{39}Ar cooling ages for this pluton (179-182 Ma), which are up to 9 Ma younger than its minimum crystallization age and up to 14 Ma younger than the most precise ^{206}Pb/^{238}U titanite age, suggest that the pluton was not uplifted until several million years after it crystallized. In addition, coincident ^{40}Ar-^{39}Ar biotite and hornblende ages indicate that the plutonic body was cooled very quickly at ca. 180 Ma, likely reflecting rapid uplift and erosion. The U-Pb system in titanites in the metaplutonic units (sample RS90-24) have apparently not been disturbed significantly by the regional metamorphism that affected the study area, indicating that metamorphic temperatures did not exceed the closure temperature of the U-Pb system in titanite (~600°C; Heaman and Parrish 1991).

Metamorphic cooling ages from Teslin tectonic zone tectonites reported in previous studies (Hansen et al. 1991; Hunt and Roddick 1992) range from 184-

Sample #	RS91-421	RS91-421
Mineral	Biotite	Hornblende
Location	60°55.08'N; 133°45.31'W	60°55.08'N; 133°45.31'W
Integrated ^{40}Ar-^{39}Ar (age, % gas)	182 ± 2 Ma (96%)	179 ± 2 Ma (99%)

Table 3-2: ^{40}Ar-^{39}Ar age data

195 Ma. These cooling ages overlap with the minimum crystallization age of the massive tonalite to quartz-diorite pluton and are up to 16 Ma older than the cooling/uplift age of the pluton. If the ^{40}Ar-^{39}Ar ages on the massive pluton are taken as uplift ages then parts of the Teslin tectonic zone were uplifted and cooled below 300°C (the argon closure temperature in biotite; Harrison et al. 1985) at different times during the period extending from 179-195 Ma. This is contrary to the interpretation of Hansen (1992a, 1992b) who suggested that rocks of the Teslin tectonic zone were uplifted rapidly as a "coherent block" in the early Jurassic.

REFERENCES

Brown, P., and Kahlert, B. 1986. Geology and mineralization of the Red Mountain porphyry molybdenum deposit south-central Yukon. *In* Mineral Deposits of the Northern Canadian Cordillera. *Edited by* J.A. Morin; Canadian Institute of Mining and Metallurgy, Special Volume 37, pp. 288-297.

Erdmer, P., and Armstrong. R.L. 1988. Permo-Triassic isotopic dates for blueschist, Ross River area, Yukon. *In* Yukon Geology vol. 2. Exploration and Geological Services Division, Yukon, Indian and Northern Affairs Canada, pp. 33-36.

Gareau, S.A., and Mortensen, J.K. 1993. Deformation and metamorphism in the southern Big Salmon Complex, Teslin area, Yukon Territory; field, petrographic and age constraints. *In* Geological Association of Canada/Mineralogical Association of Canada Program and Abstracts, v. 18, p. A33.

Hansen, V.L. 1992a. Backflow and margin-parallel shear within an ancient subduction complex. Geology, **20**: 71-74.

Hansen, V.L. 1992b. P-T evolution of the Teslin suture zone and Cassiar tectonites, Yukon, Canada: evidence for A- and B-type subduction. Journal of Metamorphic Geology, **10**: 239-263.

Hansen, V.L., Heizler, M.T., and Harrison, T.M. 1991. Mesozoic thermal evolution of the Yukon-Tanana composite terrane: new evidence from $^{40}Ar/^{39}Ar$ data. Tectonics, **10**: 51-76.

Hansen, V.L., Mortensen, J.K., and Armstrong, R.L. 1989. U-Pb, Rb-Sr, and K-Ar isotopic constraints for ductile deformation and related metamorphism in the Teslin suture zone, Yukon-Tanana terrane, south-central Yukon. Canadian Journal of Earth Sciences, **26**: 2224-2235.

Harrison, T.M., Duncan, I., and McDougal, I. 1985. Diffusion of ^{40}Ar in biotite: temperature, pressure and compositional effects. Geochimica et Cosmochimica Acta, **49**: 2461-2468.

Heaman, L., and Parrish, R.R. 1991. U-Pb geochronology of accessory minerals. *In* Applications of Radiogenic isotope systems to Problems in Geology. *Edited by* L. Heaman and J.N. Ludden, Mineralogical Association of Canada, Short Course Handbook, vol. 19, pp. 59-102.

Hunt, P.A., and Roddick, J.C. 1992. A compilation of K-Ar and ^{40}Ar/^{39}Ar ages: Report 22. *In* Radiogenic Age and Isotopic Studies: Report 6. Geological Survey of Canada, Paper 92-2, pp. 179-226.

Hunt, P.A., and Roddick, J.C. 1993. A compilation of K-Ar and ^{40}Ar/^{39}Ar ages: Report 23; *In* Radiogenic Age and Isotopic Studies: Report 7. Geological Survey of Canada, Paper 93-2, pp. 127-148.

Monger, J.W.H., and Berg, H.C. 1987. Lithotectonic terrane map of western Canada and southeastern Alaska. United States Geological Survey Miscellaneous Field Studies Map MF-1874-B, scale 1:2 500 000.

Mortensen, J.K. 1992. Pre-mid-Mesozoic tectonic evolution of the Yukon-Tanana terrane, Yukon and Alaska. Tectonics, **11**: 836-853.

Parrish, R.R., Roddick, J.C., Loveridge, W.D., and Sullivan, R.W. 1987.

Uranium-lead analytical techniques at the Geochronology Laboratory, Geological Survey of Canada. *In* Radiogenic Age and Isotopic Studies, Report 1. Geological Survey of Canada, Paper 87-2, pp. 3-7.

Parrish, R.R., Bellerive, D., and Sullivan, R.W. 1992. U-Pb chemical procedures for titanite and allanite in the Geochronology Lab, Geological Survey of Canada. *In* Radiogenic Age and Isotopic Studies, Part 5, Geological Survey of Canada, Paper 91-2, pp. 187-190.

Stevens, R.A. 1991. The Teslin suture zone in northwest Teslin map area, Yukon. *In* Current Research, Part A. Geological Survey of Canada, Paper 91-1A, pp. 271-277. *See appendix 1*

Stevens, R.A. 1992. Regional geology, fabric, and structure of the Teslin suture zone in northwest Teslin map area, Yukon Territory. *In* Current Research, Part A. Geological Survey of Canada, Paper 92-1A, pp. 287-295. *See appendix 2*

Stevens, R.A. 1994. Geology of the Teslin suture zone in parts of Laberge (105E/1), Quiet Lake (105F/4) and Teslin (105C/11, 13, 14) map areas, Yukon Territory. Geological Survey of Canada, Open File 2768. *See appendix 6*

Stevens, R.A., and Erdmer, P. 1993a. Geology and structure of the Teslin suture zone and related rocks in parts of Laberge, Quiet Lake, and Teslin map areas, Yukon Territory. *In* Current research, part A. Geological Survey of Canada, Paper 93-1A, pp. 11-20. *See appendix 3*

Stevens, R.A., and Erdmer, P. 1993b. Tectonic evolution of the Teslin suture zone, south-central Yukon Territory: subduction, transpression and extrusion. *In* Geological Association of Canada/Mineralogical Association of Canada Program and Abstracts, v. 18, p. A100.

Stevens, R.D., Delabio, R.N., and Lachance, G.R. 1982. Age determinations and geological studies, K-Ar isotopic ages, report 15. Geological Survey of Canada, Paper 81-2, pp. 19-21.

Tempelman-Kluit, D.J. 1979. Transported cataclasite, ophiolite and granodiorite in Yukon: evidence of arc-continent collision. Geological Survey of Canada, Paper 79-14.

Wanless, R.K., Stevens, R.D., Lachance, G.R., and Delabio, R.N. 1978. Age determinations and geological studies, K-Ar isotopic ages, report 13. Geological Survey of Canada, Paper 77-2.

Wheeler, J.O., Brookfield, A.J., Gabrielse, H., Monger, J.W.H., Tipper, H.W., and Woodsworth, G.J. 1991. Terrane map of the Canadian Cordillera; Geological Survey of Canada Map 1713A, scale 1:2 000 000.

Wheeler, J.O., and McFeely, P., (comp.). 1991. Tectonic assemblage map of the Canadian Cordilleran and adjacent parts of the United States of America. Geological Survey of Canada Map 1712A, scale 1:2 000 000.

CHAPTER 4 - CHARACTERISTICS OF DUCTILE TRANSPRESSION AND AN EXAMPLE FROM THE TESLIN TECTONIC ZONE, NORTHERN CANADIAN CORDILLERA*

---

*A version of this chapter has been submitted for publication. Stevens and Erdmer, Journal of Structural Geology.

INTRODUCTION

Crustal-scale transpressive deformation zones, such as the San Andreas fault zone (Sylvester and Smith 1976), or the Spitsbergen Tertiary Orogenic Belt (Lowell 1972), are generally high level, brittle-deformed zones. The lower, ductile part of such deformation zones is rarely considered. For example, it is unclear whether the structural characteristics of flower structures, which are common in brittle crustal-scale transpressive zones, continue below the ductile transition. In the literature, a variety of structural features are used to support a transpression interpretation, but correlations are rarely made between the observed ductile deformation features and the structures common to brittle transpression.

This is addressed in two principal ways. Firstly, the structural characteristics of ductile transpression are summarized into a general model for crustal-scale transpression (Fig. 4-1) that correlates the fabric orientations and kinematics of ductile transpression with analogous features in brittle flower structures. As part of this summary, four new terms are introduced: homogeneous, heterogeneous, thrust, and strike-slip transpression. These terms identify the regime under which a zone was deformed and provide criteria for identifying transpressive shear zones in the field. Secondly, the structural characteristics of the Teslin tectonic zone, a crustal-scale, ductile shear zone in the northern Canadian Cordillera are presented. Detailed structural analysis combined with regional geological data lead to the conclusion that the Teslin tectonic zone formed under heterogeneous, thrust-transpression and that it preserves the ductile root of a crustal-scale "flower structure".

THE CHARACTERISTICS OF DUCTILE TRANSPRESSION

General

Structural transpression is defined as oblique convergence in which a

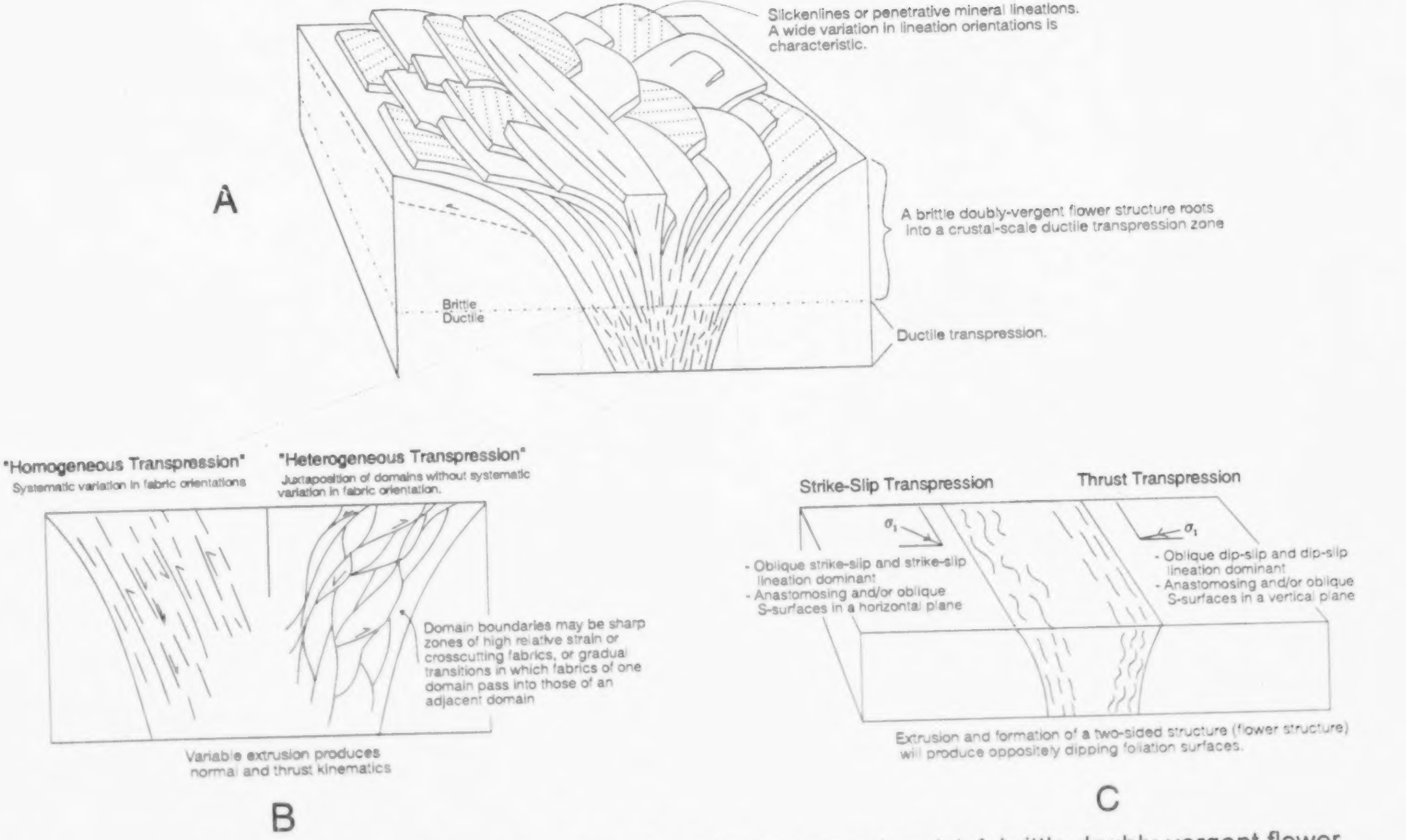
A
Slickenlines or penetrative mineral lineations. A wide variation in lineation orientations is characteristic.
A brittle doubly-vergent flower structure roots into a crustal-scale ductile transpression zone
Brittle
Ductile
Ductile transpression.
"Homogeneous Transpression"
Systematic variation in fabric orientations
"Heterogeneous Transpression"
Juxtaposition of domains without systematic variation in fabric orientation.
Domain boundaries may be sharp zones of high relative strain or crosscutting fabrics, or gradual transitions in which fabrics of one domain pass into those of an adjacent domain
Variable extrusion produces normal and thrust kinematics
B
Strike-Slip Transpression
Thrust Transpression
σ_1
σ_1
- Oblique strike-slip and strike-slip lineation dominant
- Anastomosing and/or oblique S-surfaces in a horizontal plane
- Oblique dip-slip and dip-slip lineation dominant
- Anastomosing and/or oblique S-surfaces in a vertical plane
Extrusion and formation of a two-sided structure (flower structure) will produce oppositely dipping foliation surfaces.
C

Figure 4-1: Characteristics and regimes of crustal-scale and ductile transpression. (a) A brittle doubly-vergent flower structure roots into a crustal-scale ductile transpressive shear zone. (b) Homogeneous and heterogeneous transpression describe the strain variations between domains in ductile transpression. (c) Strike-slip and thrust transpression describe characteristic fabric orientations of ductile transpression.

zone of rock is subjected to simultaneous compression and wrenching (Harland 1971; Robin and Cruden in press). A consequence of the compressive component is that a space problem arises. If the zone of deformation is confined at depth and laterally, then the space problem can be overcome by volume loss or upward extrusion of material. In a brittle environment, extrusion is commonly accompanied by the development of a flower structure with oppositely-dipping, convex upward, fault geometry (Fig. 4-1a) (Harding and Lowell 1979; Harding 1985; Sylvester and Smith 1976). Dip-slip faults with either normal or reverse separation and strike-slip faults are characteristic. In a ductile environment, the influence of transpression and extrusion on fabric orientation and kinematics is not as well documented. Several recent studies invoke a transpression model for ductile deformation (e.g. Lagarde and Michard 1986; Robert 1989; Jolivet and Huchon 1989; Borradaile and Spark 1991; Culshaw 1991; Holdsworth and Strachan 1991; Goodwin and Williams 1993; Kirkwood and Malo 1993; Lin and Williams 1993; Stauffer and Lewry 1993; Robin and Cruden in press). However, only a few of these studies propose correlations between the ductile fabrics and the features common to flower structures.

It is proposed that ties between the two transpressive regimes exist in many cases. In Fig. 4-1(a), a crustal-scale ductile transpressive zone is shown to be the root of a flower structure, and its penetrative fabrics are interpreted to be similar to the brittle structures common to flower structures. In this paper, crustal-scale refers to a transpressive zone with a strike length of many tens or even hundreds of kilometres. The general configuration of this crustal deformation zone and the internal fabrics and shear sense of its ductile portion are considered below. Although the emphasis is placed on "crustal-scale", many features are common to ductile transpressive zones at all scales.

Extrusion and Boundary Conditions

Above the brittle-ductile transition, the extrusion process may transport coherent thrust sheets of ductilely deformed rock upward, preserving ductile fabrics at shallow levels in the crust. However, the amount of lateral and vertical displacement that can be attributed to the extrusion process is not well documented. Lateral displacement, which will occur well above the level of ductile deformation, is estimated to be 5 km or more for a zone in Western Spitsbergen (Lowell 1972), and at least 25-30 km for the Iwanai nappe of the Hokkaido Central Belt, Japan (Jolivet and Huchon 1989). Modelling (P.-Y. Robin, pers. comm. 1992) suggests that rock can be uplifted vertically, from a depth six times the width of the deformation zone. In addition, transpression can occur under a number of strain configurations. In situations such as transpression above a low-angle detachment (e.g. Holdsworth and Strachan 1991), or in conjunction with wedging and back-thrusting, lateral displacement of thrust sheets may not result from extrusion only and may, therefore, be much greater.

Extrusion also implies that brittle deformation will follow ductile deformation and that brittle fabrics will commonly overprint or cut earlier ductile fabrics (e.g. Stauffer and Lewry 1993; Kirkwood and Malo 1993). These crosscutting and overprinting fabrics develop during the same deformation and are distinct from those representing separate events.

A zone of transpression (Fig. 4-1a) may be bound by rocks of different assemblages or terranes (e.g. Robert 1989) or by less deformed or undeformed rock of the same assemblage or terrane (e.g. Lin and Williams 1993). The boundaries of the zone may be a strain gradient or they may be sharp and marked by a discrete thrust fault. Along the boundaries, rock is free to move in any direction.

Foliation and Lineation

Ductile transpression produces a number of characteristic fabric orientations. Foliation (XY plane of the finite strain ellipsoid) is commonly homoclinally steeply dipping, but oppositely-dipping foliation orientations may be present when the zone is the root of a flower structure (Fig. 4-1a). Variably plunging lineation (X-direction of the finite strain ellipsoid) is characteristic (Fig.

4-1a). This is one of the principal differences between deformation under transpression and that under "normal" progressive simple shear.

Shear Sense

The combination of compression and wrenching and the extrusion process are responsible for a range of shear directions and sense in transpression. Strike-slip fabrics commonly show a single shear sense, consistent with the displacement of the zone. Dip-slip fabrics, resulting from the compressive component and the extrusion process, commonly show two opposite shear senses. Reverse sense is the most common, and occurs as a consequence of upward extrusion. However, variable extrusion also produces local zones of normal dip-slip shear (Fig. 4-1b). Oblique-slip movement, resulting from a combination of compression, wrenching, and extrusion, shows a component of normal and/or reverse dip-slip shear and a component of dextral and/or sinistral strike-slip shear. Variable rates of extrusion and the development of normal oblique-slip zones suggest that, locally, the strike-slip component of oblique-slip zones may have a different shear sense than the overall displacement of the zone.

Transpression is considered in some instances to result from a combination of pure shear (compression) and simple shear (wrenching) and is referred to as general non-coaxial shear (Hanmer and Passchier 1991). In this interpretation, pure shear compression produces both normal and reverse dip-slip movement, independent of the extrusion process. Scale may be an important factor, as a zone undergoing overall pure shear compression may develop internal dip-slip zones that display fabrics apparently consistent with simple shear (e.g. Lin and Williams 1993).

REGIMES OF DUCTILE TRANSPRESSION

In ductile transpressive zones, a wide range of structural features have been used to support the interpretation of transpression. Subdivision on the basis of fabric characteristics identified in the field can help to classify these zones and identify the transpressive regime under which it was formed. In particular, fabric variations (i.e. systematic vs. non-systematic) and the orientations of lineation (i.e. sub-horizontal vs. down-dip) can be recognized in the field and used to subdivide ductile transpressive zones.

Homogeneous and Heterogeneous Transpression

Homogeneous and heterogeneous transpression describe the strain variations of structural domains in a transpressive shear zone (Fig. 4-1b). A domain is defined as a volume of rock within the shear zone that contains uniform foliation and lineation orientations and/or shear sense. Transpression, by nature, results in heterogeneous deformation, and these terms are used to qualify the overall character of this heterogeneity.

A zone deformed by homogeneous transpression will show systematic change from steep- to shallow-plunging lineation (e.g. The Mylonite Zone, Robin and Cruden in press) or will simply be partitioned into steep- or shallow-plunging lineation domains (e.g. Goodwin and Williams 1993). Shallow-plunging lineation is commonly found in the centre of a zone, and steep-plunging near the margins (e.g. Lin and Williams 1993). Foliation is commonly homoclinally dipping but may change dip direction across the axis of the zone in a "flower structure".

Heterogeneous transpression results in the juxtaposition of domains without systematic variation of fabric orientations. Domains with oblique-slip, as well as horizontal and down-dip lineation occur (this study). Domain boundaries may be sharp zones of high relative strain, or crosscutting fabrics, or gradual transitions in which fabrics of one domain pass into those of an adjacent domain. In crustal-scale zones, the variety of rock types will control fabric orientations and kinematics, and influence the development of heterogeneous transpression.

Strike-slip and Thrust Transpression

Strike-slip transpression characterizes a zone of wrenching with a small component of compression. Sub-horizontal lineation is dominant, although steeply-plunging lineation may be common. The strike of the plane of instantaneous flattening (S-surfaces) will be at a moderate angle to the strike of the zone (i.e. shear zone wall). Thus, oblique and/or anastomosing foliation is more likely in a horizontal plane (e.g. Robert 1989). Transpression is commonly considered to be a type of strike-slip deformation (Sylvester 1988), but, under the general definition of oblique convergence, transpression is not restricted to strike-slip deformation and can occur in zones dominated by thrust faulting. In thrust-transpression, principle stresses are sub-perpendicular to the strike of the zone, producing dominantly steeply-plunging lineation and oblique and/or anastomosing foliation in a vertical plane (e.g. this study; Lin and Williams 1993). Knowledge of horizontal displacement, or other features external to a zone may be necessary to determine whether strike-slip or thrust transpression dominated.

Examples

Most transpressive shear zones can be described using one of the four terms above. For example, Lin and Williams (1993) described a transpressive shear zone from the Cape Breton Highlands which shows a gradual change from down-dip lineation near the boundaries to shallow plunging lineation in the centre. Transcurrent movement was interpreted to be concentrated in a narrow zone at the centre of a wider zone under compression. This shear zone is a homogeneous-thrust transpressive shear zone.

The Teslin tectonic zone is a crustal-scale ductile deformation zone containing many domains with distinct lineation orientations. Between domains, lineation orientations vary nonsystematically from sub-horizontal to sub-vertical and are dominantly moderately- to steeply-plunging. The Teslin tectonic zone is a heterogeneous thrust-transpressive shear zone.

Classification helps to differentiate between ductile transpressive zones and provides a set of field characteristics to identify transpressive shear zones.

THE TESLIN TECTONIC ZONE, YUKON; A CRUSTAL-SCALE HETEROGENEOUS THRUST-TRANSPRESSIVE SHEAR ZONE

Geological Setting and Previous Work

The Teslin tectonic zone of south-central Yukon, (Fig. 4-2) is part of the Yukon-Tanana terrane (Monger and Berg 1987; Jones et al. 1987) or Nisutlin terrane (Wheeler et al. 1991) and marks the fundamental boundary between deformed autochthonous North American miogeoclinal strata to the east and accreted terranes to the west. It includes S-, L-S and L-tectonites derived from sedimentary, volcanic and plutonic rocks metamorphosed under greenschist to amphibolite facies conditions (Hansen et al. 1989; Read et al. 1991; Stevens 1991, 1992, in review; Stevens and Erdmer 1993). Eclogite is preserved in one locality (Erdmer and Helmstaedt 1983)

The Teslin tectonic zone was defined on a structural basis by Tempelman-Kluit (1979) as "a northwest trending zone of steeply dipping cataclastic rocks 15 km wide [that] separates the Omineca and Intermontane belts". The Teslin tectonic zone averages 15-20 km wide and extends for more than 200 km (Fig. 4-2). Its northern and southern limits are undefined. Its western margin is marked by post-accretionary strike-slip faults, and the eastern margin by the D'Abbadie strike-slip fault to the north and an un-named thrust fault to the south (Hansen 1989; Gordey & Stevens 1994).

In the Laberge map area (Fig. 4-2) the Teslin tectonic zone has been divided into three elongate structural domains on the basis of fabric orientation and shear sense (Hansen 1989, 1992a): a domain of apparent normal shear, a

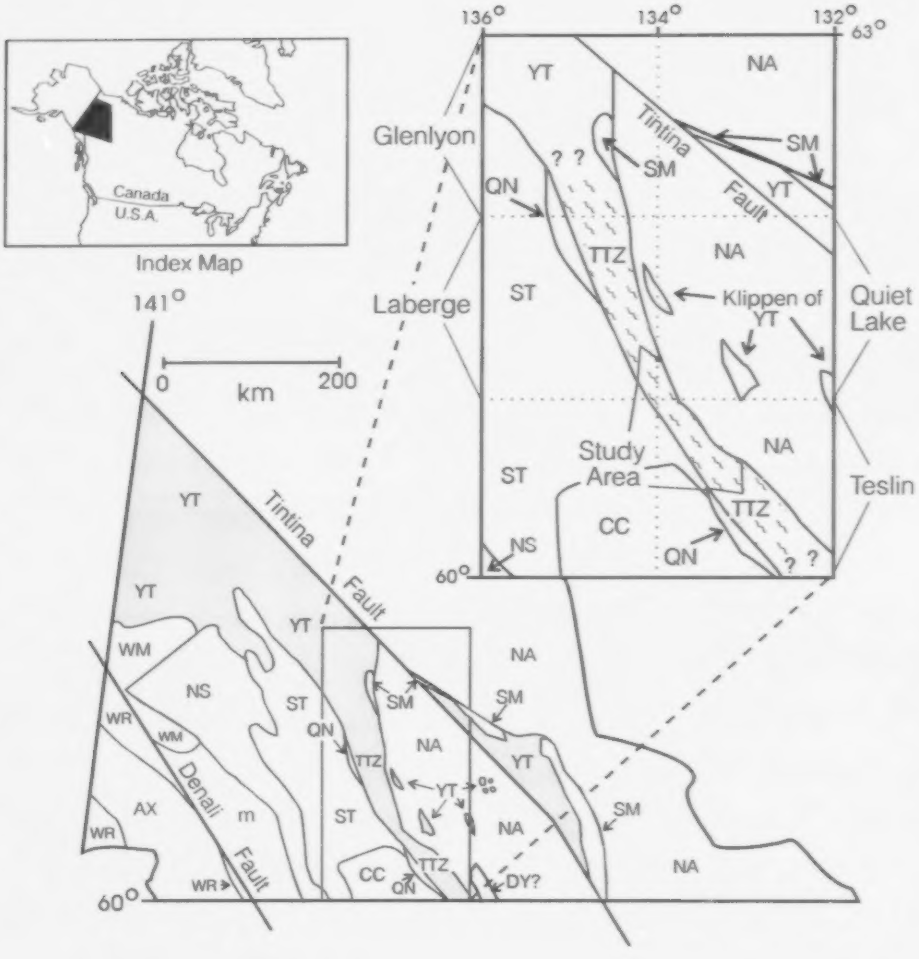
Canada
U.S.A.
Index Map
141°
0
km
200
60°
YT
YT
YT
WM
NS
WR
WM
AX
WR
m
WR
Denali
Fault
ST
QN
SM
TTZ
NA
YT
ST
CC
TTZ
QN
DY?
NA
SM
YT
SM
NA
NA
Tintina
Fault
136°
134°
132°
63°
Glenlyon
Laberge
Quiet Lake
Teslin
YT
NA
SM
SM
? ?
QN
YT
TTZ
NA
ST
Klippen of YT
ST
Study Area
NA
CC
TTZ
NS
QN
? ?
60°

Figure 4-2: Terrane map of Yukon, highlighting the Yukon-Tanana terrane, the Teslin tectonic zone and the location of this study. Glenlyon, Laberge, Quiet Lake and Teslin are 1:250 000 scale map areas. Terranes are: NA = North America, SM = Slide Mountain, YT = Yukon Tanana, TTZ = Teslin tectonic zone, NS = Nisling, DY = Dorsey, QN = Quesnellia, CC = Cache Creek, ST = Stikinia, WM = Windy McKinley, m = undivided metamorphics, AX = Alexander, WR = Wrangellia, (Modified from Monger & Berg 1989; Wheeler & McFeely 1991; Stevens in review; Gordey & Stevens 1994).

domain of dextral strike-slip shear and a domain of apparent reverse shear. Fabrics in the central strike-slip shear domain cut those in the two adjacent domains. Planar fabrics in all domains dip steeply southwest. The domains were interpreted to result from backflow, margin-parallel flow, and downflow in a subduction channel within the deep-seated portion of a west-dipping B-type Permo-Triassic subduction complex. The tectonites were interpreted to have been subsequently thrust eastward as a coherent sheet onto autochthonous strata in the Early Jurassic as a result of A-type subduction (Hansen 1992a).

New mapping and structural analysis summarized below lead to an alternative interpretation. I propose that the Teslin tectonic zone is a heterogeneous thrust-transpressive shear zone representing the ductile root of a crustal-scale "flower structure". The Teslin tectonic zone is an example of the development of characteristics typical of a brittle "flower structure" within a ductile deformation zone.

The geology of the study area (Fig. 4-2) is summarized in Fig. 4-3. Ductilely deformed rocks include siliceous schist, quartzite, graphitic phyllite, marble, greenstone, metatonalite and metagabbro metamorphosed under greenschist to amphibolite facies conditions. Garnet thermobarometry and site-chemistry of amphiboles shows that peak metamorphism occurred under "medium pressure" greenschist to amphibolite facies conditions at 450-650°C (Stevens in review). U-Pb analysis of zircons from metatonalite yielded Early Mississippian crystallization ages (Fig. 4-3) (Stevens et al. 1993). ^{40}Ar-^{39}Ar analysis of hornblende and biotite from the area of Fig. 4-3 and from rocks to the north yielded Early to Middle Jurassic cooling/uplift ages (179-195 Ma) (Hansen et al. 1991; Stevens et al. 1993). The preservation of primary depositional and intrusive contacts and the isotopic ages are interpreted to indicate that the area represents part of a continental-crust terrane (Nisutlin Terrane) formed by mid-Mississippian time that underwent ductile deformation and metamorphism prior to the Middle Jurassic (Stevens in review; Stevens et al. 1993).

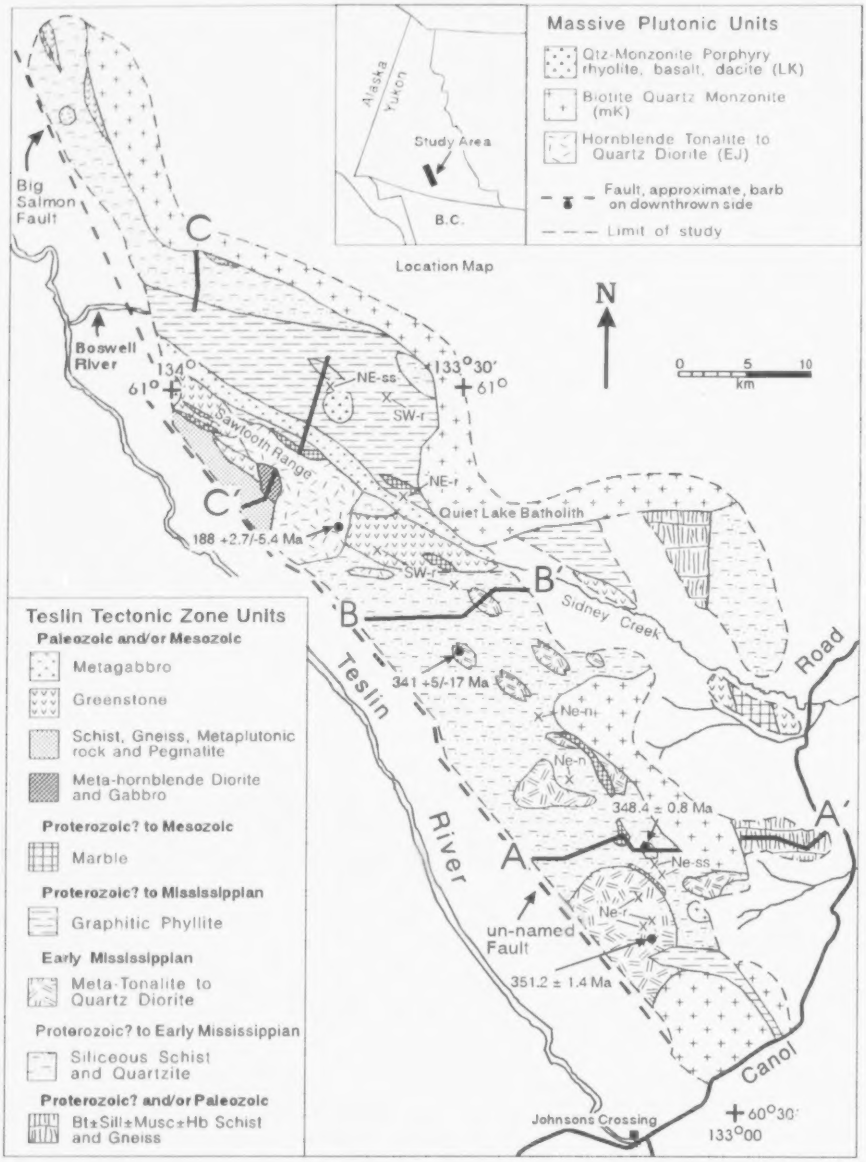
Massive Plutonic Units
Qtz-Monzonite Porphyry rhyolite, basalt, dacite (LK)
Biotite Quartz Monzonite (mK)
Hornblende Tonalite to Quartz Diorite (EJ)
Fault, approximate, barb on downthrown side
Limit of study
Alaska
Yukon
Study Area
B.C.
Location Map
N
0 5 10
km
Big Salmon Fault
Boswell River
C
C'
B
B'
A
A'
134°
61°
133°30'
61°
NE-ss
SW-r
NE-r
SW-r
Sawtooth Range
Quiet Lake Batholith
188 +2.7/-5.4 Ma
Sidney Creek
Road
Teslin River
341 +5/-17 Ma
Ne-n
Ne-n
348.4 ± 0.8 Ma
Ne-ss
Ne-r
un-named Fault
351.2 ± 1.4 Ma
Canol
Johnsons Crossing
60°30'
133°00
Teslin Tectonic Zone Units
Paleozoic and/or Mesozoic
Metagabbro
Greenstone
Schist, Gneiss, Metaplutonic rock and Pegmatite
Meta-hornblende Diorite and Gabbro
Proterozoic? to Mesozoic
Marble
Proterozoic? to Mississippian
Graphitic Phyllite
Early Mississippian
Meta-Tonalite to Quartz Diorite
Proterozoic? to Early Mississippian
Siliceous Schist and Quartzite
Proterozoic? and/or Paleozoic
Bt±Sill±Musc±Hb Schist and Gneiss

Figure 4-3: Simplified geology map of the study area (modified from Stevens 1994, in review). Teslin tectonic zone units display penetrative ductile deformation fabrics and most are part of the Yukon-Tanana terrane. Massive plutonic units post-date penetrative deformation in the zone. AA', BB', and CC' are the location of structural transects. Shear-sense indicator occurrences outside of the transects are shown with an "x". NE, SW refer to foliation dip direction, and n, r and ss refer to normal, reverse or strike-slip shear. Ages are U-Pb zircon dates from Stevens et al. (1993).

Structural Characteristics

At least two phases of deformation have affected rocks of the Teslin tectonic zone. An early penetrative ductile deformation phase and a later and weaker folding/cleavage phase (Stevens and Erdmer 1993). The early penetrative deformation produced lineated protomylonite and mylonite amounting to more than 50% of the deformed rock. Schistosity and mylonitic foliation are defined by micas, chlorite, amphiboles and tabular quartz grains. Mineral and/or stretching lineation are defined by the same minerals and are considered to be parallel to the local shear direction (Plates 4-1a, 4-1b). Shear-sense indicators in the XZ plane of the finite strain ellipsoid are well developed locally, but are not abundant. The most common are strain-insensitive Sa/Sb fabric (Hanmer and Passchier 1991) in quartzite and quartz-schist, strain-sensitive C/S fabric and asymmetrical extensional shear bands in a variety of rock types, pressure shadows around pyrite in graphitic phyllite, and, rarely, rotated feldspars in metaplutonic rock (Plates 4-2a, 4-2b). Strain partitioning at the scale of tens to hundreds of metres is well developed and best observed in metaplutonic rock (Plates 4-3a, 4-3b). Rootless isoclinal folds preserved locally are interpreted to record this early penetrative deformation.

The later weak folding/cleavage phase is primarily manifested by crenulation of the earlier schistosity and mylonitic fabrics. (Plates 4-4a, 4-4b). Hand-specimen scale open to tight, commonly disharmonic folds are found in a few areas (Plates 4-5a, 4-5b). These generally have axes parallel to mineral lineations. The parallelism of these linear features may be fortuitous; however, a pre-existing linear anisotropy (i.e. the mineral lineation) is interpreted to have controlled the subsequent formation and orientation of the folds (cf. Cobbold and Watkinson 1981; Watkinson 1983). Rotation of the axes into parallelism with the shear direction is unlikely, as the folds formed after the penetrative shearing and many are open in form. A spaced (5-50 cm) crenulation cleavage has formed locally, in particular in the area north and south of the Boswell River (see Fig. 4-3 for location). This cleavage cuts earlier schistose and mylonitic foliations.

Plate 4-1: Some structural characteristics of the penetrative deformation phase. These photographs show well developed L-S tectonites (mylonites), (a) is a muscovite-chlorite quartzite with prominent quartz-rodding, and (b) is a biotite-muscovite quartzofeldspathic schist with horizontal quartz-rodding and phyllosilicate alignment.

A

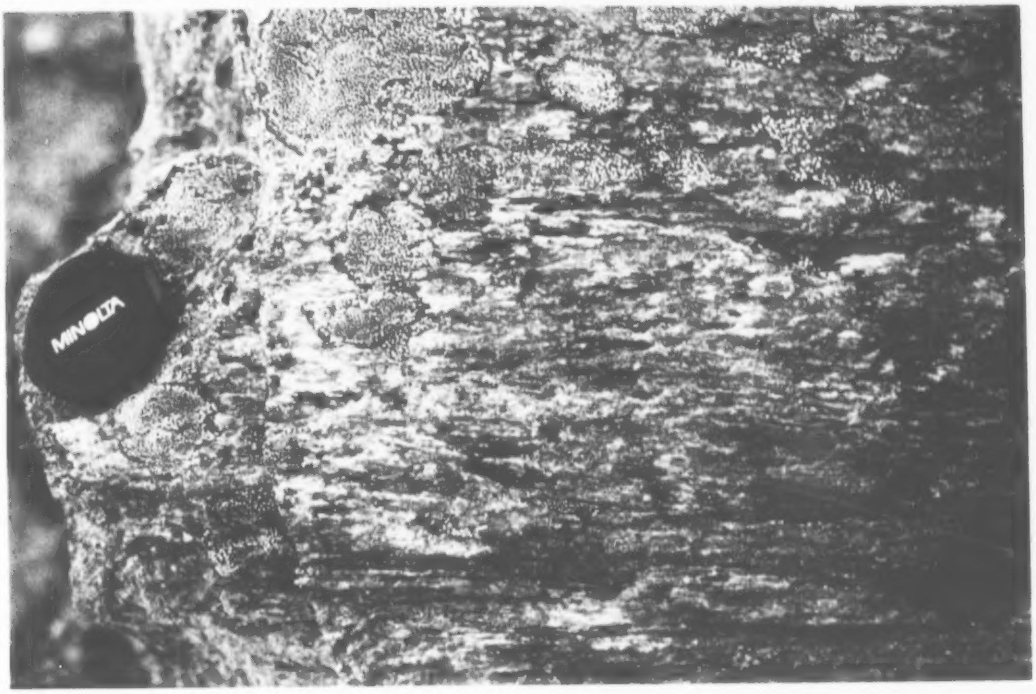

B

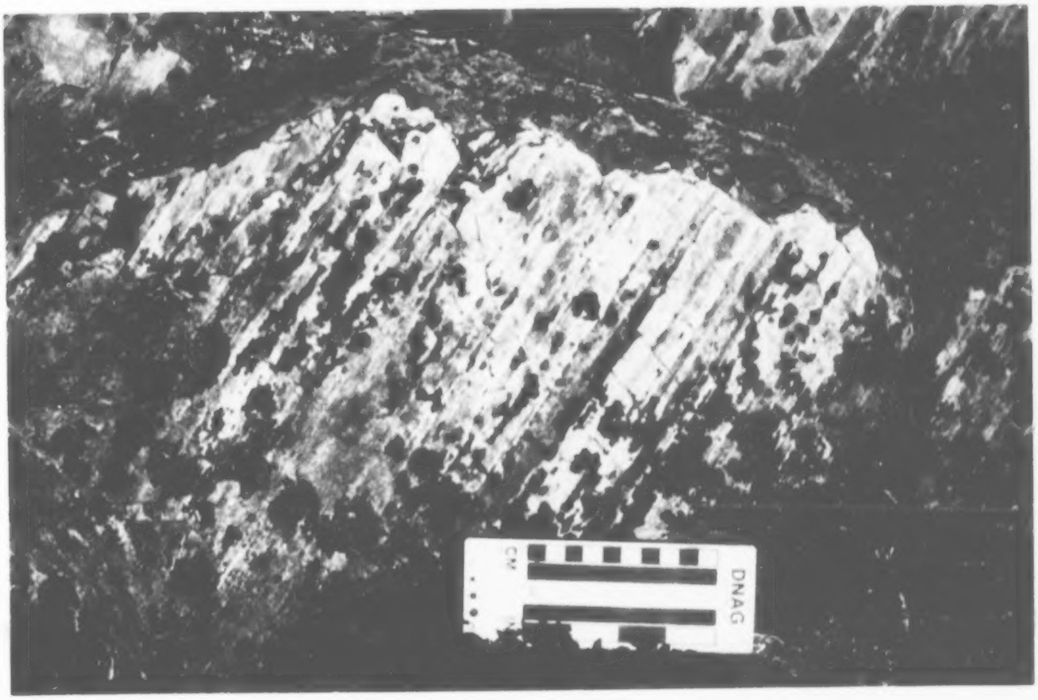

Plate 4-2: Some structural characteristics of the penetrative deformation phase. Both photographs illustrate examples of shear-sense indicators: (a) shows sinistral asymmetrical extension shear bands and (b) shows dextral strain-insensitive Sa/Sb fabric

A

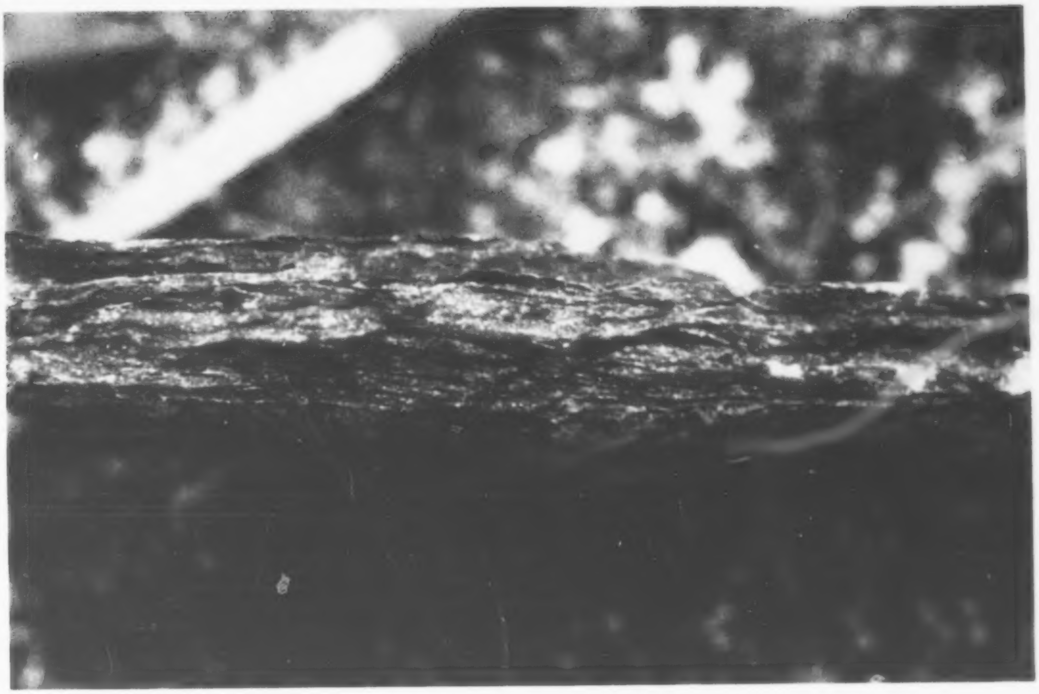

B

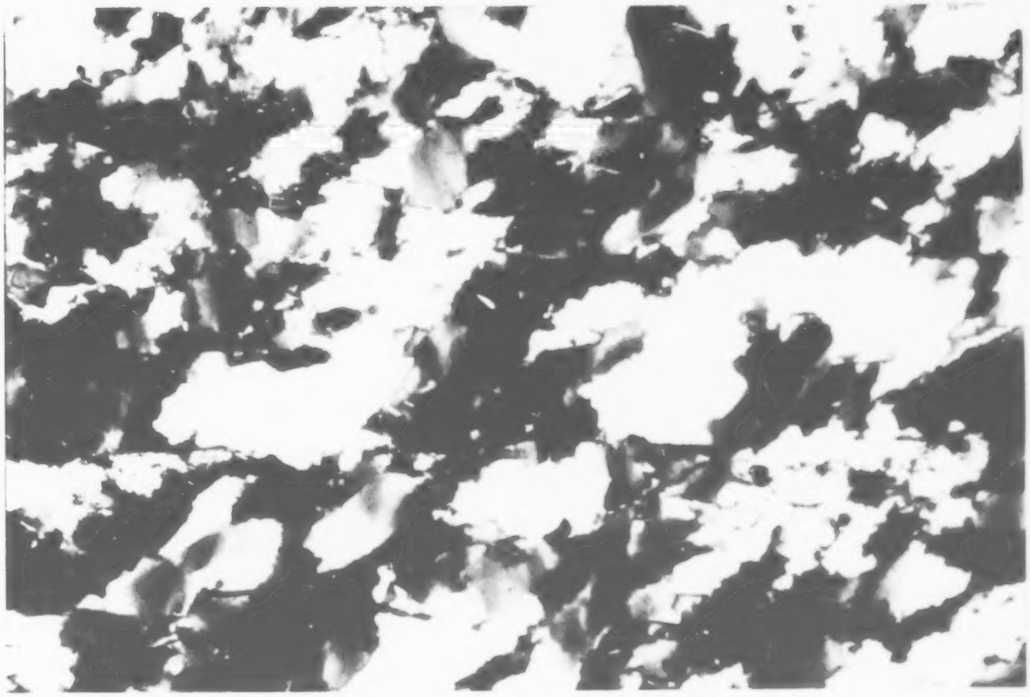

Plate 4-3: Some structural characteristics of the penetrative deformation phase. Both photographs illustrate the degree of strain partitioning, (a) shows weakly deformed metagabbro that grades over tens to hundreds of metres into (b) which shows highly sheared/mylonitic metagabbro.

A

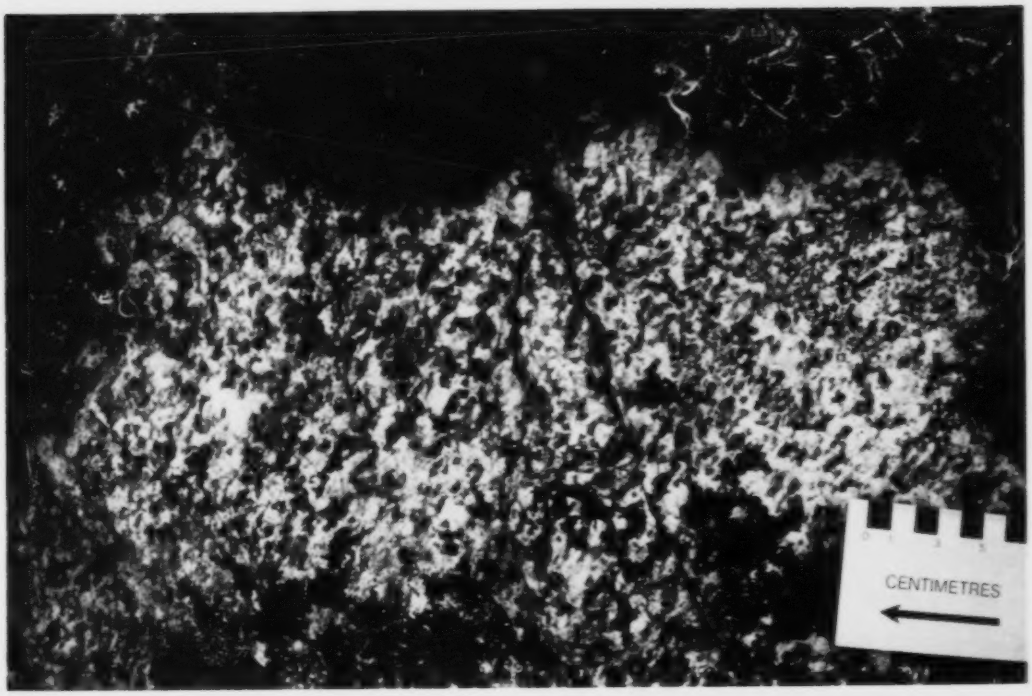
0 1 3 5
CENTIMETRES

B

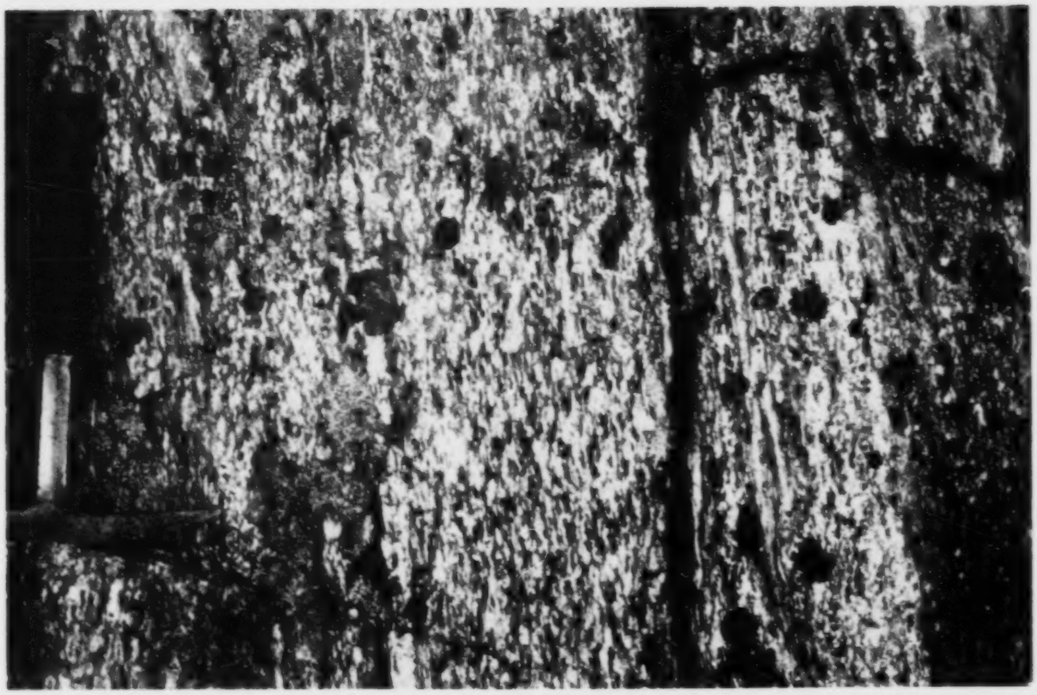

Plate 4-4: some structural characteristics of the folding/cleavage phase. Both photographs are examples of the widespread crenulations that dominate this deformation phase. (a) shows sub-horizontal crenulation axes in a quartz-muscovite schist, and (b) shows moderately-plunging axes (appears horizontal in the photograph) in a quartzite and quartz-mica schist.

A

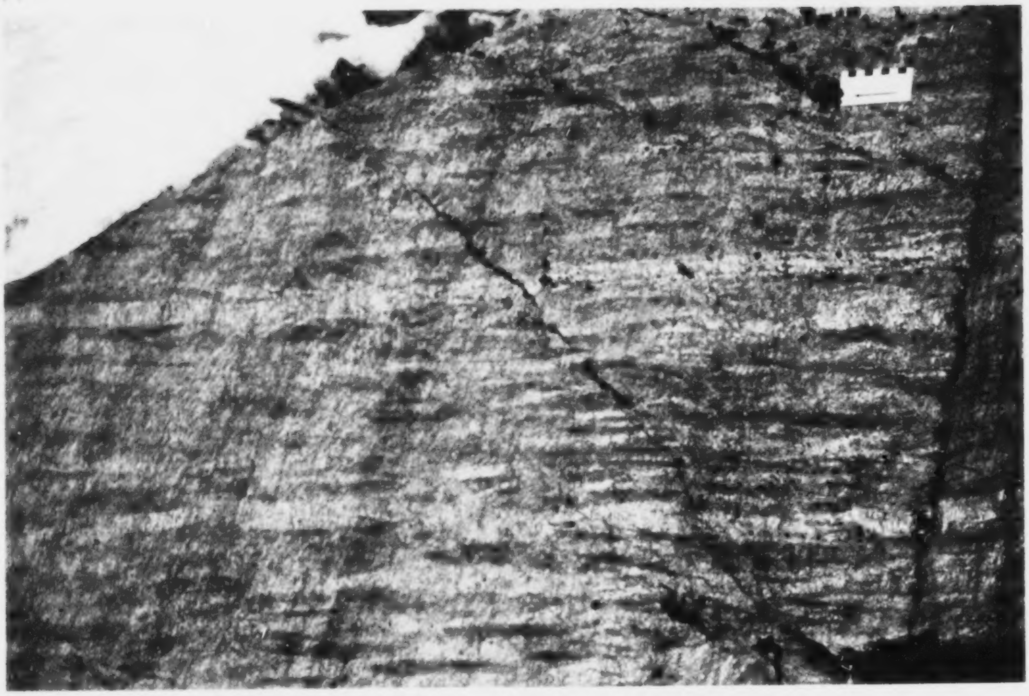

B

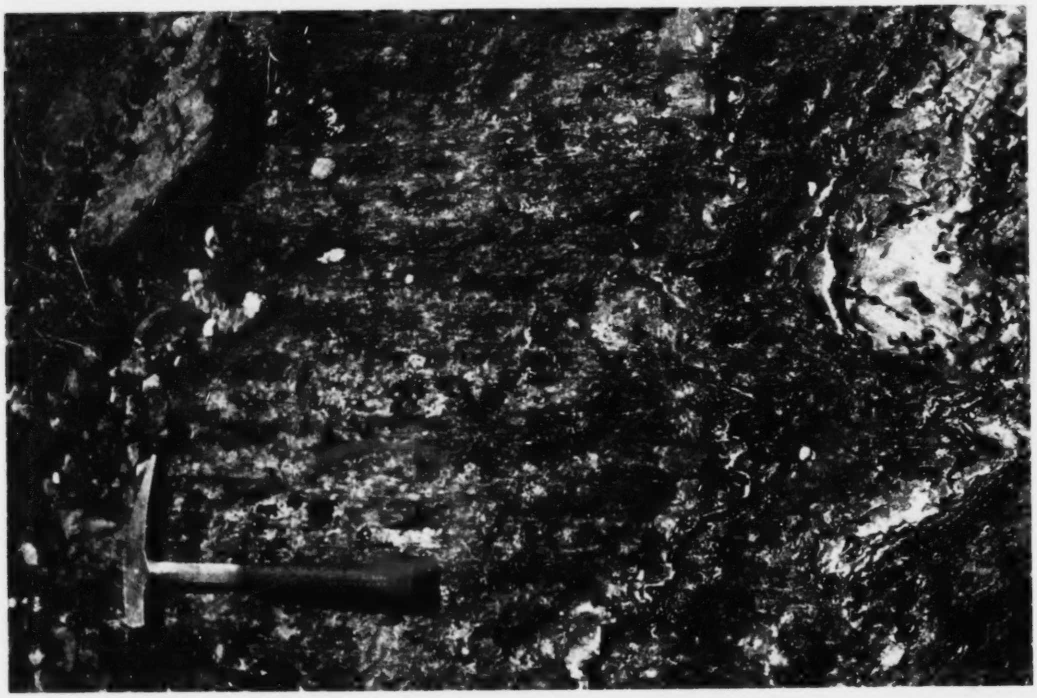

Plate 4-5: Some structural characteristics of the folding/cleavage phase. Both photographs are examples of hand-specimen-scale folds that occur locally, and which commonly have mineral lineations parallel to their fold axes. (a) is a biotite-muscovite-amphibole quartzofeldspathic schist, and (b) is a quartz-muscovite schist.

A

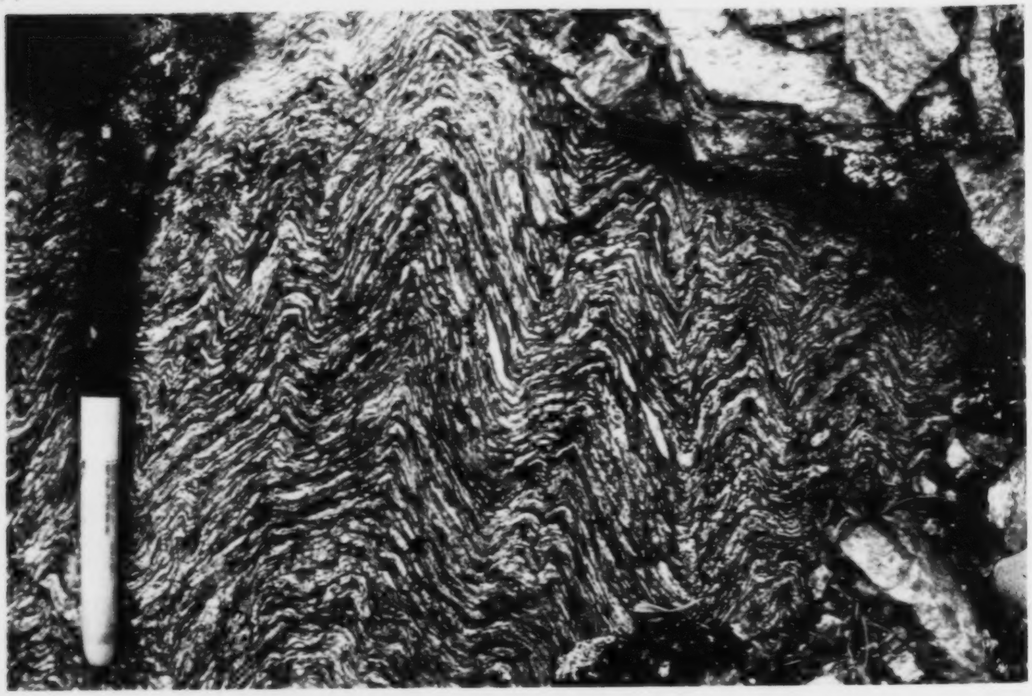

B

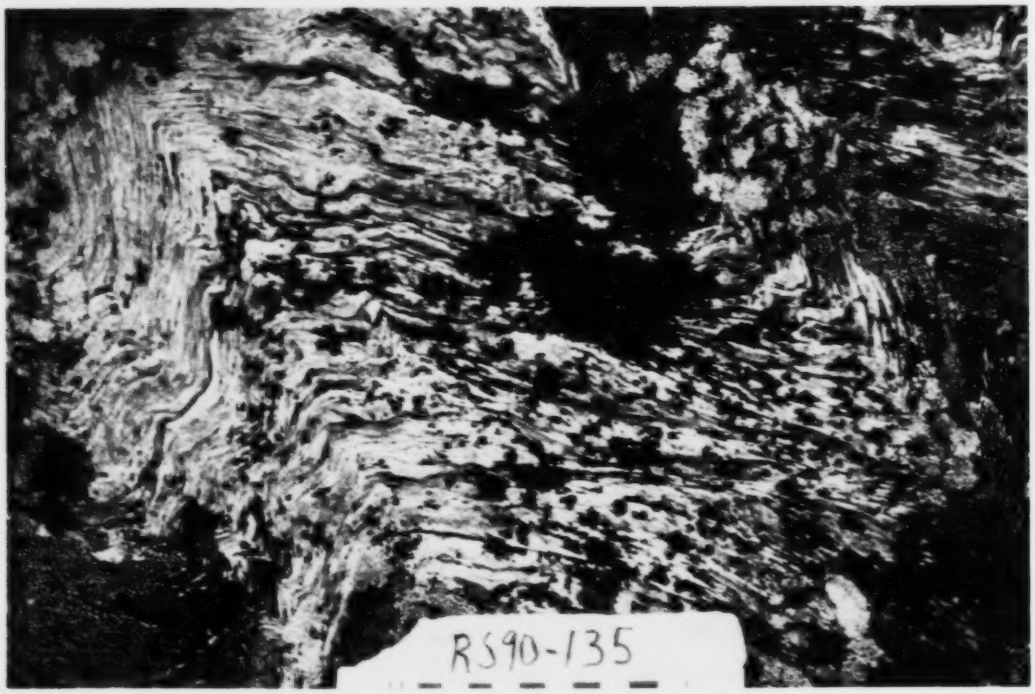

Shear sense can commonly be determined from fabric asymmetry between cleavage surfaces (Plate 4-6) (cf. Bell and Johnson 1992). Muscovite grains generally grow around fold hinges, but are kinked in places, and crenulation cleavages show both continuation of offset fabrics across the cleavage (ductile deformation) and clear separation of offset fabrics (brittle deformation). This leads me to suggest that folding occurred near the brittle-ductile transition. Retrograde metamorphic minerals associated with folding are not apparent, although the local chloritization of garnet and biotite is common.

Microstructures generally show preservation of abundant strain fabrics, such as undulose extinction, deformation bands, deformation lamellae, subgrains and new grains (Plate 4-7), in both crenulated and uncrenulated rock. In the Teslin tectonic zone north of the area, Hansen (1992b) found that microstructures generally show annealed textures. The reason for this difference is unclear, especially as the two areas are similar in most other respects (see discussion below).

Structural Domains

Detailed structural analysis along three transects (AA', BB', CC' on Fig. 4-3), revealed a variety of structural domains, each with unique linear and/or planar fabric orientations and, in some cases, structural style or shear-sense. The characteristic linear and planar fabrics are shown in Figs. 4-4 and 4-5. Domain boundaries are usually less than 0.5 km wide and are marked by a change in fabric orientation; elsewhere, boundaries are sharp and defined by a change in rock type (Stevens and Erdmer 1993). Zones of high relative strain were not identified at these domain boundaries, but strain is generally high throughout the studied area. Domains from one transect are not readily correlated with those of adjacent transects. Regional mapping (1:50 000 scale) between the transects was ineffective at placing along-strike limits for most domains, and it is likely that additional domains occur between the transects in Figs. 4-4 and 4-5.

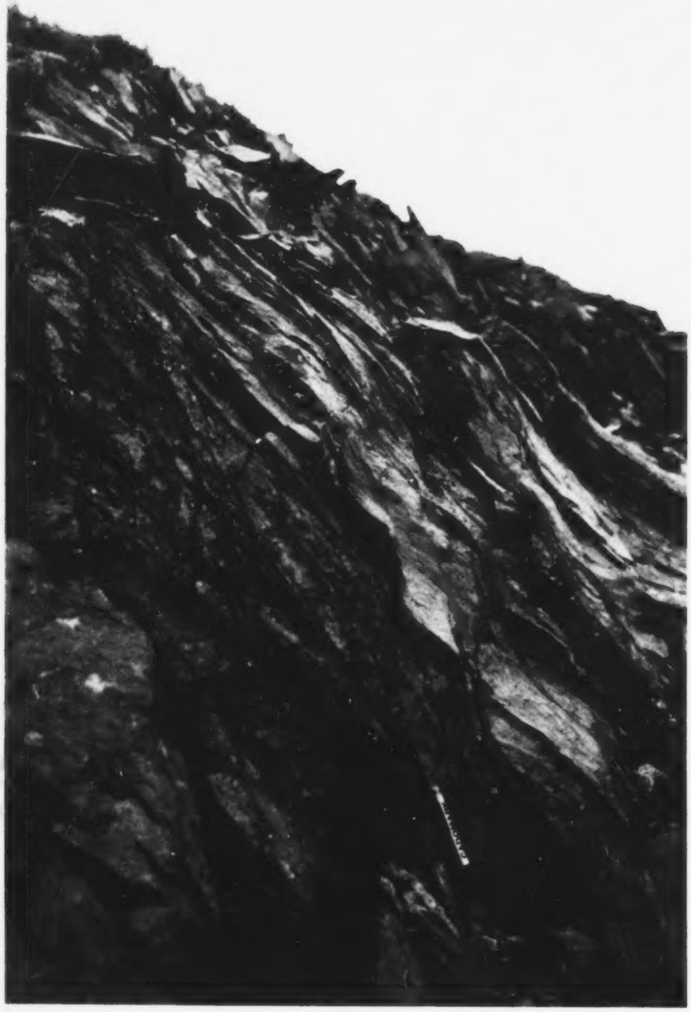

Plate 4-6: A structural characteristic of the folding/cleavage phase. The photograph illustrates the spaced (5-50 cm) cleavage that occurs locally. The cleavage dips steeply to the right or is sub-vertical and shear-sense from the fabric asymmetry between cleavage surfaces is normal. See also photograph in appendix 3.

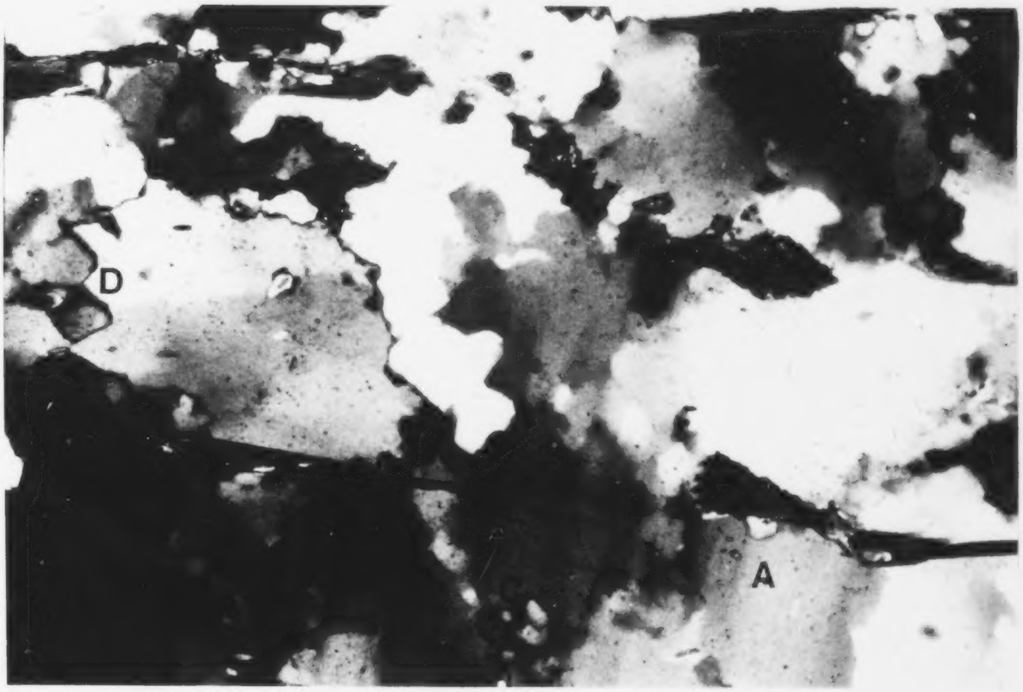

Plate 4-7. Strain microfabrics are preserved throughout the study area. Examples are: A=undulose extinction, B=deformation bands, C=sub-grains, D=new grains.

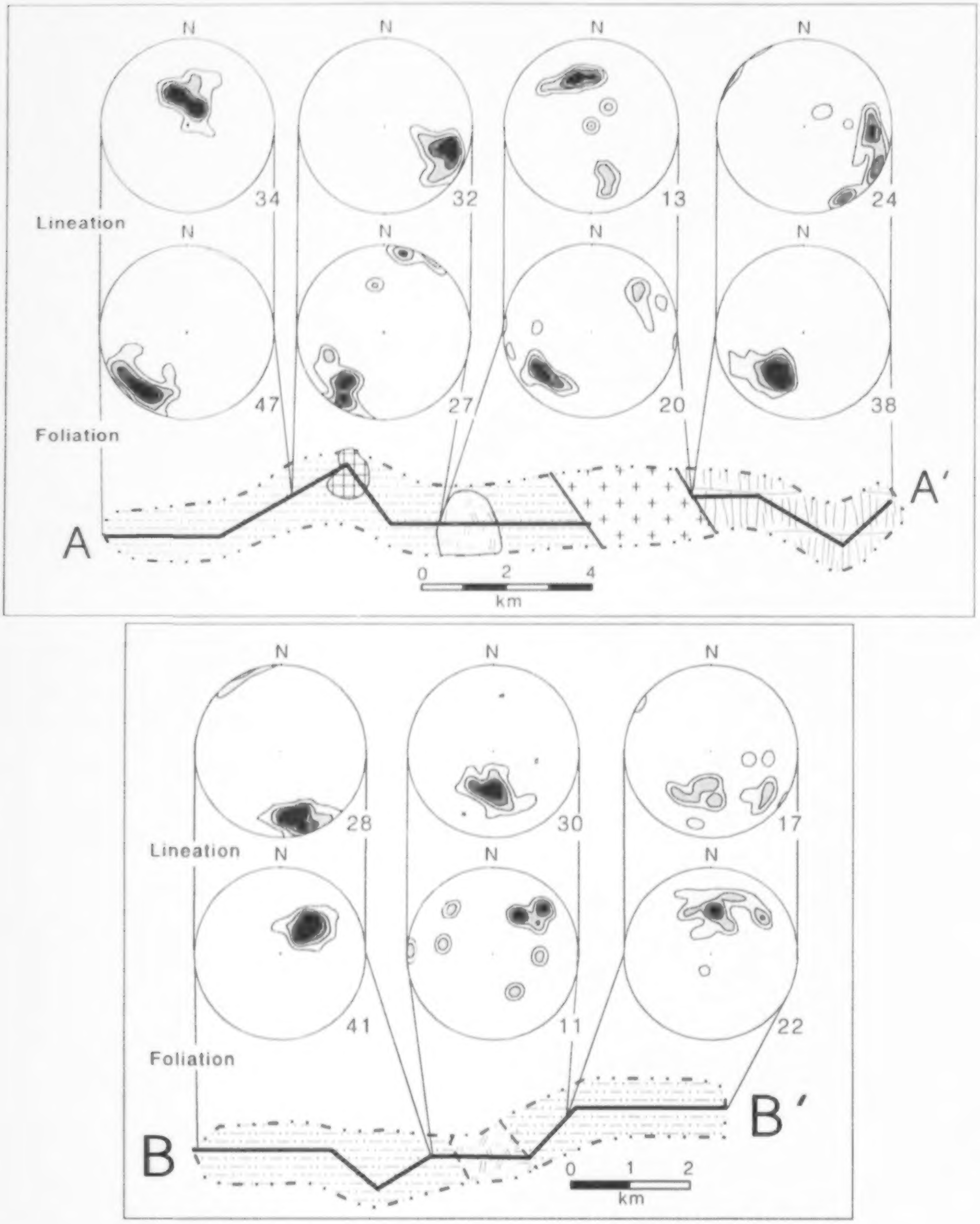
N
N
N
N
34
32
13
24
Lineation
N
N
N
N
47
27
20
38
Foliation
A
A′
0
2
4
km
N
N
N
28
30
17
Lineation
N
N
N
41
11
22
Foliation
B
B′
0
1
2
km

Figure 4-4: Strip maps for structural transects AA' and BB', with accompanying contoured equal-area projection plots of lineation and poles to foliation developed during the penetrative deformation phase. Contours are multiples of the density of a uniform distribution of orientations. Contours are at densities of 3, 6, 9, and 12.

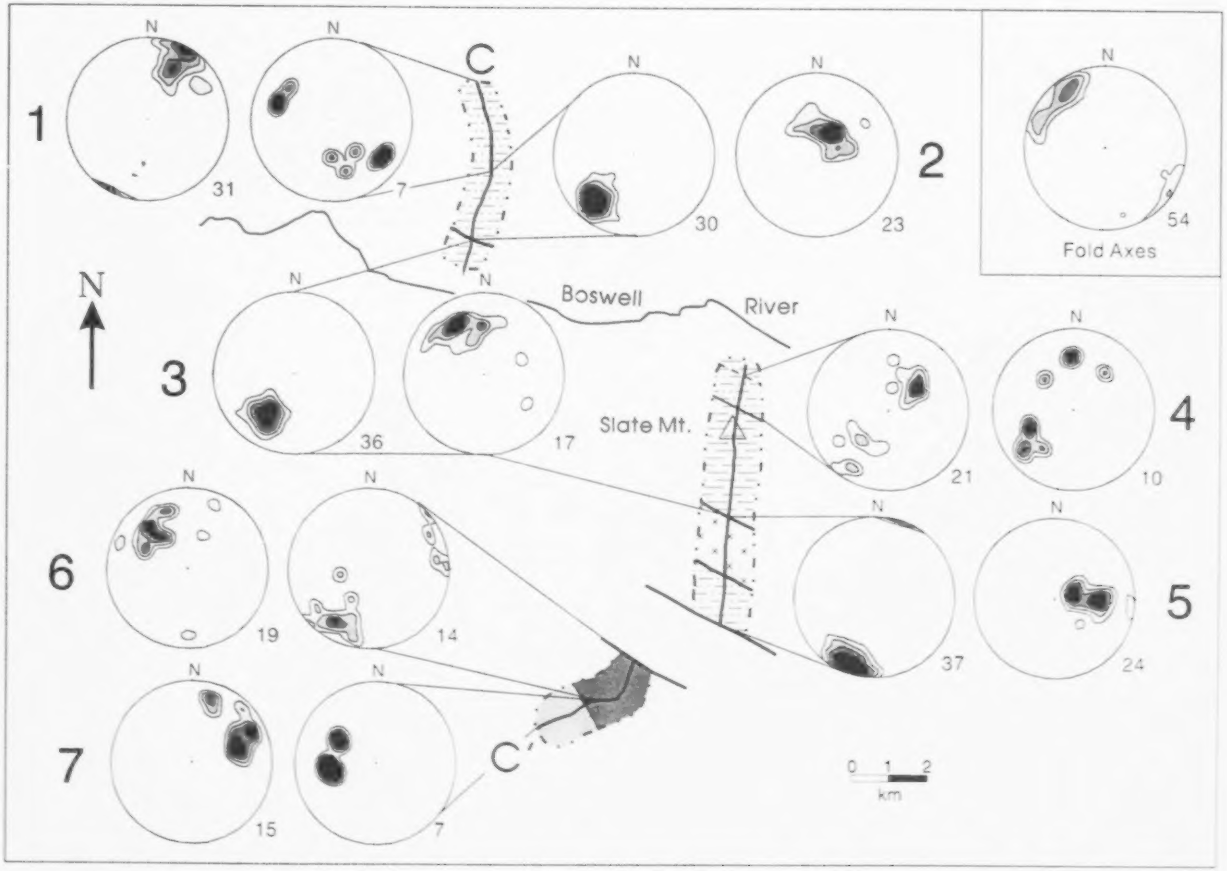
1
2
3
4
5
6
7
N
C
C'
Boswell
River
Slate Mt.
Fold Axes
N
31
7
30
23
54
36
17
21
10
37
24
19
14
15
7
0
1
2
km

Figure 4-5: Strip maps for structural transect CC', with accompanying contoured equal-area projection plots of lineation and poles to foliation developed during the penetrative deformation phase. Fold axes from the folding/cleavage phase are shown in the top right corner. The left plot is of poles to foliation and the right is of lineation. Contours are multiples of the density of a uniform distribution of orientations. Contours are at densities of 3, 6, 9, and 12.

Shear-sense indicators are well preserved in a few domains, in particular the western two domains of transect A and the westernmost in transect B. Elsewhere well preserved and unambiguous shear-sense indicators are uncommon.

The structural variations across transect C, summarized in Table 4-1, provide an example of variation across the Teslin tectonic zone. Detailed descriptions of transects A and B were presented by Stevens (1992).

Fabric orientations and shear sense from the penetrative deformation phase for all three transects are summarized in a 3-dimensional diagram (Fig. 4-6) One of the most striking characteristics of the Teslin tectonic zone is that foliation surfaces dip in one of two opposite, but well confined directions. In transect A, fabrics dip northeast, in B they dip southwest, and in C they dip either northeast or southwest (Fig. 4-6). Lineation shows a wide range of orientations, but is mostly moderately- to steeply-plunging, indicating that oblique- or dip-slip movement was dominant.

Shear-sense indicators were found in a little more than half of the domains (Fig. 4-6). They indicate that both oblique-normal and oblique-reverse shear are preserved in both the northeast- and southwest-dipping fabrics. This is also the case for shear-sense indicators outside the three transects (see Fig. 4-3).

The fabric orientations and shear sense imposed by the penetrative phase continued into the folding phase. For example, in the northern part of transect C, a spaced (5-50 cm) crenulation cleavage is developed locally. It dips either northeast or southwest, and shows reverse offset or normal offset, respectively.

Folding is not considered responsible for the opposite dips of planar fabrics in the Teslin tectonic zone, for three main reasons. Firstly, there is no evidence of large-scale chevron folding necessary to produce the two dip directions. Folding is generally confined to minor crenulations that do not alter the overall dip of the foliation, and to mesoscopic folds in a few localized areas.

Table 4-1: Structural Characteristics of Transect CC'

Domain	Penetrative Phase		Folding/Cleavage Phase		Shear-Sense Indicators		Domain Boundaries
	Planar Fabrics[1]	Linear Fabrics[2]	Planar Fabrics	Linear Fabrics	Type	occurrence	
1	-strong -steeply-southwest dipping	-a few in the southern half -rare elsewhere	-moderately southwest-dipping spaced (5-30cm) cleavage -localized	-crenulation hinges -abundant	-oblique-normal C/S (penetrative phase) -thrust asymmetry between cleavage (folding phase)	1 common	-northern is the edge of the massive Quiet Lake Batholith -southern is a 200-300 m wide zone across which foliation changes dip-direction
2	-strong to mylonitic -steeply-northeast dipping	-well developed	-moderately northeast-dipping spaced (5-30cm) cleavage -localized	-crenulation and mesoscopic fold hinges -common	-oblique-reverse C/S -oblique-normal C/S and Sa/Sb (penetrative phase) -extension asymmetry between cleavage (folding phase)	1 3 common	-southern is marked by a change from siliceous schist to graphitic phyllite
3	-moderate to strong -moderately- to steeply-northeast dipping	-best developed north of Slate Mountain in siliceous graphitic schist	-moderately northeast-dipping spaced (5-30cm) cleavage -localized	-crenulation hinges -abundant	-oblique-normal C/S and asymmetric extensional shear bands (penetrative phase) -extension asymmetry between cleavage (folding phase)	2 common	-northern and southern are the boundaries of the graphitic phyllite unit
4	-strong -folded with wavelengths of 10-30m and amplitudes of 10-40m	-well developed -variably oriented probably as a result of folding	-none	-rounded to chevron hinges -abundant	none	n/a	-domain is confined to an area of strongly folded siliceous schist within the graphitic phyllite unit of domain 3.
5	-massive to mylonitic in gabbro and strong to mylonitic is schist -steeply-northeast dipping	-well developed throughout, except in massive to moderately deformed gabbro	-none	-none	-oblique-normal C/S and asymmetric extensional shear bands	3	-northern is the contact with graphitic phyllite and southern is an intrusive contact with massive tonalite
6	-moderate to ultramylonitic -moderately- to steeply-southwest dipping	-moderately well developed -variable oriented	-none	-macroscopic fold hinges locally	-none	n/a	-northern is an intrusive contact with massive tonalite and the southern is at an inferred fault, where southeast-dipping foliation changes to southwest-dipping
7	-moderate to strong -steeply-southwest dipping	-locally developed	-none	-a few mesoscopic hinges locally	-none	n/a	-southern is placed at the western bounding fault of the Teslin tectonic zone

[1] A rock with moderate planar fabric has a foliation defined by quartz and phyllosilicates. Quartz shows undulose extinction, deformation bands, deformation lamellae and subgrains. New grains and minor grain size reduction are evident. A rock with strong planar fabric is protomylonitic, with extensive strain microstructures, prominent grain size reduction, and a strong foliation defined by all mineral grains. A mylonite is a lineated rock consisting of 10-50% porphyroclasts of strained primary grains in a strongly foliated matrix of smaller, strain-free grains. Phyllosilicates show dimensional and crystallographic alignment.

[2] The linear fabric is defined by aligned mineral grains or mineral aggregates which are commonly muscovite, chlorite, biotite and amphiboles.

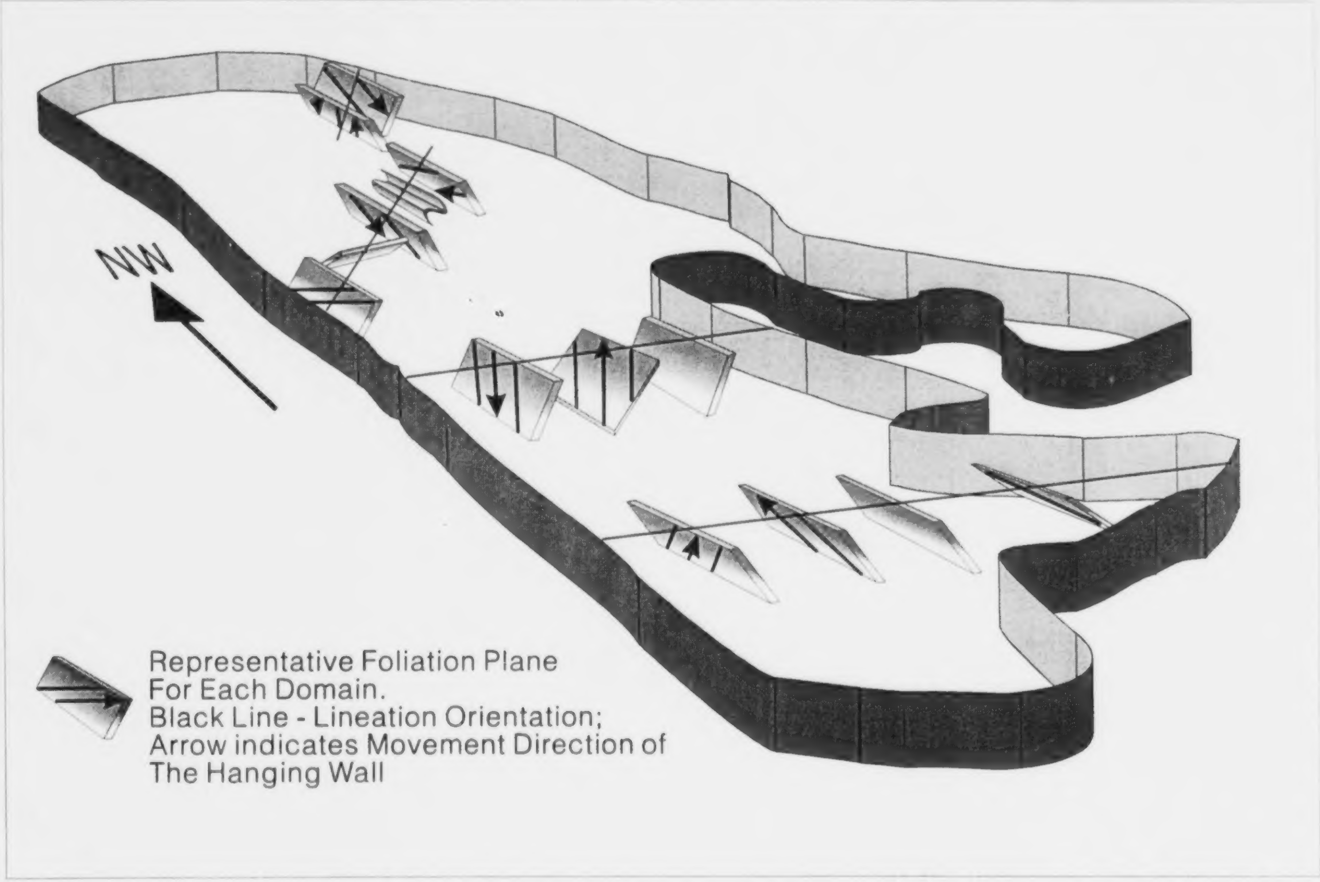
NW
Representative Foliation Plane
For Each Domain.
Black Line - Lineation Orientation;
Arrow indicates Movement Direction of
The Hanging Wall

Figure 4-6: 3-dimensional diagram that summarizes the fabric orientations and shear-sense developed during the penetrative deformation phase for each domain. Two opposite well defined dip directions, variable lineation orientations, and normal and reverse shear are characteristic.

The largest folds occur in domain 4 of transect C where they have wavelengths of 10-30 m, amplitudes of 10-40 m and closures are clearly evident. Large chevron folds do not occur. Secondly, folding cannot explain the observed changes in stratigraphy in the northern part of transect C. The only location in the study area where compositional layering is continuous for more than a few tens of metres is in the northern part of transect C (domains 1 and 2) (see chapter 2). There, a broad lithologic layering or stratigraphy can be followed for at least 7 km along strike and 5 km across strike (Fig. 4-7) (see also Stevens 1994). If folding was responsible for the two dip directions, stratigraphy should be repeated (Fig. 4-7). However, repetition in the stratigraphy is not seen when passing from the southwest dipping fabrics of domain 1 into the northeast dipping fabrics of domain 2. Thirdly, geometric rotation of planar structures into parallelism (unfolding) does not bring corresponding linear structures into alignment. This is true for adjacent domains in a single transect, such as domain 1 and 2 of transect C, and for domains from adjacent transects, such as the western domains in transects A and B.

Comparison with other parts of the Teslin tectonic zone

To the north, Hansen (1989, 1992a) suggested that the Teslin tectonic zone consists of three distinct elongate structural domains defined by fabric orientation and shear-sense. However, Hansen's (1989) data indicate that there may be more than three domains. For example, Hansen (1992a) concluded that an elongate domain of west dipping fabrics, with apparent normal shear extends across the western edge of the tectonic zone. However, the structural data for this area (see Fig. 9 in Hansen 1989) clearly include west-southwest and east-northeast dipping planar fabric orientations with both normal and reverse shear. Similar alternative interpretations can be made for the two other elongate structural domains identified by Hansen (1992a).

To the north, the Teslin tectonic zone contains domains with sub-horizontal lineation and dextral shear-sense indicators (Hansen 1989). These

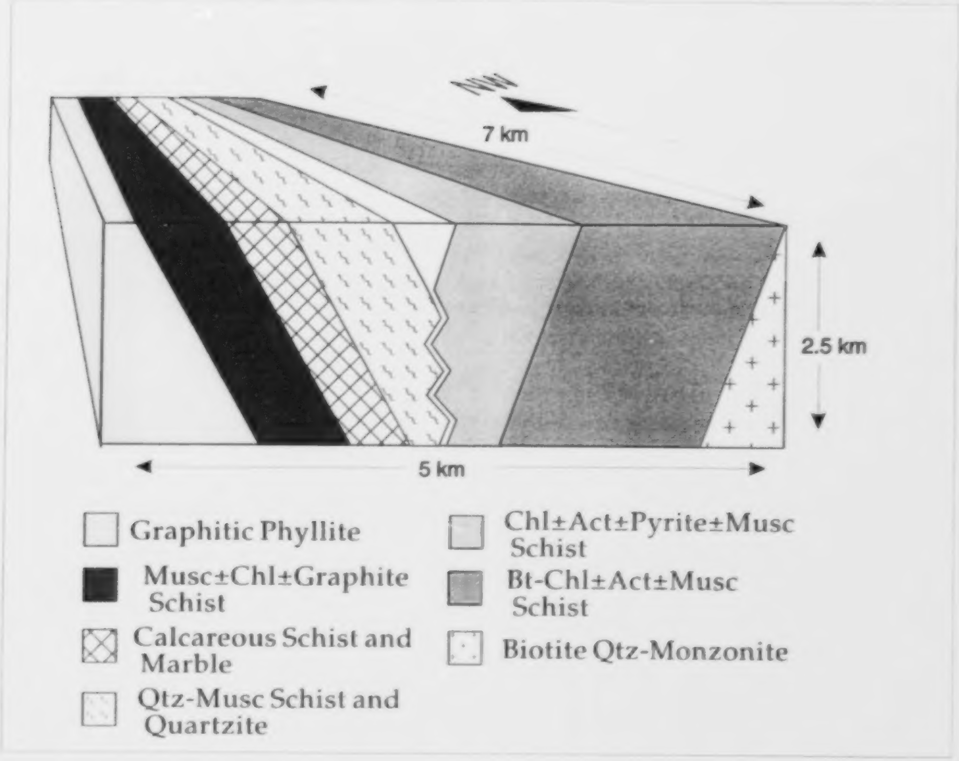
NW
7 km
2.5 km
5 km
Graphitic Phyllite
Musc±Chl±Graphite Schist
Calcareous Schist and Marble
Qtz-Musc Schist and Quartzite
Chl±Act±Pyrite±Musc Schist
Bt-Chl±Act±Musc Schist
Biotite Qtz-Monzonite

Figure 4-7: Block diagram which shows that changes in stratigraphy, in the northern part of transect C (domain 1 and 2, see Fig. 4-5), cannot be attributed to folding. For this and other reasons (see text), folding cannot explain the two opposite dip-directions in the Teslin tectonic zone.

domains indicate that strike-slip shear, in addition to the dip-slip and oblique-slip shear identified in this study, occur in the Teslin tectonic zone.

The average orientation of foliation and lineation from this study and from Hansen (1989) are summarized in Fig. 4-8. They show that the Teslin tectonic zone, with a strike length of more than 200 km, includes more than 25 domains in which planar fabrics dip either northeasterly or southwesterly, and where lineation is variable. A change in foliation strike from northwest in the study area to more northerly in the Laberge area follows an overall change in the orientation of the Teslin tectonic zone. The inflection zone over which the strike changes direction may reflect the location of a promontory in the Paleozoic North American margin and may have had strong influence on the formation of a transpressional deformation environment within the Teslin tectonic zone.

DISCUSSION

The structural characteristics of the Teslin tectonic zone are interpreted to result from heterogeneous-thrust transpression at the ductile root of a crustal-scale "flower structure" (Fig. 4-9).

Various combinations of compression, wrenching, and extrusion, in space and in time, imposed in part by heterogeneities in the rock assemblages, produced domains with different lineation orientations. As rock is extruded upward it becomes separated into these domains which preserve unique fabric orientations. Systematic variations in lineation orientations, between domains does not occur. Some domains were likely uplifted along high strain zones and juxtaposed against domains with different fabic orientations. Changes in the kinematics of deformation with time will also result in separation of rock into domains. A volume of rock with the same fabric orientations at one time may be separated into two or more domains with different fabric orientation as changing kinematics affect different parts of the original volume. The preponderance of

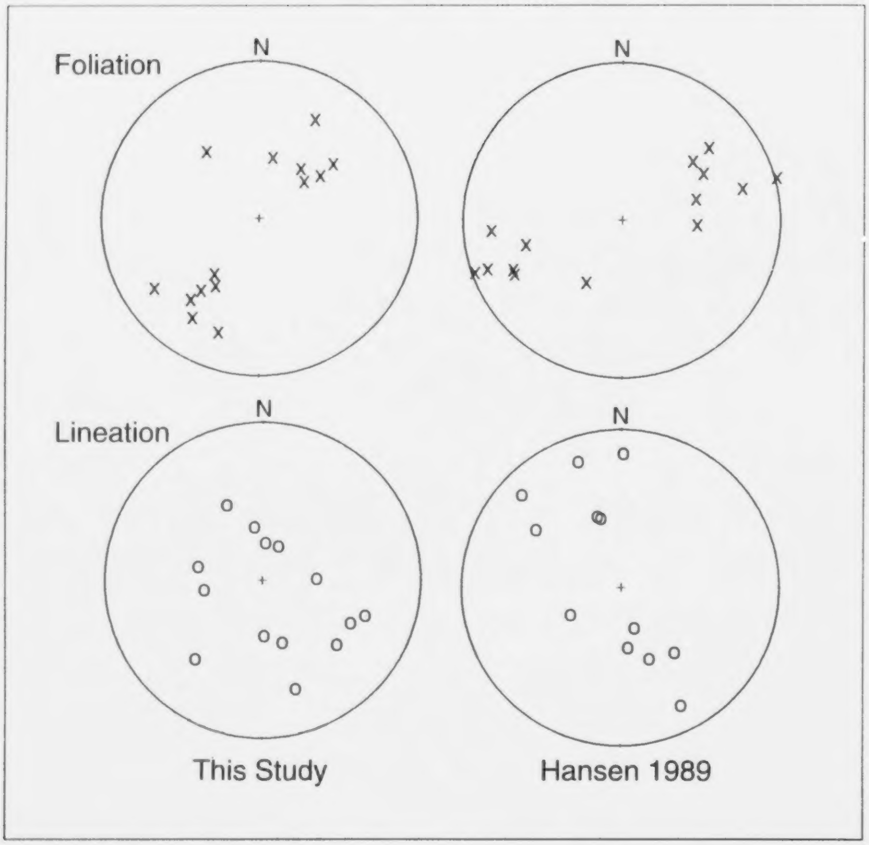

Figure 4-8: Comparison of the average fabric orientations for domains from this study with those recognized by Hansen (1989). Both areas are characterized by opposite foliation dip-directions and variable lineation orientations. The moderate difference in strike direction between the two areas results from an overall change in the strike of the Teslin tectonic zone (see text).

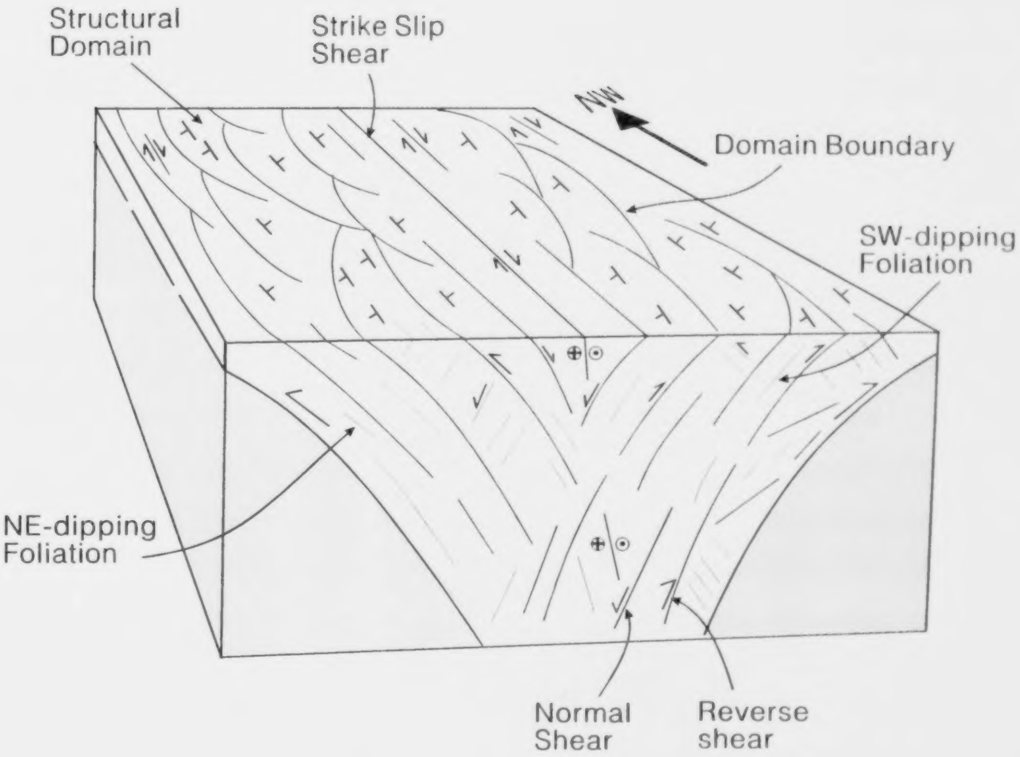
Structural Domain
Strike Slip Shear
NW
Domain Boundary
SW-dipping Foliation
NE-dipping Foliation
Normal Shear
Reverse shear

Figure 4-9: Structural model for the Teslin tectonic zone. The western margin of the zone was truncated by post-accretionary strike-slip faults, and that side of the structure is not preserved. Northeast- and southwest-dipping foliation with normal, reverse and dextral strike-slip shear and variable lineation orientations are characteristic. As rock is extruded upward it becomes separated into domains which preserve unique fabric orientations. Some domains were likely uplifted along high strain zones and juxtaposed against domains with different fabic orientations. Changes in the kinematics of deformation with time will also result in separation of rock into domains. A domain is a volume of rock that contains uniform foliation and lineation orientations. Domain boundaries are commonly less than 0.5 km wide and marked by a change in fabic orientation or are sharp and defined by a change in rock type. There are no systematic fabric variations from one domain to the next.

oblique-slip and dip-slip lineation over strike-slip in the Teslin tectonic zone suggests that thrust transpression was dominant. Strike-slip domains identified by Hansen (1989) cut dip-slip domains, suggesting that strike-slip deformation may have been confined to the later stages of ductile deformation.

A "flower structure" transpression model effectively accommodates all of the main features of the Teslin tectonic zone such as opposite dip directions with normal, reverse and strike-slip separation, and the extrusion characterisitics. Extrusion/thrusting is recorded by flat-lying klippen of Teslin tectonic zone related rocks resting on Paleozoic North American strata east of the zone (Tempelman-Kluit 1979; Gordey 1981; Erdmer 1992). As in flower structures, surface extrusion/thrusting is interpreted to have been contemporaneous with internal deformation of Teslin tectonic zone rocks. Isotopic age data indicate that rocks of Early Mississippian to mid-Permian age were ductilely deformed, and then uplifted and cooled between 179 and 195 Ma (Stevens et al. 1993; Hansen et al. 1991; Mortensen 1992). The timing of ductile deformation is not well constrained within that range, but the widespread preservation of ductile strain fabrics indicates that ductile deformation continued until the rocks were uplifted and cooled. Ductile deformation and extrusion were thus simultaneous. Cleavage and folds formed during the second deformation phase reflect the transition from penetrative ductile deformation to discrete brittle deformation as the rocks were extruded upward. The ductile deformation and extrusion may have occurred above a low angle west-dipping detachment such that the entire zone was translating eastward during internal penetrative deformation (eg. Holdsworth and Strachan 1991). It may also have been accompanied by wedging such as that proposed by Price (1985) for the southeastern Canadian Cordillera Columbia.

In the final stages of deformation, during uplift and cooling, regional thrusting was dominant (Mortensen 1992; Hansen 1992a). The initial stages of this phase are interpreted to be recorded in the Teslin tectonic zone by the crenulation and folding of ductile fabrics and by the development of cleavage.

Deformation continued from the ductile phase to the folding/cleavage phase with similar characteristics (i.e. two dip-directions and normal and reverse separation). This is taken to indicate that a "flower-structure" deformation zone was continuous through the ductile to the brittle deformation phase. Regional data support this interpretation as the Teslin tectonic zone marks the boundary between east- and west-verging thrust structures. To the east, thrust sheets of rock interpreted to root in the Teslin tectonic zone are preserved as klippen on unmetamorphosed or low grade North American strata (Tempelman-Kluit 1979; Gordey 1981; Erdmer 1985, 1992). Some of the klippen are up to 100 km away from the zone (Gordey 1981) and may not have travelled by extrusion alone. Extension (gravitational collapse) off the uplifted block (cf. Sanderson and Marchini 1984), Middle Jurassic to mid-Cretaceous thrust-and-fold belt deformation east of the Teslin tectonic zone (Gordey 1981), and Cretaceous extension east of the zone (see Wheeler and McFeely 1991; Mortensen & Hansen 1992) may have added to their translation. To the west, the data are not as well constrained and Cretaceous strike-slip faulting and extension have obscured original relationships. However, in south-central Yukon, structural data show that planar fabrics in Yukon-Tanana terrane rocks dip dominantly northeast (Fig. 4-10). This is consistent with the interpretation that rocks were thrust to the southwest and thrust sheets may have rooted in the Teslin tectonic zone prior to Cretaceous strike-slip and extensional deformation. In addition, major regional thrust structures in the Intermontane Belt west of the Teslin tectonic zone are west-verging, whereas major structures east of the Teslin tectonic zone are east-verging (Gordey and Stevens 1994; Wheeler and McFeely 1991). Active movement on the west verging structures is constrained between ~170 and ~195 Ma (Ricketts et al. 1992; Gordey and Stevens 1994), which is the time of uplift and cooling (thrusting) of Teslin tectonic zone rocks.

Heterogeneous transpression and extrusion also provide a mechanism for the uplift of eclogite (Erdmer and Helmstaedt 1983), and its incorporation within

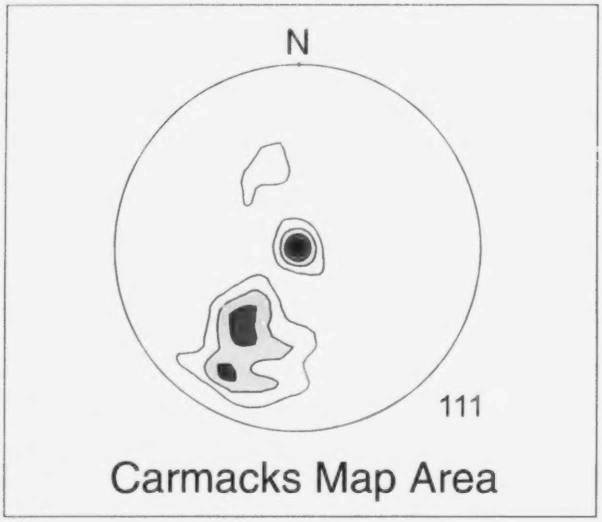

Figure 4-10: Orientation of foliation in Yukon-Tanana terrane rocks of the Carmacks 1:250 000 map area, after Tempelman-Kluit (1984). A prominent northeast dip is consistent with the interpretation that these rocks were thrust to the southwest and form a sheet that may have rooted in the Teslin tectonic zone to the northeast prior to Cretaceous strike-slip and extensional deformation.

schist of lower metamorphic grade.

The Teslin tectonic zone confirms the link between the structures of a ductile transpressive deformation zone and those commonly attributed to brittle transpression. It shows that "flower structures" are not confined to brittle deformation, but extend to mid-crustal levels and form at crustal-scale, as proposed by Jolivet and Huchon (1989). The preponderance of oblique dip-slip and pure dip-slip lineation over strike-slip indicates that thrust transpression dominated in the Teslin tectonic zone, and that a "flower structure" zone can occur in thrust dominated as well as strike-slip dominated regimes.

REFERENCES

Bell, T.H., and Johnson, S.E. 1992. Shear sense: a new approach that resolves conflicts between criteria in metamorphic rocks. Journal of Metamorphic Geology, **10**: 99-124.

Borradaile, G., and Spark, R. 1991. Deformation of the Archean Quetico-Shebandowan subprovince boundary in the Canadian Shield near Kashabowie, northern Ontario. Canadian Journal of Earth Sciences, **28**: 116-125.

Cobbold, P.R, and Watkinson, A.J. 1981. Bending anisotropy: a mechanical constraint on the orientation of fold axes in an anisotropic medium. Tectonophysics, **72**: T1-T10.

Culshaw, N. 1991. Post-collisional oblique convergence along the Thelon Tectonic Zone, north of the Bathurst Fault, NWT, Canada. Journal of Structural Geology, **13**: 501-516.

Erdmer, P. 1985. An examination of the cataclastic fabrics and structures of parts of Nisutlin, Anvil and Simpson allochthons, central Yukon: test of the arc-continent collision model. Journal of Structural Geology, **7**: 57-72.

Erdmer, P. 1992. Eclogitic rocks in the St. Cyr klippe, Yukon, and their tectonic significance. Canadian Journal of Earth Sciences, **29**: 1296-1304.

Erdmer, P., and Helmstaedt, H. 1983. Eclogite from central Yukon: a record of subduction at the western margin of ancient North America. Canadian Journal of Earth Sciences, **20**: 1389-1408.

Goodwin, L.B., and Williams, P.F. 1993. Partitioning of strike-slip and dip-slip movement within a transpressive shear zone; an example from the Appalachians. Geological Society of America, Abstracts with Programs, vol. 25, p. A-477.

Gordey, S.P. 1981. Stratigraphy, structure and tectonic evolution of southern Pelly Mountains in the Indigo Lake area, Yukon Territory. Geological Survey of Canada Bulletin 318.

Gordey, S.P., and Stevens, R.A. 1994. Tectonic framework of southern Yukon in the Teslin region. *In* Current research, 1994-A. Geological Survey of Canada, pp. 11-18.

Hanmer, S., and Passchier, C. 1991. Shear-sense indicators: a review. Geological Survey of Canada Paper 90-17.

Hansen, V.L. 1989. Structural and kinematic evolution of the Teslin suture zone, Yukon: record of an ancient transpressional margin. Journal of Structural Geology, **11**: 717-733.

Hansen, V.L. 1992a. Backflow and margin-parallel shear within an ancient subduction complex. Geology, **20**: 71-74.

Hansen, V.L. 1992b. P-T evolution of the Teslin suture zone and Cassiar tectonites, Yukon, Canada: evidence for A- and B-type subduction. Journal of Metamorphic Geology, **10**: 239-263.

Hansen, V.L., Mortensen, J.K., and Armstrong, R.L. 1989. U-Pb, Rb-Sr, and K-Ar isotopic constraints for ductile deformation and related metamorphism in the Teslin suture zone, Yukon-Tanana terrane, south-central Yukon.

Canadian Journal of Earth Sciences, **26**: 2224-2235.

Hansen, V.L., Heizler, M.T., and Harrison, T.M. 1991. Mesozoic thermal evolution of the Yukon-Tanana composite Terrane: new evidence from $^{40}Ar/^{39}Ar$ data. Tectonics, **10**: 51-76.

Harding, T.P. 1985. Seismic characteristics and identification of negative flower structures, positive flower structures, and positive structural inversions. American Association of Petroleum Geologists Bulletin, **69**: 582-600.

Harding, T.P., and Lowell, J.D. 1979. Structural styles, their plate-tectonic habitats, and hydrocarbon traps in petroleum provinces. American Association of Petroleum Geologists Bulletin, **63**: 1016-1058.

Harland, W.B. 1971. Tectonic transpression in Caledonian Spitsbergen. Geological Magazine, **108**: 27-42.

Holdsworth, R.E, and Strachan, R.A. 1991. Interlinked system of ductile strike slip and thrusting formed by Caledonian sinistral transpression in northeastern Greenland. Geology, **19**: 510-513.

Jolivet, L.. and Huchon, P. 1989. Crustal-scale strike-slip deformation in Hokkaido, northern Japan. Journal of Structural Geology, **11**: 509-522.

Jones, D.L., Silberling, N.J., Coney, P.J., and Plafker, G. 1987. Lithotectonic terrane map of Alaska (west of the 141st Meridian). United States Geological Survey Miscellaneous Field Studies Map MF-1874-A, scale, 1:2 500 000.

Kirkwood, D., and Malo, M. 1993. Across-strike geometry of the Grand Pabos fault zone: evidence for Devonian dextral transpression in the Quebec Appalachians. Canadian Journal of Earth Sciences, **30**: 1363-1373.

Lagarde, J.L., and Michard, A. 1986. Stretching normal to the regional thrust displacement in a thrust-wrench shear zone, Rehamna Massif, Morocco. Journal of Structural Geology, **8**: 483-492.

Lin, S., and Williams, P.F. 1993. A transpressional model for interpreting the variation in the pitch of the stretching lineation across the shear zone. Geological Association of Canada Abstracts with Programs, vol.18, p. A-60.

Lowell, J.D. 1972. Spitsbergen Tertiary orogenic belt and the Spitsbergen fracture zone. Geological Society of America Bulletin, **83**: 3091-3102.

Monger, J.W.H., and Berg, H.C. 1987. Lithotectonic terrane map of western Canada and southeastern Alaska. United States Geological Survey Miscellaneous Field Studies Map MF-1874-B, scale 1:2 500 000.

Mortensen, J.K. 1992. Pre-mid-Mesozoic tectonic evolution of the Yukon-Tanana Terrane, Yukon and Alaska. Tectonics, **11**: 836-853.

Mortensen, J.K., and Hansen, V.L. 1992. U-Pb and ^{40}Ar-^{39}Ar geochronology of granodioritic orthogneiss in the Western Pelly Mountains, Yukon Territory. *In* Geological Survey of Canada, Paper 92-2, pp. 125-128.

Price, R.A. 1986. The southeastern Canadian Cordillera: thrust faulting, tectonic wedging, and delamination of the lithosphere. Journal of Structural Geology, **8**: 239-254.

Read, P.B., Woodsworth, G.J., Greenwood, H.J., Ghent, E.D., and Evenchick, C.A. 1991. Metamorphic map of the Canadian Cordillera. Geological Survey of Canada Map 1714A, scale 1:2 000 000.

Ricketts, B.D., Evenchick, C.A., Anderson, R.G., and Murphy, D.C. 1992. Bowser basin, northern British Columbia: constraints on the timing of initial subsidence and Stikinia-North America terrane interactions. Geology, **20**: 1119-1122.

Robert, F. 1989. Internal structure of the Cadillac tectonic zone southeast of Val d'Or, Abitibi greenstone belt, Quebec. Canadian Journal of Earth Sciences, **26**: 2661-2675.

Robin, P.-Y.F., and Cruden, A.R. in press. Strain and vorticity patterns in ideally ductile transpressive zones. Journal of Structural Geology.

Sanderson, D.J., and Marchini, W.R.D. 1984. Transpression. Journal of Structural Geology, **6**: 449-458.

Stauffer, M.R., and Lewry, J.F. 1993. Regional setting and kinematic features of the Needle Falls Shear Zone, Trans-Hudson Orogen. Canadian Journal of Earth Sciences, **30**: 1338-1354.

Stevens, R.A. 1991. The Teslin suture zone in northwest Teslin map area, Yukon. *In* Current research, part A. Geological Survey of Canada, Paper 91-1A, pp. 271-277. *See appendix 1*

Stevens, R.A. 1992. Regional geology, fabric, and structure of the Teslin suture zone in northwest Teslin map area, Yukon Territory. *In* Current Research, part A. Geological Survey of Canada, Paper 92-1A, pp. 287-295. *See* *appendix 2*

Stevens, R.A. 1994. Geology of the Teslin suture zone in parts of Laberge (105E/1), Quiet Lake (105F/4) and Teslin (105C/11, 13, 14) map areas, Yukon Territory. Geological Survey of Canada, Open File 2768. *See appendix 6*

Stevens, R.A. in review. Regional geological correlations and metamorphism in the Teslin suture zone, south-central Yukon. Canadian Journal of Earth Sciences. *See chapter 2*

Stevens, R.A, and Erdmer. P. 1993. Geology and structure of the Teslin suture zone and related rocks in parts of Laberge, Quiet Lake, and Teslin map areas, Yukon Territory. *In* Current research, part A. Geological Survey of Canada, Paper 93-1A, pp. 11-20. *See appendix 3*

Stevens, R.A., Mortensen, J.K, and Hunt, P. A. 1993. U-Pb and ^{40}Ar-^{39}Ar geochronology of plutonic rocks from the Teslin suture zone, Yukon Territory. *In* Radiogenic age and isotopic studies, report 7. Geological Survey of Canada Paper 93-2, pp. 83-90. *See chapter 3*

Sylvester, A.G, and Smith, R.R. 1976. Tectonic transpression and basement-controlled deformation in San Andreas fault zone, Salton Trough, California. American Association of Petroleum Geologists Bulletin, **60**: 173-194.

Sylvester, A.G. 1988. Strike-slip faults. Geological Society of America Bulletin, **100**: 1666-1703.

Tempelman-Kluit, D.J. 1979. Transported cataclasite, ophiolite and granodiorite in Yukon: evidence of arc-continent collision. Geological Survey of Canada, Paper 79-14.

Tempelman-Kluit, D.J. 1984. Geology, Laberge (105E) and Carmacks (115I), Yukon Territory. Geological Survey of Canada, Open File 1101.

Watkinson, A.J. 1983. Patterns of folding and strain influenced by linearly anisotropic bands. Journal of Structural Geology, **5**: 449-454.

Wheeler, J.O., and McFeely, P., (comp.). 1991. Tectonic assemblage map of the Canadian Cordilleran and adjacent parts of the United States of America. Geological Survey of Canada, Map 1712A, scale 1:2 000 000.

Wheeler, J.O., Brookfield, A.J., Gabrielse, H., Monger, J.W.H., Tipper, H.W., and Woodsworth, G.J., (comp.). 1991. Terrane map of the Canadian Cordillera. Geological Survey of Canada, Map 1713A, scale 1:2 000 000.

CHAPTER 5 - TECTONIC EVOLUTION OF THE TESLIN TECTONIC ZONE, YUKON; SUBDUCTION, DUCTILE TRANSPRESSION, THRUSTING AND DEVELOPMENT OF A DOUBLY-VERGENT OROGEN*

*A version of this chapter has been submitted for publication. Stevens & Erdmer, 1994, Geology.

INTRODUCTION

The Teslin tectonic zone, one of the largest zones of ductilely deformed (sheared) rock in the North American Cordillera, records a complex history of ductile deformation and terrane accretion. Its position at the boundary between the accreted and autochthonous parts of the orogen make it a key tectonic element. When first named by Tempelman-Kluit (1979), the Teslin tectonic zone was interpreted as a Late Triassic to Early Jurassic subduction complex formed at an arc-ocean boundary outboard from the ancient North American passive margin. Collision of the arc terrane in the Late Jurassic resulted in obduction of trench melange onto North American shelf strata. This model was refined by Erdmer and Helmstaedt (1983) and Erdmer (1985) with the documentation of eclogite in the Teslin tectonic zone and the recognition that rocks of the Teslin tectonic zone record a wide range of strains and P-T conditions interpreted to reflect nearly all levels of a zone of subduction and collision. Subsequently, the importance of subduction-zone processes was emphasized by Hansen (1989, 1992a, 1992b), and Hansen et al. (1989, 1991). In Hansen's (1992a, 1992b) interpretation the Teslin tectonic zone preserves widespread high P/T metamorphic conditions that record backflow, margin-parallel flow, and downflow within a west-dipping B-type Permo-Triassic subduction complex. Recently, several aspects of this model have been re-evaluated by Stevens (in review) and Stevens and Erdmer (submitted). In particular, new field and analytical data lead Stevens (in review) to propose that most rocks of the Teslin tectonic zone are not the product of subduction accretion as previously thought, but rather form part of a coherent crustal terrane of Early Mississippian age, and that they generally preserve medium-, rather than high-pressure metamorphic assemblages. In addition, Stevens and Erdmer (submitted) proposed that the Teslin tectonic zone reflects deformation at the root of a crustal-scale transpressive, doubly-vergent shear zone rather than deformation in a subduction zone.

This paper incorporates the new data with existing local and regional geological data into a tectonic model of evolution for the Teslin tectonic zone from Early Permian to Late Cretaceous time and relates it to Cordilleran terrane evolution. As the proposed model departs from previous interpretations, several tests that can be applied to validate it are proposed.

TERRANE DIVISIONS

The Yukon-Tanana composite terrane, as defined by Monger and Berg (1987) and Jones et al. (1987), has been divided into several sub-terranes (Churkin et al. 1982; Aleinikoff et al. 1987; Wheeler et al. 1991; Hansen et al. 1991). In Yukon, Wheeler et al. (1991) divided the Yukon-Tanana terrane into the Pelly Gneiss and the Nisling, Slide Mountain and Nisutlin terranes, and Hansen et al. (1991) divided it into a "lower plate" of Devono-Mississippian peraluminous orthogneiss and host metasedimentary rock (referred to here as the peraluminous orthogneiss assemblage) and an "upper plate" consisting of the Nisutlin and Teslin-Taylor Mountain terranes. In this paper, the two-fold division of Hansen et al. (1991) is used, but the "upper plate" is not divided into two terranes. Here, the "upper plate" is the Nisutlin terrane as defined by Wheeler et al. (1991) and consists of Late Proterozoic?, Paleozoic, and possibly early Mesozoic metamorphosed and intensely deformed sedimentary, volcanic and plutonic rocks. The Slide Mountain terrane, which consists primarily of Mississippian to Permian oceanic sedimentary and volcanic strata (Nelson 1993), is distinct from the Nisutlin terrane, although it may be closely related (Hansen et al. 1991; Nelson 1993). Terranes west of the Teslin tectonic zone are not subdivided and are referred to here as the Intermontane superterrane. North America refers to strata of the Proterozoic to early Mesozoic passive western margin of cratonic North America.

GEOLOGY OF THE TESLIN TECTONIC ZONE

The Teslin tectonic zone, part of the Nisutlin terrane (Fig. 5-1), includes S-L-S and L-tectonites derived from sedimentary, volcanic and plutonic rocks metamorphosed under greenschist to amphibolite facies conditions (Hansen et al. 1989; Read et al. 1991; Stevens 1994, in review; Stevens and Erdmer 1993). Eclogite is preserved in one locality (Erdmer and Helmstaedt 1983). Garnet thermobarometry and the site-chemistry of amphiboles show that peak metamorphism occurred under "medium pressure" greenschist to amphibolite-facies conditions at 450-650°C (Stevens in review), with local preservation of higher P/T assemblages (Hansen 1992b). U-Pb analysis of zircon from metatonalite yielded Early Mississippian crystallization ages (Stevens et al. 1993) and ^{40}Ar-^{39}Ar analysis of hornblende, biotite and muscovite from several rock types yielded Early to Middle Jurassic cooling/uplift ages (179-195 Ma) (Hansen et al. 1991; Stevens et al. 1993). Preserved primary depositional and intrusive contacts, isotopic ages, and regional lithologic correlations indicate that the Teslin tectonic zone represents part of a regionally extensive continental-crust terrane (Nisutlin terrane) formed by mid-Mississippian time that underwent ductile deformation and metamorphism prior to the Middle Jurassic (Stevens in review).

At least two phases of deformation, an early penetrative ductile phase and a later and weaker folding/cleavage phase, have affected rocks of the Teslin tectonic zone (Stevens and Erdmer submitted). The penetrative ductile phase is characterized by lineated protomylonite and mylonite with local shear-sense indicators and by marked strain partitioning. The folding/cleavage phase is primarily recorded by the crenulation of the earlier fabrics, but also by local mesoscopic folds and a spaced brittle-ductile cleavage. Structural analysis revealed that the tectonic zone contains more than 25 domains each with different linear and/or planar fabric orientations and, in some cases, shear sense or structural style (Erdmer 1985; Hansen 1989; Stevens and Erdmer submitted).

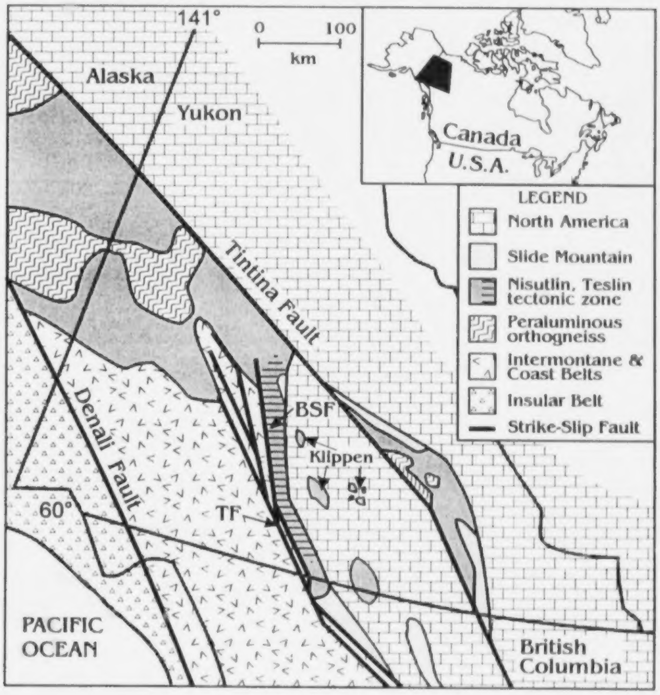
141°
0
100
km
Alaska
Yukon
Canada
U.S.A.
LEGEND
North America
Slide Mountain
Nisutlin, Teslin tectonic zone
Peraluminous orthogneiss
Intermontane & Coast Belts
Insular Belt
Strike-Slip Fault
Tintina Fault
Denali Fault
BSF
Klippen
TF
60°
PACIFIC OCEAN
British Columbia

Figure 5-1: Simplified terrane map of the northern Canadian and eastern Alaskan Cordillera (Modified from Abbott 1981; Hansen et al. 1991; Gordey and Stevens 1994; Wheeler et al. 1991). BSF = Big Salmon fault, TF = Teslin fault.

The characteristic features of these domains are northeast- or southwest-dipping foliation, variable but generally moderate- to steep-plunging lineation, and strike-slip, oblique-normal or oblique-reverse shear sense on both northeast- and southwest-dipping foliation. These features are consistent with formation under ductile transpression and are interpreted to reflect heterogeneous-thrust transpression at the ductile root of a crustal-scale, doubly-verging "flower structure" (Stevens and Erdmer submitted).

TECTONIC EVOLUTION

The proposed model of evolution is outlined schematically in Fig. 5-2. Tectonic events are interpreted to be part of a continuum and are separated into six stages in order to highlight the principal features.

Early Permian

By Early Permian time, the Nisutlin terrane (including rocks that comprise the Teslin tectonic zone) was part of a regionally extensive continental terrane outboard from the North American margin and separated from it by the Slide Mountain/Anvil Ocean (Fig. 5-2a) (Mortensen and Jilson 1985; Mortensen 1992; Stevens in review). At the present latitude of southern Yukon and northern British Columbia the Slide Mountain/Anvil Ocean is represented by Mississippian to Permian oceanic sedimentary and volcanic strata and is interpreted to have been a marginal sea (Nelson 1993). The peraluminous orthogneiss assemblage or "lower plate" of Yukon-Tanana terrane is interpreted to have been west of the Nisutlin terrane. The link between the Nisutlin terrane and the peraluminous orthogneiss assemblage is unconstrained, but the Nisutlin terrane may represent, in part, a continental margin assemblage formed along the eastern edge of a craton or continental arc represented by the peraluminous orthogneiss assemblage during the Devonian and Early Mississippian. To the west of the

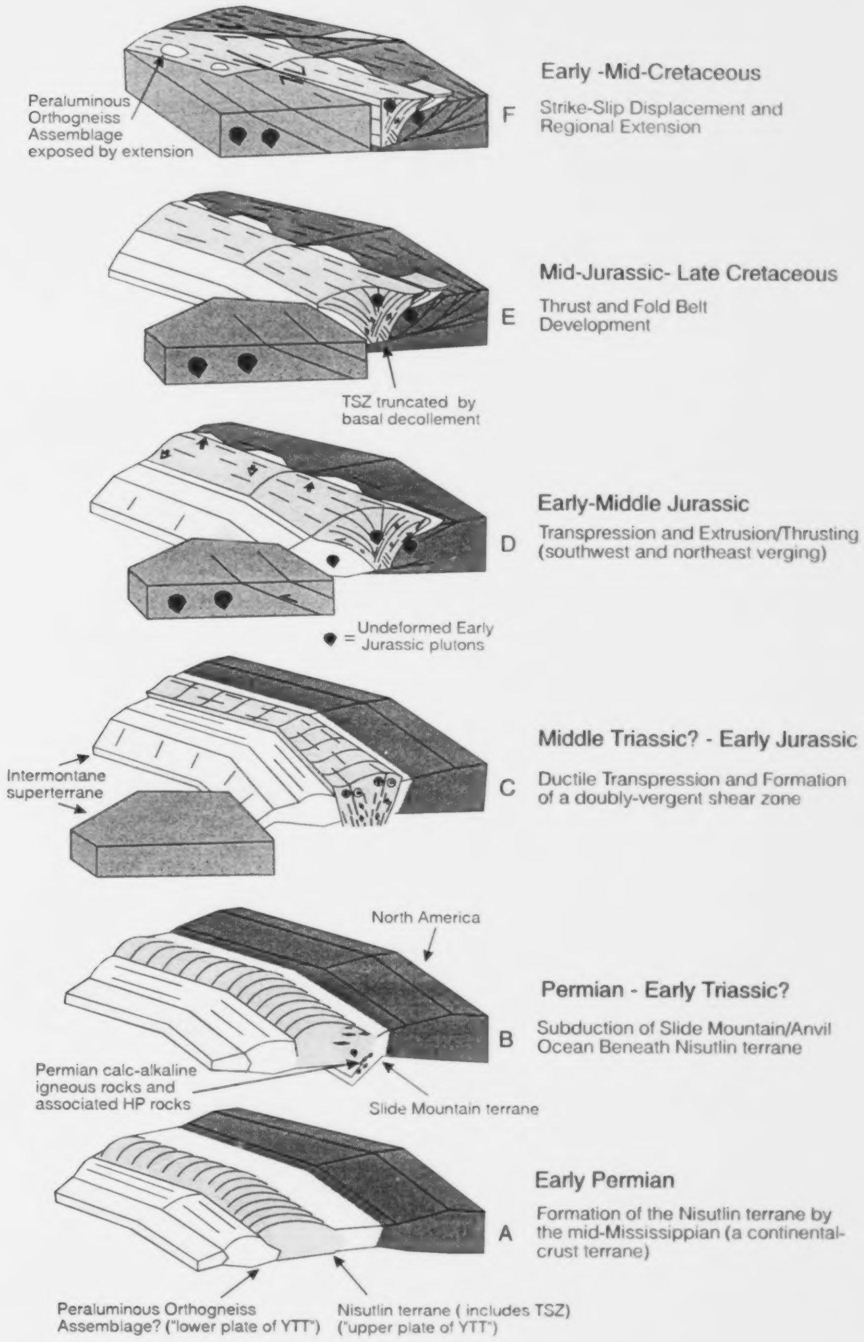
Early -Mid-Cretaceous
F
Strike-Slip Displacement and Regional Extension
Peraluminous Orthogneiss Assemblage exposed by extension
Mid-Jurassic- Late Cretaceous
E
Thrust and Fold Belt Development
TSZ truncated by basal decollement
Early-Middle Jurassic
D
Transpression and Extrusion/Thrusting (southwest and northeast verging)
= Undeformed Early Jurassic plutons
Middle Triassic? - Early Jurassic
C
Ductile Transpression and Formation of a doubly-vergent shear zone
Intermontane superterrane
North America
Permian - Early Triassic?
B
Subduction of Slide Mountain/Anvil Ocean Beneath Nisutlin terrane
Permian calc-alkaline igneous rocks and associated HP rocks
Slide Mountain terrane
Early Permian
A
Formation of the Nisutlin terrane by the mid-Mississippian (a continental-crust terrane)
Peraluminous Orthogneiss Assemblage? ("lower plate of YTT")
Nisutlin terrane (includes TSZ) ("upper plate of YTT")

Figure 5-2: Tectonic evolution model for the Teslin tectonic zone, which includes a history of subduction, ductile transpression, uplift and thrusting, development of a doubly-vergent orogen, and strike-slip faulting.

peraluminous orthogneiss assemblage were oceanic domains represented by the Intermontane superterrane (possibly Cache Creek or Windy-McKinley terranes; see Wheeler et al. 1991).

Permian to Early Triassic?

During Permian to Early Triassic time, the Slide Mountain/Anvil Ocean crust subducted beneath the Nisutlin terrane (Fig. 5-2b), with possible secondary subduction within the Slide Mountain/Anvil ocean to the east (see Nelson 1993). Subduction is recorded by Permian calc-alkaline igneous rocks in central Yukon (Mortensen 1992) and by high-pressure metamorphic rocks with Permian cooling ages (Fig. 5-2b) (Erdmer and Armstrong 1988; Wanless et al. 1978). The calc-alkaline rocks have continental-arc geochemical affinities and are interpreted to reflect the presence of a short-lived northeast facing arc, built on the Nisutlin terrane (Mortensen 1992). Ductile deformation of Nisutlin terrane rocks began at this time.

Middle Triassic? to Early Jurassic

The main penetrative deformation of rocks in the Teslin tectonic zone and Nisutlin terrane occurred from Middle Triassic? to Early Jurassic. Closure of the Slide Mountain/Anvil Ocean by the Middle Triassic? juxtaposed the Nisutlin terrane with the North American margin and formed a crustal-scale ductile, heterogeneous transpression deformation environment in the Teslin tectonic zone (Fig. 5-2c). The penetrative strain zone was bound to the east by North America and to the west by the Nisutlin terrane and/or the peraluminous orthogneiss assemblage. Northeasterly- and southwesterly-dipping mylonitic foliation, variable lineation orientations, and normal, reverse, and strike-slip shear with northeast or southwest vergence record this deformation. Heterogenous transpressional strain and extrusion, a consequence of transpression, provide a mechanism for the preservation of a wide range of strains and metamorphic environments (including eclogite facies) in the Teslin tectonic zone.

Extrusion/thrusting of Teslin tectonic zone tectonites out of the zone and the formation of a topographic welt also likely began at this time.

Early to Middle Jurassic

The main phase of regional west- and east-verging thrusting out of the Teslin tectonic zone was confined to the Early to Middle Jurassic. Cooling/uplift ages from Teslin tectonic zone rocks range from 184 to 195 Ma (Hansen et al. 1991; Hunt and Roddick 1992), and an undeformed pluton cutting Teslin tectonic zone tectonites yields U-Pb crystallization ages of 193-188 Ma and ^{40}Ar-^{39}Ar cooling ages of 179-182 Ma (Stevens et al. 1993). In addition, hornblende and biotite pairs yielded cooling ages within a few million years of each other (Stevens et al. 1993). These data indicate that different parts of the zone were uplifted and rapidly cooled at different times during the Early-Middle Jurassic. Thrusts separating individual sheets that presumably cooled coherently have not been recognized, possibly because of the complex mix of strains and juxtaposition of similar rock types make them difficult to identify. Regionally, rocks of the Nisutlin terrane were involved in thrusting as early as Late Triassic time (Mortensen 1992)

The initial stages of this thrusting event are interpreted to be preserved in the Teslin tectonic zone by the crenulation and folding of ductile fabrics and by the development of cleavage. The doubly-vergent character of the tectonic zone continues and is preserved by brittle-ductile cleavage with opposite dip-directions and normal or reverse separation. The Teslin tectonic zone also marks the regional boundary between east- and west-verging structures. To the east, thrust sheets of rock interpreted to root in the Teslin tectonic zone are preserved as klippen on unmetamorphosed or low grade North American strata (Tempelman-Kluit 1979; Gordey 1981; Erdmer 1992). To the west, in central Yukon, the data are poorly constrained, but allow the interpretation that rocks of the Nisutlin terrane occur in west-verging thrust sheets (see chapter 4; Stevens and Erdmer submitted). In addition, major regional thrusts in the Intermontane superterrane are west-verging, whereas major structures east of the Teslin tectonic zone are east-verging (Gordey 1981; Gordey and Stevens 1994; Wheeler and McFeely 1991). Movement on west-verging structures is constrained between ≈170 and ≈195 Ma (Ricketts et al. 1992; Gordey and Stevens 1994), which is the time of uplift and cooling (thrusting) of Teslin tectonic zone rocks.

Middle Jurassic to Late Cretaceous

Thrusting and folding of North American strata east of the Teslin tectonic zone characterize this period. In southern Yukon, the Teslin tectonic zone marks the western limit of foreland thrust- and fold-belt deformation in North American strata (Fig. 5-2e). The uplift and thrusting of Teslin tectonic zone tectonites out of the zone may mark the beginning of the foreland deformation, as deformed rocks interpreted to be part of the North American margin are cut by an Early Jurassic pluton (^{40}Ar-^{39}Ar hornblende age of 185 ± 3 Ma; Gordey and Stevens 1994), suggesting foreland deformation had begun by the Early Jurassic. Elsewhere, the timing of thrusting and folding is not well constrained. In the Cassiar terrane it is interpreted to have occurred after Late Triassic and before mid-Cretaceous time (Gordey 1981) and it lasted until at least the Early Cretaceous in the Selwyn and Mackenzie mountains (Gordey and Anderson 1993).

After uplift and cooling of Teslin tectonic zone tectonites in the Early to Middle Jurassic, the foreland deformation does not appear to have affected Teslin tectonic zone rocks. It is suggested that subsequent to uplift the Teslin tectonic zone was transported eastward as a coherent block over a decollement related to thrust- and fold-belt deformation (Fig. 5-2e).

Klippen of rock interpreted to root into the Teslin tectonic zone are found up to 100 km to the northeast of the tectonic zone (Fig. 5-1) (Gordey 1981) and may not have travelled as a result of Early to Middle Jurassic thrusting alone. Extensional sliding (gravitational collapse) off the uplifted block (Fig 5-2e) (c.f. Sanderson and Marchini 1984), Middle Jurassic to mid-Cretaceous thrusting and folding east of the tectonic zone, and possible Cretaceous extensional faulting east of the tectonic zone (see below) may have contributed to post-Middle Jurassic movement of these far travelled klippen.

Early to Mid-Cretaceous

Strike-slip deformation and extensional unroofing dominated during the Early- to mid-Cretaceous (Fig. 5-2f). The western margin of the Teslin tectonic zone was truncated and it is interpreted that strike-slip along the Teslin and Big Salmon faults and possibly along several other faults in the Intermontane superterrane transported part of the Teslin tectonic zone northwards together with any thrust sheets to the west (Fig. 5-2f). The displaced rocks may now be exposed in central Yukon (Fig. 5-1).

Relatively primitive isotopic signatures for mid-Cretaceous and younger plutonic rocks in the Intermontane superterrane west of the Teslin tectonic zone have been interpreted to indicate that no North American Precambrian continental basement is present (Morrison et al. 1979; Mihalynuk et al. 1992). This suggests that the Teslin tectonic zone may have been transported eastward over transitional crust during Middle Jurassic to mid-Cretaceous thrusting and folding (i.e. continental basement does not extend west of the Teslin tectonic zone), or alternatively, that basement rocks were truncated by strike-slip faulting (Fig. 5-2f), and transported northward along with the western margin of the tectonic zone.

In east-central Alaska, Hansen et al. (1991) and Dusel-Bacon and Hansen (1992) reported that the peraluminous orthogneiss assemblage (Lake George subterrane) generally yielded Early Cretaceous cooling ages which they interpreted to result from extensional unroofing. It is suggested that rocks of the peraluminous orthogneiss assemblage in west-central and southeastern Yukon were originally overthrust in the Early to Middle Jurassic by west-verging slices of Nisutlin terrane which rooted into the Teslin tectonic zone or its possible extension, the Finlayson fault zone (see Mortensen and Jilson 1985). They were subsequently exposed during Cretaceous extension. Extension may also have affected parts of the Cassiar terrane east of the Teslin tectonic zone, where Hansen et al. (1991) determined Cretaceous cooling ages and where Mortensen and Hansen (1992) suggested that rocks were ductilely deformed and metamorphosed at mid-crustal levels and then cooled rapidly through ~300°C during the mid-Cretaceous.

TESTS OF THE MODEL

Much of the geology of the Yukon Territory is known only at a reconnaissance level which means that several aspects of this model are supported by only a limited database and are testable with additional study. In the Teslin tectonic zone, further identification of primary depositional and intrusive relationships can test the interpretation that most rocks of the Teslin tectonic zone were together by the Early Mississippian. Additional metamorphic P-T study and cooling age data can help determine the degree of preservation and age of subduction zone metamorphism in the Teslin tectonic zone, and indicate whether relatively uniform P-T and cooling histories are preserved in individual thrust slices.

Elsewhere in the northern Cordillera, additional data are required to: 1) evaluate the size and age of the Permian continental arc interpreted to have formed on Nisutlin terrane and determine whether the arc rocks continue to be coeval with high pressure metamorphic rocks in the Nisutlin terrane; 2) delineate thrust sheets in the Nisutlin terrane in central Yukon and confirm their southwest vergence; 3) determine cooling ages for peraluminous orthogneiss assemblage rocks in Yukon to confirm whether they are similar to those in Alaska; 4) determine the amount of Cretaceous extension in the Cassiar terrane east of the tectonic zone; 5) establish whether some klippen were transported eastward by processes other than Early to Middle Jurassic thrusting and; 6) estimate the amount of strike-slip displacement on the Teslin and Big Salmon faults and identify the offset western margin of the tectonic zone.

REFERENCES

Abbott, J.G. 1981. Geology of the Seagull tin district. *In* Yukon Geology and Exploration 1979-1980, Indian and Northern Affairs Canada, pp. 32-44.

Aleinikoff, J.N., Dusel-Bacon, C., Foster, H.L., and Nokleberg, W.J. 1987. Lead isotopic fingerprinting of tectonostratigraphic terranes, east-central Alaska. Canadian Journal of Earth Sciences, **24**: 2089-2098.

Churkin, M., Jr., Foster, H.L., Chapman, R.M., and Weber, F.R. 1892. Terranes and suture zones in east-central Alaska. Journal of Geophysical Research, **87**: 3178-3730.

Dusel-Bacon, C., Hansen, V.L. 1992. High-pressure amphibolite-facies metamorphism and deformation within the Yukon-Tanana and Taylor Mountain terranes, eastern Alaska. *In* Geological Studies in Alaska by the U.S. Geological Survey, 1991. *Edited by* D.C. Bradely and C. Dusel-Bacon. U.S. Geological Survey Bulletin 2041, pp. 140-159.

Erdmer, P. 1985. An examination of the cataclastic fabrics and structures of parts of Nisutlin, Anvil and Simpson allochthons, central Yukon: test of the arc-continent collision model. Journal of Structural Geology, **7**: 57-72.

Erdmer, P. 1992. Eclogitic rocks in the St. Cyr klippe, Yukon, and their tectonic significance. Canadian Journal of Earth Sciences, **20**: 1296-1304.

Erdmer, P., and Helmstaedt, H. 1983. Eclogite from central Yukon: a record of subduction at the western margin of ancient North America. Canadian Journal of Earth Sciences, **20**: 1389-1408.

Erdmer, P., and Armstrong, R.L., 1988, Permo-Triassic isotopic dates for blueschist, Ross River area, Yukon. *In* Yukon Geology vol. 2, Exploration and Geological Services Division, Yukon, Indian and Northern Affairs Canada, pp. 33-36.

Gordey, S.P. 1981. Stratigraphy, structure and tectonic evolution of southern Pelly Mountains in the Indigo Lake area, Yukon Territory. Geological Survey of Canada, Bulletin 318, 54 p.

Gordey, S.P., and Anderson, R.G. 1993. Evolution of the northern Cordilleran miogeocline, Nahanni map area (105I), Yukon and Northwest territories. Geological Survey of Canada, Memoir 428, 214 p.

Gordey, S.P., and Stevens, R.A. 1994. Tectonic framework of southern Yukon in the Teslin region. *In* Current research, 1994-A, Geological Survey of Canada, pp. 11-18.

Hansen, V.L. 1989. Structural and kinematic evolution of the Teslin suture zone, Yukon: record of an ancient transpressional margin. Journal of Structural Geology, **11**: 717-733.

Hansen, V.L. 1992a. Backflow and margin-parallel shear within an ancient subduction complex. Geology, **20**: 71-74.

Hansen, V.L. 1992b. P-T evolution of the Teslin suture zone and Cassiar tectonites, Yukon, Canada: evidence for A- and B-type subduction. Journal of Metamorphic Geology, **10**: 239-263.

Hansen, V.L., Mortensen, J.K., and Armstrong, R.L. 1989. U-Pb, Rb-Sr, and K-Ar isotopic constraints for ductile deformation and related metamorphism in the Teslin suture zone, Yukon-Tanana Terrane, south-central Yukon. Canadian Journal of Earth Sciences, **20**: 2224-2235.

Hansen, V.L., Heizler, M.T., and Harrison, T.M. 1991. Mesozoic thermal evolution of the Yukon-Tanana composite Terrane: new evidence from $^{40}Ar/^{39}Ar$ data. Tectonics, **10**: 51-76.

Hunt, P.A., and Roddick, J.C. 1992. A compilation of K-Ar and ^{40}Ar-^{39}Ar ages: report 22. *In* Radiogenic Age and Isotopic Studies: Report 6, Geological Survey of Canada, Paper 92-2, pp. 192-193.

Jones, D.L., Silberling, N.J., Coney, P.J. and Plafker, G. 1987. Lithotectonic terrane map of Alaska (west of the 141st Meridian). U.S. Geological Survey Miscellaneous Field Studies Map MF-1874-A, scale, 1:2 500 000.

Mihalynuk, M.G., Smith, M.T., Gabites, J.E., Runkle, D., and Lefebure, D. 1992. Age of emplacement and basement character of the Cache Creek terrane as constrained by new isotopic and geochemical data. Canadian Journal of Earth Sciences, **29**: 2463-2477.

Monger, J.W.H., and Berg, H.C. 1987. Lithotectonic terrane map of western Canada and southeastern Alaska. U.S. Geological Survey Miscellaneous Field Studies Map MF-1874-B, scale 1:2 500 000.

Morrison, G.W., Godwin, C.I., and Armstrong, R.L. 1979. Interpretation of isotopic ages and $^{87}Sr/^{86}Sr$ initial ratios for plutonic rocks in the Whitehorse map area, Yukon. Canadian Journal of Earth Sciences, **16**: 1988-1997.

Mortensen, J.K. 1992. Pre-mid-Mesozoic tectonic evolution of the Yukon-Tanana terrane, Yukon and Alaska. Tectonics, **11**: 836-853.

Mortensen, J.K., and Jilson, G.A. 1985. Evolution of the Yukon-Tanana Terrane: evidence from southeastern Yukon Territory. Geology, **13**: 806-810.

Mortensen, J.K., and Hansen, V.L. 1992. U-Pb and ^{40}Ar-^{39}Ar geochronology of granodioritic orthogneiss in the Western Pelly Mountains, Yukon Territory. *In* Geological Survey of Canada, Paper 92-2, pp. 125-128.

Nelson, J.L. 1993. The Sylvester Allochthon: upper Paleozoic marginal-basin and island-arc terranes in northern British Columbia. Canadian Journal of Earth Sciences, **30**: 631-643.

Read, P.B., Woodsworth, G.J., Greenwood, H.J., Ghent, E.D., and Evenchick, C.A. 1991. Metamorphic map of the Canadian Cordillera. Geological Survey of Canada, Map 1714A, scale 1:2 000 000.

Ricketts, B.D., Evenchick, C.A., Anderson, R.G., and Murphy, D.C. 1992. Bowser basin, northern British Columbia: constraints on the timing of initial subsidence and Stikinia-North America terrane interactions. Geology, **20**: 1119-1122.

Sanderson, D.J., and Marchini, W.R.D. 1984. Transpression. Journal of Structural Geology, **6**: 449-458.

Stevens, R.A. 1994. Geology of the Teslin suture zone in parts of Laberge (105E/1), Quiet Lake (105F/4) and Teslin (105C/11, 13, 14) map areas, Yukon Territory. Geological Survey of Canada, Open File 2768. *See appendix 6*

Stevens, R.A. in review. Regional geological correlations and metamorphism in the Teslin suture zone, south-central Yukon. Canadian Journal of Earth

Sciences. *See chapter 2*

Stevens, R.A., and Erdmer, P. 1993. Geology and structure of the Teslin suture zone and related rocks in parts of Laberge, Quiet Lake, and Teslin map areas, Yukon Territory. *In* Current Research, Part A, Geological Survey of Canada, Paper 93-1A, pp. 11-20.

Stevens, R.A., and Erdmer, P. submitted. Characteristics of ductile transpression and an example from the Teslin suture zone, northern Canadian Cordillera. Journal of Structural Geology. *See chapter 4*

Stevens, R.A., Mortensen, J.K., and Hunt, P. A. 1993. U-Pb and ^{40}Ar-^{39}Ar geochronology of plutonic rocks from the Teslin suture zone, Yukon Territory. *In* Radiogenic Age and Isotopic Studies, Report 7, Geological Survey of Canada, Paper 93-2, pp. 83-90. *See chapter 3*

Tempelman-Kluit, D.J. 1979. Transported cataclasite, ophiolite and granodiorite in Yukon: evidence of arc-continent collision. Geological Survey of Canada, Paper 79-14, 27 p.

Wanless, R.K., Stevens, R.D., Lachance, G.R., and Delabio, R.N. 1978. Age determinations and geological studies, K-Ar isotopic ages, report 13. Geological Survey of Canada, Paper 77-2, p. 60.

Wheeler, J.O., and McFeely, P., (comp.). 1991. Tectonic assemblage map of the Canadian Cordilleran and adjacent parts of the United States of America. Geological Survey of Canada Map 1712A, scale 1:2 000 000.

Wheeler, J.O., Brookfield, A.J., Gabrielse, H., Monger, J.W.H., Tipper, H.W., and Woodsworth, G.J., (comp.). 1991. Terrane map of the Canadian

Cordillera. Geological Survey of Canada Map 1713A, scale 1:2 000 000.

CHAPTER 6 - CONCLUSIONS

This study documents the geology, metamorphism, geochronology, structure and tectonic evolution of the Teslin tectonic zone, a part of the Yukon-Tanana or Nisutlin terrane in the northern Canadian Cordillera.

Most of the study area is underlain by four units of ductilely deformed rock; a siliceous schist and quartzite unit, a graphitic phyllite unit, a meta-tonalite to quartz-diorite unit and a metagabbro and greenstone unit. U-Pb zircon dating of meta-tonalite yielded Early Mississippian crystallization ages. This data combined with preservation of primary depositional and intrusive relationships reveal that most rocks in the study area were together by the mid-Mississippian. Rocks from this study are also readily correlated with rocks of the Yukon-Tanana or Nisutlin terrane described by Tempelman-Kluit (1979), Hansen et al. (1991), and Mortensen (1992). This is interpreted to indicate that the Teslin tectonic zone is part of a regionally extensive continental terrane formed by the mid-Mississippian.

Amphibole chemistry and garnet-based geothermobarometry from this study and re-evaluation of P-T data from previous studies (Hansen 1987, 1992b) indicate that most rocks were metamorphosed under medium pressure at 450-650°C, with local preservation of higher P/T assemblages. Subduction zone metamorphism is not required to explain most of the available P-T data.

At least two phases of deformation, an early penetrative ductile phase and a later and weaker folding/cleavage phase, have affected rocks of the Teslin tectonic zone. The penetrative ductile phase is characterized by lineated protomylonite and mylonite with local shear-sense indicators and by marked strain partitioning. The folding/cleavage phase is primarily recorded by the crenulation of the earlier fabrics, but also by local mesoscopic folds and a spaced brittle-ductile cleavage. Structural analysis revealed that the Teslin tectonic zone contains more than 25 domains each with different linear and/or planar fabric orientations and, in some cases, shear sense or structural style. The characteristic features of these domains are northeast- or southwest-dipping foliation, variable but generally moderate- to steep-plunging lineation, and strike-slip, oblique-normal or oblique-reverse shear sense on both northeast- and southwest-dipping foliation. These features are consistent with formation under ductile transpression and are interpreted to reflect heterogeneous-thrust transpression at the ductile root of a crustal-scale, doubly-vergent "flower structure".

Previous models for the tectonic evolution of the Teslin tectonic zone proposed that its rocks are the product of deformation within the deep-seated portion of a west-dipping B-type Permo-Triassic subduction complex. The tectonites were interpreted to have been subsequently thrust eastward as a coherent sheet onto autochthonous strata in the Early Jurassic as a result of A-type subduction (Hansen 1992a). The results of this study cannot support this model in several respects. In particular, the notion that rocks of the Teslin tectonic zone are the product of subduction accretion and that there is widespread preservation of subduction zone metamorphic conditions needs to be re-evaluated; and the doubly-vergent character of the zone, as identified in this study, needs to be addressed.

In order to accommodate the results of this study, a new tectonic model of evolution for the Teslin tectonic zone is proposed that includes: 1) formation of the continental Nisutlin terrane (including the rocks that comprise the Teslin tectonic zone) by the mid-Mississippian; 2) Permian - Early Triassic? west-dipping subduction of the Slide Mountain Ocean crust beneath the Nisutlin terrane; 3) Middle Triassic? - Early Jurassic crustal-scale, ductile, heterogeneous, thrust transpressive shearing and formation of a doubly-vergent shear zone; 4) Early - Middle Jurassic, regional northeast and southwest-verging thrusting; 5) Middle Jurassic to mid-Cretaceous foreland thrust and fold belt development which transported the Teslin tectonic zone eastward as a coherent package over a basal decollement; and 6) Mid-Cretaceous extensional unroofing, and dextral strike-slip faulting which truncated the western margin of the Teslin tectonic zone and transported it northward.

REFERENCES

Hansen, V.L. 1987. Structural, metamorphic, and geochronologic evolution of the Teslin suture zone, Yukon: evidence from Mesozoic oblique convergence outboard of the northern Canadian Cordillera. Ph.D. thesis, University of California, Los Angeles, California.

Hansen, V.L. 1992a. Backflow and margin-parallel shear within an ancient subduction complex. Geology, **20**: 71-74.

Hansen, V.L. 1992b. P-T evolution of the Teslin suture zone and Cassiar tectonites, Yukon, Canada: evidence for A- and B-type subduction. Journal of Metamorphic Geology, **10**: 239-263.

Hansen, V.L., Heizler, M.T., and Harrison, T.M. 1991. Mesozoic thermal evolution of the Yukon-Tanana composite Terrane: new evidence from $^{40}Ar/^{39}Ar$ data. Tectonics, **10**: 51-76.

Mortensen, J.K. 1992. Pre-mid-Mesozoic tectonic evolution of the Yukon-Tanana Terrane, Yukon and Alaska. Tectonics, **11**: 836-853.

Tempelman-Kluit, D.J. 1979. Transported cataclasite, ophiolite and granodiorite in Yukon: evidence of arc-continent collision. Geological Survey of Canada, Paper 79-14.

APPENDIX 1 - THE TESLIN SUTURE ZONE IN NORTHWEST TESLIN MAP AREA, YUKON: PUBLISHED IN GEOLOGICAL SURVEY OF CANADA PAPER 91-1A*

---

*A version of this appendix has been published. Stevens, R.A., 1991. *In* Current Research, Part A, Geological Survey of Canada, Paper 91-1A, pp. 271-277.

The Teslin suture zone in northwest Teslin map area, Yukon

R.A. Stevens[1]
Cordilleran Division, Vancouver

Stevens, R.A., The Teslin suture zone in northwest Teslin map area, Yukon; in Current Research, Part A, Geological Survey of Canada, Paper 91-1A, p. 271-277, 1991.

Abstract

The geology of the study area can be divided into two categories. The first is Teslin suture zone map units and consists of graphitic phyllite, siliceous schist and quartzite, an intermediate plutonic unit, marble, greenstone, hornblende tonalite to quartz diorite and diorite. Rocks in this category display mylonitic fabrics and thus are considered to be older than, or coeval with, deformation in the suture zone. Rocks of the second category, lack foliation and thus are considered to postdate deformation in the suture zone. Teslin suture zone map units can be further subdivided based on the penetrativeness of strain. The first four rock types display almost continuous ductile deformation, whereas the remaining two are ductilely deformed in zones bordered by massive to weakly deformed rock. All ductilely deformed rocks show a variety of planar and linear fabrics, folds and rare kinematic indicators.

Résumé

La géologie de la région à l'étude a été divisée en deux catégories. La première est constituée des unités cartographiques de la zone de suture de Teslin et est composée de phyllite graphitique, de schiste siliceux et de quartzite, d'une unité plutonique intermédiaire, de marbre, de roches vertes, de tonalite à hornblende se transformant en diorite quartzitique et de diorite. Les roches de cette catégorie présentent une fabrique mylonitique et sont donc considérées plus anciennes que la déformation de la zone de suture ou du moins contemporaine à celle-ci. Les roches de la seconde catégorie ne présentent pas de foliation et sont donc considérées postérieures à la déformation de la zone de suture. Les unités cartographiques de la carte de la zone de suture de Teslin peuvent être davantage subdivisées en fonction de la pénétration de la déformation. Les quatre premiers types de roches présentent une déformation ductile presque continue tandis que les deux autres types ont été déformés de façon ductile dans des zones bordées de roches dont le degré de déformation varie d'énorme à faible. Toutes les roches déformées de façon ductile sont caractérisées par diverses fabriques planaires et linéaires, des plis et de rares indicateurs cinématiques.

---

[1] Department of Geology, University of Alberta, Edmonton, Alberta T6G 2E3

INTRODUCTION

This report presents the results of field mapping in part of the Teslin suture zone located in the northwest quarter of the Teslin map area (NTS 105C). During June and July of 1990, mapping at 1:50 000 scale was accomplished northwest of the Canol Road, east of Johnsons Crossing, to Slate Mountain at the northern limit of the Teslin map area (Fig. 1). This mapping forms part of the author's Ph.D. project to investigate the geological evolution of the Teslin suture zone and to contribute towards understanding the tectonic history of the southern Yukon-Tanana Terrane.

REGIONAL SETTING AND PREVIOUS WORK

The Yukon-Tanana Terrane (Kootenay terrane of Wheeler et al., 1988) is a metamorphic-plutonic assemblage exposed in southern Yukon and east-central Alaska. It rests structurally above and adjacent to autochthonous North American rocks on the east and is in fault contact with accreted oceanic and island arc terranes of the Intermontane Belt to the west (Tempelman-Kluit, 1979; Hansen, 1989; Mortensen, in press). Over most of its length its characteristic fabrics are relatively flat-lying, however in southern Yukon they become steeply dipping within a mélange of ductilely deformed rocks of the Teslin suture zone (Erdmer, 1985; Hansen, 1989). The Teslin suture zone was named by Tempelman-Kluit (1979) and extends from north of the Laberge map area (NTS 105E), into the northwest part of the Teslin map area (Fig. 2). Hansen (1989) defined the Teslin suture zone to be "The package of rocks comprising the 15-20 km wide steeply-dipping portion of the Yukon-Tanana Terrane in southern Yukon."

In the Laberge map area the Teslin suture zone has been the locus of several studies (Tempelman-Kluit, 1979, 1984; Erdmer, 1985; Hansen, 1989; Hansen et al., 1989). These demonstrate that the suture zone consists of three assemblages of ductilely deformed metamorphic rocks with L-S tectonite fabrics. Individual assemblages outcrop as discrete, lensoid belts, 3-4 km wide and 20-30 km long. They include mylonitic siliceous and calcareous metasedimentary rocks (Nisutlin Allochthon or Assemblage), mafic metasedimentary and metavolcanic rocks (Anvil Allochthon or Assemblage) and orthogneiss (Simpson Allochthon in Erdmer, 1985 and Tempelman-Kluit, 1979 or peraluminous orthogneiss assemblage in Hansen et al., 1989). The Nisutlin and Anvil allochthons are metamorphosed to greenschist and albite-epidote amphibolite facies and preserve pre-Late Jurassic metamorphic cooling ages (Hansen, 1990). Orthogneiss of the Simpson Allochthon or peraluminous orthogneiss assemblage preserve Devono-Mississippian crystallization ages with Jurassic to Early Cretaceous metamorphic cooling ages (Hansen, 1990).

Hansen (1989) divided the Teslin suture zone into two structural domains, "Based on the distribution of two well-defined but differently oriented stretching lineations." These structures record a complex history of deformation that involved extensional shear, thrust shear and strike-slip shear and are interpreted to result from terrane accretion during oblique plate convergence.

Reconnaissance geology of the Teslin map area was described by Mulligan (1963). In addition, the geology of the northwest part of the map area is described by Lees (1936). The Teslin map area is presently being remapped at 1:50 000 and 1:250 000 scale by S.P. Gordey of the Geological Survey of Canada.

TESLIN SUTURE ZONE MAP UNITS

The geology of the study area is shown in Figure 1. On the basis of fabric development rock units can be divided into two categories. Rocks in the first, described under the heading Teslin Suture Zone Map Units, consist of three metasedimentary and four meta-igneous units which display mylonitic textures and are therefore considered to be older than, or coeval with, deformation in the suture zone. Rocks in the second category, described under the heading Other Map Units, consist of one sedimentary and three igneous units that lack foliation and are therefore considered to postdate development of the Teslin suture zone.

Graphitic Phyllite Unit (OD_N?)

This unit includes fissile, rusty red to black, fine grained (<1 mm), pyritic, graphitic phyllite, as well as calcareous graphitic phyllite, siliceous graphitic phyllite and marble. The rock types outcrop on ridges east and west of Red Mountain Creek, along a ridge northwest of the confluence of Sidney and Iron creeks, and near Muskrat Lake. Pyrite occurs as fine grained, variably oriented to layer parallel crystals or as coarse grained (>5 mm), cubic to subcubic crystals with quartz pressure shadows and tails. Chlorite and minor micas occur on foliation surfaces. Marble bands 10-30 m wide are locally interlayered with the graphitic phyllite and larger bands several hundred metres wide are also found. Minor greenstone and muscovite-biotite-graphite bearing impure quartzite are associated with the unit.

Contact relations indicate that rocks of units PMtqd, Kqm and K_{RM} (see descriptions below) intrude the Graphitic Phyllite unit. Sharp, fabric parallel contacts with diorite of unit PMd and in a few places with unit PMtqd are the result of strain along the contact.

North of the study area rocks similar to this assemblage have been described within the Teslin suture zone and are interpreted to be part of the autochthonous Nasina Formation (Tempelman-Kluit, 1977, 1984) or part of the Nisutlin Allochthon (Erdmer, 1985). Rocks of the Nasina Formation are primarily graphitic siltstones (Tempelman-Kluit, 1984), whereas rocks of the Nisutlin Allochthon are primarily muscovite-quartz schists and other siliceous rocks that are interfoliated with minor graphitic phyllites, slates and quartzites (Erdmer, 1985). At present it appears that the Graphitic Phyllite unit in the Teslin map area is not part of Nisutlin Allochthon, because although siliceous rocks (unit PMs) possibly correlative with the Nisutlin Allochthon are found in the map area, they are spatially and lithologically distinct from the graphitic phyllite rocks. The Graphitic Phyllite unit is interpreted to be part of the autochthonous Ordovician-Devonian Nasina Formation which has been caught up in the deformation of, and incorporated into the Teslin suture zone.

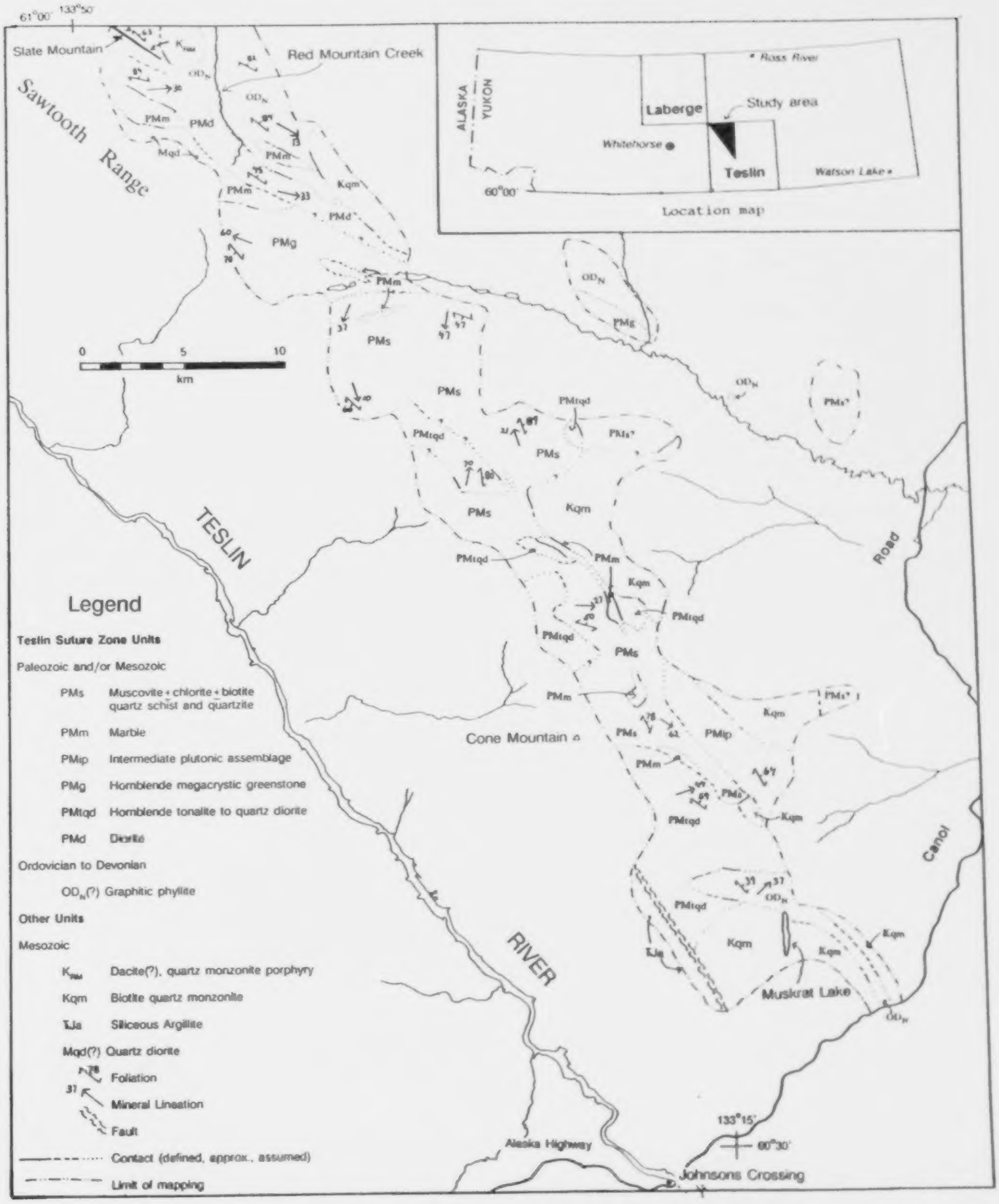
61°00'
133°50'
Slate Mountain
Red Mountain Creek
Sawtooth Range
ALASKA
YUKON
Laberge
Ross River
Study area
Whitehorse
Teslin
Watson Lake
60°00'
Location map
PMs
PMm
PMd
PMg
PMtqd
PMip
Mqd
Kqm
ODN
0
5
10
km
TESLIN
RIVER
Road
Canol
Cone Mountain
Muskrat Lake
Alaska Highway
Johnsons Crossing
133°15'
60°30'
Legend
Teslin Suture Zone Units
Paleozoic and/or Mesozoic
PMs Muscovite ± chlorite ± biotite quartz schist and quartzite
PMm Marble
PMip Intermediate plutonic assemblage
PMg Hornblende megacrystic greenstone
PMtqd Hornblende tonalite to quartz diorite
PMd Diorite
Ordovician to Devonian
ODN(?) Graphitic phyllite
Other Units
Mesozoic
KQM Dacite(?), quartz monzonite porphyry
Kqm Biotite quartz monzonite
TrJa Siliceous Argillite
Mqd(?) Quartz diorite
Foliation
Mineral Lineation
Fault
Contact (defined, approx., assumed)
Limit of mapping

Figure 1. Location map and simplified geological map of the study area.

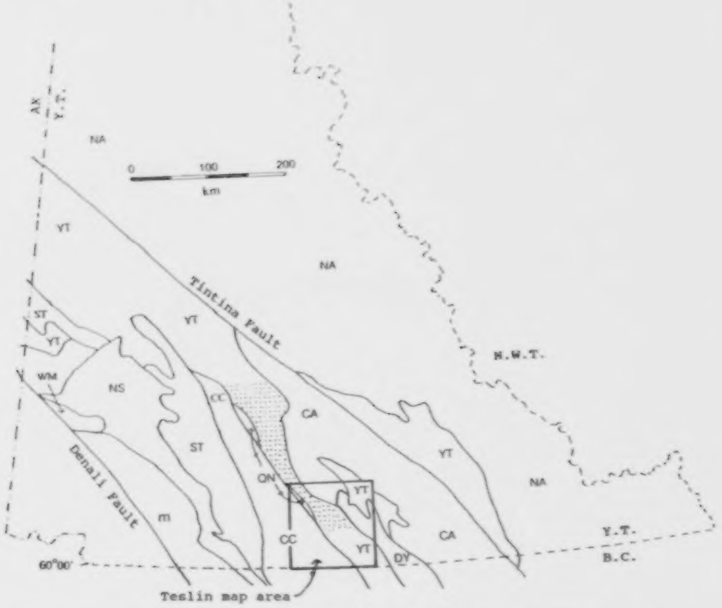

Figure 2. Generalized terrane map of Yukon between Tintina and Denali faults, including the part of the Yukon-Tanana Terrane east of Tintina Fault (modified from Wheeler and McFeely, 1987 and Hansen et al., 1989). The Teslin suture zone is shown in the stippled pattern. Terranes are: CA - Cassiar; CC - Cache Creek; DY - Dorsey; QN - Quesnellia; m - undivided metamorphics; NS - Nisling; ST - Stikinia; YT - Yukon Tanana; WM - Windy McKinley. NA represents ancestral North America.

Siliceous Schist and Quartzite Unit (PMs)

This unit outcrops as a broad band of mostly sheared siliceous schist and quartzite within the centre of the study area. The unit is lithologically heterogeneous, that is, even though end member rock types can be recognized each type shows considerable variability. In order of decreasing abundance, the prominent rock types are: mylonitic to blastomylonitic muscovite andor chlorite quartzite, muscovite-quartz schist to impure quartzite, muscovite-chlorite quartz schist to impure quartzite, chlorite schist, biotite-chlorite-pyrite-(muscovite?) schist to impure quartzite, marble, minor chloritic greenstone, possible felsic to mafic metaplutonic rocks and in one location a 5 m wide fragmental volcanic band. Schists and quartzites were seen to grade into each other commonly on the scale of metres to hundreds of metres. Slightly micaceous quartzite is the only consistently occurring rock type, although it is absent from the southern quarter of the study area. Quartz segregations are common in the schistose rocks. Marble is found both as small bands a few metres wide and as large units many hundred of metres wide. Greenstone and the possibly plutonic rocks occur as irregular bands and pods within the schist and quartzite. A band of manganese skarn 3 km northeast of Cone Mountain contains gem quality rhodonite (Marlin prospect; INAC, 1989 and references therein).

Colour and grain size vary considerably within the unit, the former ranges from medium grey-brown to silvery white to green. Grain size is primarily controlled by the intensity of shearing and ranges from microcrystalline in ultramylonites to medium grained (1-5 mm) in some schist and blastomylonite. After quartz, the major minerals are muscovite, chlorite, biotite, hornblende and pyrite. Minor feldspar is present in some rocks.

Plutonic rocks of units PMtqd and Kqm intrude the unit. Locally contacts of unit PMtqd with this unit show evidence of post-intrusive deformation and in other places, deformation has produced sharp fabric-parallel contacts and obscured any indication of an earlier intrusive contact. Rocks of units PMip grade into rocks of this unit over a diffuse, fabric parallel zone of high strain. Marble (PMm) is in conformable or possibly unconformable contact with the siliceous rocks in most places. One exception is the large marble band northeast of Cone Mountain which is at least partly in fault contact with siliceous schist. At the northern edge of this unit siliceous schist and quartzite grade into greenstones of unit PMg.

Rocks similar to those described above have been mapped in the Teslin suture zone north of the map area, and are included in Nisutlin Allochthon (Erdmer, 1985;

Tempelman-Kluit, 1984). Thus, this unit is interpreted to be part of Nisutlin Allochthon.

Marble (PMm)

Marble occurs as small 10-30 m wide bands within the stratigraphic succession of both the Graphitic Phyllite and Siliceous Schist and Quartzite units, and as mappable units several hundred metres thick located within the Graphitic Phyllite and Siliceous Schist and Quartzite units. The larger bands are mapped separately as unit PMm.

Most marble in unit PMm, consist of grey to buff and occasionally green, medium grained, sucrosic carbonate rock with 5-40 % interlayered white to colourless, 3-10 cm wide bands of fine grained quartz. In addition to carbonate and quartz, actinolite is a major component locally. Epidote, garnet and diopside were noted in a few locations. Marble south of the western edge of unit PMd has been intruded by fine grained mafic to intermediate dykes.

In the Teslin suture zone north of the map area marble was found in both the Nasina Formation and the Nisutlin Allochthon (Erdmer, 1985; Tempelman-Kluit, 1984). This correlates with marble found in the Graphitic Phyllite unit (interpreted to be part of Nasina Formation) and the Siliceous Schist and Quartzite unit (interpreted to be part of Nisutlin Allochthon).

Intermediate Plutonic Unit (PMip)

This unit outcrops east and south of the Siliceous Schist and Quartzite unit, and consists of rocks of plutonic parentage (possibly intermediate in composition), that are variably sheared and altered. Included in the unit are minor greenstone to amphibolite, fine grained rocks of unknown protolith and rare rocks of possible sedimentary origin. The typical rock type of the unit is grey to green and contains from 10-30 % medium grained megacrysts of quartz and feldspar (probably remnant igneous grains), surrounded by a fine grained matrix of chlorite, biotite, amphibole, quartz, and feldspar. Locally within small bands (<50 m thick) of weakly sheared rock, primary igneous textures can be seen. These bands are surrounded by generally fine grained, mylonitized rock of similar bulk composition, but lacking preservation of primary fabric.

The unit is in contact to the east with rocks of the Siliceous Schist and Quartzite unit. The two units appear to have undergone common deformation and the present contact is likely sheared.

It is unclear whether this unit correlates with plutonic rocks elsewhere in the Teslin suture zone or Yukon-Tanana Terrane. Its age is unknown, however it is older than or coeval with the deformation in the Teslin suture zone.

Greenstone (PMg)

A large band of greenstone outcrops to the southeast of the Sawtooth Range and is mapped as unit PMg. A number of smaller greenstone bodies (<100 m thick), most of which are included in the Graphitic Phyllite or Siliceous Schist and Quartzite units, occur in the northern half of the map area. The principal rock type is a massive, fine grained, medium to dark green mafic greenstone with 10-50 % megacrysts of medium- to coarse-grained hornblende. Other rock types in this unit include fine grained greenstone lacking hornblende megacrysts and medium grained hornblende amphibolite. Compositional layering is evident locally. In one location a 10-20 m wide band of coarse grained biotite and hornblende in a mafic matrix was found. Principal minerals of the mafic greenstone are hornblende, chlorite, epidote (as an alteration product), quartz and feldspar with accessory biotite and pyrite. Most of the unit has weak or no planar fabric; however, strong fabric is developed along the southwestern edge of the unit.

Along the northern edge of the unit carbonate rocks, similar to adjacent marble, were found as inclusions in the greenstone. This may indicate minimal dislocation along a possible original intrusive or flow contact.

In the Teslin suture zone north of the map area, greenstone, amphibolite, and other mafic and ultramafic rocks are included in the Anvil Allochthon (Erdmer, 1985; Tempelman-Kluit, 1984). It is unclear whether the rocks of this unit correlate directly with the Anvil Allochthon.

Hornblende Tonalite and Quartz Diorite (PMtqd)

This unit outcrops as a number of bodies scattered throughout the southern half of the study area. The principle rock type is blocky weathering, massive to mylonitic, grey-green medium grained hornblende tonalite to quartz diorite. In some places hornblendite and leucocratic quartz rich felsic plutonics are present. Rocks of this unit displays greater homogeneity and a lower degree of penetrative strain than rocks in unit PMip.

Several late mafic dykes cut the unit. The major minerals are feldspar, quartz (10-30 %), hornblende (10-40 %) and chlorite with accessory biotite and pyrite.

Contact metamorphism and inclusion of country rock indicates rocks of unit PMtqd intrude rocks of units OD_N and PMs. Locally intrusive relations are obscured or eliminated by deformation.

The age of this unit is unknown. However, hornblende-bearing metaplutonic rocks in the Yukon-Tanana Terrane are dominantly Devono-Mississippian or Late Triassic-Early Jurassic in age (Mortensen, in press).

In the Teslin suture zone north of the map area, hornblende-bearing plutonic rocks are included in the Simpson Allochthon (Erdmer, 1985). It is unclear if rocks of this unit are correlative with rocks of the Simpson Allochthon.

Diorite (PMd)

This unit outcrops as a northwest trending band located east of the Sawtooth Range. It comprises massive to mylonitic, green and white, coarse grained diorite cut by numerous mafic dykes. The diorite consists of 30-50 % hornblende, partly or wholly altered to chlorite and 50-70 % feldspar. The mafic dykes are dark green, fine grained and commonly well foliated. They constitute up to 5 % of the unit. At one location a small vein of serpentine asbestos was found.

Contacts relations are unclear at present but are likely structural and/or intrusive. Similarly, the age of the unit and its possible correlation with plutonic rocks elsewhere in the Teslin suture zone or Yukon-Tanana Terrane are uncertain.

OTHER MAP UNITS

Argillite (TRJa)

Along the southwestern edge of the map area, thinly laminated green to black fine grained siliceous argillite was found. The unit is bound on the east side by a brittle fault zone and on the west by the Teslin River valley. Rocks of this unit correlate with rocks of Mulligan's (1963) unit 9, which are shown to outcrop both east and west of the Teslin River valley and are thought to be Triassic and/or Jurassic in age.

Biotite Quartz Monzonite (Kqm)

A number of plutons of this unit are found in the map area. The rock is a blocky weathering, generally massive, leucocratic, medium grained equant to rarely porphyritic biotite quartz monzonite. This rock type occurs throughout the Teslin suture zone and Yukon-Tanana Terrane where it has been determined to be of mid-Cretaceous age (Tempelman-Kluit, 1984).

Red Mountain Complex (K_{RM})

Just east of Slate Mountain is a body of reddish-yellow to buff and brown, highly altered felsic rock. To the south and west of this body occurs a northwest trending, buff coloured, fine grained dyke. The protoliths of these rocks are unknown; however Brown and Kahlert (1986) called it the Red Mountain porphyry molybdenum deposit with the main body a quartz monzonite porphyry and the dyke a rhyolite porphyry. Mulligan (1963) refered to the main body as a dacite. Late Cretaceous K-Ar ages have been determined for the complex (Brown and Kahlert, 1986).

Quartz Diorite (Mqd?)

This unit outcrops near the northwestern part of the map area, in the Sawtooth Range. The unit is composed of fresh, massive, green and white, medium grained quartz diorite. Tonalite was found in one location, and coarse grained hornblendite to feldspar bearing hornblendite is present along the eastern contact. The rock is generally composed of 5-15 % quartz and 40-45 % each of feldspar and hornblende.

The rock may be part of unit PMtqd. However it appears to be fresher and more consistently massive than rocks of unit PMtqd and is thus separated here. It may also be a hornblendic phase of the Cretaceous rocks of unit Kqm.

STRUCTURAL GEOLOGY

Structurally, rock units of the Teslin suture zone (ie. those described under the heading Teslin Suture Zone Map Units), can be divided into two subsections based on the penetrativeness of strain. Rocks in the metasedimentary units OD_N and PMs and rocks of unit PMip show almost continuous ductile deformation. Marble (unit PMm) is included in this subsection although it has undergone extensive post-deformation recrystallization. The remaining units (PMg, PMtqd and PMd) show discontinuous ductile deformation. In these units massive to weakly deformed rock is bordered by zones of ductilely deformed rock 10 m to one or more kilometres in width. The structural fabrics described below are those found in the deformed rocks of all lithologies.

Planar fabrics

In the Graphitic Phyllite unit compositional layering, which likely represents transposed relict bedding, occurs in rocks east of Muskrat Lake, where marble and schistose rock interlayer with graphitic phyllite, and east of Red Mountain Creek, where graphitic rock grades into compositionally layered greenstone. In the Siliceous Schist and Quartzite unit, interlayering of quartzite and schist and compositional layering in some quartzites likely represent relict bedding. In marble, compositional variation and quartz interlayering may represent bedding. All apparent bedding planes are roughly parallel to the main orientation of metamorphic planar fabrics.

Metamorphic planar fabrics are prominent in the map area. They are: (1) strong schistosity defined by aligned chlorite and graphite in graphitic phyllite, micas and chlorite in schist and hornblende and chlorite in amphibolite and greenstone, (2) slaty cleavage in graphitic phyllite, (3) the parallel alignment of tabular quartz crystals and micas in quartzite, (4) a crenulation schistosity defined by micas in siliceous schist, (5) the parallel alignment of tabular quartz, feldspar, and hornblende crystals in plutonic rocks, and (6) the development of mylonitic fabric in all rock units, defined by elongate and/or stretched grains or aggregates of quartz, feldspar, hornblende and carbonate. Overall, planar fabrics strike northwest and dip steeply northeast. Local variations occur, particularly in the northern third of the siliceous schist and quartzite unit, where fabrics strike northwest but dip steeply to the southwest. In Laberge map area Teslin suture zone fabrics generally strike south to southeast and dip steeply west to northwest (Hansen, 1989).

Linear fabrics

Linear fabric elements are prominent in almost all the deformed rocks. They include: (1) crenulation hinges and fold axes, (2) mineral lineations defined by chlorite streaks in the graphitic rocks, alignment of quartz, mica, chlorite, hornblende, and carbonate minerals in siliceous metasedimentary rocks and of hornblende, feldspar, quartz, chlorite and biotite in plutonic rocks, (4) quartz pressure shadows around pyrite grains in graphitic rocks, and (5) boudinage structures.

Folds

Folding of compositional layering and metamorphic foliation are best developed in the graphitic phyllite and siliceous schist and quartzite units, and are rarer in marbles and plutonic rocks. Locally, folding is strongly developed in siliceous schists and calcareous graphitic phyllites. Crenulation folds, often located within larger folds, are the principal fold type. These folds are 1-10 mm in amplitude, rounded, symmetric and occur locally over wide areas of unit OD_N and PMs.

The majority of other folds are hand specimen to small outcrop scale, chevron to rounded folds with open to tight interlimb angles. Most are symmetric, but asymmetric folds were also found.

At present it appears that most of the folds observed are younger than or coeval with the deformation that produced the fabrics in schists and mylonites. This is evident by the general symmetric nature of the folds and the transposition of mylonitic and schistose fabrics into a crenulation schistosity. Folds transposed into the main planar fabric direction were found in a few locations.

Major faults

One brittle fault was found at the southwestern edge of the mapped area. It separates units Kqm and PMtqd from unit TRJa argillites. The fault is approximately 500 m wide and consists of cohesive and highly silicified bands and fragments of brittley and ductilely deformed rock derived from adjacent units and rock of unknown origin. Regional relationships indicate it is a major structural discontinuity, younger in age than Teslin suture zone deformation, that marks the boundary between the Yukon-Tanana Terrane to the east and poorly understood Mesozoic(?) volcanics and volcaniclastics to the west (see Gordey, 1991).

Kinematic indicators

Macroscopic kinematic indicators are rare in the study area. C-S fabric, asymmetric folds, tension fractures and rotated pyrite crystals occur locally. Future study will concentrate on delineating both macro- and microscopic movement indicators to understand the strain history within the suture zone.

ACKNOWLEDGMENTS

Field work was supported by a Natural Sciences and Engineering Research Council operating grant to P. Erdmer. Logistical support from the Department of Indian and Northern Development and helicopter support by the Geological Survey of Canada are gratefully acknowledged. P. Erdmer and S.P. Gordey are thanked for their visits in the field, for helpful and friendly discussions and for reviews of earlier versions of the manuscript. T. Harms is thanked for a careful review of the manuscript. Murray Rydman provided excellent assistance in the field.

REFERENCES

Brown, P. and Kahlert, B.
1986: Geology and mineralization of the Red Mountain porphyry molybdenum deposit south-central Yukon; in Mineral Deposits of the Northern Canadian Cordillera, J.A. Morin (ed.), Canadian Institute of Mining and Metallurgy, Special Volume 37, p. 288-297.

Erdmer, P.
1985: An examination of the cataclastic fabrics and structures of parts of Nisutlin, Anvil and Simpson allochthons, central Yukon: test of the arc-continent collision model; Journal of Structural Geology, v. 7, no. 1, p. 57-72.

Gordey, S.P.
1991: Teslin map area, a new geological mapping project in Southern Yukon; in Current Research, Part A, Geological Survey of Canada, Paper 91-1A.

Hansen, V.L.
1989: Structural and kinematic evolution of the Teslin suture zone, Yukon: record of an ancient transpressional margin; Journal of Structural Geology, v. 11, no. 6, p. 717-733.
1990: Yukon-Tanana Terrane: a partial acquittal; Geology, v. 18, p. 365-369.

Hansen, V.L., Mortensen, J.K., and Armstrong, R.L.
1989: U-Pb, Rb-Sr, and K-Ar isotopic constraints for ductile deformation and related metamorphism in the Teslin suture zone, Yukon-Tanana Terrane, south-central Yukon; Canadian Journal of Earth Science, v. 26, p. 2224-2235.

Indian and Northern Affairs Canada
1989: Yukon exploration 1988; Exploration and Geological Services Division, Yukon, Indian and Northern Affairs Canada, 304 p.

Lees, E.J.
1936: Geology of the Teslin-Quiet Lake area Yukon Territory; Geological Survey of Canada, Memoir 203.

Mortensen, J.K.
in press: Pre-Mid-Mesozoic tectonic evolution of the Yukon-Tanana Terrane, Yukon and Alaska; Tectonics.

Mulligan, R.
1963: Geology of the Teslin map area, Yukon Territory (105C); Geological Survey of Canada, Memoir 326.

Tempelman-Kluit, D.J.
1977: Quiet Lake (105F) and Finlayson Lake (105G) map areas, Yukon; Geological Survey of Canada, Open File 486.
1979: Transported cataclasite, ophiolite and granodiorite in Yukon: evidence of arc-continent collision; Geological Survey of Canada, Paper 79-14.
1984: Geology, Laberge (105E) and Carmacks (115I), Yukon Territory; Geological Survey of Canada, Open File 1101.

Wheeler, J.O. and McFeely, P.
1987: Tectonic assemblage map of the Canadian Cordillera and adjacent parts of the United States of America; Geological Survey of Canada, Open File 1565.

Wheeler, J.O., Brookfield, A.J., Gabrielse, H., Monger, J.W.H., Tipper, H.W., and Woodsworth, G.J.
1988: Terrane map of the Canadian Cordillera; Geological Survey of Canada, Open File 1894.

APPENDIX 2 - REGIONAL GEOLOGY, FABRIC AND STRUCTURE OF THE TESLIN SUTURE ZONE IN NORTHWEST TESLIN MAP AREA, YUKON TERRITORY: PUBLISHED IN GEOLOGICAL SURVEY OF CANADA PAPER 92-1A*

---

*A version of this appendix has been published. Stevens, R.A., 1992. *In* Current Research, Part A, Geological Survey of Canada, Paper 92-1A, pp. 287-295.

Regional geology, fabric, and structure of the Teslin suture zone in northwest Teslin map area, Yukon Territory

R.A. Stevens[1]
Cordilleran Division, Vancouver

Stevens, R.A., 1992: Regional geology, fabric, and structure of the Teslin suture zone in northwest Teslin map area, Yukon Territory; in Current Research, Part A; Geological Survey of Canada, Paper 92-1A, p. 287-295.

Abstract

The Teslin suture zone in northwest Teslin map area includes three metasedimentary and three metaigneous rock units. Ductile deformation under greenschist to lower amphibolite facies conditions produced protomylonite and mylonite in much of the area. Detailed mapping along two east trending transects about 20 km apart reveals that the suture zone has domains of contrasting structural style with different fabric orientations. In both transects, a western domain of L-S tectonites with well formed mineral lineations passes to the east into a domain dominated by ductile flexural-slip folding with mineral lineations parallel to fold axes, which in turn passes to the east into a domain of poorly formed L-S tectonites with variable fabric orientations. The southern transect intersects a fourth domain farther east that includes L-S tectonites with moderately well formed mineral lineations. The orientation of fabrics are different in the two transects.

Résumé

La zone de suture de Teslin dans le nord-ouest de la région cartographique de Teslin comprend trois unités métasédimentaires et trois unités ignées métamorphisées. La déformation ductile dans des conditions de métamorphisme allant du faciès des schistes verts au sous-faciès inférieur des amphibolites a produit des protomylonites et des mylonites dans une grande partie de cette zone. La cartographie détaillée de la zone longeant deux transects à direction est et espacés d'environ 20 km, révèle que la zone de suture comporte des domaines de style structural contrastant, caractérisés par des orientations de fabrique différentes. Le long des deux transects, un domaine occidental de tectonites L-S, présentant des linéations minérales très nettes, se transforme vers l'est en un domaine où prédomine un plissement par flexure et glissement comportant des linéations minérales parallèles aux axes des plis qui, à son tour, se transforme à l'est en un domaine de tectonites L-S mal formées à orientations de fabrique variables. Le transect sud recoupe un quatrième domaine plus à l'est qui comporte des tectonites L-S à linéations minérales modérément bien formées. Les orientations de fabrique diffèrent le long des deux transects.

---

[1] Department of Geology, University of Alberta, Edmonton, Alberta T6G 2E3

INTRODUCTION AND REGIONAL SETTING

The Teslin suture zone is part of the Yukon-Tanana composite terrane (Kootenay terrane of Wheeler et al., 1988) of southern Yukon and east-central Alaska. It forms the fundamental boundary between deformed autochthonous North American rocks of the Omineca Belt to the east and accreted terranes of the Intermontane Belt to the west. It has been defined by Hansen (1989) to be "the package of rocks comprising the 15-20 km wide steeply-dipping portion of the Yukon-Tanana terrane in southern Yukon".

Studies of the Teslin suture zone in the Laberge map area recognized three assemblages of ductilely deformed L-S tectonites metamorphosed in the greenschist to albite-epidote amphibolite facies during the early to mid-Mesozoic (Tempelman-Kluit, 1977, 1979, 1984; Erdmer, 1985; Hansen, 1989; Hansen et al., 1989). On the basis of stretching lineation orientation and shear fabric asymmetry Hansen (1989) divided the suture zone into structural domains. Together, the domains record a complex history of deformation that involves extensional shear, thrust shear and strike-slip shear, and are interpreted to result from terrane accretion during oblique plate convergence.

The geology of the Teslin map area is described by Mulligan (1963) and the geology of the northwestern quarter of the map area by Lees (1936). The Teslin map area is being remapped at 1:50 000 and 1:250 000 scales by the Geological Survey of Canada (Gordey, 1991, 1992). Teslin suture zone-related rocks in the southern half of the Teslin map area are the topic of a study in progress (see Gareau, 1992).

This report outlines the regional geology and structural characteristics of the Teslin suture zone in Northwest Teslin map area. An introduction to the regional geology of the area was presented in Stevens (1991). During the summer of 1991, 1:50 000 scale mapping expanded on that completed in 1990. Two detailed structural transects across the suture zone were also completed.

TESLIN SUTURE ZONE MAP UNITS

The geology of the study area is shown in Figure 1. Rock units are grouped into two categories on the basis of fabric development. Rock units in the first category, referred to as Teslin Suture Zone Map Units, display penetrative ductile deformation fabrics and are discussed below. Rocks in the second category, referred to as Other Units, lack a foliation and thus are considered to postdate the development of the Teslin suture zone. Descriptions of these units can be found in Stevens (1991).

Graphitic Phyllite Unit (OD$_N$?)

This unit consists of sheared, fissile, rusty red to black, fine grained (<1 mm), pyritic graphitic phyllite, calcareous graphitic phyllite, siliceous graphitic phyllite and marble. Tentative interpretations correlate this unit with the Ordovician-Devonian Nasina formation (Stevens, 1991).

Siliceous Schist and Quartzite Unit (PMs)

This unit outcrops in the central part of the map area as an elongate northwest-trending band of quartzite, schist, and phyllite. The predominant rock types are protomylonitic to mylonitic, quartz-muscovite ± chlorite ± epidote ± biotite ± amphibole schist to impure quartzite, muscovite ± chlorite quartzite, and marble. Locally the schists contain feldspar, garnet, pyrite and other opaques. Less common rock types include chlorite-quartz schist, chloritic greenstone and tremolite ± epidote ± garnet calc-silicate. Rocks of this unit are interpreted as part of the Nisutlin Allochthon (Stevens, 1991).

Structural slices of **PMtqd** rocks are interleaved within this unit locally, especially near **PMtqd** bodies. They outcrop as bands 10-300 m wide in contact with **PMs** rocks along fabric-parallel structural contacts.

A 5 m wide band of mafic intrusive rock interpreted as a volcanic fragmental in Stevens (1991), is a xenolithic dyke. It extends for at least 200 m and consists of 30-50% xenoliths in a fine-grained matrix of biotite, amphibole, feldspar and minor pyroxene. The xenoliths are mostly subrounded and show evidence of reaction with the matrix. They are 70-80% massive hornblendite and hornblende rich diorite, and foliated diorite, with 20-30% included country rocks (quartzite, marble and schist), and minor possible felsic plutonics. The dyke is massive and cuts the host rock fabric. A massive crosscutting tonalite to quartz-diorite dyke was also found within unit **PMs**; it lacks xenoliths.

Two sub-units rich of **PMs** are recognized. The first is a biotite-amphibole unit, **PMsb** (Fig. 1). The rocks are quartzofeldspathic-biotite ± amphibole schist to biotite bearing meta-arkose. The second, **PMsp**, consists of quartz-muscovite ± graphite ± biotite phyllite, quartzite and possible meta-chert. Locally, the **PMsp** rocks are schistose. The presence of graphite and the phyllitic nature distinguish this sub-unit.

Marble (PMm)

Marble, unit **PMm** in Figure 1, is grey to buff, medium grained and sucrosic-textured. It commonly contains 5-40% quartz evenly distributed throughout or in separate bands 3-10 cm wide. Tremolite and epidote are noted locally. Marble is also found within units **OD$_N$** and **PMs** as 10-30 m wide bands or pods (Stevens, 1991).

Greenstone (PMgr)

A greenstone body occurs southeast of the Sawtooth Range (Fig. 1) and includes massive, fine grained, medium to dark green amphibole-chlorite-epidote ± biotite quartzofeldspathic greenstone with 10-50% megacrysts of medium- to coarse-grained hornblende. Other rock types in this unit include fine grained greenstone and amphibolite. Most of the unit is massive, except along its southern margin where strong L-S fabric has developed (Stevens, 1991).

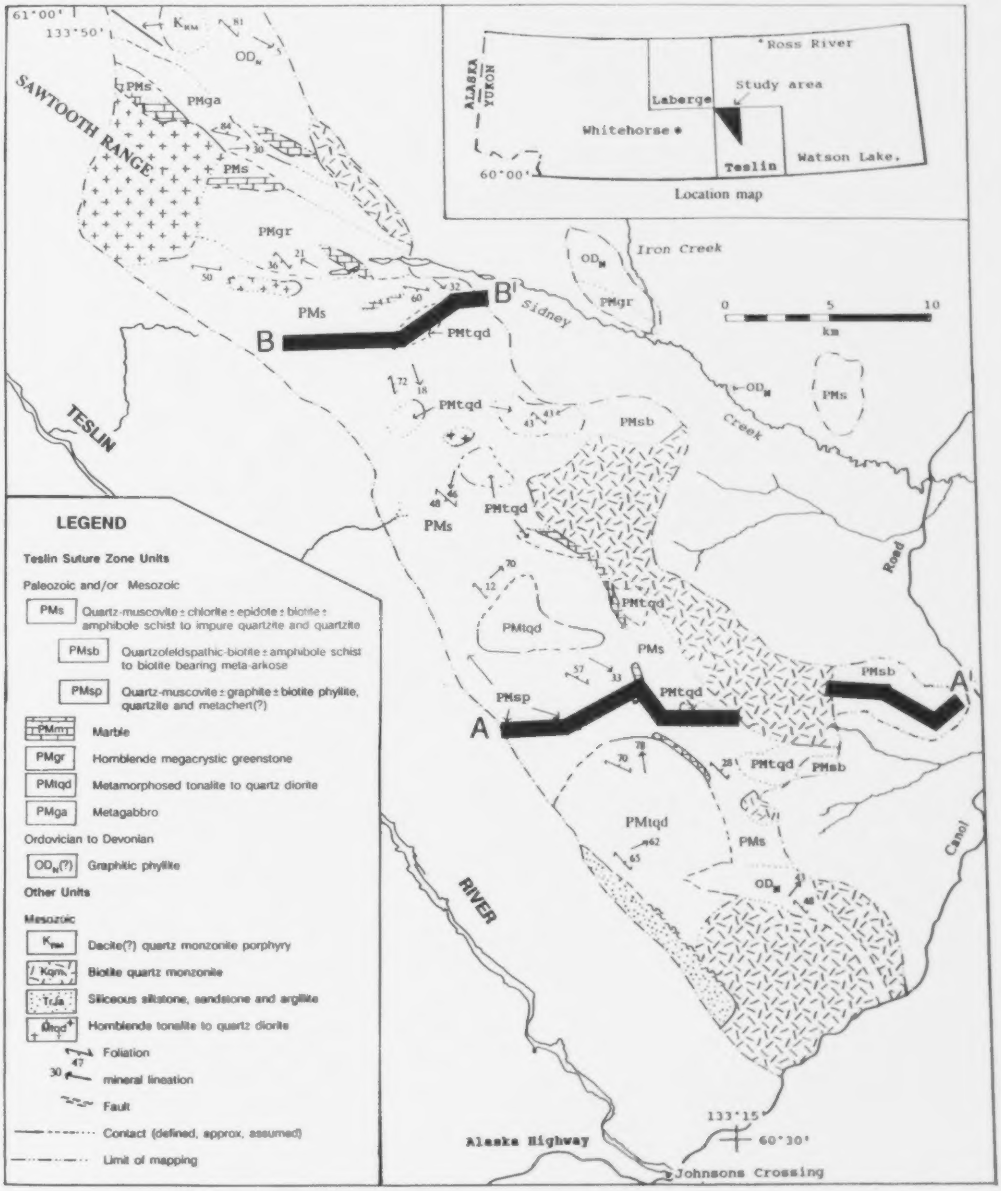
61°00'
133°50'
SAWTOOTH RANGE
TESLIN
RIVER
Sidney Creek
Iron Creek
Road
Canol
Alaska Highway
Johnsons Crossing
133°15'
60°30'
B
B'
A
A'
0
5
10
km
ALASKA
YUKON
Ross River
Study area
Laberge
Whitehorse
Teslin
Watson Lake.
60°00'
Location map
LEGEND
Teslin Suture Zone Units
Paleozoic and/or Mesozoic
PMs Quartz-muscovite ± chlorite ± epidote ± biotite ± amphibole schist to impure quartzite and quartzite
PMsb Quartzofeldspathic-biotite ± amphibole schist to biotite bearing meta-arkose
PMsp Quartz-muscovite ± graphite ± biotite phyllite, quartzite and metachert(?)
PMm Marble
PMgr Hornblende megacrystic greenstone
PMtqd Metamorphosed tonalite to quartz diorite
PMga Metagabbro
Ordovician to Devonian
OD$_N$(?) Graphitic phyllite
Other Units
Mesozoic
K$_{RM}$ Dacite(?) quartz monzonite porphyry
Kqm Biotite quartz monzonite
TrJa Siliceous siltstone, sandstone and argillite
Mtqd Hornblende tonalite to quartz diorite
47 Foliation
30 mineral lineation
Fault
Contact (defined, approx, assumed)
Limit of mapping

Figure 1. Location map and simplified geological map of the study area modified from Stevens (1991). AA' and BB' are the location of detailed structural transects.

Tonalite to Quartz Diorite (PMtqd)

Rocks of this unit outcrop as small bodies in the southern half of the map area. The main rock type is metamorphosed mesocratic tonalite to quartz diorite. Mafic minerals constitute 10-50% and are mainly hornblende, chlorite and biotite. Most of the chlorite and some biotite appear to be alteration products of hornblende. Feldspars are strongly altered to fine grained white mica and epidote. A number of massive mafic dykes cut this unit.

PMtqd rocks range from weakly deformed to mylonitic. Areas of weakly deformed rocks are commonly cut by, or grade into, areas of protomylonite and mylonite.

Intrusive contacts with units **PMs** and **OD_N** were observed in a few places, but most contacts are fabric parallel and lack intrusive characteristics. Structural slices of metasedimentary rocks of unit **PMs** are found within some of the bodies, especially near their margins.

Gabbro (PMga)

This unit outcrops as a northwest-trending band east of the Sawtooth Range (Fig. 1). It consists of massive to mylonitic green and white coarse-grained gabbro. Foliated fabric-parallel mafic dykes constitute up to 5% of this unit. The gabbro consists of 50-60% feldspar highly altered to clinozoisite and epidote, 35-60% amphibole, biotite, chlorite, white mica and possible minor pyroxene and <3% quartz. The biotite and chlorite appear to be alteration products of amphibole. This unit was reported as diorite (unit **PMd**) in Stevens (1991). However, the alteration of feldspars to calcic minerals suggests that the anorthite component of the feldspar is greater than 50%, making the rock a gabbro.

METAMORPHISM

The major syn-deformational metamorphic minerals are muscovite, biotite, chlorite, epidote, and, less commonly, amphiboles and garnet. This suggests that metamorphism took place at greenschist to lower amphibolite facies conditions. Garnet is more common in the northern and western parts of the map area than in other parts. Garnet rim-matrix biotite geothermometry on one mylonite sample from unit **PMs** gave a temperature estimate of 380°C ± 50° @ 5 kbar using the calibration of Ferry and Spear (1978). Post-deformational growth of metamorphic minerals occurred locally and may be related to thermal heating accompanying intrusion of quartz-monzonite plutons (unit **Kqm**). However, clear evidence of contact metamorphism is not apparent adjacent to these plutons.

MICROSTRUCTURES AND THE STATE OF DEFORMATION

Rocks from the study area have undergone varying amounts of ductile deformation, producing weak to mylonitic fabrics. In order to characterize the degree of ductile deformation the microstructural characteristics of quartz, and phyllosilicates and the degree of micro-fabric development are considered. Emphasis is placed on quartz microstructures as they are well documented in the literature (Bell and Etheridge, 1973; Vernon, 1976; Tullis et al., 1982; and Barker, 1990), and quartz is a major constituent of most rocks from the study area.

Under ductile conditions, quartz microstructures are produced mainly by deformation, dynamic recovery and dynamic recrystallization (Bell and Etheridge, 1973). Deformation produces undulose extinction, deformation bands and deformation lamellae developed by intracrystalline slip (Barker, 1990). These dislocation structures impose strain energy on quartz grains that increases with the density of the dislocations. The stored strain energy provides a force for the dynamic recovery (formation of subgrains) and recrystallization (formation of new grains) of the quartz. Figure 2A illustrates some of the quartz microstructures.

Mylonite as used here is a strongly foliated and commonly lineated cohesive rock consisting of 10-50% primary grains or porphyroclasts in a matrix of dimensionally aligned finer grains. The primary grains or porphyroclasts are usually remnant quartz or feldspar grains that are commonly strongly strained, with subgrains and new grains developed at their margins. Mylonite is produced by tectonic grain-size reduction by crystal-plastic processes (ductile deformation).

The following section describes the transition of microstructural characteristics in four stages ranging from weakly deformed to mylonitic. The characteristics are based on observation of more than 175 thin sections from the map area.

Weakly deformed rocks (Fig. 2B) appear massive and undeformed in the field. In thin section quartz grains locally show undulose extinction and deformation bands. Feldspars are unaffected by deformation and phyllosilicates may show minor undulose extinction. Grain size reduction and alignment of minerals is not apparent. Weakly deformed Teslin suture rocks comprise up to 10% of the map area. They occur mostly in units **PMtqd** and **PMgr** and rarely in other units.

In moderately deformed rocks (Fig. 2C), quartz grains display undulose extinction, deformation bands, deformation lamellae and subgrains. Some development of new grains and minor grain size reduction is visible. Feldspars, if present, are commonly fractured. Phyllosilicates and occasionally quartz define a weak to moderate foliation, although phyllosilicates are locally variably oriented. Rocks at about the moderately deformed stage underlie 15-20% of the map area and occur predominately in units **PMtqd**, **PMgr** and **PMga**.

In strongly deformed and/or protomylonitic rocks (Fig. 2D), many new grains have formed, but 50-90% of the rock consists of strained primary grains or porphyroclasts. The strained primary grains or porphyroclasts are mostly quartz, showing strong undulose extinction, deformation bands, deformation lamellae and subgrains. The margins of many grains include strain-free new grains one-half to one-tenth the size of the original grain. These new grains are

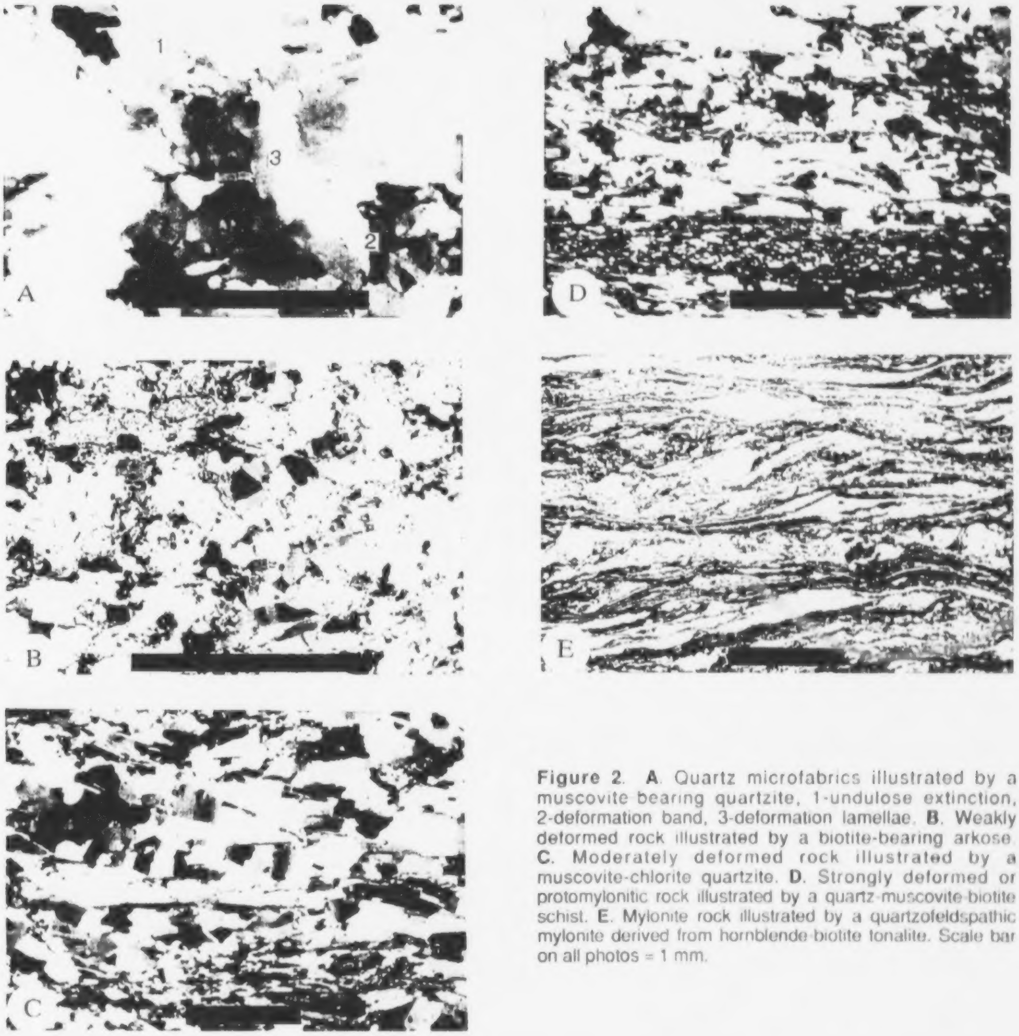

Figure 2. **A**. Quartz microfabrics illustrated by a muscovite-bearing quartzite, 1-undulose extinction, 2-deformation band, 3-deformation lamellae. **B**. Weakly deformed rock illustrated by a biotite-bearing arkose. **C**. Moderately deformed rock illustrated by a muscovite-chlorite quartzite. **D**. Strongly deformed or protomylonitic rock illustrated by a quartz-muscovite-biotite schist. **E**. Mylonite rock illustrated by a quartzofeldspathic mylonite derived from hornblende-biotite tonalite. Scale bar on all photos = 1 mm.

commonly elongate in the fabric direction. Areas of small (<0.1 mm) new grains may form bands or zones that alternate or mix with areas, usually augen shaped, of larger (>0.2 mm) strained grains. Phyllosilicates do not show grain size reduction, but are smaller and more elongate than in moderately deformed rocks. They define a moderate to strong foliation that anastomoses around porphyroclasts or augens of strained grains. Kinematic indicators are present in these rocks. Protomylonitic rocks make up 40-60% of the rocks from the map area, mainly in units **PMs** and **ODn**.

The most strongly deformed rocks from the map area are mylonite (Fig. 2E) and rarely ultramylonite. Mylonite consists of 10-50% porphyroclasts or strained primary grains, in a strongly foliated matrix of elongate strain-free grains consisting mostly of quartz and phyllosilicates. The phyllosilicates show dimensional and crystallographic alignment. Grain size reduction is widespread and apparent around the margins of strained primary grains, where smaller new grains formed at the expense of the original larger grains. Kinematic indicators are present in these rocks. Mylonite underlies about 20-30% of the map area particularly in units

PMs and **ODn**. Mylonite is found locally throughout units **PMs** and **OD$_N$**, and is not confined to zones of high strain but occurs locally throughout these units. In units **PMtqd**, **PMga** and **PMgr**, mylonite is not common and occurs in narrow zones of high strain.

STRUCTURAL TRANSECTS

Mapping along two detailed structural transects was completed in the summer of 1991. The southern transect (AA′ on Fig. 1) is approximately 18 km wide, the northern (BB′ on Fig. 1) about 9 km wide. Measurement stations were located 150-250 m apart, resulting in a total of 91 stations across AA′ and 45 across BB′. At least one oriented sample was collected at each station.

Four separate structural domains are recognized along AA′ and three along BB′. Figures 3 and 4 are strip maps of these transects with contoured stereoplots for each domain.

AA′ -Domain 1

L-S tectonites characterize the structure of this domain. Planar fabrics are dominated by mylonitic foliation which clusters near an orientation of 310°/70° (Fig. 3). Mineral and stretching lineations consist of smeared graphite and muscovite, alignment of elongate muscovite, biotite and quartz grains and rodding of quartz. The lineations form a tight cluster plunging 64° towards 2°. C-S fabrics observed in thin sections cut perpendicular to foliation and parallel to the mineral and/or stretching lineations indicate that displacement was top to the south, or right-reverse, oblique shear.

Folds are developed locally in this domain. The most common are tight to isoclinal with amplitudes of 5-30 cm, developed in small (<10 cm) quartz bands within the phyllite (Fig. 5A). They appear to be transposed into the mylonitic fabric direction. Folds are also found within large (>1 m) quartzite bands in the eastern half of this domain. These are small (amplitudes 1-2 cm) and irregular open to tight folds marked by thin (<1 mm) layers of muscovite within the quartzite. These folds were not noted in phyllite bands.

The western boundary of this domain coincides with the approximate western margin of Teslin suture zone rocks. The eastern boundary occurs over a distance of 0.5-0.75 km where there is a change of structural style.

AA′ - Domain 2

Pervasive, flexural slip folds with stretching and/or mineral lineations parallel to folds axes dominate this domain. The folds are open to tight, rounded to chevron, with amplitudes averaging 5-15 cm (Fig. 5B). They fold schistosity and mylonitic foliation. Intense folding across most of this domain commonly obscures the orientation of planar fabrics. An axial planar cleavage was noted in two locations. Bands up to 100 m wide that lack folding or are weakly folded

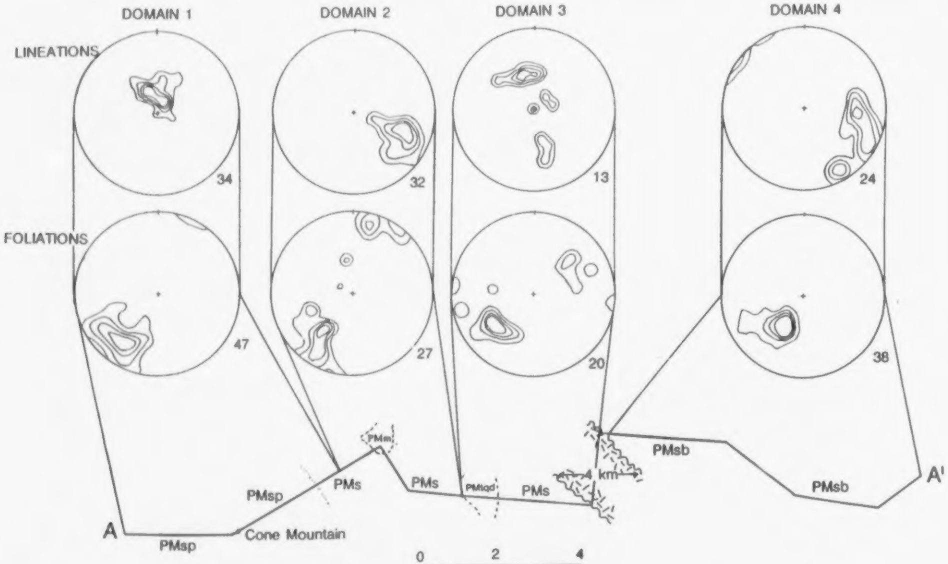

Figure 3. Strip map for transect AA′ showing rock types along the transect line. Stereographic projection plots are for the four structural domains recognized in this transect. Contours are densities expressed as multiples of a uniform density. Contours are at densities of 3, 6, 9 and 12.

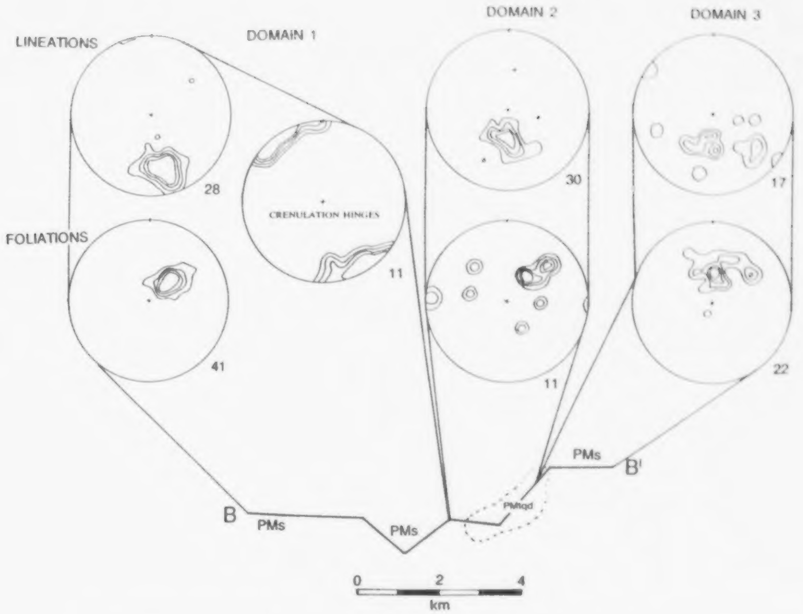

Figure 4. Strip map for transect BB′ showing rock types along the transect line. Stereographic projection plots are for the three structural domains recognized in this transect. Contours are densities expressed as multiples of a uniform density. Contours are at densities of 3, 6, 9 and 12.

commonly display mineral lineations defined by quartz, muscovite, chlorite and elongate blade-like grains of chlorite after hornblende. Mineral lineations can also be found within the folded layers. Mineral lineations and fold axes plunge 27° towards 117° on average.

Folds at the outcrop scale or larger are not readily evident in the field. However, poles to schistosity and mylonitic foliation roughly form a great circle perpendicular to the average fold axis, suggesting that the planar fabrics are folded (Fig. 3).

The eastern boundary is <0.5 km wide and is marked by the loss of folds and by the contact to a small body of **PMtqd** rocks in domain 3.

AA′ - Domain 3

Moderately to strongly deformed and variably oriented L-S tectonites are the most common features of this domain. Figure 3 illustrates the variations in orientation of planar and linear fabrics. Lineations are found in about half of the outcrops. None are strongly developed. Folds are rare and are rootless tight to isoclinal structures transposed into the foliation.

The eastern boundary of this domain is the contact with a massive biotite quartz-monzonite pluton (unit **Kqm**).

AA′ - Domain 4

Structures are dominated by L-S tectonites with poorly formed mineral lineations. Foliations cluster around 310°/50°. Mineral lineations defined by biotite, amphibole and quartz trend southeast and plunge 0-30° (Fig. 3). Tight to isoclinal, hand-specimen scale folds are present locally. These appear to be transposed into the fabric.

The western boundary of this domain is at the contact with a massive biotite quartz-monzonite pluton of unit **Kqm**, and the eastern margin is constrained by lack of exposure.

BB′ - Domain 1

L-S tectonites dominate this zone. Schistosity and mylonitic foliations cluster near 143°/40°. Mineral lineations defined by quartz rodding and elongate grains of quartz, muscovite, chlorite, biotite and amphibole plunge 24° towards 170° on average (Fig. 4). A second, less common and generally obscure subhorizontal, crenulation lineation trends northwest or southeast. The relative ages of the two lineations are not clear, but the crenulation lineations are related to minor crenulations that fold the planar fabrics containing the mineral lineations. Small (amplitudes <10 cm), isolated tight to isoclinal folds transposed into the schistosity are present locally.

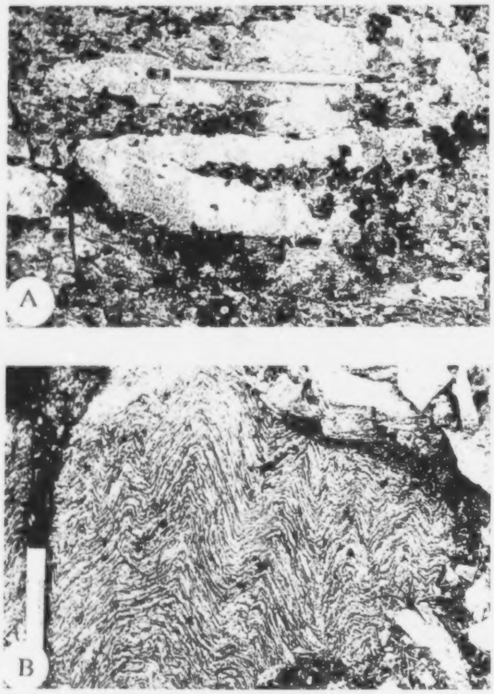

Figure 5. A. Transposed, isoclinal fold of quartzite within a muscovite-biotite-graphite phyllitic mylonite. The pencil is roughly parallel to the mylonitic foliation. This type of fold is present locally in most structural domains. **B.** Ductile flexural-slip folds that have mineral lineations parallel to their fold axes. These folds characterize the structure of domain 2 in AA′ and BB′.

The western margin of this domain is constrained by lack of outcrop near the western margin of the suture zone. The eastern boundary is a zone 0.5-1.0 km wide in which folding gradually increases in intensity, mineral lineations are less apparent and fold axes begin to plunge moderately steeply.

BB′ – Domain 2

Pervasive, disharmonic, flexural-slip folds with stretching and/or mineral lineations parallel to fold axes dominate this domain. Folds are open to tight and rarely isoclinal, with rounded to chevron hinges. Amplitudes range from <5-30 cm. Mineral lineations defined by quartz rodding, muscovite, biotite, amphibole and elongate chlorite after hornblende can be found in bands of weakly folded rock and less commonly within the folds. Mineral lineations and folds axes plunge 50° towards 180° on average (Fig. 4). Folding has obscured the original orientation of planar fabrics over much of this domain.

The eastern limit of this domain is a zone <0.5 km wide in which folding decreases and becomes a minor component of the structure.

BB′ – Domain 3

Inconsistent and commonly weak planar and linear structures are typical of this domain. Foliations strike east to southeast with dips of 40-50° south to southwest (Fig. 4). Mineral lineations are locally developed. The most common trends are south to southeast, with plunges of 30-50°. Small folds, similar to those in domain 2 are present locally.

The eastern limit of the domain is constrained by loss of outcrop in the valley of Sidney Creek.

DISCUSSION

Transects AA′ and BB′ have similarities and differences. Both have well developed L-S tectonites in the west that pass to the east into a domain dominated by folding, with mineral lineations parallel to fold axes. This in turn grades eastward into a zone of less deformed L-S tectonites with variable mineral lineations. Domain 4 of transect AA′ has no equivalent in transect BB′. Deformation decreases eastward in both transects. The difference lies in the orientation of structural fabrics, particularity schistosity and mylonitic foliation which dip north to northeast along AA′ but dip south to southwest along BB′. Broad scale late folding may explain the difference in dip direction. However, a simple rotation of structures about the fold axes from the map area do not bring the fabrics from similar domains into common orientation.

Two generations of folds are present. The first, found locally in all domains, are transposed, tight to isoclinal, and commonly rootless. They likely formed as more open folds early in the deformation event, and were subsequently rotated into the X-Y plane of the strain ellipsoid. The later generation are flexural-slip folds that dominate the structure of domain 2 in AA′ and BB′. They fold mylonitic foliations and have stretching and/or mineral lineations parallel to their fold axes. Folds with axes parallel to mineral lineations are found within many ductile shear zones (Mattauer et al., 1981; Ghosh and Sengupta, 1987; Malavieille, 1987; and Hansen, 1989; Henderson and Broome, 1990). They are commonly thought to have formed oblique to the shear direction and progressively rotated with increasing strain (Malavieille, 1987). The folds in this study appear to have formed late in the shearing event and do not show evidence of rotation. The origin of this type of folds is poorly understood (Bell and Hammond, 1984; Malavieille, 1987).

ACKNOWLEDGMENTS

Field work was supported by a joint EMR/NSERC research agreement to P. Erdmer and a Northern Scientific Training Program grant from the Department of Indian Affairs and Northern Development, a grant from the Canadian

Circumpolar Institute of the University of Alberta and a Geological Society of America grant awarded to R.A. Stevens. Logistical support provided by the Department of Indian Affairs and Northern Development and the Geological Survey of Canada is greatly appreciated. While in the field I enjoyed visits by S.A. Gareau and D.A. Jones. P. Erdmer is thanked for his help in preparing this manuscript and for reviewing an earlier version of it. D.J. Tempelman-Kluit is thanked for reviewing the manuscript. Andy Turnbull provided excellent assistance in the field.

REFERENCES

Barker, A.J.
1990: Introduction to metamorphic textures and microstructures; Blackie and Sons Ltd., London, 169 p.

Bell, T.H. and Etheridge, M.A.
1973: Microstructure of mylonites and their descriptive terminology; Lithos, v. 6, p. 337-348.

Bell, T.H. and Hammond, R.L.
1984: On the internal geometry of mylonites zones; Journal of Geology, v. 92, p. 667-686.

Erdmer, P.
1985: An examination of the cataclastic fabrics and structures of parts of Nisutlin, Anvil and Simpson allochthons, central Yukon: test of the arc-continent collision model; Journal of Structural Geology, v. 7, no. 1, p. 57-72.

Ferry, J.M. and Spear, F.S.
1978: Experimental calibration of the partitioning of Fe and Mg between biotite and garnet; Contributions to Mineralogy and Petrology, v. 66, p. 113-117.

Gareau, S.A.
1992: Report on fieldwork in the southern Big Salmon metamorphic complex, Teslin map area, Yukon; in Current Research, Part A; Geological Survey of Canada, Paper 92-1A.

Ghosh, S.K. and Sengupta, S.
1987: Progressive development of structures in a ductile shear zone; Journal of Structural Geology, v. 9, no. 3, p. 277-287.

Gordey, S.P.
1991: Teslin map area, a new geological mapping project in Southern Yukon; in Current Research, Part A; Geological Survey of Canada, Paper 91-1A, p. 171-178.
1992: Geological fieldwork in Teslin map area, southern Yukon; in Current Research, Part A; Geological Survey of Canada, Paper 92-1A.

Hansen, V.L.
1989: Structural and kinematic evolution of the Teslin suture zone, Yukon record of an ancient transpressional margin; Journal of Structural Geology, v. 11, no. 6, p. 717-733.

Hansen, V.L., Mortensen, J.K., and Armstrong, R.L.
1989: U-Pb, Rb-Sr, and K-Ar isotopic constraints for ductile deformation and related metamorphism in the Teslin suture zone, Yukon-Tanana terrane, south-central Yukon; Canadian Journal of Earth Sciences, v. 26, p. 2224-2235.

Henderson, J.R. and Broome, J.
1990: Geometry and kinematics of Wager shear zone interpreted from structural fabrics and magnetic data; Canadian Journal of Earth Sciences, v. 27, p. 590-604.

Lees, E.J.
1936: Geology of the Teslin-Quiet Lake area Yukon Territory; Geological Survey of Canada, Memoir 203.

Malavieille, J.
1987: Kinematics of compressional and extensional ductile shearing deformation in a metamorphic core complex of the northeastern Basin and Range; Journal of Structural Geology, v. 9, no. 5/6, p. 541-554.

Mattauer, M., Faure, M., and Malavieille, J.
1981: Transverse lineation and large-scale structures related to Alpine obduction in Corsica; Journal of Structural Geology, v. 3, no. 4, p. 401-409.

Mulligan, R.
1963: Geology of the Teslin map area, Yukon Territory (105C); Geological Survey of Canada, Memoir 326.

Stevens, R.A.
1991: The Teslin suture zone in northwest Teslin map area, Yukon; in Current Research, Part A; Geological Survey of Canada, Paper 91-1A, p. 271-277.

Tempelman-Kluit, D.J.
1977: Quiet Lake (105F) and Finlayson Lake (105G) map areas, Yukon; Geological Survey of Canada, Open File 486.
1979: Transported cataclasite, ophiolite and granodiorite in Yukon: evidence of arc-continent collision; Geological Survey of Canada, Paper 79-14.
1984: Geology, Laberge (105E) and Carmacks (115I), Yukon Territory; Geological Survey of Canada, Open File 1101.

Tullis, J., Snoke, A.W., and Todd, V.R.
1982: Significance and petrogenesis of mylonitic rocks: Penrose conference report; Geology, v. 10, p. 227-230.

Vernon, R.H.
1976: Metamorphic processes: reactions and microstructure development; George Allen and Unwin Ltd., 247 p.

Wheeler, J.O., Brookfield, A.J., Gabrielse, H., Monger, J.W.H., Tipper, H.W., and Woodsworth, G.J.
1988: Terrane map of the Canadian Cordillera; Geological Survey of Canada, Open File 1894.

APPENDIX 3 - GEOLOGY AND STRUCTURE OF THE TESLIN SUTURE ZONE AND RELATED ROCKS IN PARTS OF LABERGE, QUIET LAKE, AND TESLIN MAP AREAS, YUKON TERRITORY: PUBLISHED IN GEOLOGICAL SURVEY OF CANADA PAPER 93-1A*

---

*A version of this appendix has been published. Stevens, R.A., and Erdmer, P. 1993. *In* Current Research, Part A, Geological Survey of Canada, Paper 93-1A, pp. 11-20.

Geology and structure of the Teslin suture zone and related rocks in parts of Laberge, Quiet Lake, and Teslin map areas, Yukon Territory

R.A. Stevens[1] and P. Erdmer[1]
Cordilleran Division

Stevens, R.A. and Erdmer, P., 1993: Geology and structure of the Teslin suture zone and related rocks in parts of Laberge, Quiet Lake, and Teslin map areas, Yukon Territory; in Current Research, Part A; Geological Survey of Canada, Paper 93-1A, p. 11-20.

Abstract: This report outlines the geology of four areas mapped in 1992 and describes in detail the structure along one transect across the Teslin suture zone. Several units are recognized and include: hornblende±augite diorite or gabbro (**Mhdg**), conglomeratic grit of the Boswell Formation (**PBs**), felsic to mafic schist and gneiss, quartzite, metaplutonic rock, and pegmatite (**PMv**), meta-hornblende diorite or gabbro (**PMhdg**), biotite±sillimanite±muscovite schist and gneiss (**Pn+?**), and autochthonous North American rocks (**NA?**). Along the transect seven structural domains are recognized. Each is characterized by distinct foliation and mineral lineation orientations. Structures along this transect record two deformation phases: an early penetrative ductile deformation, and late folding. Mapping along the margin of the suture zone shows that faults and undeformed volcanic rocks mark the western contact.

Résumé : Dans le présent rapport, on esquisse la géologie de quatre secteurs cartographiés en 1992, et l'on décrit en détail la structure le long d'un transect suivi de part et d'autre de la zone de suture de Teslin. Parmi les nombreuses unités reconnues, on remarque : une diorite ou un gabbro à hornblende augite (**Mhdg**), un grès grossier conglomératique de la Formation de Boswell (**PBs**), un schiste et un gneiss felsiques à mafiques, un quartzite, des roches métaplutoniques et une pegmatite (**PMv**), une métadiorite ou un métagabbro à hornblende (**PMhdg**), un schiste et un gneiss à biotite±sillimanite±muscovite (**Pn+?**) et des roches autochtones, nord-américaines (**NA?**). Le long du transect, ont été identifiés sept domaines structuraux. Chacun est caractérisé par des orientations distinctes de la foliation et de la linéation minérale. Les structures observées le long de ce transect témoignent de deux phases de déformation: une déformation ductile initiale, de type pénétratif, et un plissement tardif. La cartographie de la marge de la zone de suture montre que la présence de failles et de roches volcaniques non déformées caractérise le contact occidental.

---

[1] Department of Geology, University of Alberta, #1-26 Earth Sciences Building, Edmonton, Alberta T6G 2E3

INTRODUCTION

The Teslin suture zone, a part of the Yukon-Tanana composite terrane (Kootenay terrane of Wheeler et al., 1991) of southern Yukon and east-central Alaska, marks the fundamental boundary between deformed autochthonous North American rocks of the Omineca Belt to the east and accreted terranes of the Intermontane Belt to the west. It includes of a variety of S-, L-S, and L-tectonites derived from sedimentary, volcanic, and plutonic rocks metamorphosed under greenschist to amphibolite facies conditions (Stevens, 1991, 1992). Current models of formation of the suture zone hypothesize that its rocks were the product of deformation within the deep-seated portion of a west-dipping Permo-Triassic subduction complex west of ancient North America. The rocks were subsequently thrust eastward onto North American strata in the Early Jurassic, and the Teslin suture zone is interpreted to represent the root zone to these obducted rocks (Hansen, 1991, 1992; Tempelman-Kluit, 1979).

Exposures of Teslin suture zone rocks studied for this project underlie parts of Laberge (NTS 105E), Quiet Lake (NTS 105F), and Teslin (NTS 105C) map areas. The geology of part of all three map areas was described by Lees (1936). The Quiet Lake and Laberge map areas were mapped by

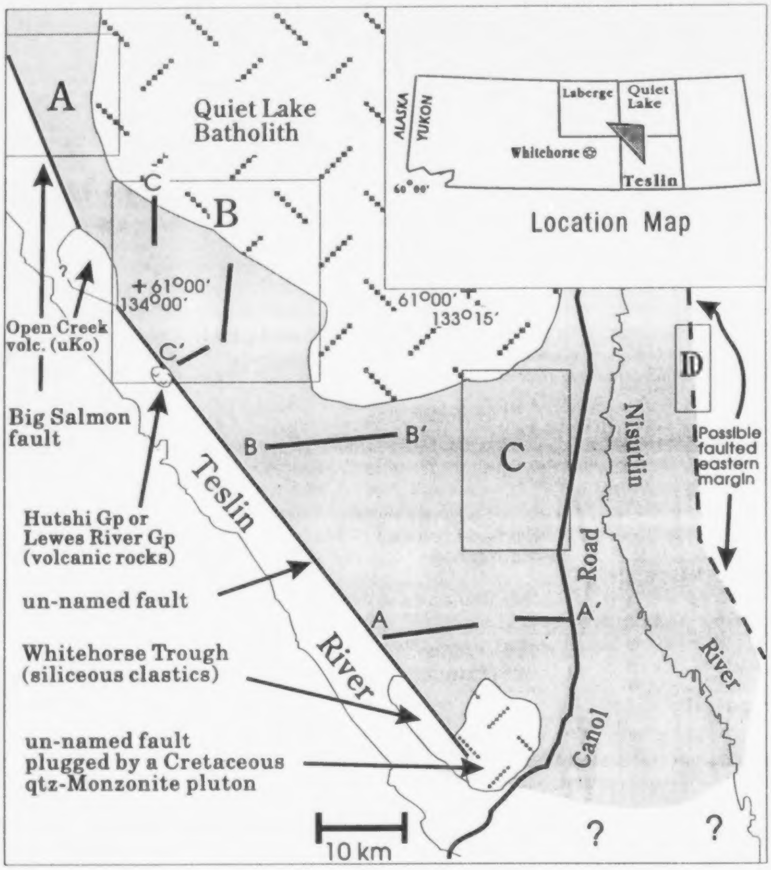
A
Quiet Lake
Batholith
C
B
+61°00′
134°00′
C′
?
Open Creek
volc. (uKo)
Big Salmon
fault
B
B′
Teslin
Hutshi Gp or
Lewes River Gp
(volcanic rocks)
un-named fault
A
A′
Whitehorse Trough
(siliceous clastics)
River
un-named fault
plugged by a Cretaceous
qtz-Monzonite pluton
10 km
61°00′
133°15′
C
Nisutlin
Road
Canol
River
D
Possible
faulted
eastern
margin
?
?
ALASKA
YUKON
Laberge
Quiet
Lake
Whitehorse
60°00′
Teslin
Location Map

Figure 1. Location map, showing the part of the Teslin suture zone considered in this study (grey shading), the type of contacts that define the margins of the Teslin suture zone, the location of three structural transects described in Stevens (1992) (AA′ and BB′) or in this report (CC′) and the location of four map areas (A-D) described in this report.

Tempelman-Kluit (1977, 1984) and the geology of the Teslin map area was described by Mulligan (1963). The Teslin map area is being remapped at 1:50 000 and 1:250 000 scales by the Geological Survey of Canada (Gordey, 1991, 1992). Teslin suture zone-related rocks in the southern half of the Teslin map area are the focus of a continuing study by Gareau (1992).

This report outlines the geology of four areas (A-D) mapped in 1992 (see Fig. 2-6), and describes the structure along one transect (CC' on Fig. 1 and 4). Many of the units recognized in areas A-D were described by Stevens (1991, 1992) (units **PMs**, **PMm**, **PMgp**, **PMga**, **Kqm**, **K$_{RM}$**, and **Mtqd**) in adjacent areas and are not described in detail here. Unit **OD$_N$** (see Stevens, 1992) is equivalent to unit **PMgp** in this report (see discussion).

MAP AREA A

Many of the units mapped in area A (Fig. 3) can be correlated with rocks to the south described by Stevens (1991, 1992) (units **PMs**, **PMm** and **Kqm**) or in this report (**PMgr**), and only brief descriptions of these are given below. Two new units (**Mhdg**, **PBs**) and one sub-unit (**PMsm**) are described in detail.

Unit **PMs** rocks are muscovite- and quartz-rich schist with minor muscovite-bearing quartzite, calcareous schist, and marble. Garnetiferous schist occurs in the northern part of the area. Unit **PMs** rocks east of the Loon Lakes locally contain biotite and chlorite. Marble (**PMm**) outcrops in the northern part of the area. Quartz-monzonite of the Quiet Lake Batholith (Tempelman-Kluit, 1977) (**Kqm**) outcrops along the western edge of the map area. Margin parallel foliation is developed within 200-300 m of the contact. Unit **PMgr** is medium to dark green chlorite-actinolite greenstone and compositionally banded chlorite-actinolite-epidote schist.

Schist (PMsm)

Brown to green weathering fine- to medium-grained chlorite-muscovite-actinolite-biotite quartzofeldspathic schist occurs in the central part of the area. Locally, medium grained phases suggest derivation from an intermediate plutonic rock. These rocks are grouped in subunit **PMsm**, because they are consistently more mafic (containing more chlorite+actinolite+biotite than muscovite) and less schistose than other **PMs** rock.

Hornblende±augite diorite or gabbro (Mhdg)

East of Loon Lakes occurs a 1 km^2 body of grey-green to slightly red weathering, massive, medium grained hornblende diorite to gabbro. Locally, the pluton is porphyritic, with up to 30% phenocrysts of medium- to coarse-grained hornblende and augite. The main mass of rock and the matrix in porphyritic phases consist of approximately 40-60% hornblende, 40-60% altered feldspar, and minor quartz. Hints of an igneous flow fabric are seen locally. The body includes screens of country rock (mostly quartzite and schist). The intrusive relationship to metamorphic rock of unit **PMs**, the massive texture, local hints of flow banding and the abundance of hornblende are similar to unit **Mtqd** mapped in the Sawtooth Range (Stevens, 1992) (Fig. 4). **Mhdg** may thus be part of an intrusive suite that includes unit **Mtqd**.

Boswell Formation (PBs)

The Boswell Formation (**PBs**) (Tempelman-Kluit, 1984) west of Loon Lakes consists of black-weathering fine- to medium-grained, unmetamorphosed, conglomeratic grit with clasts of chert, black fine grained rock, and possible hornblende or augite grains.

Regional faults

Previous maps of the area show two large faults, the d'Abbadie fault (Hansen, 1989, 1991) and the Big Salmon fault (Tempelman-Kluit, 1984). The d'Abbadie fault was interpreted to trend north and separate the Teslin suture zone proper in the west from orthogneiss to the east that is structurally similar to rock of the Teslin suture zone proper but which has undergone a different cooling history (Hansen, 1989). The Big Salmon fault was shown to trend northwest, 3-4 km east of Loon Lakes (Fig. 3) and to separate Teslin suture zone rock in the east from unmetamorphosed allochthonous rocks of the Semenof Hills Block (including the Boswell Formation) to the west.

Our mapping did not locate either of the faults in the proposed locations. In both cases the contacts are interpreted as fabric-parallel contacts within the Teslin suture zone (Fig. 3). We conclude that the d'Abbadie fault does not extend into the area as proposed by Hansen (1989, 1991), and that it terminates to the north or west. We also conclude that the Big Salmon fault is located farther west than interpreted by Tempelman-Kluit (1984), likely in the valley of the Loon Lakes separating unit **PMs** in the east from the Boswell Formation in the west.

MAP AREA B

Most of the units in map area B (Fig. 4) (**PMs**, **PMgp**, **PMm**, **PMga**, **Kqm**, **KRM**, **Mtqd**) were described by Stevens (1991, 1992). A new description of unit **PMgr** (Stevens, 1992) is presented that encompasses the results of the new mapping, and two new units are defined (**PMv** and **PMhdg**).

Mafic schist and greenstone (PMgr)

The most common rock types of this unit are: medium to dark green foliated and locally lineated actinolite-chlorite-epidote±biotite±hornblende schist and greenstone; light to dark green, sheared, compositionally banded chlorite-epidote-actinolite±biotite quartzofeldspathic schist; medium to dark green, massive, locally porphyritic hornblende-actinolite-chlorite-epidote greenstone; and sheared amphibolite. Massive hornblende-bearing greenstone is confined to

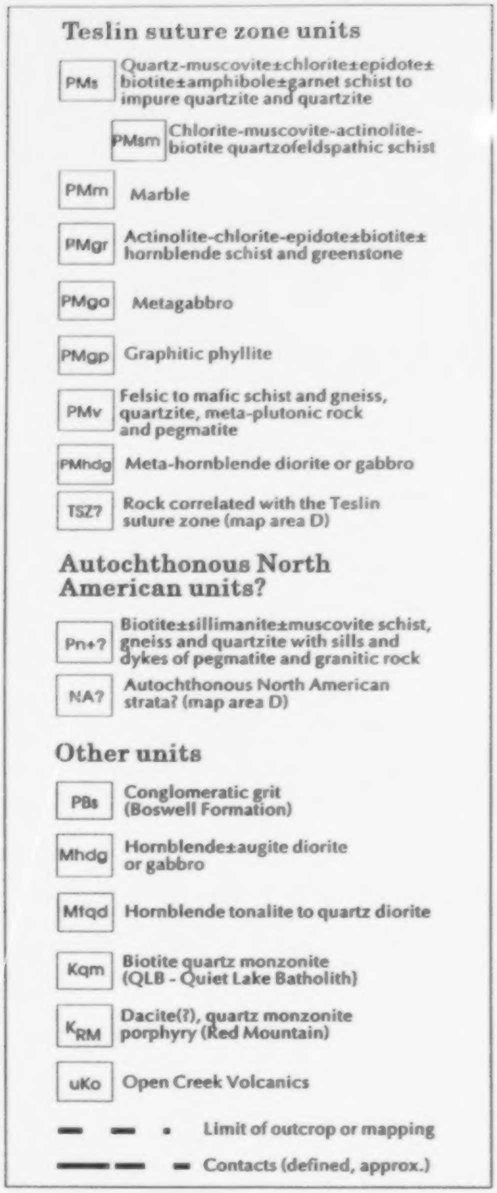

Teslin suture zone units

PMs	Quartz-muscovite±chlorite±epidote± biotite±amphibole±garnet schist to impure quartzite and quartzite
PMsm	Chlorite-muscovite-actinolite-biotite quartzofeldspathic schist
PMm	Marble
PMgr	Actinolite-chlorite-epidote±biotite± hornblende schist and greenstone
PMgo	Metagabbro
PMgp	Graphitic phyllite
PMv	Felsic to mafic schist and gneiss, quartzite, meta-plutonic rock and pegmatite
PMhdg	Meta-hornblende diorite or gabbro
TSZ?	Rock correlated with the Teslin suture zone (map area D)

Autochthonous North American units?

Pn+?	Biotite±sillimanite±muscovite schist, gneiss and quartzite with sills and dykes of pegmatite and granitic rock
NA?	Autochthonous North American strata? (map area D)

Other units

PBs	Conglomeratic grit (Boswell Formation)
Mhdg	Hornblende±augite diorite or gabbro
Mtqd	Hornblende tonalite to quartz diorite
Kqm	Biotite quartz monzonite (QLB - Quiet Lake Batholith)
K_{RM}	Dacite(?), quartz monzonite porphyry (Red Mountain)
uKo	Open Creek Volcanics

Limit of outcrop or mapping

Contacts (defined, approx.)

Figure 2. Legend for map areas A-D (Fig. 3-6). Teslin suture zone units consist of rock that shows the development of penetrative ductile deformation fabrics. Autochthonous North American units consist of rock tentatively correlated as deformed autochthonous North American strata. Other units consist of rock that lacks a foliation.

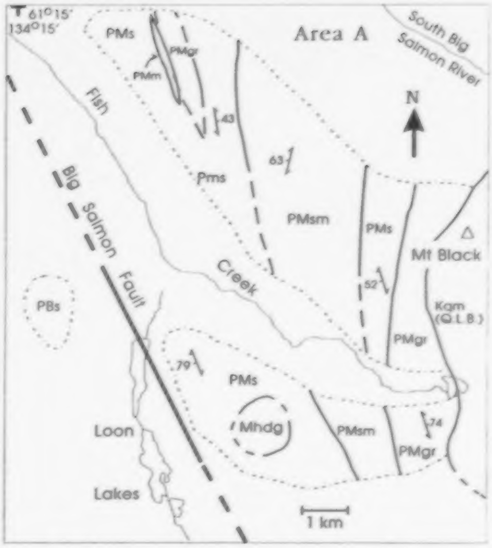
61°15'
134°15'
Area A
South Big Salmon River
N
PMs
PMgr
PMm
43
63
Pms
PMsm
PMs
Mt Black
Big Salmon Fault
Fish Creek
PBs
52
Kqm (Q.L.B.)
PMgr
79
PMs
Mhdg
PMsm
74
PMgr
Loon
Lakes
1 km

Figure 3. Simplified geology of area A.

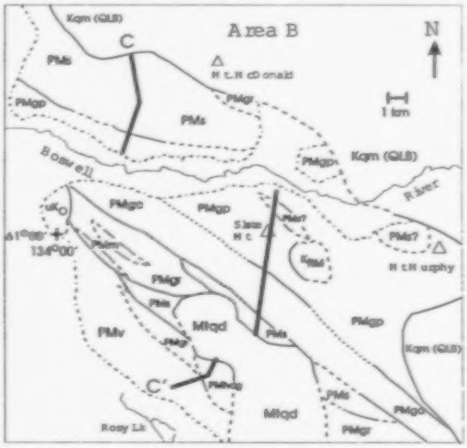
Kqm (QLB)
Area B
N
C
PMs
Mt. McDonald
PMgp
PMgr
1 km
PMs
Kqm (QLB)
PMgp
Boswell River
uKo
PMgp
PMgp
Slate Mt
PMs?
PMs?
61°08'
134°00'
PMm
KRM
Mt Murphy
PMgr
PMs
Mtqd
PMgp
PMv
PMgr
PMs
Kqm (QLB)
C'
PMhdg
PMs
PMgo
Mtqd
Rosy Lk
PMgr

Figure 4. Simplified geology of area B.

the area southeast of unit **Mtqd** (Fig. 4). Bands and pods of marble tens of metres across are common within the unit and several of these are shown on Figure 4.

The rocks of this unit are likely derived from basaltic to andesitic flows and tuffs deposited in or near a shallow water environment where small carbonate reefs or banks formed. In addition, rocks of this unit are interleaved, with gabbro of unit **PMga**, along their contact and within unit **PMga**. This suggests that the two units are genetically related, especially since **PMga** gabbro is not interlayered with other units.

Felsic to mafic schist and gneiss, quartzite, meta-plutonic rock and pegmatite (PMv)

A range of rock types, interlayered at a scale of 10 cm to several hundred metres, comprise unit **PMv**. The most common members are: sheared quartzite and muscovite quartzite, quartz-muscovite schist, biotite-muscovite-quartz-amphibole±garnet schist and gneiss, biotite-amphibole-chlorite-epidote schist and gneiss, amphibolite, massive to sheared hornblende-bearing tonalite, quartz-diorite and diorite, and massive felsic pegmatite. Pegmatite occurs as thin apparently sheared wisps and bands and as massive dykes a few metres wide.

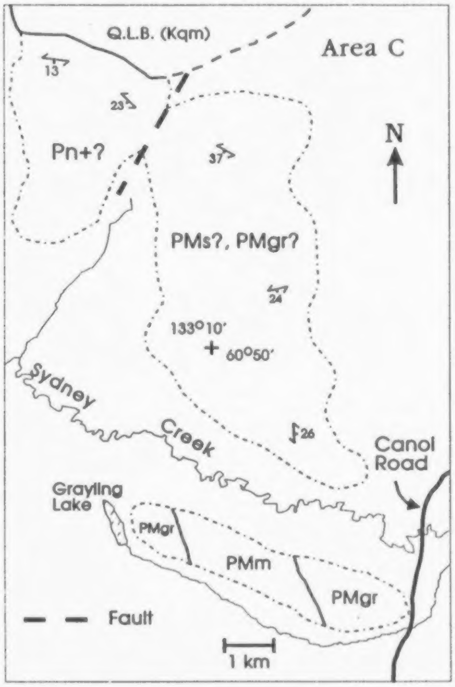

Figure 5. Simplified geology of area C.

The variety of rock types and their interlayering suggest that, prior to deformation and metamorphism, the assemblage consisted of sedimentary and possibly volcanic rocks intruded by dykes and small plugs of intermediate composition.

Meta-hornblende diorite or gabbro (PMhdg)

South of unit **Mtqd** (Fig. 4), is an area of moderately deformed to ultramylonitic S-, L-S, and L-tectonites of dark green and white hornblende diorite or gabbro and amphibolite. Cutting these rocks are massive, felsic to mafic dykes including a feldspar porphyritic phase, hornblendite and hornblende diorite. Most of the mafic intrusions are likely related to unit **Mtqd** exposed to the north. Foliation surfaces generally strike northeast and dip southeast, an orientation uncommon elsewhere in the suture zone.

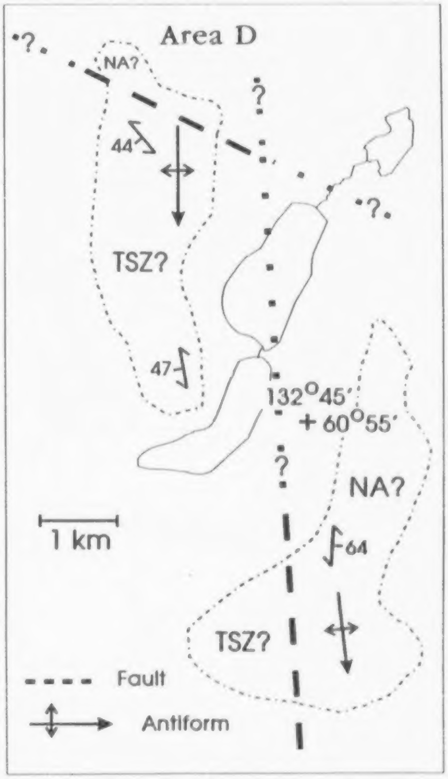

Figure 6. Simplified geology of area D.

MAP AREA C

Units **PMgr** and **PMm** outcrop south of Sydney Creek and east of Grayling Lake (see Stevens, 1992 and this report) (Fig. 5).

Biotite±sillimanite±muscovite schist, gneiss and quartzite with sills and dykes of pegmatite and granitic rock (Pn+?)

North of Sydney Creek and south of the Quiet Lake Batholith (Fig. 5) occur brownish grey to red, medium grained biotite±sillimanite±muscovite quartzofeldspathic schist to gneiss and red-weathering to strongly gossaned biotite-pyrite quartzite to quartz-schist. These are cut by and include generally massive sills and dykes of biotite-bearing quartz-monzonite and felsic pegmatite. Schist and gneiss are strongly sheared L-S tectonites with mineral lineations defined by quartz rodding and by alignment of biotite and sillimanite. The strike of foliation surfaces varies and dips average between 10° to 20°.

This unit is distinguished from other units by the presence of abundant sillimanite, local gneissic character, the abundant dykes and sills, and the subhorizontal foliation. Similar rocks in the Quiet Lake map area are included in unit **Pn+**, and are interpreted to be metamorphosed autochthonous rocks of the Omineca Belt (Tempelman-Kluit, 1977).

Heterogenous meta-sedimentary, meta-tuffaceous and meta-volcanic rocks (PMs, PMgr)

North of Sydney Creek and west of the unit described above is a unit of considerable lithological variability (Fig. 5). The main rock types are: quartzite, marble, quartz-chlorite±

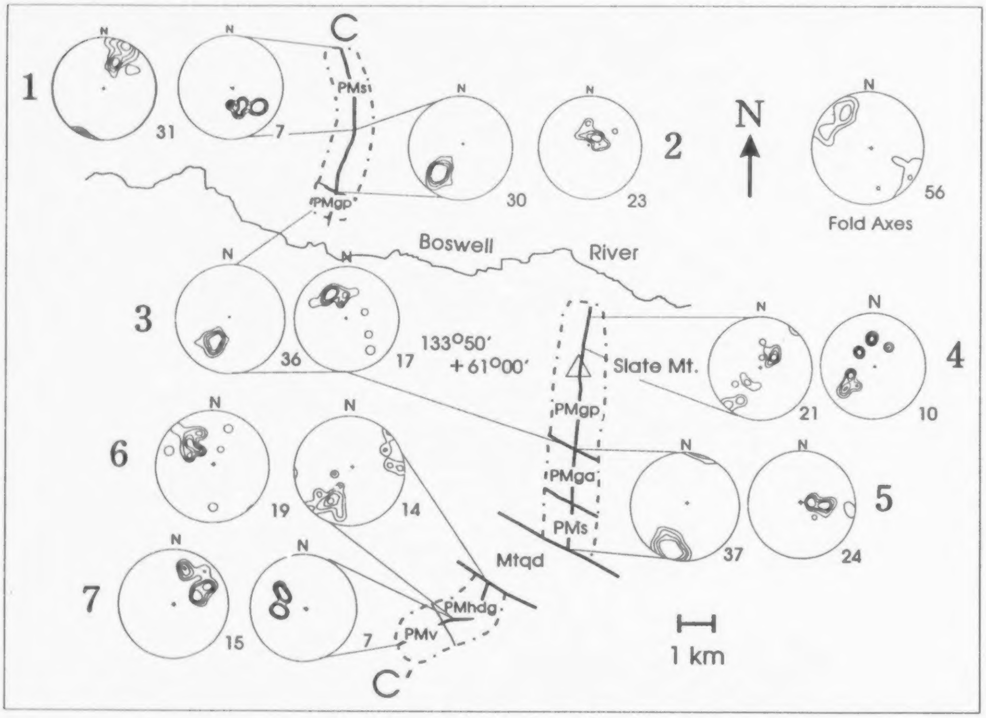

Figure 7. Strip map for transect CC' showing rock types along the transect. Stereographic projection plot are for the seven structural domains recognized in this transect. The bold number represents the domain, the left stereonet shows poles to foliation and the right stereonet, mineral/stretching lineation orientations. Contours are densities expressed as multiples of a uniform density with contours at densities of 3, 6, 9, and 12.

muscovite±actinolite schist, light to medium green, compositionally banded chlorite-epidote±actinolite-quartz schist, and actinolite-chlorite±hornblende greenstone. Green compositionally banded schist likely has tuffaceous parentage and greenstone volcanic parentage. Foliation surfaces have variable strikes, and dips between 20° and 35°. These rocks are interpreted as part of unit **PMs** possibly intercalated with unit **PMgr**.

MAP AREA D

North American rocks? (NA?)

The northern and eastern parts of area D (Fig. 6) include carbonate (locally crinoidal), impure muscovite- and chlorite-bearing metasandstone to meta-arkose, minor interlayered graphitic phyllite, and biotite-chlorite±actinolite greenstone. Most areas show weak to moderate tectonic foliation, with local development of mylonitic fabric. Quartz microstructures show evidence of recrystallization and fracturing. At least one open antiform is present (see Fig. 6). Metamorphism locally reached biotite grade, but most rocks are not strongly metamorphosed or recrystallized. Rocks similar in composition, degree of metamorphism and state of deformation outcrop in the Thirtymile Range, to the southeast (S.P. Gordey, pers. comm., 1992). Recent mapping led Gordey (1992) to suggest that strata in the Thirtymile Range are of autochthonous North American affinity.

Teslin suture zone rock? (TSZ?)

To the south and west on Figure 6 occur red-brown to green weathering, locally compositionally banded biotite-epidote± actinolite greenstone or schist. In places, they are interbanded with quartz-muscovite±biotite schist to impure quartzite and in one place with quartz-muscovite graphitic schist. The rocks are mostly L-S tectonites with foliation surfaces that strike south to southeast and dip moderately southwest or northeast. One map-scale antiform is present (Fig. 6). Rock similar in composition, metamorphic grade and state of deformation outcrop west of the Nisutlin River and are interpreted to be part of the Teslin suture zone (Stevens, 1992). These rocks are tentatively correlated with the Teslin suture zone, (units **PMgr** and/or **PMs**).

Strata in area D are folded and show widespread crenulations, cleavage, and at least two regional antiforms. Fold axes trend south and plunge 5-10°. Steep faults separate units **NA?** and **TSZ?**. One fault trends north across the centre of the area and the second trends west-northwest along the top of the map area. Rock of unit **NA?** north of the second fault may have been uplifted and may represent in part, the type of strata that unit **TSZ?** to the south of the fault are resting on.

STRUCTURAL TRANSECT

One detailed structural transect was completed during the summer of 1992 (CC' on Fig. 1). This transect complements two previous transects (Stevens, 1992) (AA' and BB' on Fig. 1). The CC' transect comprises three segments totalling 15 km. Measurement stations located 150-250 m apart, resulted in 70 stations across the transect. Oriented samples were collected at each station.

Seven structural domains are recognized. Some are rock type independent, meaning that the boundaries of the domain are not controlled by a change in rock type. In other cases, a domain is confined to, and likely controlled by, a single rock type. Figure 7 is a strip map of the transect, with contoured stereoplots of fabric orientation for each domain. Fold axis measurements along this transect are summarized in a separate stereoplot (see Fig. 7).

Domain 1

Moderately to strongly deformed S and L-S tectonites with steeply southwest-dipping foliation and crenulation hinge lineations characterize this domain. A few mineral lineations occur near the southern edge of the domain. A spaced (5-30 cm) crenulation cleavage has developed locally, which strikes roughly southeast and dips moderately southwest. These are late cleavage surfaces that cut earlier fabrics. Shear sense from the crenulation asymmetry between cleavage surfaces is hanging wall-up, or southwest face thrust to the northeast during folding (Bell and Johnson, 1992) (Fig. 8).

The northern boundary of the domain is placed at the edge of the Quiet Lake Batholith. The southern boundary is a 200-300 m wide zone where foliation surfaces switch from southwest to northeast dipping.

Domain 2

Strongly deformed to mylonitic L-S tectonites with steeply northeast dipping foliation and lineations defined by stretched and preferentially oriented minerals such as quartz, muscovite, and chlorite characterize this domain. Crenulation and mesoscopic folds are developed together with a spaced (5-30 cm) cleavage that strikes west-northwest and dips moderately northeast. Crenulation asymmetry between cleavage surfaces indicates that the hanging wall moved down to the northeast.

The southern boundary of the domain is marked by a change from muscovite- and quartz-rich schist to graphitic phyllite.

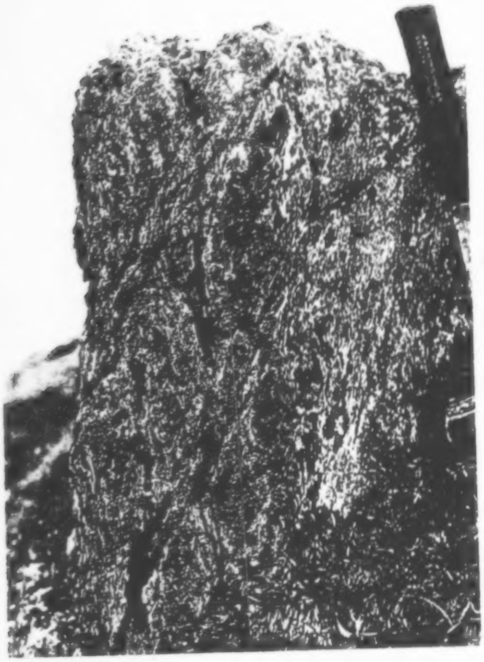

Figure 8. Shear sense from the crenulation asymmetry between cleavage surfaces is hanging wall-up, which for this figure means the southwest face was thrust to the northeast.

Domain 3

Moderately to strongly deformed S and L-S tectonites of graphitic phyllite with moderately to steeply northeast dipping foliation and crenulation hinge lineations characterize this domain. Mineral lineations are best developed north of Slate Mountain in siliceous and/or schistose graphitic phyllite. A crenulation cleavage is developed locally, with crenulation asymmetry indicating that the hanging wall moved down the northeast.

The northern and southern boundaries of this domain are defined by the contacts of the graphitic phyllite unit.

Domain 4

Domain 4 is characterized by closed to tight folds with rounded to chevron hinges, wavelengths of 10-30 m and amplitudes of approximately 10-40 m. The folds occur in an area dominated by strong L-S tectonites of quartz-chlorite±muscovite schist within the graphitic phyllite unit of domain 3. Poles to foliation surfaces approximate a great circle (Fig. 7) whose pole, oriented at 309/2, is the fold axis for the domain. This orientation is similar to the average orientation (311/9) for all fold axis measurements from the transect. Mineral/stretching lineation orientations are variable, possibly due to folding of the tectonites.

Domain 5

Domain 5 includes two rocks types. Gabbro of unit **PMga** occurs to the north. The gabbro is massive to weakly deformed, with local discrete zones of high strain. L-S tectonites are developed in these zones and rarely elsewhere in the unit. Lineations are defined by aggregates of feldspar, pyroxene, and amphibole. The southern half of the domain includes a variety of interleaved schistose rocks of unit **PMs**. These are strongly deformed to mylonitic L-S tectonites. Lineations are defined by quartz rodding and alignment of elongate muscovite, biotite, amphibole, and quartz. Folding has not developed in this domain.

The northern boundary coincides with the edge of unit **PMgp** and the southern boundary is the intrusive contact with unit **Mtqd**.

Domain 6

Moderately deformed to ultramylonitic S-, L-S, and L-tectonites of unit **PMhdg**, with foliation surfaces that strike northeast and dip moderately to steeply southeast characterize domain 6. Mineral lineations, defined by elongate trains of feldspar or by grains of amphibole, show a fair degree of scatter. Outcrop-scale folds are present locally and may be responsible for the scatter in lineation orientations.

The northern boundary of the domain is an intrusive contact with unit **Mtqd**, and the southern boundary is placed at an inferred fault, where the northeast-striking foliation surfaces change to west-northwest striking foliation surfaces.

Domain 7

Variably deformed rock of units **PMhdg** and **PMv** with northwest-striking and southwest-dipping foliation surfaces marks this domain. L-S tectonites and late folds are developed locally.

The southern boundary of the domain is unconstrained.

DISCUSSION

Two deformation events or phases of a single event are recorded in the Teslin suture zone (Fig. 1). The first was a penetrative ductile deformation event that produced mylonite and S-, L-S, and L-tectonites under greenschist to lower amphibolite facies metamorphic conditions. The second was a folding event, under similar metamorphic conditions that produced widespread crenulation of earlier fabrics and development of a cleavage.

The orientation of fabrics along CC' is characteristic of much of the Teslin suture zone considered in this study. For example early schistosity and mylonitic foliation generally strike northwest-southeast, and dip either northeast or southwest, and mineral lineations which form local orientation clusters (Fig. 7) show a wide range of orientation between the clusters. In addition, second phase folding does not appear responsible for these variations, because attempts at rotating structures about common fold axes from the map area were unsuccessful in bringing structures from adjacent or similar domains into a common orientation. We believe that most of the variations in fabric orientations developed during the early ductile deformation.

Strain partitioning throughout the map area is primarily controlled by rock type. Relatively incompetent rocks such as mica schist and graphitic phyllite are most highly deformed, followed by mafic and quartzofeldspathic schist and finally by metaplutonic rocks. The fabrics that develop are also controlled by rock type. For example, graphitic phyllite shows strong crenulation lineations but few mineral lineations, whereas schist, especially quartz rich varieties, shows strong development of mineral and fold lineations; metaplutonic rocks show little of either.

A previously defined graphitic phyllite unit (**OD$_N$**) (Stevens, 1991, 1992) is equivalent to unit **PMgp** in this report. This graphitic phyllite was correlated with the autochthonous Nasina Formation by Stevens (1991). Assignment of the graphitic phyllite to the Nasina facies (Stevens, 1991) is considered inappropriate because present mapping shows that it may be part of a single depositional sequence that includes rocks of unit **PMs**. Unit **PMs** is correlated with the Nisutlin Allochthon (Stevens, 1991). In the contact zone between **PMs** and **PMgp**, graphite first appears in unit **PMs** 400 to 600 m from the contact, and within 100-200 m one of the main rock types is quartz-muscovite-graphite schist. South of the contact, muscovite-graphite schist is interlayered with graphitic phyllite over 100-200 m. This suggests that the contact was originally depositional and that the two units may result from different depositional environments or sources within a continuous sedimentary sequence.

REGIONAL EXTENT OF THE TESLIN SUTURE ZONE

North of the study area (Fig. 1) the Teslin suture zone trends across the Laberge map area to the southern part of the Glenlyon map area (Tempelman-Kluit, 1979; Hansen 1989). Results presented by Stevens (1991, 1992) and in this report show that the suture zone continues southward from Laberge map area to the Canol Road in central Teslin map area. South of the Canol Road, the distribution of Teslin suture zone rock is unclear (see Gareau, 1992). The western margin of the suture zone in Figure 1 is marked by faults or undeformed volcanic rocks. The Big Salmon fault marks the western contact in the northern part of the map area. It is masked to the south by volcanic rocks of unit **UKo** which overlie Teslin suture zone rocks. From the northwest corner of the Teslin map area (61°00'N, 134°00'W) to the Canol Road, the contact is a second fault (unnamed) (see Gordey, 1991). Volcanic rocks equivalent to the Hutshi or Lewes River groups in the Whitehorse map area (Wheeler, 1961) and siliceous clastic rock of the Whitehorse trough (unit 9 of Mulligan, 1963) were mapped west of this unnamed fault (Fig. 1). North of the Canol Road, a massive biotite quartz-monzonite pluton cuts the fault. The location of the eastern margin of the suture zone is unclear. It may pass through map area D (Fig. 1 and Fig. 6) or, if Teslin suture zone rocks in that map area are parts of klippen, the contact may lie farther west, possibly in the Nisutlin River valley.

ACKNOWLEDGMENTS

Field work was supported by a joint EMR/NSERC research agreement to P. Erdmer and a Northern Scientific Training Program grant from the Department of Indian Affairs and Northern Development, a grant from the Canadian Circumpolar Institute of the University of Alberta and an NSERC Post Graduate Scholarship awarded to R.A. Stevens. Logistical support provided by the Department of Indian Affairs and Northern Development and the Geological Survey of Canada is greatly appreciated. S.P. Gordey is thanked for a visit in the field and for reviewing an early version of this report. D.J. Tempelman-Kluit is thanked for reviewing the manuscript. Gord Stretch provided excellent assistance in the field.

REFERENCES

Bell, T.H. and Johnson, S.E.
1992: Shear sense: a new approach that resolves conflicts between criteria in metamorphic rocks; Journal of Metamorphic Geology, v. 10, p. 99-124.
Gareau, S.A.
1992: Report on fieldwork in the southern Big Salmon metamorphic complex, Teslin map area, Yukon Territory; in Current Research, Part A; Geological Survey of Canada, Paper 92-1A, p. 267-277.
Gordey, S.P.
1991: Teslin map area, a new geological mapping project in Southern Yukon; in Current Research, Part A; Geological Survey of Canada, Paper 91-1A, p. 171-178.
1992: Geological fieldwork in Teslin map area, southern Yukon Territory; in Current Research, Part A; Geological Survey of Canada, Paper 92-1A, p. 279-286.
Hansen, V.L.
1989: Structural and kinematic evolution of the Teslin suture zone, Yukon: record of an ancient transpressional margin; Journal of Structural Geology, v. 11, no. 6, p. 717-733.
1991: Mesozoic thermal evolution of the Yukon-Tanana composite terrane: new evidence from ^{40}Ar/^{39}Ar data; Tectonics, v. 10, no. 1, p. 51-76.
1992: Backflow and margin-parallel shear within an ancient subduction complex; Geology, v. 20, no. 1, p. 71-74.

Lees, E.J.
1936: Geology of the Teslin-Quiet Lake area Yukon Territory; Geological Survey of Canada, Memoir 203.

Mulligan, R.
1963: Geology of the Teslin map area, Yukon Territory (105C); Geological Survey of Canada, Memoir 326.

Stevens, R.A.
1991: The Teslin suture zone in northwest Teslin map area, Yukon; *in* Current Research, Part A; Geological Survey of Canada, Paper 91-1A, p. 271-277.
1992: Regional geology, fabric, and structure of the Teslin suture zone in northwest Teslin map area, Yukon Territory; *in* Current Research, Part A; Geological Survey of Canada, Paper 92-1A, p. 287-295.

Tempelman-Kluit, D.J.
1977: Quiet Lake (105F) and Finlayson Lake (105G) map areas, Yukon; Geological Survey of Canada, Open File 486.

Tempelman-Kluit, D.J. (cont.)
1979: Transported cataclasite, ophiolite and granodiorite in Yukon: evidence of arc-continent collision; Geological Survey of Canada, Paper 79-14.
1984: Geology, Laberge (105E) and Carmacks (115I), Yukon Territory; Geological Survey of Canada, Open File 1101.

Wheeler, J.O.
1961: Whitehorse map-area, Yukon Territory (105 D); Geological Survey of Canada, Memoir 312.

Wheeler, J.O., Brookfield, A.J., Gabrielse, H., Monger, J.W.H., Tipper, H.W., and Woodsworth, G.J.
1991: Terrane map of the Canadian Cordillera; Geological Survey of Canada, Map 1713A, scale 1:2 000 000.

APPENDIX 4 - ABSTRACTS OF PRESENTATIONS GIVEN ON THE TESLIN TECTONIC ZONE DURING PH.D. STUDY

REGIONAL GEOLOGY AND STRUCTURE OF THE TESLIN SUTURE ZONE IN NORTHWEST TESLIN MAP AREA, YUKON

R.A. Stevens, 1992. Presented at the 1992 Western InterUniversity Geology Conference, Edmonton, Alberta, January 16-18.

The Teslin suture zone in northwest Teslin map area includes three metasedimentary and three metaigneous rock units of paleozoic and/or mesozoic age. They are: a graphitic phyllite unit, a siliceous schist and quartzite unit, marble, hornblende megacrystic greenstone, metamorphosed tonalite to quartz diorite and metagabbro. Ductile deformation under greenschist to lower amphibolite facies conditions produced protomylonite and mylonite in much of the area, particularly in the siliceous schist and quartzite unit. Detailed mapping along two east trending transects about 20 km apart reveals that the suture zone has domains of contrasting structural style with different fabric orientations. In both transects, a western domain of L-S tectonites with well formed mineral lineations passes to the east into a domain dominated by ductile flexural-slip folding with mineral lineations parallel to fold axes, which in turn passes to the east into a domain of poorly formed L-S tectonites with variable fabric orientations. The southern transect intersects a fourth domain farther east that includes L-S tectonites with moderately well formed mineral lineations. Although the structural style of the first three domains are similar the orientation of fabrics are different in the two transects. Particularly, the orientation of schistosity and mylonitic foliation which switches from northeast dipping in the southern transect to southwest dipping in the northern transect. Together the structural domains represent a change in deformation from west to east within a single package of rocks, not individual structural slices separated by thrust faults. This feature combined with the fact that deformation decreases to the east suggests that the rocks were deformed in some type of compressional event in which deformation began in the west, propagated to the east and changed style as it went.

STRUCTURE AND TECTONIC HISTORY OF THE TESLIN SUTURE ZONE, SOUTHWESTERN YUKON TERRITORY: SUBDUCTION, TRANSPRESSION AND FORMATION OF A POSITIVE FLOWER STRUCTURE

R.A. Stevens and P. Erdmer. 1992. Presented at the annual meeting of the Canadian Tectonics Group, Nordegg, Alberta, October 23-25.

The Teslin suture zone is part of the Yukon-Tanana terrane of southern Yukon and east-central Alaska. It marks the fundamental boundary between deformed autochthonous North American rocks of the Omineca Belt to the east and accreted terranes of the Intermontane Belt to the west. In parts of the Laberge, Quiet Lake and Teslin map areas the Teslin suture zone includes metasedimentary, metavolcanic and metaplutonic units of Paleozoic and/or Mesozoic age. These rocks have been metamorphosed under greenschist to lower amphibolite facies conditions. Temperature estimates of 380 to 550°C have been determined using garnet-biotite exchange thermometry.

Two deformation phases affected the map area. The earlier produced mylonite under greenschist to amphibolite facies conditions. The second, at similar metamorphic conditions, produced widespread crenulation and folding and local cleavage development. Strain partitioning is common, and is primarily controlled by rock type. Rock type also influences the type of fabrics that develop (e.g. mineral vs. fold lineation).

Detailed mapping along three structural transects revealed that the suture zone includes many domains of contrasting structural style with different fabric orientations. The following structural characteristics are present in 14 domains identified along the transects and elsewhere in the map area; 1) northeast- and southwest-dipping mylonitic fabrics, 2) normal and reverse right-oblique shear on both the northeast- and southwest-dipping fabrics; 3) domains with fold axes parallel to mineral lineations and an overall orogen-parallel subhorizontal orientation.

The current model of formation of the suture zone proposes that the rocks were deformed within the deep-seated portion of a west dipping Permo-Triassic subduction complex outboard from ancient North America. The rocks were subsequently thrust eastward onto North American strata during the Early Jurassic, and the Teslin suture zone would represent the root zone of the obducted package.

In this study, the lack of deformation under subduction zone metamorphic conditions and the presence of northeast-dipping mylonitic fabrics with apparent top-to-the-west reverse shear are difficult to accommodate into the existing model.

It is proposed that the model be revised to include early subduction zone deformation, followed by development of a right-lateral transpressive environment and the formation of a positive flower structure. The fact that subduction zone deformation comprises only part of the overall strain history explains why subduction zone metamorphism is not widespread. The transpressive environment with formation of a flower structure accounts for the existence of east- and west-verging thrust and normal shear and orogen-parallel fold axes. The lack of thrust sheets west of the suture zone as predicted by the "flower structure" model can be explained by northward translation of the thrust sheets, and underlying rocks of the Intermontane Belt, on post-accretionary dextral strike slip faults.

REGIONAL GEOLOGY, STRUCTURE AND TECTONICS OF THE TESLIN SUTURE ZONE IN NORTHWEST TESLIN MAP AREA, YUKON

R.A. Stevens and P. Erdmer, 1992. Presented at the combined meeting of the 18th annual Cordilleran Tectonics Workshop and the southern Cordillera Lithoprobe transect workshop, University of Alberta, Edmonton, Alberta, March 6-8.

The Teslin suture zone in northwest Teslin map area includes three metasedimentary and three metaigneous rock units of Paleozoic and/or Mesozoic age. They are: a graphitic phyllite unit, a siliceous schist and quartzite unit, marble, hornblende megacrystic greenstone, metamorphosed tonalite to quartz diorite and metagabbro. Rocks from the map area have been metamorphosed under greenschist to lower amphibolite facies. Temperature estimates of between 380-550°C have been determined using Garnet-Biotite exchange thermometry. Pressure estimates of between 6-10 Kbar are loosely constrained by the phengite component of white mica. Ductile deformation under the above metamorphic conditions produced protomylonite and mylonite over much of the area, particularly in the siliceous schist and quartzite unit. On average mylonitic foliations and schistosity strike northwest and dip northeast.

Detailed mapping along two east-trending transects about 20 km apart reveals that the suture zone has domains of contrasting structural style with different fabric orientations. In both transects, a western domain of L-S tectonite with well formed mineral lineations passes to the east into a domain dominated by ductile flexural-slip folding with mineral lineations parallel to fold axes, which in turn passes to the east into a domain of poorly formed L-S tectonite with variable fabric orientations. Moderately well constrained shear-sense indicators from the first two domains of the southern transect suggest thrust movement with the hanging wall transported roughly westward. The southern transect intersects a fourth domain farther east that includes L-S tectonite with moderately well formed mineral lineations. Although the structural style of the first three domains is similar, the orientation of fabrics is different in the two transects. Particularly, the orientation of schistosity and mylonitic foliation which switches from northeast dipping in the southern transect to southwest dipping in the northern transect. Together, the structural domains represent a change in deformation from west to east within a single package of rocks, not individual structural slices separated by major faults. This, combined with the fact that deformation decreases to the east suggests that deformation began in the west, propagated to the east and changed style as it went.

Current models on the formation of the suture zone place the rocks as having been deformed within the deep-seated portion of a west dipping Permo-Triassic subduction complex outboard of North America. This package of rocks was subsequently thrust eastward onto North American strata during the Early Jurassic, and the Teslin suture zone represents the root zone to this obducted package of rocks. At present many of the geological features of the suture zone in northwest Teslin map area are consistent with this model. However the northeasterly dipping fabrics with apparent top-to-the-west reverse shearing suggest that west-verging structures may play an important role in the structural evolution of the suture zone. One possibility is that these west verging structures represent back-thrusting within the package of rocks that was thrust eastward over the North America margin.

TECTONIC EVOLUTION OF THE TESLIN SUTURE ZONE, A MAJOR PLATE BOUNDARY IN SOUTH-CENTRAL YUKON TERRITORY

R.A. Stevens, 1993. Presented at the 19th annual Cordilleran Tectonics Workshop, Queen's University, Kingston, Ontario, February 19-21.

The Teslin suture zone, part of the Yukon-Tanana terrane of southern Yukon and east-central Alaska, marks the fundamental boundary between deformed autochthonous North American rocks of the Omineca Belt to the east and accreted terranes of the Intermontane Belt to the west. In parts of the Laberge, Quiet Lake and Teslin map areas the Teslin suture zone includes schist, quartzite, phyllite, marble, greenstone, meta-tonalite to quartz-diorite and metagabbro all metamorphosed under greenschist to lower amphibolite facies conditions. The largest unit, a siliceous schist and quartzite unit, is part of the Nisutlin Allochthonous Assemblage and is intruded by Late Devonian to early Mississippian hornblende-bearing tonalite to quartz diorite plutons.

Two deformation phases affected the area. The earlier and stronger phase, produced lineated protomylonite and mylonite over much of the area. Mineral and/or stretching lineations defined mostly by phyllosilicates, amphiboles and quartz are considered to be parallel to the local movement direction in the rocks. Shear-sense indicators such as strain-insensitive Sa/Sb fabric, strain-sensitive C/S fabric, asymmetrical extensional shear bands and pressure shadows have developed and help to delineate the kinematics of this early deformation phase. The second and weaker phase produced widespread crenulation, hand-specimen scale folding and local cleavage development. Shear sense can be determined locally by the crenulation asymmetry between cleavage surfaces. Strain partitioning is common, and is primarily controlled by rock type. Rock type also influences the type of fabrics that develop (e.g. mineral vs. fold lineation).

Detailed mapping along three structural transects revealed that the suture zone includes many domains of contrasting structural style with different foliation and lineation fabric orientations. The following structural characteristics are present in 14 domains identified along the transects and elsewhere in the map area; 1) steeply northeast- and southwest-dipping mylonitic fabrics, 2) normal and reverse oblique shear on both the northeast- and southwest-dipping fabrics; 3) an overall subhorizontal, suborogen-parallel crenulation axis; 4) open to tight handspecimen-scale folds with axes parallel to mineral lineations; and 5) a local spaced (10-30 cm) crenulation cleavage that dips northeast or southwest. Folding is not responsible for the two dip directions displayed by the mylonitic fabrics.

Existing models for formation of the suture zone propose that the rocks were deformed within the deep-seated portion of a west dipping Permo-Triassic subduction complex outboard from ancient North America. The rocks were subsequently thrust eastward onto North American strata during the Early Jurassic, and the Teslin suture zone would represent the root zone of the obducted package. However, the lack of deformation under subduction zone metamorphic conditions and the presence of northeast-dipping mylonitic fabrics with apparent top-to-the-west reverse shear, seen in this study, are difficult to accommodate into the existing model. In addition, it would be difficult to transport, down the subduction zone, a Devono-Mississippian pluton from the study area that is at least 6 km wide and 10 km long, without it recording this transport.

It is proposed that the evolutionary model include early subduction zone deformation, followed by development of a transpressive environment and formation of a two-sided orogen. This revised model accounts for the lack of widespread subduction zone metamorphism and for the existence of east- and west-verging thrust and normal shear and orogen-parallel fold axes. Sheets of suture zone rock thrust to the west are interpreted to have been translated northward on post-accretionary dextral strike-slip faults.

STRUCTURAL CHARACTERISTICS OF THE TESLIN SUTURE ZONE, A MAJOR PLATE BOUNDARY IN SOUTH-CENTRAL YUKON TERRITORY

R.A. Stevens, 1993. Presented at the Geological Association of Canada/Mineralogical Association of Canada annual meeting, Edmonton, Alberta, May 17-19, vol. 18, p. A101

The Teslin suture zone is part of the Yukon-Tanana terrane of southern Yukon and east-central Alaska. It marks the fundamental boundary between deformed autochthonous North American rocks of the Omineca Belt to the east and accreted terranes of the Intermontane Belt to the west. In parts of the Laberge, Quiet Lake and Teslin map areas the Teslin suture zone includes metasedimentary, metavolcanic and metaplutonic units of Paleozoic and/or Mesozoic age. These rocks were metamorphosed and deformed under greenschist to mid-amphibolite facies conditions from the latest Paleozoic to mid-Mesozoic.

Two deformation phases affected the area. The earlier and stronger phase, produced lineated protomylonite and mylonite over much of the area. Mineral and/or stretching lineations defined mostly by phyllosilicates, amphiboles and quartz are considered to be parallel to the local movement direction in the rocks. Shear-sense indicators such as strain-insensitive Sa/Sb fabric, strain-sensitive C/S fabric, asymmetrical extensional shear bands and pressure shadows have developed and help to delineate the kinematics of this early deformation phase. The second and weaker phase produced widespread crenulation, hand-specimen scale folding and local cleavage development. Shear sense can be determined locally by the crenulation asymmetry between cleavage surfaces. Strain partitioning is common, and is primarily controlled by rock type. Rock type also influences the type of fabrics that develop (e.g. mineral vs. fold lineation).

Detailed mapping along three structural transects revealed that the suture zone includes many domains of contrasting structural style with different foliation and lineation fabric orientations. The following structural characteristics are present in 14 domains identified along the transects and elsewhere in the map area; 1) steeply northeast- and southwest-dipping mylonitic fabrics, 2) normal and reverse oblique shear on both the northeast- and southwest-dipping fabrics; 3) an overall subhorizontal, suborogen-parallel crenulation axis; 4) open to tight handspecimen-scale folds with axes parallel to mineral lineations; and 5) a local spaced (10-30 cm) crenulation cleavage that dips northeast or southwest. Folding is not responsible for the two dip directions displayed by the mylonitic fabrics.

These structural features are consistent with formation in a crustal-scale transpressive strike-slip environment (general non-coaxial shear) with development of a two sided orogen (flower structure).

TECTONIC EVOLUTION OF THE TESLIN SUTURE ZONE, SOUTH-CENTRAL YUKON TERRITORY: SUBDUCTION, TRANSPRESSION AND EXTRUSION

R.A. Stevens, 1993. Presented at the Geological Association of Canada/Mineralogical Association of Canada annula meeting, Edmonton, Alberta, May 17-19, vol. 18, p. A100.

The Teslin suture zone, part of the Yukon-Tanana terrane of southern Yukon and east-central Alaska, marks the fundamental boundary between deformed autochthonous North American rocks of the Omineca Belt to the east and accreted terranes of the Intermontane Belt to the west. In parts of the Laberge, Quiet Lake and Teslin map areas the Teslin suture zone includes schist, quartzite, phyllite, marble, greenstone, meta-tonalite to quartz-diorite and metagabbro all metamorphosed under greenschist to lower amphibolite facies conditions. The largest unit, a siliceous schist and quartzite unit, is part of the Nisutlin Allochthonous Assemblage and is intruded by Late Devonian to early Mississippian hornblende-bearing tonalite to quartz diorite plutons. The Nisutlin Allochthonous Assemblage may be a fragment of the pre-Late Devonian North American margin that separated from North America and was intruded by plutons during the Late Devonian to early Mississippian.

Two deformation phases affected the map area. The earlier produced northeast- and southwest-dipping mylonitic fabrics. Shear sense indicators show both normal and reverse oblique shear. The second and weaker phase, produced widespread subhorizontal, suborogen-parallel crenulation axes, hand specimen-scale folds and local cleavage.

Existing models for formation of the suture zone propose that the rocks were deformed within the deep-seated portion of a west dipping Permo-Triassic subduction complex outboard from ancient North America. The rocks were subsequently thrust eastward onto North American strata during the Early

Jurassic, and the Teslin suture zone would represent the root zone of the obducted package. However, the lack of deformation under subduction zone metamorphic conditions and the presence of northeast-dipping mylonitic fabrics with apparent top-to-the-west reverse shear, seen in this study, are difficult to accommodate into the existing model. In addition, it would be difficult to transport, down the subduction zone, a Devono-Mississippian pluton from the study area that is at least 6 km wide and 10 km long, without it recording this transport.

We propose that the evolutionary model include early subduction zone deformation, followed by development of a transpressive environment and formation of a two-sided orogen. This revised model accounts for the lack of widespread subduction zone metamorphism and for the existence of east- and west-verging thrust and normal shear and orogen-parallel fold axes. Sheets of suture zone rock thrust to the west are interpreted to have been translated northward on post-accretionary dextral strike-slip faults.

TESLIN SUTURE ZONE

R.A. Stevens, 1993. Contribution to the field guide to accompany the 1993 Nuna conference on the nothern Intermontane superterrane, prepared by Johnston J.T. et al., August 22-28.

The Teslin suture zone (TSZ) in south-central Yukon, is part of the Yukon Tanana Terrane (YTT) (Kootenay Terrane of Wheeler et al. 1991) and it marks the fundamental boundary between deformed autochthonous North American rocks of the Omineca Belt to the east and accreted terranes of the Intermontane Belt to the west. It was originally named and defined by Tempelman-Kluit (1979) as " a northwest trending zone of steeply dipping cataclastic rocks 15 km wide [that] separates the Omineca and Intermontane belts". The TSZ extends from the southern Glenlyon map area (Little Salmon Lake) south through the Laberge map area to a least the Canol Road in the Teslin map area. The northern and southern limits of the TSZ are undefined. The western margin is marked by late post-accretionary faults; the Big Salmon Fault in the Laberge map area (Tempelman-Kluit 1984) and an un-named fault in the Teslin map area. The eastern margin has been placed at the D'Abbadie Fault in the Quiet Lake map area (Hansen et al. 1989) and is not clearly defined in the Teslin area. Klippen of rock similar to those found in the TSZ lie in fault contact with North American strata up to 100 km east of the TSZ on a northeast trend.

The TSZ consists of metamorphosed and ductilely deformed S-, L-S, and L-tectonites derived from sedimentary, volcanic and plutonic rocks. Rock units can be divided into three broad lithotectonic assembalges, on the basis of rock type. The first consists primarily of pre-Late Devonian metasedimentary rocks and includes quartz-muscovite±chlorite schist, muscovite-chlorite quartzite, muscovite-graphite phyllite and quartzite, calcareous schist and minor marble.

These rocks comprise the Nisutlin assemblage of Tempelman-Kluit (1979). The second assemblage consists of Late Devonian-early Mississippian foliated metagranitoids that are intrusive to some or all of the metasedimentary rocks described above. This group includes peraluminous and hornblende-bearing rocks and comprises the Simpson assemblage of Tempelman-Kluit (1979) and the peraluminous orthogneiss assemblage of Hansen et al. (1989). The last assemblage consists mostly of mafic schist and greenstone, amphibolite, metagabbro and serpentinized peridotite. These rocks comprise the Anvil assemblage of Tempelman-Kluit (1979).

All rocks generally contain greenschist to amphibolite facies mineral assemblages, with rare preservation of eclogite facies minerals. Deformation has produced mylonite throughout the TSZ, particularly in the metasedimentary rocks. Strain partitioning is common and is best seen in metaplutonic rocks. At least two phases of deformation have affected rocks of the TSZ, an earlier ductile deformation phase that produced the tectonites and a later and weaker folding that produced wide-spread crenulation of the earlier fabrics. Contacts between rock units are structural/tectonic with rare preservation of primary depositional and intrusive relationships. Compositional banding is common within metasedimentary units and likely reflects transposed bedding. Detailed structural mapping in the Laberge (Hansen 1989) and Teslin (Stevens 1992; Stevens and Erdmer 1993a) map areas has shown that the TSZ consists of many structural domains each with distinct fabric orientations and/or structural style.

K-Ar, ^{40}Ar-^{39}Ar and Rb-Sr cooling ages on metamorphic minerals from TSZ and YTT rocks of southern Yukon generally yield Early to Middle Jurassic ages (Stevens et al. 1982; Hansen et al. 1991; Hunt and Roddick 1992, 1993).

One current model for the tectonic evolution of the TSZ suggests that its rocks were deformed within the deep-seated portion of a west-dipping Permo-Triassic subduction complex outboard of North American (Hansen et al. 1991). These rocks were subsequently thrust eastward as a coherent sheet onto North American strata in the Early to Middle Jurassic (Hansen 1992b and references therein). A second model suggests that the rocks underwent Permian subduction zone deformation, followed by Triassic to Middle Jurassic development of a crustal-scale transpressive shear zone and formation of a two-sided orogen. In this model rocks were thrust both eastward and westward out of the suture zone (Stevens and Erdmer 1993b).

REFERENCES

Hansen, V.L. 1989. Structural and kinematic evolution of the Teslin suture zone, Yukon: record of an ancient transpressional margin. Journal of Structural Geology, **11**: 717-733.

Hansen, V.L. 1992b. P-T evolution of the Teslin suture zone and Cassiar tectonites, Yukon, Canada: evidence for A- and B-type subduction. Journal of Metamorphic Geology, **10**: 239-263.

Hansen, V.L., Mortensen, J.K., and Armstrong, R.L. 1989. U-Pb, Rb-Sr, and K-Ar isotopic constraints for ductile deformation and related metamorphism in the Teslin suture zone, Yukon-Tanana terrane, south-central Yukon. Canadian Journal of Earth Sciences, **26**: 2224-2235.

Hansen, V.L., Heizler, M.T., and Harrison, T.M. 1991. Mesozoic thermal evolution of the Yukon-Tanana composite terrane: new evidence from $^{40}Ar/^{39}Ar$ data. Tectonics, **10**: 51-76.

Hunt, P.A., and Roddick, J.C. 1992. A compilation of K-Ar and $^{40}Ar/^{39}Ar$ ages: Report 22. *In* Radiogenic Age and Isotopic Studies: Report 6. Geological Survey of Canada, Paper 92-2, pp. 179-226.

Hunt, P.A., and Roddick, J.C. 1993. A compilation of K-Ar and $^{40}Ar/^{39}Ar$ ages: Report 23; *In* Radiogenic Age and Isotopic Studies: Report 7. Geological Survey of Canada, Paper 93-2, pp. 127-148.

Stevens, R.A., and Erdmer, P. 1993a. Geology and structure of the Teslin suture zone and related rocks in parts of Laberge, Quiet Lake, and Teslin map areas, Yukon Territory. *In* Current research, part A. Geological Survey of Canada, Paper 93-1A, pp. 11-20. *See appendix 3*

Stevens, R.A., and Erdmer, P. 1993b. Tectonic evolution of the Teslin suture zone, south-central Yukon Territory: subduction, transpression and extrusion. *In* Geological Association of Canada/Mineralogical Association of Canada Program and Abstracts, v. 18, p. A100.

Stevens, R.A. 1992. Regional geology, fabric, and structure of the Teslin suture zone in northwest Teslin map area, Yukon Territory. *In* Current Research, part A. Geological Survey of Canada, Paper 92-1A, pp. 287-295. *See appendix 2*

Stevens, R.D., Delabio, R.N., and Lachance, G.R. 1982. Age determinations and geological studies, K-Ar isotopic ages, report 15. Geological Survey of Canada, Paper 81-2, pp. 19-21.

Tempelman-Kluit, D.J. 1979. Transported cataclasite, ophiolite and granodiorite in Yukon: evidence of arc-continent collision. Geological Survey of Canada, Paper 79-14.

Tempelman-Kluit, D.J. 1984. Geology, Laberge (105E) and Carmacks (115I), Yukon Territory. Geological Survey of Canada, Open File 1101.

Wheeler, J.O., Brookfield, A.J., Gabrielse, H., Monger, J.W.H., Tipper, H.W., and Woodsworth, G.J. 1991. Terrane map of the Canadian Cordillera; Geological Survey of Canada Map 1713A, scale 1:2 000 000.

STRUCTURAL AND TECTONIC EVOLUTION OF THE TESLIN SUTURE ZONE, YUKON: A DOUBLY-VERGING, HETEROGENEOUS, TRANSPRESSIVE SHEAR ZONE

R.A. Stevens. 1994. Presented at the 20th annual Codilleran Tectonics Workshop, University of Victoria, Victoria, British Columbia, January 28-30

The Teslin suture zone (TSZ), part of the Yukon-Tanana terrane (YTT) of southern Yukon and east-central Alaska, marks the fundamental boundary between deformed autochthonous North American rocks to the east, and accreted allochthonous terranes to the west. The project area is underlain by rocks assigned to the Nisutlin terrane and it includes siliceous schist, quartzite, phyllite, marble, greenstone, metatonalite and metagabbro, all deformed under greenschist to amphibolite facies conditions. These rock types are readily correlated with similar lithologic assemblages elsewhere in the Teslin suture zone and in the Yukon Tanana terrane of southern Yukon. Garnet thermobarometry and site-chemistry of amphiboles suggests metamorphism occurred under medium pressures at 450-650°C. U-Pb analysis of zircons from metaplutonic rocks give Early Mississippian crystallization ages and ^{40}Ar-^{39}Ar analysis of biotite and hornblende suggest Early Jurassic metamorphic cooling ages (≈180-190 Ma). Rock characteristics, combined with rare preservation of primary depositional and intrusive contacts, and the U-Pb geochronology indicate that rocks of the Teslin suture zone (and Nisutlin terrane) represent part of a continental-crust terrane that had formed by the mid-Mississippian.

Two deformation phases affected the area. The earlier and stronger, produced protomylonite and mylonite, mineral and stretching lineations, shear-sense indicators and marked strain partitioning. The second and weaker phase produced widespread crenulation, hand-specimen scale folding and local cleavage. Detailed structural mapping revealed that the suture zone includes numerous domains of contrasting structural style and fabric orientation. The following structural characteristics are present in domains identified in the map area; 1) steeply northeast- or southwest-dipping mylonitic fabrics, 2) normal and reverse oblique shear on both the northeast- and southwest-dipping fabrics; 3) an overall subhorizontal, suborogen-parallel crenulation axis; 4) open to tight handspecimen-scale folds with axes parallel to mineral lineations; and 5) a local spaced (10-30 cm) crenulation cleavage that dips northeast or southwest. These structural characteristics are interpreted to result from ductile, heterogeneous thrust transpression and may preserve the root of a crustal-scale flower structure.

A six part tectonic model is proposed that includes: 1) Formation of the Nisutlin terrane, a continental-crust terrane, by the mid-Mississippian; 2) Permian - Early Triassic? subduction of the Slide Mountain/Anvil Ocean beneath the Nisutlin terrane; 3) Middle Triassic? -Early Jurassic development of a crustal-scale, ductile, heterogeneous, thrust transpressive shear zone and formation of a two-sided orogen; 4) Early - Middle Jurassic, regional thrusting with northeast and southwest verging thrusts; 5) Middle Jurassic to mid-Cretaceous foreland thrust and fold belt deformation which resulted in transportation of the Teslin suture zone eastward as a coherent package over a basal decollement located above the North American Basement; and 6) Early - mid-Cretaceous extension and dextral strike-slip faulting. The western margin of the Teslin suture zone was truncated and transported northward by the strike-slip faulting.

APPENDIX 5 - SUMMARY OF BIOTITE, MUSCOVITE, GARNET, PLAGIOCLASE AND AMPHIBOLE MICROPROBE ANALYSES

The following abbreviations are used in this appendix:

Biotite 91-366a = analysis of biotite from sample 91-366a
Xann = mole fraction of annite in biotite
Xphl = mole fraction of pholgophite in biotite
FeCel = iron celadanite mole fraction of muscovite
MgCel = magnesium celadanite mole fraction of muscovite
Xalm = mole fraction of almadine in garnet
Xpy = mole fraction of pyrope in garnet
Xgr = mole fraction of grossular in garnet
Xsps = mole fraction of spessertine in garnet
An = anorthite mole fraction of plagioclase
Ab = albite mole fraction of plagioclase
Or = orthoclase mole fraction of plagioclase

Amphibole elemental data are recalculated after:

Laird, J., and Albee, A.L. 1981. Pressure, temperature, and time indicators in mafic schist: their application to reconstructing the polymetamorphic history of Vermont. American Journal of Science, **281**: 127-175.

Biotite 91-366a

					Average
SiO_2	37.13	37.21	36.78	37.07	37.05
TiO_2	1.34	1.41	1.23	1.04	1.26
Al_2O_3	16.99	16.49	16.54	16.91	16.73
FeO	15.29	15.96	16.26	16.55	16.02
MnO	0.20	0.22	0.31	0.24	0.24
MgO	12.57	12.96	12.05	11.65	12.31
CaO	0.14	0.05	0.05	0.08	0.08
K_2O	8.34	8.92	9.10	8.59	8.74
Na_20	0.13	0.12	0.14	0.10	0.12
TOTAL	92.12	93.35	92.46	92.23	92.54
Si	5.69	5.67	5.68	5.72	5.69
Ti	0.15	0.16	0.14	0.12	0.14
Al	3.07	2.96	3.01	3.07	3.03
Fe	1.96	2.03	2.10	2.13	2.06
Mn	0.03	0.03	0.04	0.03	0.03
Mg	2.87	2.94	2.77	2.68	2.82
Ca	0.02	0.01	0.01	0.01	0.01
K	1.63	1.73	1.79	1.69	1.71
Na	0.04	0.03	0.04	0.03	0.04
O	22.00	22.00	22.00	22.00	22.00
Xann	0.34	0.35	0.37	0.37	0.36
Xphl	0.50	0.51	0.48	0.47	0.49
Fe/Fe+Mg	0.41	0.41	0.43	0.44	0.42

Biotite 91-367a

					Average
SIO_2	35.91	35.65	35.60	35.42	35.65
TIO_2	1.71	1.74	1.85	1.77	1.77
AL_2O_3	17.01	17.51	17.36	17.46	17.34
FEO	20.27	20.96	21.25	20.49	20.74
MNO	0.18	0.16	0.14	0.19	0.17
MGO	8.50	7.84	8.17	8.23	8.19
CAO	0.00	0.02	0.00	0.00	0.01
K_2O	9.43	9.33	9.52	9.46	9.44
NA_20	0.17	0.29	0.07	0.06	0.15
TOTAL	93.17	93.49	93.96	93.07	93.42
SI	5.63	5.58	5.56	5.57	5.58
TI	0.20	0.20	0.22	0.21	0.21
AL	3.14	3.23	3.20	3.23	3.20
FE	2.66	2.75	2.78	2.69	2.72
MN	0.02	0.02	0.02	0.03	0.02
MG	1.99	1.83	1.90	1.93	1.91
CA	0.00	0.00	0.00	0.00	0.00
K	1.88	1.86	1.90	1.90	1.88
NA	0.05	0.09	0.02	0.02	0.05
O	22.00	22.00	22.00	22.00	22.00
Xann	0.47	0.49	0.49	0.48	0.48
Xphl	0.35	0.33	0.34	0.34	0.34
Fe/Fe+Mg	0.57	0.60	0.59	0.58	0.59

Biotite 90-192

						Average
SiO_2	35.68	35.66	36.15	35.64	36.46	35.92
TiO_2	1.96	1.82	2.02	1.86	1.97	1.93
Al_2O_3	16.62	16.57	16.35	16.79	16.51	16.57
FeO	19.25	19.22	18.96	19.24	19.05	19.14
MnO	0.30	0.26	0.26	0.27	0.26	0.27
MgO	10.15	10.10	10.36	10.14	10.14	10.18
CaO	0.05	0.00	0.00	0.01	0.00	0.01
K_2O	9.26	9.63	9.50	9.44	9.51	9.47
Na_20	0.11	0.12	0.18	0.15	0.10	0.13
TOTAL	93.38	93.39	93.79	93.56	93.99	93.62
Si	5.56	5.57	5.60	5.55	5.63	5.58
Ti	0.23	0.21	0.24	0.22	0.23	0.22
Al	3.05	3.05	2.99	3.08	3.00	3.03
Fe	2.51	2.51	2.46	2.50	2.46	2.49
Mn	0.04	0.03	0.03	0.04	0.03	0.04
Mg	2.36	2.35	2.39	2.35	2.33	2.36
Ca	0.01	0.00	0.00	0.00	0.00	0.00
K	1.84	1.92	1.88	1.87	1.87	1.88
Na	0.03	0.03	0.05	0.05	0.03	0.04
O	22.00	22.00	22.00	22.00	22.00	22.00
Xann	0.44	0.44	0.43	0.44	0.43	0.43
Xphl	0.41	0.41	0.42	0.41	0.41	0.41
Fe/Fe+Mg	0.52	0.52	0.51	0.52	0.51	0.51

Biotite 90-116

						Average
SiO_2	34.63	36.21	38.38	36.15	36.06	36.29
TiO_2	1.47	1.09	1.83	1.78	1.35	1.50
Al_2O_3	16.65	15.56	15.45	15.91	16.09	15.93
FeO	21.63	18.82	17.97	18.41	18.61	19.09
MnO	0.16	0.33	0.25	0.24	0.22	0.24
MgO	11.40	11.62	10.55	11.22	11.42	11.24
CaO	0.17	0.10	0.04	0.07	0.09	0.09
K_2O	0.10	0.18	0.07	0.13	0.11	0.12
Na_20	8.04	8.95	9.39	9.01	8.97	8.87
TOTAL	94.24	92.85	93.92	92.92	92.92	93.37
Si	5.38	5.65	5.87	5.63	5.61	5.63
Ti	0.17	0.13	0.21	0.21	0.16	0.18
Al	3.05	2.86	2.78	2.92	2.95	2.91
Fe	2.81	2.46	2.30	2.40	2.42	2.48
Mn	0.02	0.04	0.03	0.03	0.03	0.03
Mg	2.64	2.71	2.40	2.60	2.65	2.60
Ca	0.03	0.02	0.07	0.01	0.02	0.03
K	1.59	1.78	1.83	1.79	1.78	1.76
Na	0.03	0.05	0.02	0.04	0.03	0.04
O	22.00	22.00	22.00	22.00	22.00	22.00
Xann	0.46	0.42	0.41	0.41	0.42	0.42
Xphl	0.43	0.46	0.43	0.45	0.45	0.45
Fe/Fe+Mg	0.52	0.48	0.49	0.48	0.48	0.49

Biotite 91-368

					Average
SiO_2	36.22	37.30	37.51	37.48	37.13
TiO_2	1.54	1.50	1.47	1.58	1.52
Al_2O_3	17.56	17.38	17.08	17.48	17.38
FeO	19.80	19.06	19.83	20.74	19.86
MnO	0.19	0.17	0.21	0.21	0.20
MgO	9.87	9.94	9.03	8.72	9.39
CaO	0.00	0.00	0.00	0.00	0.00
K_2O	9.66	0.17	9.27	9.49	7.15
Na_20	0.11	9.94	0.20	0.21	2.62
TOTAL	94.96	95.19	94.60	95.90	95.16
Si	5.55	5.67	5.74	5.69	5.66
Ti	0.18	0.17	0.17	0.18	0.17
Al	3.17	3.11	3.08	3.12	3.12
Fe	2.54	2.42	2.54	2.63	2.53
Mn	0.03	0.02	0.03	0.03	0.03
Mg	2.26	2.25	2.06	1.97	2.14
Ca	0.00	0.00	0.00	0.00	0.00
K	1.89	1.88	1.81	1.84	1.85
Na	0.03	0.05	0.06	0.06	0.05
O	22.00	22.00	22.00	22.00	22.00
Xann	0.44	0.43	0.45	0.47	0.45
Xphl	0.39	0.40	0.37	0.35	0.38
Fe/Fe+Mg	0.53	0.52	0.55	0.57	0.54

Biotite 90-117

				Average
SiO_2	35.83	35.83	35.60	35.75
TiO_2	1.79	1.68	1.46	1.64
Al_2O_3	15.21	15.46	15.37	15.35
FeO	20.30	19.94	19.99	20.08
MnO	0.22	0.31	0.33	0.29
MgO	10.29	10.19	10.21	10.23
CaO	0.02	0.08	0.07	0.06
K_2O	9.44	9.01	9.21	9.22
Na_20	0.16	0.21	0.08	0.15
TOTAL	93.35	92.70	92.31	92.79
Si	5.63	5.64	5.64	5.64
Ti	0.21	0.20	0.17	0.19
Al	2.82	2.87	2.87	2.85
Fe	2.67	2.63	2.65	2.65
Mn	0.04	0.04	0.04	0.04
Mg	2.41	2.39	2.41	2.40
Ca	0.00	0.01	0.01	0.01
K	1.89	1.81	1.86	1.85
Na	0.05	0.06	0.02	0.04
O	22.00	22.00	22.00	22.00
Xann	0.46	0.45	0.46	0.46
Xphl	0.42	0.41	0.42	0.42
Fe/Fe+Mg	0.53	0.52	0.52	0.52

Biotite 91-352

				Average
SiO_2	34.56	34.39	34.36	34.44
TiO_2	2.14	2.27	2.40	2.27
Al_2O_3	18.63	18.32	18.73	18.56
FeO	20.83	21.37	20.32	20.84
MnO	0.21	0.29	0.27	0.26
MgO	8.27	8.45	8.40	8.37
CaO	0.00	0.00	0.00	0.00
K_2O	9.02	9.21	9.04	9.09
Na_20	0.38	0.26	0.36	0.33
TOTAL	94.05	94.56	93.88	94.16
Si	5.38	5.35	5.35	5.36
Ti	0.25	0.27	0.28	0.27
Al	3.42	3.36	3.44	3.40
Fe	2.71	2.78	2.65	2.71
Mn	0.03	0.04	0.04	0.03
Mg	1.92	1.96	1.95	1.94
Ca	0.00	0.00	0.00	0.00
K	1.79	1.83	1.96	1.86
Na	0.11	0.08	0.11	0.10
O	22.00	22.00	22.00	22.00
Xann	0.48	0.48	0.46	0.47
Xphl	0.34	0.34	0.34	0.34
Fe/Fe+Mg	0.59	0.59	0.58	0.58

Biotite 90-266b

							Average
SiO_2	36.24	36.34	36.91	36.27	36.34	36.78	36.48
TiO_2	1.89	2.00	1.89	1.74	1.70	1.80	1.84
Al_2O_3	16.19	16.14	16.37	16.59	16.49	16.69	16.41
FeO	17.19	16.86	16.88	17.68	17.46	16.57	17.11
MnO	0.29	0.39	0.38	0.27	0.28	0.31	0.32
MgO	111.80	0.16	11.74	11.43	11.44	12.21	26.46
CaO	0.00	0.01	0.00	0.00	0.00	0.01	0.00
K_2O	9.55	0.29	9.70	9.75	9.89	9.68	8.14
Na_20	0.18	9.71	0.18	0.16	0.16	0.21	1.77
TOTAL	93.31	93.43	94.04	93.91	93.76	94.26	93.79
Si	5.60	5.61	5.64	5.58	5.60	5.60	5.61
Ti	0.22	0.23	0.22	0.20	0.20	0.21	0.21
Al	2.95	2.93	2.95	3.01	3.00	2.99	2.97
Fe	2.22	2.18	2.16	2.28	2.25	2.11	2.20
Mn	0.03	0.05	0.05	0.04	0.04	0.04	0.04
Mg	2.77	2.69	2.68	2.62	2.66	2.77	2.70
Ca	0.00	0.00	0.00	0.00	0.00	0.00	0.00
K	1.88	1.91	1.89	1.91	1.94	1.88	1.90
Na	0.05	0.09	0.05	0.05	0.05	0.02	0.05
O	22.00	22.00	22.00	22.00	22.00	22.00	22.00
Xann	0.38	0.38	0.38	0.40	0.39	0.37	0.38
Xphl	0.48	0.47	0.47	0.46	0.46	0.48	0.47
Fe/Fe+Mg	0.44	0.45	0.45	0.46	0.46	0.43	0.45

Biotite 90-119

					Average
SiO_2	36.05	35.50	35.36	35.73	35.66
TiO_2	1.88	1.82	1.87	1.83	1.85
Al_2O_3	15.92	16.07	15.85	16.11	15.98
FeO	19.64	19.61	19.77	20.26	19.82
MnO	0.12	0.17	0.13	0.10	0.13
MgO	9.75	9.61	9.73	8.99	9.52
CaO	0.08	0.00	0.05	0.04	0.04
K_2O	9.18	9.35	9.19	9.15	9.21
Na_20	0.26	0.29	0.30	0.27	0.28
TOTAL	92.86	92.40	92.24	92.46	92.49
Si	5.65	5.61	5.60	5.65	5.63
Ti	0.22	0.22	0.22	0.22	0.22
Al	2.94	2.99	2.96	3.00	2.97
Fe	2.58	2.59	2.62	2.68	2.62
Mn	0.02	0.02	0.02	0.01	0.02
Mg	2.28	2.26	2.30	2.12	2.24
Ca	0.01	0.00	0.01	0.01	0.01
K	1.84	1.88	1.86	1.84	1.86
Na	0.08	0.09	0.09	0.08	0.09
O	22.00	22.00	22.00	22.00	22.00
Xann	0.45	0.46	0.46	0.47	0.46
Xphl	0.40	0.40	0.40	0.37	0.39
Fe/Fe+Mg	0.53	0.53	0.53	0.56	0.54

Biotite 92-618b

				Average
SiO_2	35.89	36.01	35.67	35.86
TiO_2	1.81	1.87	1.54	1.74
Al_2O_3	18.01	17.92	18.43	18.12
FeO	17.89	18.30	17.39	17.86
MnO	0.07	0.12	0.09	0.09
MgO	10.87	11.44	11.02	11.11
CaO	0.00	0.00	0.00	0.00
K_2O	9.42	8.69	9.56	9.22
Na_20	0.10	0.09	0.10	0.10
TOTAL	94.08	94.45	93.80	94.11
Si	5.50	5.48	5.47	5.48
Ti	0.21	0.21	0.18	0.20
Al	3.25	3.21	3.33	3.26
Fe	2.29	2.33	2.23	2.28
Mn	0.01	0.02	0.01	0.01
Mg	2.48	2.59	2.52	2.53
Ca	0.00	0.00	0.00	0.00
K	1.84	1.69	1.87	1.80
Na	0.03	0.03	0.03	0.03
O	22.00	22.00	22.00	22.00
Xann	0.40	0.40	0.39	0.40
Xphl	0.43	0.44	0.44	0.44
Fe/Fe+Mg	0.48	0.47	0.47	0.47

Muscovite 91-367a

						Average
SiO_2	48.68	49.17	49.57	49.13	49.11	49.13
TiO_2	0.38	0.37	0.40	0.43	0.30	0.38
Al_2O_3	28.65	28.85	28.66	29.11	28.94	28.84
FeO	2.39	2.35	2.19	2.14	2.25	2.26
MnO	0.00	0.02	0.01	0.01	0.01	0.01
MgO	2.62	2.54	2.56	2.46	2.61	2.56
CaO	0.00	0.00	0.00	0.00	0.00	0.00
K_2O	10.33	10.28	10.26	10.68	10.41	10.39
Na_20	0.66	0.68	0.68	0.48	0.60	0.62
TOTAL	93.70	94.27	94.34	94.43	94.23	94.19
Si	6.62	6.64	6.68	6.63	6.63	6.64
Ti	0.00	0.04	0.04	0.04	0.03	0.03
Al	4.59	4.59	4.55	4.63	4.61	4.59
Fe	0.27	0.27	0.25	0.24	0.25	0.26
Mn	0.00	0.00	0.00	0.00	0.00	0.00
Mg	0.53	0.51	0.51	0.50	0.53	0.52
Ca	0.00	0.00	0.00	0.00	0.00	0.00
K	1.79	1.77	1.76	1.84	1.79	1.79
Na	0.17	0.18	0.18	0.12	0.16	0.16
O	22.00	22.00	22.00	22.00	22.00	22.00
FeCel	0.01	0.03	0.02	0.02	0.03	0.02
MgCel	0.03	0.06	0.04	0.04	0.07	0.05
Fe/Fe+Mg	0.34	0.34	0.32	0.33	0.33	0.33

Muscovite 90-192

								Average
SiO_2	45.80	48.82	46.76	48.18	47.67	45.95	47.51	47.24
TiO_2	0.42	0.51	0.36	0.48	0.52	0.50	0.47	0.47
Al_2O_3	34.51	30.79	33.62	31.40	31.75	34.34	31.10	32.50
FeO	1.35	0.50	1.42	2.04	1.86	1.44	1.78	1.48
MnO	0.00	0.01	0.00	0.00	0.01	0.00	0.00	0.00
MgO	0.81	2.13	1.02	1.78	1.78	0.87	1.78	1.45
CaO	0.00	0.00	0.00	0.00	0.00	0.00	0.00	0.00
K_2O	9.69	9.96	9.82	9.94	10.42	10.24	10.17	10.03
Na_20	1.33	1.09	1.35	1.10	0.80	1.04	0.98	1.10
TOTAL	93.92	95.35	94.36	94.92	94.81	94.37	93.79	94.50
Si	6.18	6.50	6.28	6.45	6.40	6.19	6.44	6.35
Ti	0.04	0.05	0.04	0.05	0.05	0.05	0.05	0.05
Al	5.49	4.83	5.32	4.95	5.02	5.45	4.97	5.15
Fe	0.15	0.23	0.16	0.23	0.21	0.16	0.20	0.19
Mn	0.00	0.02	0.00	0.00	0.00	0.00	0.00	0.00
Mg	0.16	0.42	0.20	0.36	0.36	0.17	0.36	0.29
Ca	0.00	0.00	0.00	0.00	0.00	0.00	0.00	0.00
K	1.67	1.69	1.68	1.70	1.78	1.76	1.76	1.72
Na	0.35	0.28	0.35	0.28	0.21	0.27	0.26	0.29
O	22.00	22.00	22.00	22.00	22.00	22.00	22.00	22.00
FeCel	0.01	0.03	0.00	0.02	0.02	0.01	0.01	0.02
MgCel	0.02	0.05	0.00	0.03	0.04	0.02	0.02	0.03
Fe/Fe+Mg	0.48	0.35	0.44	0.39	0.37	0.48	0.36	0.41

Muscovite 91-368

							Average
SiO_2	48.41	47.83	48.06	47.72	47.82	48.36	48.03
TiO_2	0.45	0.46	0.56	0.52	0.54	0.49	0.50
Al_2O_3	28.13	28.37	28.69	18.52	27.79	27.34	26.47
FeO	2.80	2.75	2.70	2.55	2.88	2.89	2.76
MnO	0.03	0.03	0.00	0.00	0.00	0.02	0.01
MgO	2.64	2.45	2.46	2.38	2.52	2.68	2.52
CaO	0.00	0.00	0.00	0.00	0.00	0.03	0.01
K_2O	0.62	10.25	10.11	10.14	9.89	10.38	8.57
Na_20	10.26	0.56	0.80	0.80	0.77	0.62	2.30
TOTAL	93.34	92.71	93.38	92.63	92.20	92.81	92.85
Si	6.63	6.59	6.57	6.58	6.63	6.67	6.61
Ti	0.05	0.05	0.06	0.05	0.06	0.05	0.05
Al	4.54	4.61	4.63	4.63	4.54	4.44	4.56
Fe	0.32	0.32	0.31	0.29	0.33	0.33	0.32
Mn	0.00	0.00	0.00	0.00	0.00	0.00	0.00
Mg	0.54	0.50	0.50	0.49	0.52	0.55	0.52
Ca	0.00	0.00	0.00	0.00	0.00	0.01	0.00
K	1.79	1.80	1.76	1.78	1.75	1.83	1.79
Na	0.16	0.15	0.21	0.21	0.21	0.17	0.19
O	22.00	22.00	22.00	22.00	22.00	22.00	22.00
FeCel	0.05	0.05	0.04	0.03	0.05	0.04	0.04
MgCel	0.09	0.08	0.07	0.05	0.08	0.06	0.07
Fe/Fe+Mg	0.37	0.39	0.38	0.38	0.39	0.38	0.38

Muscovite 90-117

					Average
SiO_2	49.37	49.58	49.47	49.36	49.45
TiO_2	0.24	0.26	0.23	0.22	0.24
Al_2O_3	27.65	28.20	27.66	27.77	27.82
FeO	3.32	3.28	3.32	3.37	3.32
MnO	0.02	0.02	0.06	0.00	0.03
MgO	2.45	2.33	2.28	2.34	2.35
CaO	0.00	0.00	0.00	0.00	0.00
K_2O	10.34	10.47	10.32	10.47	10.40
Na_20	0.50	0.47	0.59	0.52	0.52
TOTAL	93.89	94.62	93.93	94.06	94.13
Si	6.72	6.70	6.74	6.72	6.72
Ti	0.02	0.03	0.02	0.02	0.02
Al	4.44	4.49	4.44	4.45	4.46
Fe	0.38	0.37	0.38	0.38	0.38
Mn	0.00	0.00	0.01	0.00	0.00
Mg	0.50	0.47	0.46	0.47	0.48
Ca	0.00	0.00	0.00	0.00	0.00
K	1.80	1.80	1.79	1.82	1.80
Na	0.13	0.12	0.16	0.14	0.14
O	22.00	22.00	22.00	22.00	22.00
FeCel	0.05	0.05	0.04	0.05	0.05
MgCel	0.07	0.06	0.05	0.06	0.06
Fe/Fe+Mg	0.43	0.44	0.45	0.45	0.44

Muscovite 91-359a

					Average
SiO_2	50.05	50.29	49.09	50.16	49.90
TiO_2	0.33	0.40	0.44	0.38	0.39
Al_2O_3	29.13	29.06	30.58	28.77	29.39
FeO	2.94	2.55	2.23	2.84	2.64
MnO	0.00	0.00	0.00	0.00	0.00
MgO	2.22	2.65	1.98	2.57	2.36
CaO	0.00	0.00	0.00	0.00	0.00
K_2O	10.26	9.94	9.68	10.07	9.99
Na_20	0.61	0.83	1.07	0.72	0.81
TOTAL	95.53	95.73	95.07	95.52	95.46
Si	6.67	6.67	6.55	6.68	6.64
Ti	0.03	0.04	0.04	0.04	0.04
Al	4.58	4.54	4.81	4.52	4.61
Fe	0.33	0.28	0.25	0.32	0.29
Mn	0.00	0.00	0.00	0.00	0.00
Mg	0.44	0.52	0.39	0.51	0.47
Ca	0.00	0.00	0.00	0.00	0.00
K	1.74	1.68	1.65	1.71	1.70
Na	0.16	0.21	0.28	0.19	0.21
O	22.00	22.00	22.00	22.00	22.00
FeCel	0.04	0.04	0.03	0.05	0.04
MgCel	0.06	0.08	0.04	0.08	0.06
Fe/Fe+Mg	0.43	0.35	0.39	0.38	0.39

Muscovite 91-352

						Average
SiO_2	46.16	46.13	45.80	45.78	45.74	45.92
TiO_2	0.43	0.43	0.63	0.54	0.52	0.51
Al_2O_3	35.14	35.11	34.80	34.62	34.42	34.82
FeO	1.92	2.06	1.92	2.06	1.92	1.98
MnO	0.07	0.01	0.01	0.00	0.00	0.02
MgO	0.51	0.62	0.61	0.53	0.62	0.58
CaO	0.00	0.00	0.00	0.00	0.00	0.00
K_2O	10.54	10.39	10.60	10.44	10.32	10.46
Na_20	0.95	0.94	0.91	0.87	0.91	0.92
TOTAL	95.74	95.69	95.29	94.85	94.44	95.20
Si	6.15	6.14	6.13	6.16	6.17	6.15
Ti	0.04	0.04	0.06	0.05	0.05	0.05
Al	5.52	5.51	5.49	5.49	5.47	5.50
Fe	0.21	0.23	0.22	0.23	0.22	0.22
Mn	0.01	0.00	0.00	0.00	0.00	0.00
Mg	0.10	0.12	0.12	0.11	0.13	0.12
Ca	0.00	0.00	0.00	0.00	0.00	0.00
K	1.79	1.77	1.81	1.79	1.77	1.79
Na	0.25	0.24	0.24	0.23	0.24	0.24
O	22.00	22.00	22.00	22.00	22.00	22.00
FeCel	0.03	0.04	0.03	0.03	0.03	0.03
MgCel	0.01	0.02	0.01	0.01	0.02	0.02
Fe/Fe+Mg	0.68	0.65	0.64	0.69	0.63	0.66

Muscovite 91-389c

							Average
SiO_2	47.10	48.06	48.20	47.62	47.53	47.94	47.74
TiO_2	0.39	0.32	0.37	0.34	0.22	0.30	0.32
Al_2O_3	29.21	27.98	28.09	28.58	30.06	28.46	28.73
FeO	3.59	3.68	3.94	3.79	3.88	3.75	3.77
MnO	0.05	0.00	0.00	0.03	0.02	0.00	0.02
MgO	1.84	2.31	2.29	2.15	1.75	2.02	2.06
CaO	0.02	0.00	0.03	0.00	0.00	0.00	0.01
K_2O	9.41	9.77	9.72	9.77	9.80	10.00	9.75
Na_2O	1.42	0.96	0.96	1.08	0.91	0.93	1.04
TOTAL	93.03	93.08	93.60	93.36	94.18	93.40	93.44
Si	6.49	6.62	6.61	6.55	6.47	6.59	6.55
Ti	0.04	0.03	0.04	0.04	0.02	0.03	0.03
Al	4.74	4.54	4.54	4.63	4.82	4.61	4.65
Fe	0.41	0.42	0.45	0.44	0.44	0.43	0.43
Mn	0.01	0.00	0.00	0.00	0.00	0.00	0.00
Mg	0.38	0.47	0.47	0.44	0.36	0.41	0.42
Ca	0.00	0.00	0.00	0.00	0.00	0.00	0.00
K	1.65	1.72	1.70	1.71	1.70	1.75	1.71
Na	0.38	0.26	0.25	0.29	0.24	0.25	0.28
O	22.00	22.00	22.00	22.00	22.00	22.00	22.00
FeCel	0.06	0.07	0.09	0.08	0.10	0.06	0.08
MgCel	0.05	0.08	0.09	0.08	0.08	0.06	0.07
Fe/Fe+Mg	0.52	0.47	0.49	0.50	0.55	0.51	0.51

Muscovite 91-266b

								Average
SiO_2	47.73	48.39	47.71	47.91	47.75	48.16	48.07	47.96
TiO_2	0.35	0.35	0.41	0.46	0.31	0.43	0.48	0.40
Al_2O_3	28.96	28.63	28.65	27.87	28.84	28.02	28.52	28.50
FeO	2.57	2.48	2.83	2.76	2.58	2.74	2.21	2.60
MnO	0.00	0.01	0.00	0.00	0.00	0.02	0.01	0.01
MgO	2.21	2.51	2.20	3.11	2.26	2.38	2.58	2.46
CaO	0.00	0.00	0.00	0.00	0.00	0.00	0.00	0.00
K_2O	10.05	10.25	10.26	9.81	10.43	10.29	10.18	10.18
Na_2O	0.76	0.71	0.74	0.75	0.58	0.56	0.77	0.70
TOTAL	92.64	93.34	92.80	92.70	92.75	92.60	92.83	92.81
Si	6.57	6.61	6.58	6.60	6.58	6.64	6.60	6.60
Ti	0.04	0.04	0.04	0.05	0.03	0.04	0.05	0.04
Al	4.70	4.61	4.65	4.52	4.68	4.56	4.61	4.62
Fe	0.30	0.28	0.33	0.32	0.30	0.32	0.25	0.30
Mn	0.00	0.00	0.00	0.00	0.00	0.00	0.00	0.00
Mg	0.45	0.51	0.45	0.64	0.46	0.49	0.53	0.51
Ca	0.00	0.00	0.00	0.00	0.00	0.00	0.00	0.00
K	1.77	1.79	1.80	1.72	1.83	1.81	1.78	1.79
Na	0.20	0.19	0.20	0.20	0.15	0.15	0.21	0.19
O	22.00	22.00	22.00	22.00	22.00	22.00	22.00	22.00
FeCel	0.04	0.04	0.04	0.07	0.04	0.04	0.03	0.04
MgCel	0.06	0.06	0.05	0.14	0.06	0.06	0.06	0.07
Fe/Fe+Mg	0.39	0.36	0.42	0.33	0.39	0.39	0.32	0.37

Muscovite 91-371

						Average
SiO_2	49.49	48.90	47.89	49.15	48.59	48.80
TiO_2	0.41	0.47	0.44	0.34	0.37	0.41
Al_2O_3	29.29	29.90	31.44	28.68	29.66	29.79
FeO	2.11	2.18	1.84	2.31	2.27	2.14
MnO	0.00	0.00	0.00	0.02	0.00	0.00
MgO	2.42	2.15	1.67	2.46	1.93	2.13
CaO	0.00	0.00	0.00	0.00	0.00	0.00
K_2O	10.10	10.45	9.71	10.29	10.63	10.24
Na_20	0.87	0.86	1.22	0.68	0.56	0.84
TOTAL	94.68	94.90	94.18	93.93	94.01	94.34
Si	6.64	6.56	6.45	6.66	6.59	6.58
Ti	0.04	0.05	0.04	0.03	0.04	0.04
Al	4.63	4.73	4.99	4.58	4.74	4.73
Fe	0.24	0.24	0.21	0.26	0.26	0.24
Mn	0.00	0.00	0.00	0.00	0.00	0.00
Mg	0.48	0.43	0.33	0.50	0.39	0.43
Ca	0.00	0.00	0.00	0.00	0.00	0.00
K	1.73	1.79	1.67	1.78	1.84	1.76
Na	0.23	0.22	0.32	0.18	0.15	0.22
O	22.00	22.00	22.00	22.00	22.00	22.00
FeCel	0.02	0.01	0.01	0.02	0.01	0.01
MgCel	0.03	0.02	0.02	0.04	0.01	0.03
Fe/Fe+Mg	0.33	0.36	0.38	0.35	0.40	0.36

Muscovite 90-119

				Average
SiO_2	47.60	48.22	48.87	48.23
TiO_2	0.38	0.36	0.32	0.35
Al_2O_3	27.67	27.76	26.89	27.44
FeO	3.22	2.92	3.18	3.11
MnO	0.00	0.00	0.00	0.00
MgO	2.45	2.41	2.72	2.53
CaO	0.00	0.04	0.02	0.02
K_2O	10.01	9.75	10.21	9.99
Na_20	0.58	0.71	0.44	0.58
TOTAL	91.90	92.16	92.64	92.23
Si	6.63	6.67	6.74	6.68
Ti	0.04	0.04	0.03	0.04
Al	4.54	4.53	4.37	4.48
Fe	0.37	0.34	0.37	0.36
Mn	0.00	0.00	0.00	0.00
Mg	0.51	0.50	0.56	0.52
Ca	0.00	0.01	0.00	0.00
K	1.78	1.72	1.80	1.77
Na	0.16	0.19	0.12	0.15
O	22.00	22.00	22.00	22.00
FeCel	0.07	0.05	0.06	0.06
MgCel	0.10	0.07	0.09	0.09
Fe/Fe+Mg	0.42	0.40	0.40	0.41

Muscovite 92-487a

								Average
SiO_2	49.10	48.35	48.49	48.42	48.22	49.51	48.87	48.52
TiO_2	0.41	0.39	0.42	0.45	0.46	0.41	0.41	0.41
Al_2O_3	30.60	31.27	31.80	31.39	31.33	28.56	29.57	30.95
FeO	2.18	1.96	2.21	2.03	2.14	2.58	2.12	2.10
MnO	0.00	0.00	0.01	0.02	0.01	0.00	0.05	0.01
MgO	2.38	1.93	1.90	2.10	2.02	2.75	2.35	2.13
CaO	0.00	0.00	0.00	0.00	0.00	0.00	0.00	0.00
K_2O	9.53	9.84	9.99	9.88	9.93	10.21	10.46	9.95
Na_20	0.88	0.99	0.88	1.08	1.09	0.77	0.45	0.93
TOTAL	95.08	95.16	95.71	95.35	95.19	94.79	94.29	95.05
Si	6.54	6.44	6.44	6.45	6.44	6.66	6.59	6.48
Ti	0.04	0.04	0.04	0.04	0.05	0.04	0.04	0.04
Al	4.80	4.98	4.97	4.93	4.93	4.53	4.70	4.88
Fe	0.24	0.22	0.25	0.23	0.24	0.29	0.24	0.23
Mn	0.00	0.00	0.00	0.00	0.00	0.00	0.01	0.00
Mg	0.47	0.38	0.38	0.42	0.40	0.55	0.47	0.43
Ca	0.00	0.00	0.00	0.00	0.00	0.00	0.00	0.00
K	1.62	1.67	1.69	1.68	1.69	1.75	1.80	1.70
Na	0.23	0.25	0.23	0.28	0.28	0.20	0.12	0.24
O	22.00	22.00	22.00	22.00	22.00	22.00	22.00	22.00
FeCel	0.05	0.03	0.05	0.03	0.03	0.04	0.03	0.04
MgCel	0.10	0.06	0.07	0.06	0.06	0.07	0.06	0.07
Fe/Fe+Mg	0.34	0.36	0.39	0.35	0.37	0.35	0.34	0.36

Muscovite-618b

						Average
SiO_2	47.74	48.49	49.58	49.55	49.49	48.97
TiO_2	0.08	0.55	0.03	0.12	0.02	0.16
Al_2O_3	32.02	25.87	30.06	29.82	31.95	29.94
FeO	2.35	5.95	2.55	2.90	1.55	3.06
MnO	0.00	0.06	0.03	0.00	0.05	0.03
MgO	1.54	4.64	1.30	1.94	1.21	2.13
CaO	0.00	0.00	0.00	0.00	0.00	0.00
K_2O	10.48	10.14	9.79	9.88	9.30	9.92
Na_20	0.09	0.14	0.78	1.52	1.64	0.83
TOTAL	94.30	95.84	94.12	95.73	95.21	95.04
Si	6.43	6.58	6.67	6.61	6.58	6.57
Ti	0.08	0.06	0.00	0.01	0.02	0.03
Al	5.09	4.14	4.78	4.69	5.01	4.74
Fe	0.27	0.62	0.29	0.32	0.17	0.33
Mn	0.00	0.01	0.00	0.00	0.01	0.00
Mg	0.31	0.86	0.26	0.39	0.24	0.41
Ca	0.00	0.00	0.00	0.00	0.00	0.00
K	1.80	1.76	1.68	1.68	1.58	1.70
Na	0.02	0.04	0.20	0.39	0.42	0.22
O	22.00	22.00	22.00	22.00	22.00	22.00
FeCel	0.14	0.21	0.01	0.02	0.01	0.07
MgCel	0.17	0.29	0.00	0.03	0.02	0.09
Fe/Fe+Mg	0.46	0.42	0.53	0.45	0.41	0.45

Garnet 91-366a

									Average
SiO_2	37.74	37.44	37.71	37.41	37.64	37.42	37.53	37.95	37.61
TiO_2	0.22	0.15	0.10	0.09	0.09	0.10	0.08	0.05	0.11
Al_2O_3	20.91	21.43	21.39	21.51	21.37	21.25	21.15	21.40	21.30
FeO	28.40	29.02	29.19	28.75	28.68	29.00	28.83	29.52	28.92
MnO	4.45	4.44	4.44	4.26	4.25	4.21	4.57	4.29	4.36
MgO	2.43	2.61	2.45	2.47	2.46	2.48	2.48	2.46	2.48
CaO	5.45	5.50	5.53	6.02	6.11	5.66	5.17	5.74	5.65
TOTAL	99.60	100.58	100.81	100.51	100.61	100.12	99.81	101.41	100.43
Si	3.02	2.98	2.99	2.98	2.99	2.99	3.01	3.00	2.99
Ti	0.01	0.01	0.01	0.01	0.01	0.01	0.01	0.00	0.01
Al	1.97	2.01	2.00	2.02	2.00	2.00	2.00	1.99	2.00
Fe	1.90	1.93	2.94	1.91	1.91	1.94	1.93	1.95	2.05
Mn	0.30	0.30	0.30	0.29	0.29	0.28	0.31	0.29	0.29
Mg	0.29	0.31	0.29	0.29	0.29	0.30	0.30	0.29	0.29
Ca	0.47	0.47	0.47	0.51	0.52	0.48	0.44	0.49	0.48
O	12.00	12.00	12.00	12.00	12.00	12.00	12.00	12.00	12.00
Xalm	0.64	0.64	0.74	0.64	0.63	0.65	0.65	0.65	0.66
Xpy	0.10	0.10	0.07	0.10	0.10	0.10	0.10	0.10	0.09
Xgr	0.16	0.16	0.12	0.17	0.17	0.16	0.15	0.16	0.15
Xsps	0.10	0.10	0.07	0.10	0.10	0.09	0.10	0.10	0.09
Fe/Fe+Mg	0.87	0.86	0.91	0.87	0.87	0.87	0.87	0.87	0.87

Garnet 91-367a

					Average
SiO_2	37.28	37.54	37.69	37.56	37.52
TiO_2	0.31	0.05	0.16	0.36	0.22
Al_2O_3	20.74	21.27	20.69	20.31	20.75
FeO	29.79	31.45	31.76	30.32	30.83
MnO	0.92	0.52	0.74	1.78	0.99
MgO	1.76	1.50	1.51	1.65	1.61
CaO	8.75	8.34	2.67	7.55	6.83
TOTAL	99.55	100.69	100.57	99.53	100.09
Si	2.99	2.99	3.01	3.03	3.01
Ti	0.02	0.00	0.01	0.02	0.01
Al	1.96	2.00	1.95	1.93	1.96
Fe	2.00	2.09	2.12	2.04	2.06
Mn	0.06	0.04	0.05	0.12	0.07
Mg	0.21	0.18	0.18	0.20	0.19
Ca	0.75	0.72	0.69	0.65	0.70
O	12.00	12.00	12.00	12.00	12.00
Xalm	0.66	0.69	0.70	0.68	0.68
Xpy	0.07	0.06	0.06	0.07	0.06
Xgr	0.25	0.24	0.23	0.22	0.23
Xsps	0.02	0.01	0.02	0.04	0.02
Fe/Fe+Mg	0.90	0.92	0.92	0.91	0.92

Garnet 90-192

							Average
SiO_2	36.89	37.73	36.61	36.82	37.50	37.42	37.16
TiO_2	1.28	0.03	0.01	0.16	0.00	0.00	0.25
Al_2O_3	20.75	21.36	20.72	20.80	21.23	20.84	20.95
FeO	32.80	32.64	32.61	31.86	33.40	32.13	32.57
MnO	1.58	0.99	4.61	4.47	4.49	4.73	3.48
MgO	2.77	2.99	2.70	2.73	2.75	2.64	2.76
CaO	4.04	4.54	1.96	2.62	1.15	1.64	2.66
TOTAL	100.11	100.28	99.23	99.47	100.52	99.40	99.84
Si	2.96	3.00	2.98	2.99	3.01	3.03	3.00
Ti	0.08	0.00	0.00	0.10	0.00	0.00	0.03
Al	1.96	2.00	1.99	1.99	2.01	1.99	1.99
Fe	2.20	2.17	2.22	2.16	2.24	2.17	2.20
Mn	0.11	0.07	0.32	0.31	0.31	0.32	0.24
Mg	0.33	0.35	0.33	0.33	0.33	0.22	0.32
Ca	0.35	0.39	0.17	0.23	0.10	0.14	0.23
O	12.00	12.00	12.00	12.00	12.00	12.00	12.00
Xalm	0.74	0.73	0.73	0.71	0.75	0.76	0.74
Xpy	0.11	0.12	0.11	0.11	0.11	0.08	0.11
Xgr	0.12	0.13	0.06	0.08	0.03	0.05	0.08
Xsps	0.04	0.02	0.10	0.10	0.10	0.11	0.08
Fe/Fe+Mg	0.87	0.86	0.87	0.87	0.87	0.91	0.87

Garnet 91-116

									Average
SiO_2	37.66	37.63	37.80	37.74	37.45	37.05	36.88	37.29	37.44
TiO_2	0.03	0.05	0.08	0.10	0.07	0.07	0.06	0.07	0.07
Al_2O_3	21.67	21.38	21.55	21.41	21.33	21.25	21.26	21.28	21.39
FeO	27.59	27.95	27.27	27.20	28.33	27.82	27.94	27.81	27.74
MnO	2.31	2.05	2.28	2.26	1.94	2.20	2.18	2.37	2.20
MgO	1.26	1.60	1.25	1.25	1.59	1.31	1.37	1.23	1.36
CaO	9.76	9.73	10.24	9.82	9.46	9.74	9.66	9.89	9.79
TOTAL	100.29	100.39	100.47	99.78	100.18	99.44	99.35	99.95	99.98
Si	2.99	2.99	3.00	3.01	2.98	2.98	2.97	2.98	2.99
Ti	0.00	0.00	0.00	0.01	0.00	0.00	0.00	0.00	0.00
Al	2.03	2.00	2.01	2.01	2.00	2.01	2.02	2.01	2.01
Fe	1.83	1.86	1.81	1.81	1.89	1.87	1.88	1.86	1.85
Mn	0.16	0.14	0.15	0.15	0.13	0.15	0.15	0.16	0.15
Mg	0.15	0.19	0.15	0.15	0.19	0.16	0.16	0.15	0.16
Ca	0.83	0.83	0.87	0.84	0.81	0.84	0.83	0.85	0.84
O	12.00	12.00	12.00	12.00	12.00	12.00	12.00	12.00	12.00
Xalm	0.62	0.62	0.61	0.61	0.63	0.62	0.62	0.62	0.62
Xpy	0.05	0.06	0.05	0.05	0.06	0.05	0.05	0.05	0.05
Xgr	0.28	0.28	0.29	0.28	0.27	0.28	0.28	0.28	0.28
Xsps	0.05	0.05	0.05	0.05	0.04	0.05	0.05	0.05	0.05
Fe/Fe+Mg	0.92	0.91	0.92	0.92	0.91	0.92	0.92	0.93	0.92

Garnet 91-368

									Average
SiO_2	36.86	37.05	37.28	37.45	37.80	37.21	37.46	37.84	37.37
TiO_2	0.26	0.17	0.19	0.20	0.05	0.11	0.13	0.20	0.16
Al_2O_3	21.07	21.50	21.71	21.30	21.29	21.02	21.64	21.54	21.38
FeO	30.09	30.89	30.46	29.81	28.34	29.18	30.66	30.54	30.00
MnO	0.80	0.36	0.20	0.38	1.18	0.87	1.00	0.21	0.63
MgO	1.62	1.62	1.53	1.44	1.43	1.23	1.73	1.46	1.51
CaO	8.58	8.51	9.03	9.62	9.95	9.49	7.84	9.19	9.03
TOTAL	99.29	100.09	100.40	100.21	100.05	99.10	100.45	100.97	100.07
Si	2.97	2.96	2.97	2.99	3.01	3.00	2.98	2.99	2.98
Ti	0.02	0.01	0.01	0.01	0.00	0.01	0.01	0.00	0.01
Al	2.00	2.03	2.04	2.00	2.00	2.00	2.03	2.01	2.01
Fe	2.03	2.07	2.03	1.99	1.89	2.00	2.04	2.02	2.01
Mn	0.05	0.02	0.01	0.03	0.08	0.06	0.07	0.01	0.04
Mg	0.19	0.19	0.18	0.17	0.17	0.15	0.20	0.17	0.18
Ca	0.74	0.73	0.77	0.82	0.85	0.82	0.67	0.78	0.77
O	12.00	12.00	12.00	12.00	12.00	12.00	12.00	12.00	12.00
Xalm	0.67	0.69	0.68	0.66	0.63	0.66	0.68	0.68	0.67
Xpy	0.06	0.06	0.06	0.06	0.06	0.05	0.07	0.06	0.06
Xgr	0.25	0.24	0.26	0.27	0.28	0.27	0.22	0.26	0.26
Xsps	0.02	0.01	0.00	0.01	0.03	0.02	0.02	0.00	0.01
Fe/Fe+Mg	0.91	0.91	0.92	0.92	0.92	0.93	0.91	0.92	0.92

Garnet 90-117

									Average
SiO_2	37.37	37.43	37.45	37.85	36.99	37.27	37.41	36.60	37.30
TiO_2	0.03	0.07	0.09	0.07	0.04	0.07	0.06	0.03	0.06
Al_2O_3	21.22	21.03	21.15	21.38	21.51	21.39	21.17	21.30	21.27
FeO	27.86	26.94	26.81	26.15	28.46	28.32	28.84	28.03	27.68
MnO	2.78	3.66	4.22	4.38	2.04	1.91	2.31	2.85	3.02
MgO	0.97	0.88	0.93	1.05	1.22	0.99	0.98	1.00	1.00
CaO	9.56	9.66	9.57	8.91	9.15	9.56	9.44	9.29	9.39
TOTAL	99.78	99.67	100.22	99.78	99.41	99.50	100.21	99.10	99.71
Si	3.00	3.01	2.99	3.02	2.97	2.99	2.99	2.96	2.99
Ti	0.00	0.00	0.01	0.00	0.00	0.00	0.00	0.00	0.00
Al	2.01	1.99	1.99	2.01	2.04	2.02	2.00	2.03	2.01
Fe	1.87	1.81	1.79	1.75	1.91	1.90	1.93	1.90	1.86
Mn	0.19	0.25	0.29	0.30	0.14	0.13	0.16	0.20	0.21
Mg	0.12	0.11	0.11	0.12	0.15	0.12	0.12	0.12	0.12
Ca	0.82	0.83	0.82	0.76	0.79	0.82	0.81	0.81	0.81
O	12.00	12.00	12.00	12.00	12.00	12.00	12.00	12.00	12.00
Xalm	0.62	0.60	0.60	0.60	0.64	0.64	0.64	0.63	0.62
Xpy	0.04	0.04	0.04	0.04	0.05	0.04	0.04	0.04	0.04
Xgr	0.27	0.28	0.27	0.26	0.26	0.28	0.27	0.27	0.27
Xsps	0.06	0.08	0.09	0.10	0.05	0.04	0.05	0.06	0.07
Fe/Fe+Mg	0.94	0.94	0.94	0.93	0.93	0.94	0.94	0.94	0.94

Garnet 91-359a

							Average
SiO_2	37.21	37.31	37.11	37.43	37.18	37.17	37.24
TiO_2	0.06	0.06	0.07	0.05	0.04	0.03	0.05
Al_2O_3	21.76	21.67	21.51	21.54	21.88	21.84	21.70
FeO	31.55	32.13	31.29	32.28	31.75	32.17	31.86
MnO	0.27	0.17	0.19	0.11	0.18	0.21	0.19
MgO	1.92	1.76	1.91	1.80	1.93	1.81	1.86
CaO	7.11	6.59	7.05	7.29	7.50	7.05	7.10
TOTAL	99.88	99.69	99.13	100.50	100.46	100.28	99.99
Si	2.98	2.99	2.99	2.98	2.96	2.97	2.98
Ti	0.00	0.00	0.00	0.00	0.00	0.00	0.00
Al	2.05	2.05	2.04	2.02	2.05	2.05	2.04
Fe	2.11	2.15	2.11	2.15	2.11	2.15	2.13
Mn	0.02	0.01	0.01	0.01	0.01	0.01	0.01
Mg	0.23	0.21	0.23	0.21	0.23	0.22	0.22
Ca	0.61	0.57	0.61	0.62	0.64	0.60	0.61
O	12.00	12.00	12.00	12.00	12.00	12.00	12.00
Xalm	0.71	0.73	0.71	0.72	0.71	0.72	0.72
Xpy	0.08	0.07	0.08	0.07	0.08	0.07	0.07
Xgr	0.21	0.19	0.21	0.21	0.21	0.20	0.20
Xsps	0.01	0.00	0.00	0.00	0.00	0.00	0.00
Fe/Fe+Mg	0.90	0.91	0.90	0.91	0.90	0.91	0.91

Garnet 91-352

							Average
SiO_2	36.55	36.90	36.78	36.80	36.66	36.71	36.73
TiO_2	0.01	0.04	0.00	0.02	0.07	0.00	0.02
Al_2O_3	21.34	21.56	21.39	21.43	21.07	21.30	21.35
FeO	29.58	29.42	29.80	29.64	28.79	29.27	29.42
MnO	8.37	7.97	7.80	7.72	9.16	8.33	8.23
MgO	2.08	2.18	2.19	2.19	1.85	1.95	2.07
CaO	1.86	1.88	1.89	1.79	1.83	1.84	1.85
TOTAL	99.78	99.94	99.84	99.59	99.42	99.38	99.66
Si	2.70	2.98	2.98	2.98	2.99	2.99	2.94
Ti	0.00	0.00	0.00	0.00	0.00	0.00	0.00
Al	2.04	2.05	2.04	2.05	2.02	2.04	2.04
Fe	2.01	1.99	2.02	2.01	1.96	1.99	2.00
Mn	0.58	0.54	0.53	0.53	0.63	0.57	0.57
Mg	0.25	0.26	0.26	0.27	0.22	0.24	0.25
Ca	0.16	0.16	0.16	0.16	0.16	0.16	0.16
O	12.00	12.00	12.00	12.00	12.00	12.00	12.00
Xalm	0.67	0.67	0.68	0.68	0.66	0.67	0.67
Xpy	0.08	0.09	0.09	0.09	0.08	0.08	0.08
Xgr	0.05	0.05	0.05	0.05	0.05	0.05	0.05
Xsps	0.19	0.18	0.18	0.18	0.21	0.19	0.19
Fe/Fe+Mg	0.89	0.88	0.88	0.88	0.90	0.89	0.89

Garnet 91-389c

						Average
SiO_2	36.66	37.19	37.00	37.11	36.98	36.99
TiO_2	0.13	0.14	0.09	0.11	0.10	0.11
Al_2O_3	20.99	20.88	20.93	21.08	20.43	20.86
FeO	19.28	19.36	21.60	21.80	21.25	20.66
MnO	14.28	14.03	11.62	10.96	11.72	12.52
MgO	0.99	1.02	1.35	1.55	1.18	1.22
CaO	6.90	6.85	6.36	6.47	6.96	6.71
TOTAL	99.23	99.47	98.96	99.08	98.62	99.07
Si	2.98	3.01	3.00	3.00	3.02	3.00
Ti	0.01	0.01	0.01	0.01	0.01	0.01
Al	2.01	1.99	2.00	2.01	1.96	1.99
Fe	1.31	1.31	1.47	1.47	1.45	1.40
Mn	0.98	0.96	0.80	0.75	0.81	0.86
Mg	0.12	0.12	0.16	0.19	0.14	0.15
Ca	0.60	0.59	0.55	0.56	0.61	0.58
O	12.00	12.00	12.00	12.00	12.00	12.00
Xalm	0.43	0.44	0.49	0.50	0.48	0.47
Xpy	0.04	0.04	0.05	0.06	0.05	0.05
Xgr	0.20	0.20	0.19	0.19	0.20	0.19
Xsps	0.33	0.32	0.27	0.25	0.27	0.29
Fe/Fe+Mg	0.92	0.91	0.90	0.89	0.91	0.90

Garnet 91-266b

								Average
SiO_2	38.01	37.72	37.40	37.56	37.57	37.72	37.94	37.70
TiO_2	0.13	0.05	0.06	0.09	0.14	0.08	0.08	0.09
Al_2O_3	21.62	21.66	21.27	21.40	21.60	21.52	21.77	21.55
FeO	27.53	25.77	28.55	27.25	27.44	27.05	27.51	27.30
MnO	3.91	3.07	3.13	4.09	3.95	3.92	3.52	3.66
MgO	1.89	1.72	1.77	1.81	1.85	1.88	1.88	1.83
CaO	7.62	9.97	7.72	7.62	7.57	7.33	7.72	7.94
TOTAL	100.72	99.95	99.90	99.82	100.12	99.50	100.42	100.06
Si	3.01	2.99	2.99	3.00	2.99	3.01	3.00	3.00
Ti	0.01	0.00	0.00	0.01	0.01	0.01	0.00	0.01
Al	2.02	2.03	2.01	2.02	2.03	2.03	2.03	2.02
Fe	1.82	1.71	1.91	1.82	1.83	1.81	1.82	1.82
Mn	0.26	0.21	0.21	0.28	0.27	0.27	0.24	0.25
Mg	0.22	0.20	0.21	0.22	0.22	0.22	0.22	0.22
Ca	0.65	0.85	0.66	0.65	0.65	0.63	0.65	0.68
O	12.00	12.00	12.00	12.00	12.00	12.00	12.00	12.00
Xalm	0.62	0.58	0.64	0.61	0.62	0.62	0.62	0.61
Xpy	0.08	0.07	0.07	0.07	0.07	0.08	0.08	0.07
Xgr	0.22	0.29	0.22	0.22	0.22	0.21	0.22	0.23
Xsps	0.09	0.07	0.07	0.09	0.09	0.09	0.08	0.08
Fe/Fe+Mg	0.89	0.89	0.90	0.89	0.89	0.89	0.89	0.89

Garnet 91-371

									Average
SiO_2	37.74	37.63	37.70	37.57	37.67	37.66	37.25	37.43	37.58
TiO_2	0.05	0.04	0.08	0.04	0.08	0.06	0.06	0.05	0.06
Al_2O_3	21.45	21.62	21.79	22.00	21.71	21.65	21.49	21.76	21.68
FeO	31.77	30.27	31.40	31.67	30.58	31.42	31.10	30.07	31.04
MnO	0.64	0.40	0.58	0.50	0.45	0.58	0.63	0.73	0.56
MgO	1.70	1.81	1.50	1.85	1.84	1.59	1.44	1.53	1.66
CaO	7.76	8.34	8.16	7.44	8.21	7.88	8.20	8.37	8.05
TOTAL	101.11	100.11	101.19	101.07	100.53	100.84	100.17	99.93	100.62
Si	2.99	2.99	2.98	2.97	2.99	2.99	2.98	2.99	2.98
Ti	0.00	0.00	0.00	0.00	0.00	0.00	0.00	0.00	0.00
Al	2.00	2.03	2.03	2.05	2.03	2.02	2.03	2.05	2.03
Fe	2.11	2.01	2.08	2.09	2.03	2.08	2.08	2.01	2.06
Mn	0.04	0.03	0.04	0.03	0.03	0.04	0.04	0.05	0.04
Mg	0.20	0.21	0.18	0.22	0.22	0.19	0.17	0.18	0.20
Ca	0.66	0.71	0.69	0.63	0.70	0.67	0.70	0.72	0.68
O	12.00	12.00	12.00	12.00	12.00	12.00	12.00	12.00	12.00
Xalm	0.70	0.68	0.70	0.70	0.68	0.70	0.69	0.68	0.69
Xpy	0.07	0.07	0.06	0.07	0.07	0.06	0.06	0.06	0.07
Xgr	0.22	0.24	0.23	0.21	0.23	0.22	0.23	0.24	0.23
Xsps	0.01	0.01	0.01	0.01	0.01	0.01	0.01	0.02	0.01
Fe/Fe+Mg	0.91	0.90	0.92	0.91	0.90	0.92	0.92	0.92	0.91

Garnet 90-119

				Average
SiO_2	36.91	37.34	37.23	37.16
TiO_2	0.00	0.00	0.00	0.00
Al_2O_3	20.56	20.10	20.61	20.42
FeO	28.43	27.00	26.66	27.36
MnO	3.08	4.26	5.17	4.17
MgO	1.03	0.86	0.89	0.92
CaO	8.84	9.68	9.02	9.18
TOTAL	99.45	99.22	99.57	99.41
Si	2.99	3.03	3.01	3.01
Ti	0.00	0.00	0.00	0.00
Al	1.97	1.92	1.96	1.95
Fe	1.97	1.83	1.80	1.87
Mn	0.22	0.29	0.35	0.29
Mg	0.12	0.10	0.11	0.11
Ca	0.76	0.84	0.78	0.79
O	12.00	12.00	12.00	12.00
Xalm	0.64	0.60	0.59	0.61
Xpy	0.04	0.03	0.04	0.04
Xgr	0.25	0.27	0.26	0.26
Xsps	0.07	0.10	0.12	0.09
Fe/Fe+Mg	0.94	0.95	0.94	0.94

Garnet 92-487a

									Average
SiO_2	37.82	37.27	37.77	37.83	37.58	37.12	37.19	37.45	37.50
TiO_2	0.05	0.05	0.05	0.07	0.08	0.04	0.05	0.06	0.06
Al_2O_3	22.28	22.19	22.28	22.32	22.40	22.26	22.19	22.28	22.28
FeO	34.58	35.43	33.07	34.58	34.39	34.84	33.95	35.39	34.53
MnO	0.08	0.12	0.15	0.12	0.24	0.16	0.06	0.13	0.13
MgO	2.00	2.12	2.07	1.83	2.46	1.89	2.03	1.94	2.04
CaO	5.96	5.26	7.32	6.21	5.89	5.90	6.34	5.36	6.03
TOTAL	102.77	102.44	102.70	102.95	103.05	102.20	101.81	102.60	102.57
Si	2.96	2.94	2.95	2.95	2.93	2.93	2.94	2.94	2.94
Ti	0.00	0.00	0.00	0.00	0.00	0.00	0.00	0.00	0.00
Al	2.05	2.06	2.05	2.06	2.06	2.07	2.07	2.06	2.06
Fe	2.26	2.33	2.16	2.26	2.24	2.30	2.24	2.33	2.27
Mn	0.01	0.01	0.01	0.01	0.02	0.01	0.00	0.01	0.01
Mg	0.23	0.25	0.24	0.21	0.29	0.22	0.24	0.23	0.24
Ca	0.50	0.44	0.61	0.52	0.49	0.50	0.54	0.45	0.51
O	12.00	12.00	12.00	12.00	12.00	12.00	12.00	12.00	12.00
Xalm	0.75	0.77	0.71	0.75	0.74	0.76	0.74	0.77	0.75
Xpy	0.08	0.08	0.08	0.07	0.09	0.07	0.08	0.08	0.08
Xgr	0.17	0.15	0.20	0.17	0.16	0.16	0.18	0.15	0.17
Xsps	0.00	0.00	0.00	0.00	0.01	0.00	0.00	0.00	0.00
Fe/Fe+Mg	0.91	0.90	0.90	0.91	0.89	0.91	0.90	0.91	0.90

Garnet 92-618b

							Average
SiO_2	37.89	38.14	37.87	37.66	37.67	37.48	37.79
TiO_2	0.13	0.17	0.11	0.14	0.13	0.17	0.14
Al_2O_3	22.68	22.38	22.32	22.37	22.30	22.37	22.40
FeO	27.36	27.36	27.94	28.07	27.65	27.60	27.66
MnO	1.43	1.35	1.35	1.28	2.39	3.07	1.81
MgO	2.57	2.58	2.52	2.61	2.39	2.23	2.48
CaO	10.24	10.40	10.21	10.21	9.95	9.25	10.04
TOTAL	102.31	102.38	102.32	102.35	102.48	102.17	102.34
Si	2.93	2.95	2.94	2.93	2.93	2.93	2.93
Ti	0.01	0.01	0.01	0.01	0.01	0.01	0.01
Al	2.07	2.04	2.04	2.05	2.04	2.06	2.05
Fe	1.77	1.77	1.81	1.82	1.79	1.80	1.79
Mn	0.09	0.09	0.09	0.08	0.16	0.20	0.12
Mg	0.30	0.30	0.29	0.30	0.28	0.26	0.29
Ca	0.85	0.86	0.85	0.85	0.83	0.77	0.84
O	12.00	12.00	12.00	12.00	12.00	12.00	12.00
Xalm	0.59	0.59	0.60	0.60	0.59	0.59	0.59
Xpy	0.10	0.10	0.10	0.10	0.09	0.09	0.09
Xgr	0.28	0.29	0.28	0.28	0.27	0.25	0.28
Xsps	0.03	0.03	0.03	0.03	0.05	0.07	0.04
Fe/Fe+Mg	0.86	0.86	0.86	0.86	0.87	0.87	0.86

Plagioclase 92-618b

								Average
SiO_2	58.76	57.41	56.72	58.50	56.15	58.03	57.46	57.58
Al_2O_3	24.66	25.00	26.52	25.54	26.64	26.05	25.85	25.75
FeO	0.05	0.10	0.01	0.02	0.06	0.06	0.05	0.05
MgO	0.02	0.07	0.01	0.02	0.06	0.05	0.02	0.04
CaO	7.09	8.01	9.07	7.79	9.36	8.44	8.45	8.32
Na_2O	7.41	6.95	6.80	6.97	6.12	6.82	6.86	6.85
K_20	0.08	0.06	0.06	0.07	0.05	0.06	0.05	0.06
TOTAL	98.06	97.61	99.20	98.91	98.44	99.52	98.74	98.64
Si	2.67	2.63	2.57	2.64	2.56	2.61	2.61	2.61
Al	1.32	1.35	1.42	1.36	1.43	1.38	1.31	1.37
Fe	0.00	0.00	0.00	0.00	0.00	0.00	0.00	0.00
Mg	0.00	0.01	0.00	0.00	0.00	0.00	0.00	0.00
Ca	0.35	0.39	0.44	0.38	0.46	0.41	0.41	0.40
Na	0.65	0.62	0.60	0.61	0.54	0.59	0.60	0.60
K	0.00	0.00	0.00	0.00	0.00	0.00	0.00	0.00
O	8.00	8.00	8.00	8.00	8.00	8.00	8.00	8.00
An	0.34	0.39	0.42	0.38	0.46	0.40	0.40	0.40
Ab	0.65	0.61	0.57	0.62	0.54	0.59	0.59	0.60
Or	0.00	0.00	0.00	0.00	0.00	0.00	0.00	0.00
Ca\Ca+Na	0.35	0.39	0.42	0.38	0.46	0.41	0.41	0.40

Plagioclase 92-618c

								Average
SiO_2	63.60	63.25	62.82	63.34	60.98	61.44	61.30	62.39
Al_2O_3	23.52	23.57	23.33	22.05	22.30	22.48	22.69	22.85
FeO	0.16	0.11	0.15	0.21	0.11	0.12	0.13	0.14
MgO	0.04	0.05	0.03	0.03	0.04	0.02	0.04	0.04
CaO	4.72	4.62	4.89	4.13	4.57	4.47	4.66	4.58
Na_2O	9.01	8.92	8.99	9.80	8.89	8.98	8.75	9.05
K_20	0.06	0.07	0.06	0.06	0.06	0.07	0.08	0.07
TOTAL	101.12	100.60	100.27	99.62	96.95	97.58	97.65	99.11
Si	2.78	2.78	2.78	2.82	2.79	2.79	2.78	2.79
Al	1.21	1.22	1.22	1.16	1.20	1.20	1.21	1.20
Fe	0.01	0.00	0.01	0.01	0.00	0.00	0.00	0.01
Mg	0.00	0.00	0.00	0.00	0.00	0.00	0.00	0.00
Ca	0.22	0.22	0.23	0.20	0.22	0.22	0.23	0.22
Na	0.76	0.76	0.77	0.85	0.79	0.79	0.77	0.78
K	0.00	0.00	0.00	0.00	0.00	0.00	0.00	0.00
O	8.00	8.00	8.00	8.00	8.00	8.00	8.00	8.00
An	0.22	0.22	0.23	0.19	0.22	0.21	0.23	0.22
Ab	0.77	0.77	0.77	0.81	0.78	0.78	0.77	0.78
Or	0.00	0.00	0.00	0.00	0.00	0.00	0.00	0.00
Ca\Ca+Na	0.22	0.22	0.23	0.19	0.22	0.22	0.23	0.22

Plagioclase 92-483a

					Average
SiO_2	66.44	68.57	67.26	68.93	67.80
Al_2O_3	21.92	20.01	21.44	19.88	20.81
FeO	0.02	0.00	0.06	0.00	0.02
MgO	0.04	0.05	0.02	0.04	0.04
CaO	2.55	0.63	2.11	0.40	1.42
Na_2O	10.12	11.39	10.55	11.56	10.91
K_20	0.12	0.08	0.11	0.08	0.10
TOTAL	101.22	100.73	101.56	100.88	101.10
Si	2.88	2.98	2.91	2.98	2.94
Al	1.12	1.02	1.09	1.01	1.06
Fe	0.00	0.00	0.00	0.00	0.00
Mg	0.00	0.00	0.00	0.00	0.00
Ca	0.12	0.03	0.10	0.02	0.07
Na	0.85	0.96	0.88	0.97	0.92
K	0.01	0.00	0.01	0.00	0.01
O	8.00	8.00	8.00	8.00	8.00
An	0.12	0.03	0.10	0.02	0.07
Ab	0.87	0.97	0.90	0.98	0.93
Or	0.01	0.00	0.01	0.00	0.01
Ca\Ca+Na	0.12	0.03	0.10	0.02	0.07

Plagioclase 91-367a

						Average
SiO_2	62.86	61.87	65.19	67.86	68.61	65.28
Al_2O_3	23.60	23.83	22.84	20.23	19.68	22.04
FeO	0.49	0.55	0.23	0.12	0.03	0.28
MgO	0.10	0.02	0.02	0.05	0.00	0.04
CaO	4.68	4.85	3.58	0.93	0.33	2.87
Na_2O	9.13	9.02	9.34	11.02	11.50	10.00
K_20	0.09	0.08	0.09	0.08	0.09	0.09
TOTAL	100.94	100.21	101.30	100.28	100.25	100.60
Si	2.76	2.74	2.84	2.96	2.99	2.86
Al	1.22	1.25	1.17	1.04	1.01	1.14
Fe	0.02	0.02	0.01	0.00	0.00	0.01
Mg	0.01	0.00	0.00	0.00	0.00	0.00
Ca	0.22	0.23	0.17	0.04	0.02	0.14
Na	0.78	0.78	0.79	0.93	0.97	0.85
K	0.01	0.00	0.01	0.00	0.01	0.00
O	8.00	8.00	8.00	8.00	8.00	8.00
An	0.22	0.23	0.17	0.04	0.02	0.14
Ab	0.78	0.77	0.82	0.95	0.98	0.86
Or	0.00	0.00	0.01	0.00	0.01	0.00
Ca\Ca+Na	0.22	0.23	0.17	0.04	0.02	0.14

Amphibole 92-618C

SIO$_2$	44.26	41.32	40.36	43.06	45.19	43.91	42.66	44.44	43.60
TIO$_2$	0.53	0.27	0.25	0.30	0.28	0.31	0.61	0.32	0.21
AL$_2$O$_3$	11.02	15.54	14.68	12.11	10.78	13.93	12.35	13.49	14.20
FEO	20.84	19.77	21.89	20.72	18.44	18.06	19.88	16.80	18.24
MNO	0.28	0.31	0.31	0.30	0.29	0.17	0.31	0.12	0.23
MGO	8.74	7.26	6.52	8.22	10.14	8.90	8.61	9.88	8.54
CAO	10.96	10.76	11.24	10.92	10.53	10.39	11.01	9.78	10.73
NA$_2$O	1.75	2.01	2.12	1.82	1.58	2.04	1.93	2.20	1.90
K$_2$O	0.32	0.58	0.63	0.47	0.31	0.45	0.48	0.46	0.45
TOTAL	98.70	97.82	98.00	97.92	97.54	98.16	97.84	97.49	98.10
SI	6.51	6.14	6.09	6.41	6.61	6.41	6.35	6.46	6.39
TI	0.06	0.03	0.03	0.03	0.03	0.03	0.07	0.03	0.02
AL	1.91	2.72	2.61	2.12	1.86	2.40	2.17	2.31	2.45
FE	2.56	2.46	2.76	2.58	2.26	2.20	2.47	2.04	2.24
MN	0.03	0.04	0.04	0.04	0.04	0.02	0.04	0.01	0.03
MG	1.92	1.61	1.47	1.82	2.21	1.94	1.91	2.14	1.87
CA	1.73	1.71	1.82	1.74	1.65	1.62	1.75	1.52	1.69
NA	0.50	0.58	0.62	0.52	0.45	0.58	0.56	0.62	0.54
K	0.06	0.11	0.12	0.09	0.06	0.08	0.09	0.09	0.08
O	23.00	23.00	23.00	23.00	23.00	23.00	23.00	23.00	23.00
SI	6.51	6.14	6.09	6.41	6.61	6.41	6.35	6.46	6.39
AL(IV)	1.49	1.86	1.91	1.59	1.39	1.59	1.65	1.54	1.61
AL(VI)	0.42	0.86	0.70	0.53	0.47	0.80	0.51	0.77	0.85
TI	0.06	0.03	0.03	0.03	0.03	0.03	0.07	0.03	0.02
FE(3+)	0.93	0.82	0.77	0.90	1.06	0.81	0.85	0.95	0.72
FE(2+)	1.64	1.64	1.99	1.67	1.20	1.40	1.62	1.09	1.52
MN	0.03	0.04	0.04	0.04	0.04	0.02	0.04	0.01	0.03
MG	1.92	1.61	1.47	1.82	2.21	1.94	1.91	2.14	1.87
CA	1.73	1.71	1.82	1.74	1.65	1.62	1.75	1.52	1.69
NA(M4)	0.27	0.29	0.18	0.26	0.35	0.38	0.25	0.48	0.31
NA(A)	0.23	0.29	0.44	0.27	0.10	0.20	0.31	0.14	0.23
K	0.06	0.11	0.12	0.09	0.06	0.08	0.09	0.09	0.08
TOTAL	15.29	15.40	15.56	15.35	15.16	15.29	15.40	15.23	15.31
Na^A+K	0.29	0.40	0.56	0.35	0.16	0.29	0.40	0.23	0.31
Al^{vi}+Fe^{3+}+T	1.41	1.71	1.50	1.47	1.55	1.65	1.43	1.76	1.59
Na/Ca+Na	22.42	25.26	25.45	23.17	21.35	26.22	24.08	28.93	24.27
Al/Si+Al	22.69	30.72	30.01	24.90	21.95	27.22	25.45	26.36	27.74

Amphibole 91-369A

SIO$_2$	47.78	47.85	46.40	49.11
TIO$_2$	0.21	0.22	0.28	0.12
AL$_2$O$_3$	9.67	9.66	10.86	8.16
FEO	15.11	14.67	14.87	16.01
MNO	0.22	0.20	0.21	0.22
MGO	12.06	12.33	12.03	12.47
CAO	10.08	10.44	10.94	9.43
NA$_2$O	2.20	2.24	1.69	2.10
K$_2$O	0.47	0.47	0.42	0.26
TOTAL	97.80	98.08	97.70	97.88
SI	6.89	6.89	6.71	7.02
TI	0.02	0.02	0.03	0.01
AL	1.64	1.64	1.85	1.37
FE	1.82	1.77	1.80	1.91
MN	0.03	0.02	0.03	0.03
MG	2.59	2.65	2.59	2.66
CA	1.56	1.61	1.69	1.44
NA	0.62	0.63	0.47	0.58
K	0.09	0.09	0.08	0.05
O	23.00	23.00	23.00	23.00
SI	6.89	6.89	6.71	7.02
AL(IV)	1.11	1.11	1.29	0.98
AL(VI)	0.54	0.54	0.56	0.39
TI	0.02	0.02	0.03	0.01
FE(3+)	0.71	0.59	0.74	1.05
FE(2+)	1.11	1.18	1.06	0.86
MN	0.03	0.02	0.03	0.03
MG	2.59	2.65	2.59	2.66
CA	1.56	1.61	1.69	1.44
NA(M4)	0.44	0.39	0.31	0.56
NA(A)	0.17	0.24	0.17	0.03
K	0.09	0.09	0.08	0.05
TOTAL	15.26	15.32	15.25	15.07
Na^A+K	0.26	0.32	0.25	0.07
Al^{VI}+Fe^{3+}+T	1.27	1.15	1.33	1.45
Na/Ca+Na	28.31	27.97	21.85	28.72
Al/Si+Al	19.26	19.22	21.63	16.38

Amphibole 91-372A

SIO_2	46.75	49.05	45.06	47.42
TIO_2	0.28	0.29	0.30	0.21
AL_2O_3	11.38	8.42	12.48	11.10
FEO	14.04	13.03	14.81	13.87
MNO	0.32	0.36	0.32	0.31
MGO	12.10	14.18	11.69	12.32
CAO	9.21	10.36	10.35	8.86
NA_2O	2.84	1.76	2.32	2.95
K_2O	0.32	0.39	0.38	0.27
TOTAL	97.24	97.84	97.71	97.31
SI	6.72	6.97	6.50	6.78
TI	0.03	0.03	0.03	0.02
AL	1.93	1.41	2.12	1.87
FE	1.69	1.55	1.79	1.66
MN	0.04	0.04	0.04	0.04
MG	2.59	3.00	2.51	2.63
CA	1.42	1.58	1.60	1.36
NA	0.79	0.48	0.65	0.82
K	0.06	0.07	0.07	0.05
O	23.00	23.00	23.00	23.00
SI	6.72	6.97	6.50	6.78
AL(IV)	1.28	1.03	1.50	1.22
AL(VI)	0.65	0.38	0.63	0.65
TI	0.03	0.03	0.03	0.02
FE(3+)	0.88	0.89	0.89	0.93
FE(2+)	0.81	0.66	0.90	0.72
MN	0.04	0.04	0.04	0.04
MG	2.59	3.00	2.51	2.63
CA	1.42	1.58	1.60	1.36
NA(M4)	0.58	0.42	0.40	0.64
NA(A)	0.21	0.06	0.25	0.18
K	0.06	0.07	0.07	0.05
TOTAL	15.27	15.13	15.32	15.23
Na^A+K	0.27	0.13	0.32	0.23
Al^{VI}+Fe^{3+}+T	1.56	1.29	1.54	1.61
Na/Ca+Na	35.82	23.51	28.86	37.60
Al/Si+Al	22.30	16.83	24.61	21.63

Amphibole 90-49B

SIO$_2$	42.09	47.41	44.47	46.25
TIO$_2$	0.77	0.20	0.56	0.46
AL$_2$O$_3$	13.25	8.21	10.44	9.51
FEO	17.47	14.59	15.55	15.33
MNO	0.31	0.30	0.38	0.30
MGO	9.90	13.66	12.17	12.72
CAO	11.35	11.21	11.35	11.15
NA$_2$O	2.07	1.34	1.73	1.57
K$_2$O	0.31	0.11	0.19	0.15
TOTAL	97.52	97.03	96.84	97.44
SI	6.22	6.84	6.52	6.69
TI	0.09	0.02	0.06	0.05
AL	2.31	1.40	1.80	1.62
FE	2.16	1.76	1.91	1.86
MN	0.04	0.04	0.05	0.04
MG	2.18	2.94	2.66	2.74
CA	1.80	1.73	1.78	1.73
NA	0.59	0.38	0.49	0.44
K	0.06	0.02	0.04	0.03
O	23.00	23.00	23.00	23.00
SI	6.22	6.84	6.52	6.69
AL(IV)	1.78	1.16	1.48	1.31
AL(VI)	0.53	0.24	0.32	0.31
TI	0.09	0.02	0.06	0.05
FE(3+)	0.82	1.01	0.94	0.97
FE(2+)	1.34	0.75	0.97	0.89
MN	0.04	0.04	0.05	0.04
MG	2.18	2.94	2.66	2.74
CA	1.80	1.73	1.78	1.73
NA(M4)	0.20	0.27	0.22	0.27
NA(A)	0.39	0.11	0.28	0.17
K	0.06	0.02	0.04	0.03
TOTAL	15.45	15.13	15.31	15.20
Na^A+K	0.45	0.13	0.31	0.20
Al^{vi}+Fe^{3+}+T	1.44	1.27	1.32	1.33
Na/Ca+Na	24.81	17.78	21.62	20.31
Al/Si+Al	27.07	16.95	21.68	19.51

Amphibole 92-617B

SIO_2	47.08	49.71	46.82	46.48
TIO_2	0.37	0.07	0.28	0.26
AL_2O_3	9.49	7.39	9.81	10.49
FEO	11.41	8.41	11.02	13.43
MNO	0.33	0.20	0.27	0.35
MGO	15.62	18.31	15.81	13.30
CAO	11.85	12.29	12.08	10.88
NA_2O	1.84	1.66	2.32	2.15
K_2O	0.31	0.18	0.47	0.30
TOTAL	98.30	98.22	98.88	97.64
SI	6.68	6.95	6.64	6.68
TI	0.04	0.01	0.03	0.03
AL	1.59	1.22	1.64	1.78
FE	1.35	0.98	1.31	1.62
MN	0.04	0.02	0.03	0.04
MG	3.30	3.82	3.34	2.85
CA	1.80	1.84	1.84	1.68
NA	0.51	0.45	0.64	0.60
K	0.06	0.03	0.09	0.06
O	23.00	23.00	23.00	23.00
SI	6.68	6.95	6.64	6.68
AL(IV)	1.32	1.05	1.36	1.32
AL(VI)	0.27	0.17	0.29	0.46
TI	0.04	0.01	0.03	0.03
FE(3+)	0.81	0.70	0.61	0.79
FE(2+)	0.54	0.28	0.70	0.83
MN	0.04	0.02	0.03	0.04
MG	3.30	3.82	3.34	2.85
CA	1.80	1.84	1.84	1.68
NA(M4)	0.20	0.16	0.16	0.32
NA(A)	0.31	0.29	0.48	0.28
K	0.06	0.03	0.09	0.06
TOTAL	15.36	15.32	15.56	15.33
Na^A+K	0.36	0.32	0.56	0.33
Al^{vi}+Fe^{3+}+T	1.12	0.88	0.93	1.28
Na/Ca+Na	21.94	19.64	25.79	26.34
Al/Si+Al	19.20	14.91	19.81	21.02

Amphibole 90-30

SIO_2	44.17	44.84	45.99	44.31
TIO_2	0.96	0.87	0.78	0.93
AL_2O_3	9.28	8.99	8.18	9.29
FEO	18.80	18.19	18.16	18.58
MNO	0.64	0.76	0.78	0.66
MGO	9.88	10.37	10.82	10.00
CAO	11.71	11.51	11.59	11.37
NA_2O	1.37	1.33	1.31	1.56
K_2O	0.66	0.72	0.53	0.76
TOTAL	97.47	97.58	98.14	97.46
SI	6.61	6.67	6.78	6.62
TI	0.11	0.10	0.09	0.10
AL	1.64	1.58	1.42	1.64
FE	2.35	2.26	2.24	2.32
MN	0.08	0.10	0.10	0.08
MG	2.20	2.30	2.38	2.23
CA	1.88	1.83	1.83	1.82
NA	0.40	0.38	0.37	0.45
K	0.13	0.14	0.10	0.14
O	23.00	23.00	23.00	23.00
SI	6.61	6.67	6.78	6.62
AL(IV)	1.39	1.33	1.22	1.38
AL(VI)	0.25	0.25	0.20	0.26
TI	0.11	0.10	0.09	0.10
FE(3+)	0.64	0.70	0.71	0.67
FE(2+)	1.72	1.56	1.53	1.66
MN	0.08	0.10	0.10	0.08
MG	2.20	2.30	2.38	2.23
CA	1.88	1.83	1.83	1.82
NA(M4)	0.12	0.17	0.17	0.18
NA(A)	0.28	0.22	0.20	0.27
K	0.13	0.14	0.10	0.14
TOTAL	15.40	15.35	15.30	15.42
Na^A+K	0.40	0.35	0.30	0.42
Al^{vi}+Fe^{3+}+T	1.00	1.04	1.00	1.03
Na/Ca+Na	17.47	17.29	16.98	19.89
Al/Si+Al	19.85	19.12	17.33	19.82

Amphibole 92-607

SIO_2	42.85	43.17	43.53	43.68
TIO_2	1.02	1.07	0.69	0.83
AL_2O_3	11.05	10.97	10.52	9.95
FEO	17.17	17.43	16.49	15.94
MNO	0.24	0.21	0.22	0.24
MGO	11.16	11.17	11.76	12.21
CAO	11.55	11.46	11.47	11.58
NA_2O	2.53	2.44	2.30	2.38
K_2O	0.80	0.84	0.69	0.63
TOTAL	98.37	98.76	97.67	97.44
SI	6.34	6.36	6.43	6.47
TI	0.11	0.12	0.08	0.09
AL	1.93	1.90	1.83	1.74
FE	2.13	2.15	2.04	1.97
MN	0.03	0.03	0.03	0.03
MG	2.46	2.45	2.59	2.70
CA	1.83	1.81	1.82	1.84
NA	0.73	0.70	0.66	0.68
K	0.15	0.16	0.13	0.12
O	23.00	23.00	23.00	23.00
SI	6.34	6.36	6.43	6.47
AL(IV)	1.66	1.64	1.57	1.53
AL(VI)	0.27	0.26	0.27	0.21
TI	0.11	0.12	0.08	0.09
FE(3+)	0.62	0.68	0.72	0.66
FE(2+)	1.50	1.47	1.31	1.32
MN	0.03	0.03	0.03	0.03
MG	2.46	2.45	2.59	2.70
CA	1.83	1.81	1.82	1.84
NA(M4)	0.17	0.19	0.18	0.16
NA(A)	0.56	0.50	0.48	0.52
K	0.15	0.16	0.13	0.12
TOTAL	15.71	15.66	15.61	15.64
Na^A+K	0.71	0.66	0.61	0.64
Al^{VI}+Fe^{3+}+T	1.00	1.06	1.07	0.96
Na/Ca+Na	28.39	27.81	26.63	27.11
Al/Si+Al	23.31	23.05	22.17	21.17

Amphibole 91-366A

SIO_2	49.86	46.69	46.35	42.44
TIO_2	0.19	0.26	0.21	0.15
AL_2O_3	10.40	11.54	12.83	11.83
FEO	14.20	15.18	14.76	16.81
MNO	0.31	0.45	0.34	0.38
MGO	12.34	11.57	11.16	10.66
CAO	8.11	10.59	9.01	11.78
NA_2O	2.81	1.93	2.70	1.85
K_2O	0.22	0.27	0.30	0.51
TOTAL	98.44	98.48	97.66	96.41
SI	6.99	6.68	6.63	6.36
TI	0.02	0.03	0.02	0.02
AL	1.72	1.95	2.16	2.09
FE	1.66	1.82	1.77	2.11
MN	0.04	0.05	0.04	0.05
MG	2.58	2.47	2.33	2.38
CA	1.22	1.62	1.38	1.89
NA	0.76	0.54	0.75	0.54
K	0.04	0.05	0.05	0.10
O	23.00	23.00	23.00	23.00
SI	6.99	6.68	6.63	6.36
AL(IV)	1.01	1.32	1.37	1.64
AL(VI)	0.70	0.63	0.79	0.45
TI	0.02	0.03	0.02	0.02
FE(3+)	1.03	0.79	0.97	0.74
FE(2+)	0.63	1.02	0.80	1.36
MN	0.04	0.05	0.04	0.05
MG	2.58	2.47	2.38	2.38
CA	1.22	1.62	1.38	1.89
NA(M4)	0.78	0.38	0.62	0.11
NA(A)	-0.02	0.16	0.13	0.43
K	0.04	0.05	0.05	0.10
TOTAL	15.02	15.21	15.18	15.53
Na^A+K	0.02	0.21	0.18	0.53
Al^{vi}+Fe^{3+}+T	1.76	1.45	1.78	1.21
Na/Ca+Na	38.54	24.80	35.16	22.13
Al/Si+Al	19.74	22.56	24.60	24.73

APPENDIX 6 - STATION LOCATIONS AND STRUCTURAL DATA

The following terms are used in this appendix:

Structure = tectonic fabrics

s1, s1b, s1c, etc. = foliation measurements at a given station.

l1, l1b, l1c, etc. = mineral lineation measurements at a given station

fa, fab, etc = fold axis measurements at a given station

apc, apcb, etc. = axial planar cleavage measurements at a given station

Domain = structural domains indentified along transects AA', BB', and CC'

A1...C7 = measurements taken in structural domains A1 to C7. These measurements were used to produce the equal-area plots in figures 4-4 and 4-5.

Station	Location (UTM)		Strike/	Dip/	Structure	Domain
	Easting	Northing	Trend	Plunge		
"001"	590140	6749900	306	80	"s1"	
"002"	589010	6750980	146	72	"s1"	
"002"	589010	6750980	140	66	"s1b"	
"002"	589010	6750980	140	05	"fa"	
"003"	587970	6752310	132	39	"s1"	
"003"	587970	6752310	130	01	"fa"	
"004"	590280	6749270	140	50	"s1"	
"005"	600000	6744590	340	44	"s1"	
"005"	600000	6744590	130	15	"fa"	
"006"	600300	6744960	006	18	"s1"	
"006"	600300	6744960	010	26	"s1b"	
"006"	600300	6744960	180	18	"fa"	
"007"	601210	6745980	352	26	"s1"	
"007"	601210	6745980	016	30	"l1"	
"008"	600580	6747050	353	18	"s1"	
"008"	600580	6747050	011	23	"l1"	
"009"	600130	6746660	002	30	"s1"	
"009"	600130	6746660	127	18	"fa"	
"009"	600130	6746660	012	24	"l1"	
"010"	599930	6746170	060	29	"s1"	
"010"	599930	6746170	147	12	"fa"	
"010"	599930	6746170	209	11	"l1"	
"011"	591800	6748000	305	87	"s1"	
"011"	591800	6748000	305	00	"l1"	
"012"	596140	6745530	317	77	"s1"	
"012"	596140	6745530	142	12	"fa"	
"013"	600960	6742930	002	19	"s1"	
"013"	600960	6742930	127	07	"fa"	
"013"	600960	6742930	167	18	"l1"	
"014"	603610	6742030				
"015"	604940	6737810	290	34	"s1"	
"016"	607250	6760450	318	76	"s1"	
"017"	606950	6759650	023	34	"s1"	
"018"	602800	6716230	307	44	"s1"	
"018"	602800	6716230	303	44	"s1b"	
"018"	602800	6716230	042	49	"l1"	
"019"	602360	6716540	344	53	"s1"	
"019"	602360	6716540	330	40	"s1b"	
"019"	602360	6716540	090	40	"l1"	
"020"	602000	6717690	315	64	"s1"	
"020"	602000	6717690	147	09	"fa"	
"021"	601130	6718600	323	52	"s1"	

Station	Location (UTM) Easting	Northing	Strike/ Trend	Dip/ Plunge	Structure	Domain
"021"	601130	6718600	305	84	"s1b"	
"021"	601130	6718600	162	67	"fa"	
"022"	595090	6723650	327	69	"s1"	
"022"	595090	6723650	253	59	"s1b"	
"022"	595090	6723650	356	62	"l1"	
"023"	594490	6723510	132	88	"s1"	
"023"	594490	6723510	250	90	"l1"	
"024"	593750	6722870	332	57	"s1"	
"024"	593750	6722870	315	42	"s1b"	
"024"	593750	6722870	043	28	"l1"	
"024"	593750	6722870	036	36	"l1b"	
"025"	593160	6722700				
"026"	592590	6722880				
"027"	591930	6722340				
"028"	591190	6721680				
"029"	590830	6721200				
"030"	595790	6721530				
"031"	595710	6721280	084	67	"s1"	
"031"	595710	6721280	086	33	"l1"	
"031"	595710	6721280	090	44	"fa"	
"032"	595270	6720800	297	65	"s1"	
"032"	595270	6720800	293	62	"s1b"	
"032"	595270	6720800	272	64	"s1c"	
"032"	595270	6720800	272	64	"s1d"	
"032"	595270	6720800	048	40	"l1"	
"032"	595270	6720800	042	39	"l1b"	
"032"	595270	6720800	050	39	"l1c"	
"032"	595270	6720800	043	38	"l1d"	
"032"	595270	6720800	072	36	"l1e"	
"032"	595270	6720800	073	45	"l1f"	
"033"	594440	6721430	313	83	"s1"	
"033"	594440	6721430	125	62	"l1"	
"034"	594310	6720710	310	51	"s1"	
"034"	594310	6720710	050	38	"l1"	
"034"	594310	6720710	012	42	"l1b"	
"035"	593420	6721520				
"036"	592800	6721140	290	66	"s1"	
"037"	592430	6720580				
"038"	592140	6719860				
"039"	592040	6719470	323	82	"s1"	
"039"	592040	6719470	325	04	"fa"	
"039"	592040	6719470	063	86	"l1"	
"039"	592040	6719470	086	74	"l1b"	
"040"	591830	6719300	252	52	"s1"	
"041"	593790	6718480	324	79	"s1"	

Station	Location (UTM)		Strike/ Trend	Dip/ Plunge	Structure	Domain
	Easting	Northing				
"042"	594230	6719500				
"043"	597380	6721270	338	31	"s1"	
"043"	597380	6721270	260	62	"s1b"	
"043"	597380	6721270	060	50	"fa"	
"043"	597380	6721270	080	45	"fab"	
"043"	597380	6721270	068	32	"l1"	
"044"	596550	6720830	310	46	"s1"	
"044"	596550	6720830	327	49	"s1b"	
"044"	596550	6720830	332	41	"s1c"	
"044"	596550	6720830	047	28	"l1"	
"044"	596550	6720830	054	52	"l1b"	
"044"	596550	6720830	058	38	"l1c"	
"044"	596550	6720830	070	42	"l1d"	
"045"	595880	6720560	320	39	"s1"	
"045"	595880	6720560	047	37	"l1"	
"046"	595790	6719640				
"047"	595250	6715560	313	75	"s1"	
"047"	595250	6715560	300	54	"s1b"	
"048"	595180	6716190				
"049"	598230	6726650	336	46	"s1"	
"050"	596850	6726240	331	64	"s1"	
"050"	596850	6726240	343	61	"s1b"	
"051"	596490	6726110	331	79	"s1"	
"052"	595960	6725480	312	82	"s1"	
"052"	595960	6725480	274	43	"s1b"	
"052"	595960	6725480	258	36	"s1c"	
"053"	594810	6725160	308	28	"s1"	
"053"	594810	6725160	045	22	"fa"	
"054"	596390	6725000	274	60	"s1"	
"055"	588270	6730130	297	07	"s1"	
"056"	590640	6730480	327	59	"s1"	
"056"	590640	6730480	298	57	"s1b"	
"056"	590640	6730480	049	63	"l1"	
"056"	590640	6730480	115	33	"l1b"	
"056"	590640	6730480	327	07	"l1c"	
"057"	590930	6730340	102	77	"s1"	
"057"	590930	6730340	095	12	"l1"	
"058"	589310	6730420	124	88	"s1"	
"058"	589310	6730420	120	83	"s1b"	
"058"	589310	6730420	154	34	"fa"	
"058"	589310	6730420	155	59	"fab"	
"058"	589310	6730420	124	49	"fac"	
"058"	589310	6730420	153	42	"fad"	
"059"	589390	6730890	090	68	"s1"	
"059"	589390	6730890	105	11	"fa"	

Station	Location (UTM) Easting	 Northing	Strike/ Trend	Dip/ Plunge	Structure	Domain
"059"	589390	6730890	088	02	"fab"	
"060"	589920	6731320	088	56	"s1"	
"060"	589920	6731320	084	60	"s1b"	
"061"	591490	6732430	298	45	"s1"	
"061"	591490	6732430	300	34	"fa"	
"061"	591490	6732430	302	49	"fab"	
"061"	591490	6732430	302	60	"fac"	
"061"	591490	6732430	258	33	"fad"	
"062"	591500	6731230	309	43	"s1"	
"062"	591500	6731230	090	70	"fa"	
"063"	593080	6730780	168	72	"s1"	
"063"	593080	6730780	177	41	"s1b"	
"064"	592760	6730000	310	80	"s1"	
"064"	592760	6730000	347	86	"s1b"	
"064"	592760	6730000	150	42	"l1"	
"065"	592530	6729350	317	62	"s1"	
"065"	592530	6729350	310	56	"s1b"	
"065"	592530	6729350	100	44	"fa"	
"065"	592530	6729350	097	37	"fab"	
"065"	592530	6729350	108	27	"fac"	
"065"	592530	6729350	108	12	"l1"	
"066"	595950	6729600				
"067"	601100	6730650	174	78	"s1"	
"068"	602590	6730430	302	60	"s1"	
"068"	602590	6730430	137	00	"l1"	
"069"	595430	6729340	332	76	"s1"	
"069"	595430	6729340	320	85	"s1b"	
"069"	595430	6729340	315	68	"s1c"	
"069"	595430	6729340	050	63	"l1"	
"069"	595430	6729340	096	75	"l1b"	
"070"	596390	6728720	316	70	"s1"	
"071"	595530	6728570	335	79	"s1"	
"071"	595530	6728570	322	82	"s1b"	
"071"	595530	6728570	079	74	"l1"	
"072"	594210	6728930	331	56	"s1"	
"072"	594210	6728930	316	58	"s1b"	
"073"	594330	6728800	293	57	"s1"	
"073"	594330	6728800	170	69	"s1b"	
"074"	593380	6729000	352	41	"s1"	
"074"	593380	6729000	162	20	"l1"	
"075"	592900	6729940	344	76	"s1"	
"075"	592900	6729940	156	15	"fa"	
"076"	591900	6729130	112	67	"s1"	
"076"	591900	6729130	108	77	"s1b"	
"076"	591900	6729130	088	51	"s1c"	

Station	Location (UTM)		Strike/	Dip/	Structure	Domain
	Easting	Northing	Trend	Plunge		
"076"	591900	6729130	127	19	"l1"	
"077"	591550	6729890	334	78	"s1"	
"077"	591550	6729890	290	77	"s1b"	
"077"	591550	6729890	355	42	"s1c"	
"077"	591550	6729890	355	77	"s1d"	
"077"	591550	6729890	125	62	"l1"	
"077"	591550	6729890	124	36	"fa"	
"077"	591550	6729890	104	42	"apc"	
"078"	591200	6730200	047	56	"s1"	
"078"	591200	6730200	047	53	"s1b"	
"078"	591200	6730200	047	74	"s1c"	
"078"	591200	6730200	044	76	"s1d"	
"078"	591200	6730200	054	58	"s1e"	
"078"	591200	6730200	026	44	"s1f"	
"078"	591200	6730200	090	50	"s1g"	
"078"	591200	6730200	327	74	"s1h"	
"079"	590720	6729800	293	80	"s1"	
"079"	590720	6729800	095	47	"fa"	
"079"	590720	6729800	297	21	"l1"	
"080"	590080	6729130	304	64	"s1"	
"080"	590080	6729130	302	47	"s1b"	
"080"	590080	6729130	308	60	"s1c"	
"080"	590080	6729130	332	38	"l1"	
"081"	589550	6728970	312	72	"s1"	
"081"	589550	6728970	297	69	"s1b"	
"081"	589550	6728970	047	72	"l1"	
"081"	589550	6728970	035	69	"l1b"	
"082"	592940	6728320	346	75	"s1"	
"082"	592940	6728320	125	45	"fa"	
"082"	592940	6728320	128	48	"fab"	
"082"	592940	6728320	118	46	"fac"	
"083"	593280	6727530	310	80	"s1"	
"083"	593280	6727530	138	75	"s1b"	
"083"	593280	6727530	124	13	"fa"	
"084"	594180	6727440	336	50	"s1"	
"084"	594180	6727440	340	54	"s1b"	
"084"	594180	6727440	143	26	"fa"	
"084"	594180	6727440	174	28	"fab"	
"084"	594180	6727440	084	58	"l1"	
"085"	593530	6725220	334	60	"s1"	
"085"	593530	6725220	308	59	"s1b"	
"085"	593530	6725220	074	44	"l1"	
"086"	592740	6725350	304	69	"s1"	
"086"	592740	6725350	350	50	"l1"	
"086"	592740	6725350	110	53	"l1b"	

Station	Location (UTM)		Strike/ Trend	Dip/ Plunge	Structure	Domain
	Easting	Northing				
"086"	592740	6725350	221	71	"l1c"	
"087"	591900	6726310	330	50	"s1"	
"088"	584990	6740030	328	49	"s1"	
"088"	584990	6740030	296	80	"s1b"	
"088"	584990	6740030	346	78	"s1c"	
"088"	584990	6740030	076	78	"l1"	
"089"	585320	6739150	336	70	"s1"	
"090"	585220	6738680	331	71	"s1"	
"090"	585220	6738680	071	78	"s1b"	
"090"	585220	6738680	072	71	"s1c"	
"090"	585220	6738680	078	74	"fa"	
"090"	585220	6738680	154	60	"l1"	
"090"	585220	6738680	110	66	"l1b"	
"090"	585220	6738680	198	81	"l1c"	
"091"	585640	6737830	312	68	"s1"	
"091"	585640	6737830	330	58	"s1b"	
"091"	585640	6737830	060	68	"l1"	
"092"	585720	6737250	287	85	"s1"	
"092"	585720	6737250	170	88	"l1"	
"093"	586200	6737390	125	83	"s1"	
"093"	586200	6737390	204	86	"l1"	
"094"	586650	6737570	127	74	"s1"	
"095"	584540	6740670	330	81	"s1"	
"095"	584540	6740670	322	90	"s1b"	
"095"	584540	6740670	323	78	"s1c"	
"095"	584540	6740670	323	73	"l1"	
"095"	584540	6740670	232	90	"l1b"	
"096"	583710	6741120	355	70	"s1"	
"097"	583230	6741540	350	74	"s1"	
"097"	583230	6741540	354	80	"s1b"	
"097"	583230	6741540	008	40	"s1c"	
"097"	583230	6741540	012	70	"l1"	
"098"	582520	6740930	132	74	"s1"	
"098"	582520	6740930	124	80	"s1b"	
"098"	582520	6740930	148	72	"s1c"	
"098"	582520	6740930	154	34	"fa"	
"098"	582520	6740930	210	59	"fab"	
"098"	582520	6740930	085	78	"fac"	
"098"	582520	6740930	226	74	"l1"	
"099"	581500	6740700	110	75	"s1"	
"099"	581500	6740700	136	71	"fa"	
"099"	581500	6740700	235	67	"fab"	
"099"	581500	6740700	095	82	"l1"	
"099"	581500	6740700	315	66	"apc"	
"100"	581060	6739930	136	90	"s1"	

Station	Location (UTM)		Strike/ Trend	Dip/ Plunge	Structure	Domain
	Easting	Northing				
"100"	581060	6739930	276	66	"l1"	
"101"	584250	6741590	304	88	"s1"	
"101"	584250	6741590	332	79	"s1b"	
"101"	584250	6741590	110	76	"s1c"	
"101"	584250	6741590	057	68	"fa"	
"102"	584410	6742420	324	81	"s1"	
"102"	584410	6742420	334	71	"s1b"	
"102"	584410	6742420	065	50	"s1c"	
"102"	584410	6742420	322	27	"fa"	
"103"	584610	6743390	328	48	"s1"	
"103"	584610	6743390	341	89	"s1b"	
"103"	584610	6743390	341	21	"l1"	
"104"	585180	6742500	353	70	"s1"	
"104"	585180	6742500	012	80	"s1b"	
"104"	585180	6742500	123	27	"fa"	
"104"	585180	6742500	108	74	"fab"	
"104"	585180	6742500	063	47	"apc"	
"105"	585730	6742750				
"106"	586260	6743480	185	42	"s1"	
"107"	587690	6743050	305	82	"s1"	
"108"	588440	6743250	352	70	"s1"	
"108"	588440	6743250	003	58	"s1b"	
"109"	589740	6742900	026	76	"s1"	
"110"	590720	6742990	020	57	"s1"	
"110"	590720	6742990	123	68	"l1"	
"111"	591710	6742930	093	27	"s1"	
"111"	591710	6742930	092	43	"s1b"	
"111"	591710	6742930	235	32	"l1"	
"111"	591710	6742930	092	05	"l1b"	
"112"	592060	6742850	021	70	"s1"	
"113"	588460	6742100				
"114"	587710	6740600				
"115"	587310	6736850	305	45	"s1"	
"115"	587310	6736850	308	85	"s1b"	
"115"	587310	6736850	304	61	"s1c"	
"115"	587310	6736850	324	84	"s1d"	
"115"	587310	6736850	133	42	"fa"	
"115"	587310	6736850	143	44	"fab"	
"115"	587310	6736850	105	05	"fac"	
"115"	587310	6736850	022	78	"l1"	
"115"	587310	6736850	062	82	"l1b"	
"115"	587310	6736850	214	83	"l1c"	
"116"	587120	6736000	302	56	"s1"	
"117"	587380	6734830	322	12	"s1"	
"117"	587380	6734830	345	22	"s1b"	

Station	Location (UTM)		Strike/	Dip/	Structure	Domain
	Easting	Northing	Trend	Plunge		
"117"	587380	6734830	050	00	"l1"	
"118"	588000	6734670	316	35	"s1"	
"118"	588000	6734670	286	78	"s1b"	
"118"	588000	6734670	096	29	"fa"	
"118"	588000	6734670	095	40	"l1"	
"119"	587810	6733980	304	65	"s1"	
"119"	587810	6733980	285	50	"s1b"	
"119"	587810	6733980	279	65	"s1c"	
"119"	587810	6733980	087	33	"fa"	
"119"	587810	6733980	093	27	"l1"	
"120"	588740	6733450	329	53	"s1"	
"120"	588740	6733450	340	77	"s1b"	
"120"	588740	6733450	312	77	"s1c"	
"120"	588740	6733450	294	65	"s1d"	
"120"	588740	6733450	150	26	"fa"	
"120"	588740	6733450	127	22	"fab"	
"120"	588740	6733450	127	22	"l1"	
"120"	588740	6733450	055	54	"l1b"	
"120"	588740	6733450	064	59	"apc"	
"121"	589100	6732800	295	58	"s1"	
"121"	589100	6732800	294	75	"s1b"	
"121"	589100	6732800	312	46	"s1c"	
"121"	589100	6732800	358	50	"s1d"	
"121"	589100	6732800	067	42	"fa"	
"121"	589100	6732800	095	32	"l1"	
"122"	589820	6734110	325	60	"s1"	
"122"	589820	6734110	337	52	"s1b"	
"122"	589820	6734110	054	35	"s1c"	
"122"	589820	6734110	098	44	"fa"	
"123"	590430	6734200	080	34	"s1"	
"124"	590960	6734470	320	62	"s1"	
"124"	590960	6734470	326	71	"s1b"	
"124"	590960	6734470	324	82	"s1c"	
"124"	590960	6734470	075	66	"l1"	
"124"	590960	6734470	056	82	"l1b"	
"125"	591490	6735070				
"126"	590660	6735130	326	64	"s1"	
"126"	590660	6735130	042	57	"l1"	
"127"	590250	6734730	323	63	"s1"	
"127"	590250	6734730	088	42	"fa"	
"128"	589800	6735230	318	45	"s1"	
"128"	589800	6735230	102	13	"fa"	
"129"	586960	6734090	287	54	"s1"	
"129"	586960	6734090	287	80	"s1b"	
"129"	586960	6734090	098	66	"s1c"	

Station	Location (UTM)		Strike/	Dip/	Structure	Domain
	Easting	Northing	Trend	Plunge		
"130"	586510	6733520	298	90	"s1"	
"130"	586510	6733520	288	79	"s1b"	
"130"	586510	6733520	110	70	"s1c"	
"131"	585840	6732490	287	78	"s1"	
"131"	585840	6732490	295	80	"s1b"	
"131"	585840	6732490	297	68	"s1c"	
"131"	585840	6732490	295	07	"fa"	
"131"	585840	6732490	092	33	"l1"	
"131"	585840	6732490	119	27	"l1b"	
"132"	584330	6738550	313	85	"s1"	
"132"	584330	6738550	320	76	"s1b"	
"132"	584330	6738550	336	69	"s1c"	
"132"	584330	6738550	334	72	"s1d"	
"132"	584330	6738550	108	55	"fa"	
"132"	584330	6738550	104	56	"fab"	
"132"	584330	6738550	054	85	"l1"	
"132"	584330	6738550	047	76	"l1b"	
"133"	583500	6738900	170	73	"s1"	
"133"	583500	6738900	252	73	"l1"	
"134"	582700	6738620	124	48	"s1"	
"134"	582700	6738620	138	88	"s1b"	
"134"	582700	6738620	108	86	"s1c"	
"134"	582700	6738620	195	46	"l1"	
"134"	582700	6738620	198	88	"l1b"	
"135"	582580	6737650	308	16	"s1"	
"135"	582580	6737650	108	17	"fa"	
"135"	582580	6737650	110	12	"fab"	
"135"	582580	6737650	129	10	"fac"	
"135"	582580	6737650	097	13	"fad"	
"136"	582180	6736770	132	25	"s1"	
"137"	567810	6762100				
"138"	567500	6761700	312	81	"s1"	
"138"	567500	6761700	308	82	"s1b"	
"138"	567500	6761700	330	73	"s1c"	
"138"	567500	6761700	123	10	"fa"	
"138"	567500	6761700	144	18	"l1"	
"138"	567500	6761700	125	05	"l1b"	
"139"	566720	6762100				
"140"	566050	6763130	314	63	"s1"	
"140"	566050	6763130	327	51	"s1b"	
"140"	566050	6763130	135	04	"fa"	
"140"	566050	6763130	322	04	"fab"	
"140"	566050	6763130	111	34	"l1"	
"140"	566050	6763130	092	42	"l1b"	
"141"	565780	6762400	300	17	"s1"	

Station	Location (UTM)		Strike/ Trend	Dip/ Plunge	Structure	Domain
	Easting	Northing				
"141"	565780	6762400	312	21	"s1b"	
"141"	565780	6762400	297	20	"s1c"	
"141"	565780	6762400	102	02	"l1"	
"142"	565460	6757280				
"143"	565860	6757800	008	90	"s1"	
"144"	566050	6758260	304	74	"s1"	C5
"144"	566050	6758260	305	83	"s1b"	C5
"144"	566050	6758260	298	90	"s1c"	C5
"144"	566050	6758260	270	79	"s1d"	C5
"144"	566050	6758260	265	53	"l1"	C5
"145"	566140	6758450	290	82	"s1"	C5
"145"	566140	6758450	284	75	"s1b"	C5
"145"	566140	6758450	113	71	"l1"	C5
"146"	566180	6758970	292	81	"s1"	C5
"146"	566180	6758970	280	84	"s1b"	C5
"146"	566180	6758970	273	81	"s1c"	C5
"146"	566180	6758970	270	84	"s1d"	C5
"146"	566180	6758970	097	49	"l1"	C5
"146"	566180	6758970	065	68	"l1b"	C5
"146"	566180	6758970	076	70	"l1c"	C5
"146"	566180	6758970	136	67	"l1d"	C5
"147"	566320	6759470	282	65	"s1"	C5
"148"	566200	6760300	288	78	"s1"	C5
"148"	566200	6760300	282	84	"s1b"	C5
"148"	566200	6760300	085	30	"l1"	C5
"149"	566190	6760880	310	79	"s1"	C5
"149"	566190	6760880	310	60	"s1b"	C5
"150"	571690	6762100	110	44	"s1"	
"150"	571690	6762100	095	31	"s1b"	
"151"	572090	6761130	300	82	"s1"	
"151"	572090	6761130	305	90	"s1b"	
"152"	572100	6760460	310	81	"s1"	
"152"	572100	6760460	300	78	"s1b"	
"152"	572100	6760460	164	62	"s1c"	
"152"	572100	6760460	125	12	"l1"	
"152"	572100	6760460	334	45	"l1b"	
"153"	572000	6759480	320	39	"s1"	
"153"	572000	6759480	290	63	"s1b"	
"153"	572000	6759480	077	28	"fa"	
"153"	572000	6759480	108	04	"l1"	
"153"	572000	6759480	102	06	"l1b"	
"154"	571950	6758640	268	29	"s1"	
"154"	571950	6758640	265	44	"s1b"	
"154"	571950	6758640	254	18	"s1c"	
"154"	571950	6758640	250	90	"s1d"	

Station	Location (UTM)		Strike/ Trend	Dip/ Plunge	Structure	Domain
	Easting	Northing				
"154"	571950	6758640	292	16	"fa"	
"154"	571950	6758640	286	03	"fab"	
"155"	572850	6758480	311	84	"s1"	
"155"	572850	6758480	105	88	"s1b"	
"155"	572850	6758480	122	13	"fa"	
"156"	572970	6757530	292	55	"s1"	
"156"	572970	6757530	312	72	"s1b"	
"157"	566900	6757880				
"158"	567490	6758100	275	74	"s1"	
"158"	567490	6758100	287	82	"s1b"	
"158"	567490	6758100	270	60	"s1c"	
"158"	567490	6758100	062	54	"l1"	
"158"	567490	6758100	055	50	"l1b"	
"159"	568090	6758630	272	52	"s1"	
"160"	572960	6750310	137	71	"s1"	
"160"	572960	6750310	150	57	"s1b"	
"160"	572960	6750310	295	26	"l1"	
"160"	572960	6750310	252	40	"l1b"	
"161"	574010	6751580	325	85	"s1"	
"162"	573570	6752130				
"163"	573690	6752800	320	55	"s1"	
"163"	573690	6752800	302	71	"s1b"	
"164"	572790	6752450				
"165"	571170	6751870	147	62	"s1"	
"165"	571170	6751870	152	60	"s1b"	
"165"	571170	6751870	146	70	"s1c"	
"165"	571170	6751870	292	60	"l1"	
"166"	572270	6752970				
"167"	571590	6753440				
"168"	571070	6753880	308	88	"s1"	
"168"	571070	6753880	264	67	"s1b"	
"168"	571070	6753880	270	18	"l1"	
"169"	572270	6754270	113	83	"s1"	
"169"	572270	6754270	262	60	"l1"	
"170"	572830	6755380				
"171"	571740	6755970	318	40	"s1"	
"171"	571740	6755970	306	45	"s1b"	
"171"	571740	6755970	074	59	"s1c"	
"171"	571740	6755970	104	33	"l1"	
"172"	573800	6754900	275	81	"s1"	
"173"	573180	6755880	304	88	"s1"	
"174"	573370	6756080	301	61	"s1"	
"174"	573370	6756080	297	56	"s1b"	
"174"	573370	6756080	305	60	"s1c"	
"174"	573370	6756080	078	43	"l1"	

Station	Location (UTM) Easting	 Northing	Strike/ Trend	Dip/ Plunge	Structure	Domain
"174"	573370	6756080	097	32	"l1b"	
"174"	573370	6756080	110	34	"l1c"	
"175"	573380	6756780	136	73	"s1"	
"176"	574270	6756520	318	75	"s1"	
"176"	574270	6756520	123	24	"l1"	
"177"	575010	6756080	277	29	"s1"	
"177"	575010	6756080	064	07	"l1"	
"178"	575830	6754050	280	85	"s1"	
"178"	575830	6754050	122	32	"l1"	
"179"	578030	6753200				
"180"	577520	6752830	280	65	"s1"	
"181"	577080	6752560				
"182"	578890	6752170	322	61	"s1"	
"182"	578890	6752170	310	64	"s1b"	
"182"	578890	6752170	334	50	"s1c"	
"183"	579130	6750590	110	63	"s1"	
"183"	579130	6750590	098	43	"s1b"	
"183"	579130	6750590	104	20	"l1"	
"184"	579150	6750340	097	60	"s1"	
"184"	579150	6750340	125	32	"fa"	
"185"	579800	6746930	160	87	"s1"	
"185"	579800	6746930	160	87	"s1b"	
"185"	579800	6746930	155	84	"s1c"	
"185"	579800	6746930	180	85	"s1d"	
"185"	579800	6746930	013	67	"s1e"	
"185"	579800	6746930	041	12	"s1f"	
"185"	579800	6746930	170	36	"fa"	
"185"	579800	6746930	180	40	"fab"	
"185"	579800	6746930	168	54	"l1"	
"186"	579870	6747560	145	39	"s1"	
"186"	579870	6747560	155	39	"s1b"	
"186"	579870	6747560	118	39	"s1c"	
"186"	579870	6747560	165	13	"fa"	
"186"	579870	6747560	246	31	"l1"	
"186"	579870	6747560	340	50	"apc"	
"187"	579660	6748000	295	57	"s1"	
"187"	579660	6748000	301	87	"s1b"	
"187"	579660	6748000	308	60	"s1c"	
"187"	579660	6748000	114	05	"fa"	
"187"	579660	6748000	142	47	"fab"	
"187"	579660	6748000	050	56	"fac"	
"188"	579230	6749070	114	57	"s1"	
"188"	579230	6749070	125	40	"s1b"	
"188"	579230	6749070	095	58	"s1c"	
"188"	579230	6749070	224	57	"l1"	

Station	Location (UTM)		Strike/ Trend	Dip/ Plunge	Structure	Domain
	Easting	Northing				
"188"	579230	6749070	200	45	"l1b"	
"188"	579230	6749070	225	43	"l1c"	
"189"	579540	6749630	112	63	"s1"	
"190"	578700	6749210	095	75	"s1"	
"190"	578700	6749210	070	81	"s1b"	
"190"	578700	6749210	241	44	"l1"	
"191"	577910	6748850	080	62	"s1"	
"191"	577910	6748850	110	47	"fa"	
"191"	577910	6748850	225	41	"l1"	
"192"	577030	6749070	190	75	"s1"	
"192"	577030	6749070	204	37	"l1"	
"192"	577030	6749070	212	22	"l1b"	
"193"	580200	6747860	150	60	"s1"	
"193"	580200	6747860	035	83	"s1b"	
"193"	580200	6747860	152	44	"fa"	
"193"	580200	6747860	231	36	"l1"	
"194"	580550	6748280	133	56	"s1"	
"194"	580550	6748280	121	57	"s1b"	
"194"	580550	6748280	117	27	"s1c"	
"194"	580550	6748280	132	33	"s1d"	
"194"	580550	6748280	153	17	"fa"	
"194"	580550	6748280	164	34	"l1"	
"195"	581180	6748800	111	47	"s1"	
"195"	581180	6748800	190	47	"l1"	
"196"	582180	6749000	164	47	"s1"	
"197"	584010	6748690	123	57	"s1"	
"198"	579320	6747300	125	60	"s1"	
"198"	579320	6747300	195	57	"fa"	
"198"	579320	6747300	190	59	"fab"	
"198"	579320	6747300	205	59	"fac"	
"198"	579320	6747300	187	51	"fad"	
"199"	578500	6747460	135	37	"s1"	
"199"	578500	6747460	132	33	"s1b"	
"199"	578500	6747460	153	65	"s1c"	
"199"	578500	6747460	150	03	"fa"	
"199"	578500	6747460	155	22	"l1"	
"199"	578500	6747460	180	22	"l1b"	
"200"	577760	6746820	155	57	"s1"	
"200"	577760	6746820	159	63	"s1b"	
"200"	577760	6746820	175	61	"s1c"	
"200"	577760	6746820	175	14	"fa"	
"200"	577760	6746820	164	06	"fab"	
"200"	577760	6746820	167	14	"l1"	
"201"	576390	6747000	140	24	"s1"	
"201"	576390	6747000	150	58	"s1b"	

Station	Location (UTM)		Strike/ Trend	Dip/ Plunge	Structure	Domain
	Easting	Northing				
"201"	576390	6747000	344	10	"l1"	
"201"	576390	6747000	344	07	"l1b"	
"201"	576390	6747000	330	20	"l1c"	
"202"	577020	6746750	142	47	"s1"	
"202"	577020	6746750	102	34	"s1b"	
"202"	577020	6746750	186	35	"l1"	
"203"	577080	6745870	135	60	"s1"	
"203"	577080	6745870	162	10	"l1"	
"204"	576920	6744890	109	61	"s1"	
"204"	576920	6744890	105	71	"s1b"	
"204"	576920	6744890	233	44	"fa"	
"205"	580190	6746470	157	51	"s1"	
"205"	580190	6746470	205	84	"s1b"	
"205"	580190	6746470	207	46	"fa"	
"205"	580190	6746470	207	49	"fab"	
"205"	580190	6746470	196	35	"fac"	
"205"	580190	6746470	247	51	"l1"	
"206"	580730	6745880	352	56	"s1"	
"206"	580730	6745880	003	65	"s1b"	
"206"	580730	6745880	052	47	"s1c"	
"206"	580730	6745880	017	49	"s1d"	
"206"	580730	6745880	154	31	"fa"	
"206"	580730	6745880	112	30	"fab"	
"206"	580730	6745880	165	40	"l1"	
"206"	580730	6745880	164	18	"l1b"	
"207"	581380	6746300	172	77	"s1"	
"207"	581380	6746300	038	58	"s1b"	
"207"	581380	6746300	172	47	"l1"	
"208"	580930	6745060	167	75	"s1"	
"208"	580930	6745060	327	88	"s1b"	
"208"	580930	6745060	142	40	"fa"	
"208"	580930	6745060	135	17	"fab"	
"209"	581760	6744170	155	74	"s1"	
"209"	581760	6744170	304	33	"s1b"	
"209"	581760	6744170	030	40	"s1c"	
"209"	581760	6744170	032	37	"s1d"	
"209"	581760	6744170	084	27	"fa"	
"209"	581760	6744170	054	48	"fab"	
"210"	580300	6744420	342	72	"s1"	
"210"	580300	6744420	165	18	"fa"	
"211"	579920	6743530				
"212"	579490	6743130	145	52	"s1"	
"213"	581950	6738100	265	81	"s1"	
"213"	581950	6738100	005	33	"s1b"	
"213"	581950	6738100	143	42	"fa"	

Station	Location (UTM)		Strike/ Trend	Dip/ Plunge	Structure	Domain
	Easting	Northing				
"214"	580410	6737580	083	19	"s1"	
"215"	580600	6736000	095	51	"s1"	
"215"	580600	6736000	115	18	"l1"	
"216"	581350	6736100	130	59	"s1"	
"217"	585050	6736850	305	47	"s1"	
"218"	586640	6736600	281	59	"s1"	
"218"	586640	6736600	170	27	"fa"	
"219"	582350	6731040	358	73	"s1"	
"220"	583410	6731100	295	57	"s1"	
"220"	583410	6731100	322	53	"l1"	
"221"	583820	6731560	352	80	"s1"	
"221"	583820	6731560	035	37	"fa"	
"221"	583820	6731560	005	62	"l1"	
"222"	584100	6732720	130	50	"s1"	
"222"	584100	6732720	141	52	"fa"	
"222"	584100	6732720	265	35	"l1"	
"222"	584100	6732720	326	73	"apc"	
"223"	584740	6733200	125	72	"s1"	
"224"	585740	6733700	130	50	"s1"	
"225"	587780	6733600	010	37	"s1"	
"225"	587780	6733600	105	32	"fa"	
"226"	589450	6732040	328	33	"s1"	
"226"	589450	6732040	100	19	"fa"	
"226"	589450	6732040	097	61	"apc"	
"227"	588690	6731400	053	32	"s1"	
"227"	588690	6731400	104	21	"fa"	
"227"	588690	6731400	094	75	"apc"	
"228"	588120	6729760	283	56	"s1"	
"228"	588120	6729760	321	78	"fa"	
"229"	585140	6727780	325	74	"s1"	A1
"230"	585320	6727920	320	80	"s1"	A1
"230"	585320	6727920	343	51	"s1b"	A1
"230"	585320	6727920	137	30	"fa"	
"231"	585460	6727960	338	46	"s1"	A1
"231"	585460	6727960	340	60	"s1b"	A1
"231"	585460	6727960	345	62	"s1c"	A1
"231"	585460	6727960	329	65	"s1d"	A1
"231"	585460	6727960	010	54	"l1"	A1
"231"	585460	6727960	010	40	"l1b"	A1
"231"	585460	6727960	005	54	"l1c"	A1
"232"	585620	6728020	322	75	"s1"	A1
"232"	585620	6728020	350	63	"l1"	A1
"233"	585740	6728100	335	75	"s1"	A1
"233"	585740	6728100	164	74	"s1b"	A1
"234"	586620	6728030	285	56	"s1"	A1

Station	Location (UTM) Easting	Northing	Strike/ Trend	Dip/ Plunge	Structure	Domain
"234"	586620	6728030	033	56	"l1"	A1
"235"	586760	6728160	297	87	"s1"	A1
"235"	586760	6728160	285	62	"s1b"	A1
"235"	586760	6728160	111	65	"l1"	A1
"236"	586910	6727950	281	60	"s1"	A1
"236"	586910	6727950	305	86	"s1b"	A1
"237"	587040	6727830	305	73	"s1"	A1
"237"	587040	6727830	025	73	"l1"	A1
"238"	587190	6727780	298	71	"s1"	A1
"238"	587190	6727780	337	61	"l1"	A1
"239"	587440	6727570	307	69	"s1"	A1
"239"	587440	6727570	105	64	"fa"	
"239"	587440	6727570	098	60	"fab"	
"239"	587440	6727570	034	69	"l1"	A1
"240"	587520	6727780	300	75	"s1"	A1
"240"	587520	6727780	040	74	"l1"	A1
"241"	587690	6727890	315	75	"s1"	A1
"241"	587690	6727890	359	69	"l1"	A1
"242"	587800	6728100	329	79	"s1"	A1
"242"	587800	6728100	280	90	"s1b"	A1
"242"	587800	6728100	100	75	"l1"	A1
"242"	587800	6728100	345	62	"l1b"	A1
"243"	588050	6728120	307	79	"s1"	A1
"243"	588050	6728120	292	76	"s1b"	A1
"243"	588050	6728120	334	86	"s1c"	A1
"243"	588050	6728120	342	71	"l1"	A1
"243"	588050	6728120	022	76	"l1b"	A1
"243"	588050	6728120	339	50	"l1c"	A1
"244"	588160	6728220	292	65	"s1"	A1
"244"	588160	6728220	317	72	"s1b"	A1
"244"	588160	6728220	332	54	"l1"	A1
"244"	588160	6728220	345	55	"l1b"	A1
"245"	588390	6728320	292	75	"s1"	A1
"245"	588390	6728320	290	88	"s1b"	A1
"245"	588390	6728320	310	59	"fa"	
"245"	588390	6728320	318	59	"l1"	A1
"246"	588610	6728510	305	76	"s1"	A1
"246"	588610	6728510	322	36	"fa"	
"246"	588610	6728510	300	30	"fab"	
"246"	588610	6728510	300	30	"fac"	
"246"	588610	6728510	324	58	"l1"	A1
"247"	587310	6726460	320	64	"s1"	A1
"248"	587360	6726880	327	77	"s1"	A1
"248"	587360	6726880	335	85	"s1b"	A1
"248"	587360	6726880	087	85	"l1"	A1

Station	Location (UTM)		Strike/ Trend	Dip/ Plunge	Structure	Domain
	Easting	Northing				
"249"	587430	6727190	312	73	"s1"	A1
"249"	587430	6727190	045	73	"l1"	A1
"250"	588830	6728570	298	64	"s1"	A1
"250"	588830	6728570	325	43	"l1"	A1
"251"	589040	6728690	297	67	"s1"	A1
"251"	589040	6728690	128	27	"fa"	
"251"	589040	6728690	344	60	"l1"	A1
"252"	589530	6728450	300	66	"s1"	A1
"253"	589500	6728640	294	42	"s1"	A1
"253"	589500	6728640	290	43	"s1b"	A1
"253"	589500	6728640	302	33	"s1c"	A1
"253"	589500	6728640	036	41	"l1"	A1
"253"	589500	6728640	002	42	"l1b"	A1
"253"	589500	6728640	028	33	"l1c"	A1
"254"	589600	6728740	310	50	"s1"	A1
"254"	589600	6728740	335	71	"s1b"	A1
"254"	589600	6728740	018	46	"l1"	A1
"254"	589600	6728740	037	69	"l1b"	A1
"255"	589750	6728930	310	71	"s1"	A1
"255"	589750	6728930	309	70	"s1b"	A1
"255"	589750	6728930	025	70	"l1"	A1
"255"	589750	6728930	012	68	"l1b"	A1
"256"	589910	6729000	297	86	"s1"	A1
"256"	589910	6729000	010	46	"fa"	
"256"	589910	6729000	120	45	"fab"	
"256"	589910	6729000	335	51	"l1"	A1
"257"	590140	6729190	296	56	"s1"	A1
"257"	590140	6729190	095	29	"fa"	
"257"	590140	6729190	326	37	"l1"	A1
"258"	590270	6729350	300	79	"s1"	A2
"258"	590270	6729350	097	85	"s1b"	A2
"258"	590270	6729350	283	75	"fa"	
"258"	590270	6729350	098	63	"l1"	A2
"258"	590270	6729350	274	32	"l1b"	A2
"259"	590310	6729540	105	82	"s1"	A2
"259"	590310	6729540	105	83	"s1b"	A2
"259"	590310	6729540	108	22	"l1"	A2
"259"	590310	6729540	112	45	"l1b"	A2
"260"	590500	6729640	310	56	"s1"	A2
"260"	590500	6729640	305	90	"s1b"	A2
"260"	590500	6729640	303	73	"s1c"	A2
"260"	590500	6729640	303	73	"s1d"	
"260"	590500	6729640	303	73	"s1e"	
"260"	590500	6729640	339	31	"l1"	A2
"260"	590500	6729640	125	13	"l1b"	A2

Station	Location (UTM)		Strike/ Trend	Dip/ Plunge	Structure	Domain
	Easting	Northing				
"260"	590500	6729640	118	15	"l1c"	A2
"260"	590500	6729640	118	15	"l1d"	
"261"	590690	6729720	297	78	"s1"	A2
"261"	590690	6729720	090	37	"fa"	
"261"	590690	6729720	309	44	"l1"	A2
"261"	590690	6729720	095	47	"apc"	
"262"	578920	6739780	177	20	"s1"	
"262"	578920	6739780	158	28	"fa"	
"262"	578920	6739780	280	20	"l1"	
"262"	578920	6739780	150	75	"apc"	
"263"	579820	6740440	311	84	"s1"	
"263"	579820	6740440	323	85	"s1b"	
"263"	579820	6740440	150	42	"fa"	
"263"	579820	6740440	325	66	"l1"	
"263"	579820	6740440	332	61	"l1b"	
"263"	579820	6740440	099	52	"apc"	
"264"	580420	6740820	146	80	"s1"	
"264"	580420	6740820	127	82	"s1b"	
"264"	580420	6740820	191	73	"l1"	
"264"	580420	6740820	195	81	"l1b"	
"265"	581200	6741050	157	70	"s1"	
"265"	581200	6741050	142	73	"s1b"	
"265"	581200	6741050	256	70	"l1"	
"265"	581200	6741050	268	69	"l1b"	
"266"	581850	6740820				
"267"	582320	6741030	350	90	"s1"	
"267"	582320	6741030	350	52	"l1"	
"268"	584620	6742030	329	87	"s1"	
"268"	584620	6742030	105	65	"fa"	
"268"	584620	6742030	095	75	"fab"	
"268"	584620	6742030	080	80	"apc"	
"269"	585150	6742520	154	68	"s1"	
"270"	585650	6742650	348	75	"s1"	
"270"	585650	6742650	097	74	"l1"	
"271"	585120	6743760	137	43	"s1"	
"271"	585120	6743760	125	60	"fa"	
"271"	585120	6743760	243	43	"l1"	
"272"	585950	6744750				
"273"	585130	6744050	308	53	"s1"	
"273"	585130	6744050	338	42	"s1b"	
"274"	583620	6743110	268	65	"s1"	
"274"	583620	6743110	297	15	"fa"	
"274"	583620	6743110	265	14	"fab"	
"275"	582510	6742290	040	90	"s1"	
"276"	583450	6741300	330	72	"s1"	

Station	Location (UTM) Easting	Northing	Strike/ Trend	Dip/ Plunge	Structure	Domain
"276"	583450	6741300	015	50	"s1b"	
"277"	589530	6721440	296	65	"s1"	
"278"	589520	6721740	320	70	"s1"	
"278"	589520	6721740	035	58	"l1"	
"279"	589520	6722360				
"280"	589650	6723450				
"281"	590550	6723800	320	65	"s1"	
"281"	590550	6723800	021	62	"l1"	
"282"	591290	6723620	294	77	"s1"	
"283"	593130	6723730	323	73	"s1"	
"283"	593130	6723730	349	55	"l1"	
"284"	592270	6724300	277	85	"s1"	
"284"	592270	6724300	295	74	"l1"	
"285"	590650	6726590	295	70	"s1"	
"285"	590650	6726590	295	70	"s1b"	
"285"	590650	6726590	351	68	"l1"	
"285"	590650	6726590	102	31	"l1b"	
"286"	591490	6727490	321	66	"s1"	
"286"	591490	6727490	009	59	"l1"	
"287"	592410	6726980	305	74	"s1"	
"287"	592410	6726980	290	62	"s1b"	
"287"	592410	6726980	344	65	"l1"	
"287"	592410	6726980	354	59	"l1b"	
"288"	592980	6727190	340	79	"s1"	
"289"	591900	6729140	077	46	"s1"	A2
"289"	591900	6729140	100	22	"l1"	A2
"290"	591900	6729330	310	66	"s1"	A2
"290"	591900	6729330	115	11	"fa"	A2
"290"	591900	6729330	117	09	"fab"	A2
"290"	591900	6729330	105	64	"apc"	
"291"	592100	6729260	307	57	"s1"	A2
"291"	592100	6729260	110	21	"fa"	A2
"292"	592290	6729260	320	73	"s1"	A2
"292"	592290	6729260	133	21	"l1"	A2
"293"	592490	6729320	303	61	"s1"	A2
"293"	592490	6729320	125	25	"fa"	A2
"293"	592490	6729320	107	26	"l1"	A2
"294"	592610	6729210	287	85	"s1"	A2
"294"	592610	6729210	104	28	"l1"	A2
"295"	592790	6729090	310	56	"s1"	A2
"295"	592790	6729090	335	54	"s1b"	A2
"295"	592790	6729090	108	28	"l1"	A2
"295"	592790	6729090	142	18	"l1b"	A2
"296"	590860	6729900	310	67	"s1"	A2
"296"	590860	6729900	310	67	"s1b"	

Station	Location (UTM)		Strike/ Trend	Dip/ Plunge	Structure	Domain
	Easting	Northing				
"296"	590860	6729900	299	51	"s1c"	A2
"296"	590860	6729900	105	40	"fa"	A2
"296"	590860	6729900	115	32	"l1"	A2
"296"	590860	6729900	129	02	"l1b"	A2
"296"	590860	6729900	109	18	"l1c"	A2
"297"	591050	6730150	105	74	"s1"	A2
"297"	591050	6730150	109	14	"l1"	A2
"298"	591270	6730220	082	45	"s1"	A2
"299"	591490	6730170	115	37	"fa"	A2
"300"	591550	6729940	115	37	"fa"	
"301"	591730	6729760	132	85	"s1"	A2
"301"	591730	6729760	302	78	"s1b"	A2
"301"	591730	6729760	105	56	"fa"	A2
"301"	591730	6729760	133	16	"l1"	A2
"302"	591810	6729540	301	90	"s1"	A2
"302"	591810	6729540	125	43	"fa"	A2
"302"	591810	6729540	121	34	"l1"	A2
"303"	592920	6728940	342	59	"s1"	A2
"303"	592920	6728940	142	29	"l1"	A2
"304"	593180	6728960	335	60	"s1"	A2
"304"	593180	6728960	332	75	"s1b"	A2
"304"	593180	6728960	111	51	"l1"	A2
"304"	593180	6728960	118	64	"l1b"	A2
"305"	593390	6729000	030	20	"s1"	A2
"306"	593620	6728960	006	90	"s1"	A3
"306"	593620	6728960	141	90	"l1"	A3
"307"	593800	6728880	006	53	"s1"	A3
"307"	593800	6728880	167	24	"l1"	A3
"308"	594000	6728800	347	84	"s1"	A3
"309"	594250	6728800	155	54	"s1"	A3
"309"	594250	6728800	137	68	"s1b"	A3
"309"	594250	6728800	135	61	"s1c"	A3
"309"	594250	6728800	309	31	"l1"	A3
"309"	594250	6728800	165	49	"l1b"	A3
"309"	594250	6728800	159	37	"l1c"	A3
"310"	599500	6713900				
"311"	598050	6716200	335	54	"s1"	
"312"	598150	6718100	335	47	"s1"	
"312"	598150	6718100	339	04	"l1"	
"313"	597640	6715060				
"314"	597150	6713960				
"315"	596430	6713330				
"316"	603400	6729650	318	37	"s1"	A4
"316"	603400	6729650	309	53	"s1b"	A4
"316"	603400	6729650	099	25	"l1"	A4

Station	Location (UTM)		Strike/ Trend	Dip/ Plunge	Structure	Domain
	Easting	Northing				
"317"	603580	6729610	293	73	"s1"	A4
"317"	603580	6729610	310	72	"s1b"	A4
"318"	603800	6729550	290	49	"s1"	A4
"319"	603980	6729360	288	54	"s1"	A4
"319"	603980	6729360	290	47	"s1b"	A4
"319"	603980	6729360	093	20	"l1"	A4
"319"	603980	6729360	100	11	"l1b"	A4
"320"	604140	6729280	297	30	"s1"	A4
"320"	604140	6729280	297	47	"s1b"	A4
"320"	604140	6729280	076	21	"l1"	A4
"321"	600560	6730610				
"322"	600700	6730590				
"323"	600900	6730680	330	83	"s1"	A4
"324"	601140	6730700	345	75	"s1"	A4
"324"	601140	6730700	003	69	"s1b"	A4
"324"	601140	6730700	325	52	"fa"	
"324"	601140	6730700	044	73	"l1"	A4
"324"	601140	6730700	054	64	"l1b"	A4
"325"	601470	6730700	322	50	"s1"	A4
"325"	601470	6730700	330	57	"s1b"	A4
"325"	601470	6730700	109	33	"l1"	A4
"325"	601470	6730700	147	04	"l1b"	A4
"326"	601650	6730540	335	70	"s1"	A4
"326"	601650	6730540	340	52	"s1b"	A4
"326"	601650	6730540	152	09	"l1"	A4
"326"	601650	6730540	156	06	"l1b"	A4
"327"	601880	6730430	317	56	"s1"	A4
"327"	601880	6730430	087	49	"l1"	A4
"328"	602130	6730370	322	27	"s1"	A4
"328"	602130	6730370	311	34	"s1b"	A4
"328"	602130	6730370	123	09	"l1"	A4
"328"	602130	6730370	124	04	"l1b"	A4
"329"	602310	6730420	295	51	"s1"	A4
"329"	602310	6730420	309	47	"s1b"	A4
"329"	602310	6730420	312	59	"s1c"	A4
"329"	602310	6730420	112	04	"l1"	A4
"329"	602310	6730420	129	00	"l1b"	A4
"330"	602650	6730460	319	65	"s1"	A4
"330"	602650	6730460	330	73	"s1b"	A4
"330"	602650	6730460	124	29	"l1"	A4
"330"	602650	6730460	146	11	"l1b"	A4
"331"	602870	6730370	312	44	"s1"	A4
"331"	602870	6730370	097	29	"l1"	A4
"332"	602950	6731030	302	60	"s1"	A4
"332"	602950	6731030	295	46	"s1b"	A4

Station	Location (UTM)		Strike/	Dip/	Structure	Domain
	Easting	Northing	Trend	Plunge		
"332"	602950	6731030	116	06	"l1"	A4
"333"	603170	6729780	297	60	"s1"	A4
"333"	603170	6729780	109	14	"l1"	A4
"334"	594490	6728880	172	57	"s1"	A3
"335"	594700	6728900	303	55	"s1"	A3
"335"	594700	6728900	290	56	"s1b"	A3
"335"	594700	6728900	325	62	"s1c"	A3
"335"	594700	6728900	339	40	"l1"	A3
"335"	594700	6728900	338	48	"l1b"	A3
"335"	594700	6728900	349	37	"l1c"	A3
"336"	594960	6728930	157	75	"s1"	A3
"336"	594960	6728930	312	60	"s1b"	A3
"336"	594960	6728930	324	40	"l1"	A3
"337"	595150	6728950	302	63	"s1"	A3
"338"	595420	6728840	325	61	"s1"	A3
"338"	595420	6728840	360	46	"l1"	A3
"339"	595580	6728750	337	59	"s1"	A3
"339"	595580	6728750	325	80	"s1b"	A3
"339"	595580	6728750	007	40	"l1"	A3
"340"	595820	6728600	329	67	"s1"	A3
"340"	595820	6728600	137	51	"s1b"	A3
"340"	595820	6728600	042	66	"l1"	A3
"341"	596060	6728580	318	62	"s1"	A3
"342"	596190	6728610	315	67	"s1"	A3
"342"	596190	6728610	078	63	"l1"	A3
"343"	597710	6726510	327	83	"s1"	
"343"	597710	6726510	333	80	"s1b"	
"343"	597710	6726510	334	45	"l1"	
"344"	598750	6726780	313	65	"s1"	
"344"	598750	6726780	323	58	"s1b"	
"344"	598750	6726780	007	60	"l1"	
"345"	599600	6726700	298	56	"s1"	
"346"	600000	6726800	317	45	"s1"	
"346"	600000	6726800	303	43	"s1b"	
"346"	600000	6726800	053	45	"l1"	
"346"	600000	6726800	051	42	"l1b"	
"347"	600160	6727320	321	60	"s1"	
"347"	600160	6727320	095	51	"l1"	
"348"	604460	6729200	294	50	"s1"	A4
"349"	604650	6729050	302	42	"s1"	A4
"350"	605150	6729200	306	40	"s1"	A4
"351"	605520	6729050	315	46	"s1"	A4
"352"	605760	6728900	296	47	"s1"	A4
"352"	605760	6728900	095	21	"l1"	A4
"353"	605950	6728740	303	39	"s1"	A4

Station	Location (UTM) Easting	Northing	Strike/ Trend	Dip/ Plunge	Structure	Domain
"353"	605950	6728740	296	37	"s1b"	A4
"353"	605950	6728740	080	29	"l1"	A4
"354"	606160	6728660	296	43	"s1"	A4
"354"	606160	6728660	085	25	"l1"	A4
"355"	606500	6728800	291	53	"s1"	A4
"356"	607040	6730070	301	52	"s1"	A4
"356"	607040	6730070	108	16	"l1"	A4
"357"	575420	6747460	174	31	"s1"	
"357"	575420	6747460	357	25	"fa"	
"357"	575420	6747460	298	26	"l1"	B1
"358"	575610	6747410	303	24	"s1"	B1
"358"	575610	6747410	149	53	"s1b"	B1
"358"	575610	6747410	049	23	"l1"	B1
"359"	575810	6747370	137	22	"s1"	B1
"359"	575810	6747370	119	41	"s1b"	B1
"359"	575810	6747370	165	11	"l1"	B1
"359"	575810	6747370	143	19	"l1b"	B1
"360"	575950	6747350	141	52	"s1"	B1
"360"	575950	6747350	140	25	"fa"	
"360"	575950	6747350	186	48	"l1"	B1
"361"	576150	6747320	131	37	"s1"	B1
"361"	576150	6747320	153	40	"s1b"	B1
"361"	576150	6747320	158	16	"fa"	
"361"	576150	6747320	141	08	"fab"	
"361"	576150	6747320	179	20	"l1"	B1
"362"	576300	6747560	125	41	"s1"	B1
"362"	576300	6747560	101	26	"s1b"	B1
"362"	576300	6747560	113	34	"s1c"	B1
"362"	576300	6747560	113	34	"s1d"	B1
"362"	576300	6747560	161	23	"l1"	B1
"362"	576300	6747560	179	32	"l1b"	B1
"363"	576380	6747370	093	28	"s1"	B1
"363"	576380	6747370	241	19	"fa"	
"363"	576380	6747370	168	27	"l1"	B1
"364"	576400	6747200				
"365"						
"366"	576450	6747010	135	49	"s1"	B1
"366"	576450	6747010	132	64	"s1b"	B1
"366"	576450	6747010	311	05	"fa"	
"366"	576450	6747010	154	37	"l1"	B1
"367"	576660	6747000	153	42	"s1"	B1
"367"	576660	6747000	172	16	"fa"	
"368"	576790	6746880	156	47	"s1"	B1
"368"	576790	6746880	155	20	"s1b"	B1
"368"	576790	6746880	334	02	"fa"	

Station	Location (UTM)		Strike/ Trend	Dip/ Plunge	Structure	Domain
	Easting	Northing				
"368"	576790	6746880	321	05	"fab"	
"369"	576990	6746780	133	27	"s1"	B1
"369"	576990	6746780	133	27	"s1b"	B1
"369"	576990	6746780	133	27	"s1c"	B1
"369"	576990	6746780	333	00	"fa"	
"369"	576990	6746780	175	19	"l1"	B1
"370"	577150	6746690	136	44	"s1"	B1
"370"	577150	6746690	125	18	"fa"	
"370"	577150	6746690	127	12	"fab"	
"370"	577150	6746690	164	25	"l1"	B1
"371"	577340	6746650	132	38	"s1"	B1
"371"	577340	6746650	160	35	"s1b"	B1
"371"	577340	6746650	166	04	"fa"	
"371"	577340	6746650	178	29	"l1"	B1
"372"	577510	6746710	135	33	"s1"	B1
"372"	577510	6746710	143	33	"s1b"	B1
"372"	577510	6746710	164	18	"l1"	B1
"372"	577510	6746710	178	20	"l1b"	B1
"373"	577600	6745660	138	45	"s1"	B1
"373"	577600	6745660	145	34	"s1b"	B1
"373"	577600	6745660	167	26	"l1"	B1
"373"	577600	6745660	192	25	"l1b"	B1
"374"	577710	6746850	143	62	"s1"	B1
"374"	577710	6746850	179	36	"s1b"	B1
"374"	577710	6746850	145	04	"fa"	
"374"	577710	6746850	357	01	"fab"	
"375"	577850	6746950	352	82	"s1"	B1
"375"	577850	6746950	168	26	"l1"	B1
"376"	578070	6747050	147	72	"s1"	B1
"376"	578070	6747050	150	10	"fa"	
"377"	578220	6747200	127	46	"s1"	B1
"377"	578220	6747200	159	29	"l1"	B1
"378"	578380	6747390	135	21	"s1"	B1
"378"	578380	6747390	135	21	"s1b"	B1
"378"	578380	6747390	147	30	"s1c"	B1
"378"	578380	6747390	144	48	"s1d"	B1
"378"	578380	6747390	130	46	"s1e"	B1
"378"	578380	6747390	308	03	"fa"	
"378"	578380	6747390	198	17	"l1"	B1
"378"	578380	6747390	159	07	"l1b"	B1
"378"	578380	6747390	156	13	"l1c"	B1
"378"	578380	6747390	156	24	"l1d"	B1
"379"	578460	6747550	147	23	"s1"	B1
"379"	578460	6747550	126	47	"s1b"	B1
"379"	578460	6747550	073	25	"s1c"	B1

Station	Location (UTM)		Strike/ Trend	Dip/ Plunge	Structure	Domain
	Easting	Northing				
"379"	578460	6747550	165	07	"l1"	B1
"379"	578460	6747550	156	28	"l1b"	B1
"380"	578670	6747500	122	43	"s1"	B2
"380"	578670	6747500	122	43	"s1b"	B2
"380"	578670	6747500	183	45	"s1c"	B2
"380"	578670	6747500	183	45	"s1d"	B2
"380"	578670	6747500	167	33	"l1"	B2
"380"	578670	6747500	205	21	"l1b"	B2
"381"	578830	6747410	011	49	"s1"	B2
"381"	578830	6747410	160	30	"l1"	B2
"382"	578990	6747360	127	46	"s1"	B2
"382"	578990	6747360	240	42	"s1b"	B2
"382"	578990	6747360	240	42	"s1c"	B2
"382"	578990	6747360	181	54	"fa"	B2
"382"	578990	6747360	185	43	"l1"	B2
"382"	578990	6747360	008	35	"l1b"	B2
"383"	579190	6747320	169	45	"fa"	B2
"383"	579190	6747320	163	48	"fab"	B2
"383"	579190	6747320	180	57	"fac"	B2
"383"	579190	6747320	187	51	"fad"	B2
"383"	579190	6747320	148	69	"apc"	
"384"	579380	6747320	137	64	"s1"	B2
"384"	579380	6747320	139	71	"s1b"	B2
"384"	579380	6747320	178	69	"fa"	B2
"384"	579380	6747320	177	53	"l1"	B2
"384"	579380	6747320	169	56	"l1b"	B2
"385"	579590	6747330	147	52	"s1"	B2
"385"	579590	6747330	203	53	"fa"	B2
"385"	579590	6747330	206	48	"l1"	B2
"386"	579800	6747380	217	54	"fa"	B2
"386"	579800	6747380	233	63	"fab"	B2
"387"	579920	6747540	192	73	"fa"	B2
"387"	579920	6747540	145	27	"fab"	B2
"387"	579920	6747540	177	57	"fac"	B2
"388"	580050	6747700	002	85	"s1"	B2
"388"	580050	6747700	168	40	"fa"	B2
"388"	580050	6747700	183	26	"fab"	B2
"388"	580050	6747700	178	40	"l1"	B2
"389"	580180	6747850	185	54	"fa"	B2
"389"	580180	6747850	197	40	"fab"	B2
"389"	580180	6747850	143	33	"fac"	B2
"389"	580180	6747850	103	48	"apc"	
"390"	580400	6747930	047	60	"s1"	B2
"390"	580400	6747930	215	53	"fa"	B2
"391"	580510	6748110	136	40	"s1"	B2

Station	Location (UTM)		Strike/ Trend	Dip/ Plunge	Structure	Domain
	Easting	Northing				
"391"	580510	6748110	136	40	"s1b"	B2
"391"	580510	6748110	173	34	"fa"	B2
"391"	580510	6748110	223	40	"l1"	B2
"391"	580510	6748110	070	44	"apc"	
"392"	580580	6748370	100	37	"s1"	B3
"392"	580580	6748370	090	43	"s1b"	B3
"392"	580580	6748370	087	43	"s1c"	B3
"392"	580580	6748370	127	19	"l1"	B3
"392"	580580	6748370	121	25	"l1b"	B3
"392"	580580	6748370	212	37	"l1c"	B3
"393"	580770	6748480	125	67	"s1"	B3
"393"	580770	6748480	100	46	"s1b"	B3
"393"	580770	6748480	130	42	"fa"	
"393"	580770	6748480	172	60	"l1"	B3
"393"	580770	6748480	173	44	"l1b"	B3
"394"	580890	6748600	085	22	"s1"	B3
"394"	580890	6748600	140	16	"l1"	B3
"395"	581110	6748820	116	60	"s1"	B3
"395"	581110	6748820	140	35	"l1"	B3
"396"	581310	6748790	108	60	"s1"	B3
"396"	581310	6748790	098	40	"s1b"	B3
"396"	581310	6748790	102	54	"l1"	B3
"396"	581310	6748790	176	39	"l1b"	B3
"397"	581450	6748820	077	57	"s1"	B3
"397"	581450	6748820	067	45	"s1b"	B3
"397"	581450	6748820	054	23	"s1c"	B3
"397"	581450	6748820	197	41	"l1"	B3
"397"	581450	6748820	192	16	"l1b"	B3
"398"	581670	6749000	290	17	"s1"	B3
"398"	581670	6749000	056	46	"s1b"	B3
"398"	581670	6749000	097	34	"l1"	B3
"399"	581820	6748950	064	68	"s1"	B3
"399"	581820	6748950	075	55	"fa"	
"399"	581820	6748950	090	46	"fab"	
"399"	581820	6748950	225	39	"l1"	B3
"400"	582000	6749000	147	66	"s1"	B3
"400"	582000	6749000	147	59	"s1b"	B3
"400"	582000	6749000	138	61	"s1c"	B3
"400"	582000	6749000	120	31	"s1d"	B3
"400"	582000	6749000	165	46	"fa"	
"400"	582000	6749000	157	38	"fab"	
"400"	582000	6749000	127	30	"fac"	
"400"	582000	6749000	202	54	"l1"	B3
"401"	582250	6749030	095	60	"s1"	B3
"401"	582250	6749030	189	60	"l1"	B3

Station	Location (UTM)		Strike/ Trend	Dip/ Plunge	Structure	Domain
	Easting	Northing				
"402"	582500	6749000	127	32	"s1"	B3
"402"	582500	6749000	097	30	"s1b"	B3
"402"	582500	6749000	173	56	"fa"	
"402"	582500	6749000	304	02	"l1"	B3
"402"	582500	6749000	253	18	"l1b"	B3
"403"	574350	6748000	160	56	"s1"	B1
"403"	574350	6748000	127	28	"s1b"	B1
"403"	574350	6748000	172	76	"s1c"	B1
"403"	574350	6748000	165	08	"l1"	B1
"403"	574350	6748000	177	22	"l1b"	B1
"403"	574350	6748000	181	32	"l1c"	B1
"404"	574100	6747800	004	77	"s1"	B1
"404"	574100	6747800	004	77	"s1b"	B1
"404"	574100	6747800	160	30	"fa"	
"404"	574100	6747800	163	58	"l1"	B1
"405"	573300	6747660	185	69	"s1"	B1
"406"	572650	6748140				
"407"	573840	6748840				
"408"	573950	6749300				
"409"	573250	6749200				
"410"	570820	6750050				
"411"	570610	6749290	099	50	"s1"	
"412"	569650	6749450				
"413"	570000	6750660	255	62	"s1"	
"413"	570000	6750660	253	57	"s1b"	
"413"	570000	6750660	280	39	"l1"	
"413"	570000	6750660	282	36	"l1b"	
"414"	568390	6750900	132	34	"s1"	
"414"	568390	6750900	127	41	"s1b"	
"414"	568390	6750900	103	27	"s1c"	
"414"	568390	6750900	218	34	"l1"	
"414"	568390	6750900	213	41	"l1b"	
"414"	568390	6750900	208	26	"l1c"	
"415"	568000	6750000	115	30	"s1"	
"415"	568000	6750000	097	21	"s1b"	
"415"	568000	6750000	065	29	"s1c"	
"415"	568000	6750000	150	15	"fa"	
"415"	568000	6750000	152	16	"fab"	
"415"	568000	6750000	190	29	"l1"	
"415"	568000	6750000	201	20	"l1b"	
"415"	568000	6750000	154	29	"l1c"	
"416"	568100	6751950				
"417"	567350	6752500				
"418"	566710	6751510				
"419"	567520	6753440				

Station	Location (UTM)		Strike/	Dip/	Structure	Domain
	Easting	Northing	Trend	Plunge		
"420"	568400	6753240				
"421"	567500	6754100				
"422"	568610	6754660				
"423"	567190	6754920				
"424"	566920	6755780				
"425"	568650	6756480				
"426"	569900	6757040				
"427"	565270	6753830				
"428"	564840	6751670				
"429"	563550	6756000				
"430"	553600	6764100				
"431"	554100	6763830				
"432"	554300	6763230	110	66	"s1"	
"432"	554300	6763230	112	54	"s1b"	
"432"	554300	6763230	300	37	"fa"	
"433"	555130	6762830	095	59	"s1"	
"434"	555250	6762420	088	68	"s1"	
"434"	555250	6762420	129	59	"fa"	
"434"	555250	6762420	090	06	"l1"	
"435"	555940	6762260	111	75	"s1"	
"435"	555940	6762260	278	70	"s1b"	
"435"	555940	6762260	284	17	"l1"	
"436"	556490	6762460				
"437"	556470	6764980	300	24	"s1"	
"437"	556470	6764980	272	34	"s1b"	
"437"	556470	6764980	305	15	"s1c"	
"437"	556470	6764980	008	22	"l1"	
"437"	556470	6764980	298	16	"l1b"	
"438"	556410	6764850	305	57	"s1"	
"438"	556410	6764850	100	33	"l1"	
"439"	556250	6764960	285	41	"s1"	
"440"	556370	6764590	275	25	"s1"	
"440"	556370	6764590	268	30	"s1b"	
"440"	556370	6764590	077	08	"l1"	
"440"	556370	6764590	061	14	"l1b"	
"441"	555770	6764550	278	55	"s1"	
"441"	555770	6764550	275	57	"s1b"	
"442"	556200	6763550	270	35	"s1"	
"442"	556200	6763550	282	09	"l1"	
"443"	556580	6763030	132	19	"s1"	
"443"	556580	6763030	118	17	"s1b"	
"443"	556580	6763030	272	16	"s1c"	
"443"	556580	6763030	132	00	"l1"	
"443"	556580	6763030	311	10	"l1b"	
"444"	557420	6762170	269	42	"s1"	

Station	Location (UTM)		Strike/	Dip/	Structure	Domain
	Easting	Northing	Trend	Plunge		
"444"	557420	6762170	284	13	"l1"	
"445"	557950	6764560	306	56	"s1"	
"446"	559440	6764350	310	44	"s1"	
"447"	558980	6763560	295	76	"s1"	
"447"	558980	6763560	277	43	"s1b"	
"448"	558550	6763010	276	54	"s1"	
"448"	558550	6763010	260	66	"s1b"	
"448"	558550	6763010	280	06	"l1"	
"449"	558610	6762430	287	40	"s1"	
"449"	558610	6762430	250	54	"s1b"	
"450"	557190	6761700	123	73	"s1"	
"450"	557190	6761700	230	39	"s1b"	
"450"	557190	6761700	291	33	"l1"	
"450"	557190	6761700	273	29	"l1b"	
"451"	556910	6761430				
"452"	556650	6761380	322	61	"s1"	
"452"	556650	6761380	329	41	"s1b"	
"452"	556650	6761380	125	19	"l1"	
"453"	556020	6761020	274	79	"s1"	
"453"	556020	6761020	275	90	"s1b"	
"453"	556020	6761020	275	30	"l1"	
"454"	555720	6760780	109	61	"s1"	
"455"	555110	6759440				
"456"	555360	6759260	151	63	"s1"	
"456"	555360	6759260	272	59	"l1"	
"457"	555800	6759020				
"458"	556030	6759040	150	80	"s1"	
"458"	556030	6759040	116	80	"s1b"	
"459"	556420	6758800	125	84	"s1"	
"459"	556420	6758800	125	64	"s1b"	
"459"	556420	6758800	130	63	"s1c"	
"459"	556420	6758800	277	44	"l1"	
"459"	556420	6758800	272	51	"l1b"	
"460"	556780	6758700	118	80	"s1"	
"460"	556780	6758700	296	10	"l1"	
"461"	557110	6758430	130	73	"s1"	
"461"	557110	6758430	117	77	"s1b"	
"461"	557110	6758430	296	38	"l1"	
"461"	557110	6758430	286	41	"l1b"	
"462"	556960	6757650	330	84	"s1"	
"462"	556960	6757650	144	45	"l1"	
"463"	558320	6759350	281	81	"s1"	
"464"	558400	6759670	118	63	"s1"	
"465"	558610	6760150				
"466"	559220	6760740	291	90	"s1"	

Station	Location (UTM)		Strike/	Dip/	Structure	Domain
	Easting	Northing	Trend	Plunge		
"466"	559220	6760740	291	05	"l1"	
"467"	558990	6761510				
"468"	596950	6754760				
"469"	596270	6754170	109	15	"s1"	
"469"	596270	6754170	100	13	"s1b"	
"469"	596270	6754170	144	09	"l1"	
"469"	596270	6754170	152	11	"l1b"	
"470"	596370	6753460	085	07	"s1"	
"470"	596370	6753460	095	15	"s1b"	
"470"	596370	6753460	143	06	"l1"	
"470"	596370	6753460	146	12	"l1b"	
"471"	596080	6752900	089	11	"s1"	
"471"	596080	6752900	090	02	"s1b"	
"472"	596860	6751930	090	32	"s1"	
"472"	596860	6751930	127	21	"l1"	
"472"	596860	6751930	110	02	"fa"	
"473"	596030	6750910	072	37	"s1"	
"473"	596030	6750910	187	34	"l1"	
"474"	597910	6751560	105	21	"s1"	
"474"	597910	6751560	138	23	"s1b"	
"474"	597910	6751560	275	16	"l1"	
"475"	598980	6750820	270	50	"s1"	
"476"	599530	6750840	345	24	"s1"	
"477"	599980	6750500	123	37	"s1"	
"477"	599980	6750500	152	20	"l1"	
"478"	600650	6751370	097	46	"s1"	
"478"	600650	6751370	097	00	"fa"	
"479"	600210	6749500	055	16	"s1"	
"479"	600210	6749500	063	24	"s1b"	
"479"	600210	6749500	135	16	"l1"	
"479"	600210	6749500	148	24	"l1b"	
"480"	600620	6748590	095	13	"s1"	
"480"	600620	6748590	085	14	"s1b"	
"480"	600620	6748590	203	12	"l1"	
"480"	600620	6748590	188	14	"l1b"	
"480"	600620	6748590	110	13	"fa"	
"480"	600620	6748590	120	33	"Fab"	
"481"	601660	6748260	080	24	"s1"	
"481"	601660	6748260	094	36	"s1b"	
"481"	601660	6748260	232	12	"l1"	
"481"	601660	6748260	208	34	"l1b"	
"482"	600680	6747530	010	29	"s1"	
"482"	600680	6747530	005	26	"s1b"	
"482"	600680	6747530	354	15	"s1c"	
"482"	600680	6747530	010	03	"l1"	

Station	Location (UTM) Easting	Northing	Strike/ Trend	Dip/ Plunge	Structure	Domain
"482"	600680	6747530	009	04	"l1b"	
"483"	602110	6745490	335	24	"s1"	
"483"	602110	6745490	058	24	"l1"	
"484"	602580	6744550	000	26	"s1"	
"484"	602580	6744550	037	16	"l1"	
"485"	543060	6790040	143	78	"s1"	
"485"	543060	6790040	155	79	"s1b"	
"485"	543060	6790040	160	75	"s1c"	
"485"	543060	6790040	273	74	"l1"	
"485"	543060	6790040	318	55	"l1b"	
"486"	543890	6789470	005	82	"s1"	
"487"	544640	6789250	353	43	"s1"	
"487"	544640	6789250	180	67	"s1b"	
"487"	544640	6789250	320	57	"l1"	
"488"	545620	6788430	155	63	"s1"	
"488"	545620	6788430	170	39	"s1b"	
"488"	545620	6788430	200	22	"l1"	
"489"	546440	6787860	185	63	"s1"	
"490"	546750	6786950	170	45	"s1"	
"491"	547830	6786670				
"492"	548380	6786340	175	48	"s1"	
"492"	548380	6786340	167	52	"s1b"	
"492"	548380	6786340	178	43	"s1c"	
"492"	548380	6786340	204	29	"l1"	
"492"	548380	6786340	222	46	"l1b"	
"492"	548380	6786340	235	38	"l1c"	
"492"	548380	6786340	330	24	"fa"	
"493"	549640	6785980				
"494"	550510	6785040				
"495"	549590	6784410				
"496"	549180	6784370	125	83	"s1"	
"497"	548720	6784270	152	31	"s1"	
"497"	548720	6784270	129	24	"s1b"	
"498"	549960	6782650	350	83	"s1"	
"498"	549960	6782650	350	74	"s1b"	
"499"	548910	6781830	100	43	"s1"	
"500"	548010	6782000				
"501"	547340	6782090	122	73	"s1"	
"501"	547340	6782090	132	73	"s1b"	
"501"	547340	6782090	184	69	"l1"	
"501"	547340	6782090	145	23	"fa"	
"502"	547340	6781870	162	22	"s1"	
"502"	547340	6781870	263	19	"l1"	
"503"	546510	6782100	150	26	"s1"	
"503"	546510	6782100	225	25	"l1"	

Station	Location (UTM)		Strike/ Trend	Dip/ Plunge	Structure	Domain
	Easting	Northing				
"504"	545640	6782740				
"505"	544100	6783250	160	79	"s1"	
"506"	540920	6784560				
"507"	552850	6771910	152	53	"s1"	
"507"	552850	6771910	343	88	"s1b"	
"508"	574680	6758050	115	62	"s1"	
"508"	574680	6758050	136	17	"fa"	
"509"	577140	6761480	090	45	"s1"	
"510"	569050	6767410	105	71	"s1b"	
"511"	560400	6763600	296	88	"s1"	
"511"	560400	6763600	115	15	"l1"	
"512"	560100	6762610	277	59	"s1"	
"512"	560100	6762610	281	06	"l1"	
"513"	559860	6762040	123	40	"s1"	
"513"	559860	6762040	267	27	"l1"	
"514"	559030	6761530	085	56	"s1"	
"514"	559030	6761530	078	39	"s1b"	
"514"	559030	6761530	097	25	"l1"	
"514"	559030	6761530	100	17	"l1b"	
"514"	559030	6761530	095	13	"fa"	
"515"	559890	6760660	088	61	"s1"	
"515"	559890	6760660	092	07	"l1"	
"516"	559500	6758310	315	76	"s1"	
"516"	559500	6758310	119	48	"l1"	
"517"	559940	6758750				
"518"	560100	6759360	116	20	"fa"	
"519"	560540	6759620	005	26	"s1"	
"519"	560540	6759620	345	26	"s1b"	
"519"	560540	6759620	117	24	"l1"	
"520"	561990	6761710	312	26	"s1"	
"521"	561780	6761230	267	44	"s1"	
"522"	561700	6760950	288	44	"s1"	
"522"	561700	6760950	297	74	"s1b"	
"522"	561700	6760950	100	44	"l1"	
"522"	561700	6760950	108	28	"l1b"	
"523"	561420	6759960	113	86	"s1"	
"523"	561420	6759960	114	10	"l1"	
"524"	562110	6760680	313	10	"s1"	
"524"	562110	6760680	085	07	"l1"	
"525"	562530	6759920				
"526"	620530	6756350	180	46	"s1"	
"526"	620530	6756350	170	47	"s1b"	
"526"	620530	6756350	193	13	"l1"	
"526"	620530	6756350	187	17	"l1b"	
"527"	620500	6756900	182	34	"s1"	

Station	Location (UTM)		Strike/ Trend	Dip/ Plunge	Structure	Domain
	Easting	Northing				
"527"	620500	6756900	354	06	"l1"	
"528"	620060	6757640	169	55	"s1"	
"528"	620060	6757640	155	30	"s1b"	
"528"	620060	6757640	191	19	"l1"	
"529"	619270	6757970	025	45	"s1"	
"529"	619270	6757970	142	42	"l1"	
"530"	620210	6579020	183	68	"s1"	
"530"	620210	6579020	180	09	"fa"	
"531"	620320	6759220	185	12	"fa"	
"532"	620500	6759580				
"533"	620060	6759650	140	44	"s1"	
"533"	620060	6759650	100	22	"s1b"	
"533"	620060	6759650	355	88	"apc"	
"533"	620060	6759650	175	15	"fa"	
"534"	622970	6756840	180	88	"apc"	
"535"	623160	6755900				
"536"	623070	6755280	003	64	"s1"	
"537"	622410	6754260	357	75	"s1"	
"537"	622410	6754260	002	70	"s1b"	
"537"	622410	6754260	035	56	"l1"	
"537"	622410	6754260	192	15	"fa"	
"538"	622600	6753330	354	41	"s1"	
"538"	622600	6753330	107	10	"s1b"	
"538"	622600	6753330	183	07	"fa"	
"539"	623050	6753360	183	78	"s1"	
"540"	621850	6753430	180	87	"s1"	
"541"	621030	6753280	015	55	"s1"	
"542"	563950	6768960	305	80	"s1"	
"542"	563950	6768960	308	87	"s1b"	
"543"	564330	6770350	125	67	"s1"	
"543"	564330	6770350	127	45	"s1b"	
"544"	556600	6755920				
"545"	552160	6770380	315	42	"s1"	
"546"	553160	6770460	335	35	"s1"	
"546"	553160	6770460	111	26	"l1"	
"546"	553160	6770460	035	38	"fa"	
"547"	553660	6770720	305	50	"s1"	
"547"	553660	6770720	344	41	"s1b"	
"547"	553660	6770720	103	24	"l1"	
"548"	554550	6771120	298	47	"s1"	
"548"	554550	6771120	286	24	"s1b"	
"548"	554550	6771120	315	79	"s1c"	
"548"	554550	6771120	091	26	"l1"	
"548"	554550	6771120	310	70	"apc"	
"548"	554550	6771120	305	10	"fa"	

Station	Location (UTM)		Strike/ Trend	Dip/ Plunge	Structure	Domain
	Easting	Northing				
"549"	554380	6772170	325	49	"s1"	
"549"	554380	6772170	116	29	"l1"	
"550"	555390	6772850	128	80	"s1"	
"550"	555390	6772850	154	84	"s1b"	
"551"	558380	6772500	283	60	"s1"	C1
"551"	558380	6772500	119	85	"s1b"	C1
"551"	558380	6772500	307	35	"l1"	C1
"551"	558380	6772500	286	30	"l1b"	C1
"552"	558510	6772320	122	68	"s1"	C1
"552"	558510	6772320	125	78	"s1b"	C1
"552"	558510	6772320	117	52	"s1c"	C1
"552"	558510	6772320	116	60	"s1d"	C1
"552"	558510	6772320	287	32	"l1"	C1
"552"	558510	6772320	300	21	"fa"	
"552"	558510	6772320	283	17	"fab"	
"553"	558570	6772130	100	46	"s1"	C1
"553"	558570	6772130	105	66	"s1b"	C1
"553"	558570	6772130	121	58	"s1c"	C1
"553"	558570	6772130	108	52	"s1d"	C1
"553"	558570	6772130	275	20	"fa"	
"554"	558600	6771910	130	35	"s1"	C1
"554"	558600	6771910	115	47	"s1b"	C1
"554"	558600	6771910	291	12	"fa"	
"554"	558600	6771910	281	14	"fab"	
"555"	558650	6771730	111	67	"s1"	C1
"555"	558650	6771730	279	26	"fa"	
"556"	558700	6771580	130	50	"apc"	
"556"	558700	6771580	100	40	"apcb"	
"556"	558700	6771580	102	85	"s1"	C1
"556"	558700	6771580	110	85	"s1b"	C1
"556"	558700	6771580	126	73	"s1c"	C1
"556"	558700	6771580	288	17	"fa"	
"556"	558700	6771580	300	17	"fab"	
"557"	558660	6771310	117	85	"s1"	C1
"557"	558660	6771310	097	84	"s1b"	C1
"557"	558660	6771310	114	87	"s1c"	C1
"558"	558700	6770960	115	59	"s1"	C1
"558"	558700	6770960	132	27	"l1"	C1
"559"	558690	6770780	110	60	"apc"	
"559"	558690	6770780	113	76	"s1"	C1
"559"	558690	6770780	122	87	"s1b"	C1
"559"	558690	6770780	123	87	"s1c"	C1
"559"	558690	6770780	120	90	"s1d"	C1
"559"	558690	6770780	123	23	"l1"	C1
"559"	558690	6770780	124	23	"l1b"	C1

Station	Location (UTM)		Strike/ Trend	Dip/ Plunge	Structure	Domain
	Easting	Northing				
"559"	558690	6770780	300	22	"fa"	
"560"	558740	6770590	153	74	"s1"	C1
"560"	558740	6770590	134	82	"s1b"	C1
"560"	558740	6770590	164	35	"l1"	C1
"560"	558740	6770590	143	50	"l1b"	C1
"561"	558780	6770430	148	60	"s1"	C1
"561"	558780	6770430	144	65	"s1b"	C1
"561"	558780	6770430	121	41	"s1c"	C1
"561"	558780	6770430	160	33	"fa"	
"561"	558780	6770430	180	52	"l1"	C1
"562"	558640	6770300	275	45	"s1"	C1
"562"	558640	6770300	309	29	"l1"	C1
"563"	558700	6770100	115	59	"s1"	C1
"563"	558700	6770100	105	44	"apc"	
"563"	558700	6770100	105	45	"apcb"	
"563"	558700	6770100	148	43	"l1"	C1
"563"	558700	6770100	110	23	"fa"	
"564"	558610	6769870	310	82	"s1"	C2
"564"	558610	6769870	085	79	"l1"	C2
"565"	558450	6769800	304	82	"s1"	C2
"565"	558450	6769800	311	68	"s1b"	C2
"565"	558450	6769800	090	76	"l1"	C2
"565"	558450	6769800	338	49	"l1b"	C2
"566"	558500	6769650	300	68	"s1"	C2
"566"	558500	6769650	305	62	"s1b"	C2
"566"	558500	6769650	311	64	"s1c"	C2
"566"	558500	6769650	314	67	"s1d"	C2
"566"	558500	6769650	041	62	"l1"	C2
"566"	558500	6769650	046	64	"l1b"	C2
"566"	558500	6769650	034	67	"l1c"	C2
"567"	558620	6769490	315	60	"s1"	C2
"567"	558620	6769490	316	58	"sib"	C2
"567"	558620	6769490	320	63	"s1c"	C2
"567"	558620	6769490	310	72	"s1d"	C2
"567"	558620	6769490	034	67	"l1"	C2
"567"	558620	6769490	073	57	"l1b"	C2
"567"	558620	6769490	044	58	"l1c"	C2
"567"	558620	6769490	004	54	"l1d"	C2
"568"	558580	6769370	310	74	"s1"	C2
"568"	558580	6769370	323	68	"s1b"	C2
"568"	558580	6769370	352	67	"l1"	C2
"568"	558580	6769370	089	64	"l1b"	C2
"569"	558430	6769260	318	43	"s1"	C2
"569"	558430	6769260	331	46	"s1b"	C2
"569"	558430	6769260	339	07	"fa"	

Station	Location (UTM)		Strike/ Trend	Dip/ Plunge	Structure	Domain
	Easting	Northing				
"569"	558430	6769260	325	15	"fab"	
"569"	558430	6769260	337	33	"fac"	
"569"	558430	6769260	350	19	"fad"	
"570"	558320	6769070	300	50	"apc"	
"570"	558320	6769070	313	73	"s1"	C2
"570"	558320	6769070	307	64	"s1b"	C2
"570"	558320	6769070	011	70	"l1"	C2
"570"	558320	6769070	043	64	"l1b"	C2
"570"	558320	6769070	346	47	"fa"	
"571"	558300	6768920	315	30	"s1"	C2
"571"	558300	6768920	301	71	"s1b"	C2
"571"	558300	6768920	057	30	"l1"	C2
"571"	558300	6768920	335	12	"fa"	
"571"	558300	6768920	322	46	"l1b"	C2
"572"	558400	6768810	322	57	"s1"	C2
"572"	558400	6768810	310	71	"s1b"	C2
"572"	558400	6768810	297	60	"s1c"	C2
"572"	558400	6768810	305	59	"s1d"	C2
"572"	558400	6768810	024	70	"l1"	C2
"572"	558400	6768810	082	53	"l1b"	C2
"572"	558400	6768810	328	07	"fa"	
"572"	558400	6768810	021	60	"l1c"	C2
"572"	558400	6768810	033	59	"l1d"	C2
"572"	558400	6768810	328	27	"fab"	
"573"	558370	6768640	317	56	"s1"	C2
"573"	558370	6768640	285	70	"s1b"	C2
"573"	558370	6768640	285	70	"s1c"	C2
"573"	558370	6768640	104	11	"fa"	
"573"	558370	6768640	313	53	"l1"	C2
"573"	558370	6768640	325	60	"l1b"	C2
"573"	558370	6768640	335	35	"l1c"	C2
"574"	558320	6768450	305	49	"s1"	C2
"574"	558320	6768450	304	52	"s1b"	C2
"574"	558320	6768450	031	61	"s1c"	C2
"574"	558320	6768450	353	41	"l1"	C2
"574"	558320	6768450	316	16	"fa"	
"575"	558280	6768300	297	46	"s1"	C2
"575"	558280	6768300	305	43	"s1b"	C2
"575"	558280	6768300	331	21	"fa"	
"575"	558280	6768300	319	21	"fab"	
"575"	558280	6768300	295	07	"fac"	
"575"	558280	6768300	359	37	"l1"	C2
"576"	558230	6768150	275	65	"apc"	
"576"	558230	6768150	303	52	"s1"	C3
"576"	558230	6768150	310	35	"s1b"	C3

Station	Location (UTM)		Strike/ Trend	Dip/ Plunge	Structure	Domain
	Easting	Northing				
"576"	558230	6768150	319	19	"fa"	
"576"	558230	6768150	017	33	"l1"	C3
"576"	558230	6768150	330	14	"fab"	
"576"	558230	6768150	318	29	"fac"	
"577"	558220	6767970	295	40	"s1"	C3
"577"	558220	6767970	300	53	"s1b"	C3
"577"	558220	6767970	295	58	"s1c"	C3
"577"	558220	6767970	277	62	"apc"	
"577"	558220	6767970	317	18	"fa"	
"577"	558220	6767970	326	30	"fab"	
"578"	558180	6767840	323	30	"s1"	C3
"578"	558180	6767840	340	10	"fa"	
"579"	558160	6767640	310	40	"s1"	C3
"579"	558160	6767640	332	18	"fa"	
"580"	574100	6763610	115	44	"s1"	
"580"	574100	6763610	112	31	"s1b"	
"580"	574100	6763610	136	14	"l1"	
"581"	570360	6766950				
"582"	566500	6764930	157	18	"s1"	C4
"582"	566500	6764930	148	27	"s1b"	C4
"582"	566500	6764930	144	40	"s1c"	C4
"582"	566500	6764930	316	07	"fa"	
"582"	566500	6764930	164	16	"fab"	
"582"	566500	6764930	232	27	"l1"	C4
"582"	566500	6764930	218	39	"l1b"	C4
"583"	566330	6764780	315	42	"s1"	C4
"583"	566330	6764780	310	40	"s1b"	C4
"583"	566330	6764780	328	60	"s1c"	C4
"583"	566330	6764780	359	32	"l1"	C4
"583"	566330	6764780	040	40	"l1b"	C4
"583"	566330	6764780	356	39	"l1c"	C4
"583"	566330	6764780	120	08	"fa"	
"584"	566510	6764650	097	23	"s1b"	C4
"584"	566510	6764650	303	72	"s1"	C4
"584"	566510	6764650	150	39	"s1c"	C4
"584"	566510	6764650	137	34	"s1d"	C4
"584"	566510	6764650	229	17	"l1"	C4
"584"	566510	6764650	243	39	"l1b"	C4
"584"	566510	6764650	116	22	"fa"	
"584"	566510	6764650	165	18	"fab"	
"585"	566590	6764400	095	54	"s1"	C4
"585"	566590	6764400	300	72	"s1b"	C4
"585"	566590	6764400	110	40	"s1c"	C4
"585"	566590	6764400	133	47	"s1d"	C4
"585"	566590	6764400	337	40	"s1e"	C4

Station	Location (UTM)		Strike/ Trend	Dip/ Plunge	Structure	Domain
	Easting	Northing				
"585"	566590	6764400	138	36	"s1f"	C4
"585"	566590	6764400	129	52	"s1g"	C4
"585"	566590	6764400	251	43	"l1"	C4
"585"	566590	6764400	266	12	"l1b"	C4
"585"	566590	6764400	160	51	"fab"	
"585"	566590	6764400	302	05	"fa"	
"586"	566220	6764200	290	44	"s1"	C4
"586"	566220	6764200	277	37	"s1b"	C4
"586"	566220	6764200	311	85	"s1c"	C4
"586"	566220	6764200	031	89	"s1d"	C4
"586"	566220	6764200	313	24	"fa"	
"586"	566220	6764200	316	47	"l1"	C4
"586"	566220	6764200	314	53	"l1b"	C4
"587"	566250	6763980	326	75	"s1"	C3
"587"	566250	6763980	300	68	"s1b"	C3
"587"	566250	6763980	277	41	"s1c"	C3
"587"	566250	6763980	300	62	"s1d"	C3
"587"	566250	6763980	345	50	"l1"	C3
"587"	566250	6763980	338	56	"l1b"	C3
"587"	566250	6763980	330	35	"l1c"	C3
"588"	566250	6763760	308	85	"s1"	C3
"588"	566250	6763760	308	85	"s1b"	C3
"588"	566250	6763760	315	55	"s1c"	C3
"588"	566250	6763760	136	46	"s1d"	C3
"588"	566250	6763760	335	26	"l1"	C3
"588"	566250	6763760	314	52	"l1b"	C3
"588"	566250	6763760	296	20	"l1c"	C3
"588"	566250	6763760	128	05	"fa"	
"589"	566250	6759330	287	83	"s1"	C5
"589"	566250	6759330	290	78	"s1b"	C5
"589"	566250	6759330	294	68	"s1c"	C5
"589"	566250	6759330	298	62	"s1d"	C5
"589"	566250	6759330	088	69	"l1"	C5
"589"	566250	6759330	090	58	"l1b"	C5
"589"	566250	6759330	091	44	"l1c"	C5
"589"	566250	6759330	088	43	"l1d"	C5
"590"	566170	6759140	302	78	"s1"	C5
"590"	566170	6759140	317	65	"s1b"	C5
"590"	566170	6759140	084	71	"l1"	C5
"590"	566170	6759140	059	65	"l1b"	C5
"590"	566170	6759140	144	40	"fa"	C5
"591"	566160	6758830	272	82	"s1"	C5
"591"	566160	6758830	286	89	"s1b"	C5
"591"	566160	6758830	283	84	"s1c"	C5
"591"	566160	6758830	286	81	"s1d"	C5

Station	Location (UTM)		Strike/	Dip/	Structure	Domain
	Easting	Northing	Trend	Plunge		
"591"	566160	6758830	065	73	"l1"	C5
"591"	566160	6758830	104	60	"l1b"	C5
"591"	566160	6758830	096	50	"l1c"	C5
"591"	566160	6758830	076	73	"l1d"	C5
"592"	566150	6758640	285	65	"s1"	C5
"592"	566150	6758640	285	72	"s1b"	C5
"592"	566150	6758640	081	51	"l1"	C5
"592"	566150	6758640	056	58	"l1b"	C5
"593"	566190	6759590	297	82	"s1"	C5
"594"	566140	6759840	283	58	"s1"	C5
"594"	566140	6759840	100	04	"l1"	C5
"595"	566140	6760100	303	70	"s1"	C5
"595"	566140	6760100	282	82	"s1b"	C5
"595"	566140	6760100	275	68	"s1c"	C5
"595"	566140	6760100	295	55	"s1d"	C5
"595"	566140	6760100	091	09	"l1"	C5
"595"	566140	6760100	084	36	"l1b"	C5
"596"	566250	6763650	113	49	"s1"	C3
"596"	566250	6763650	127	62	"s1b"	C3
"596"	566250	6763650	151	54	"s1c"	C3
"596"	566250	6763650	286	08	"fa"	
"596"	566250	6763650	128	03	"fab"	
"596"	566250	6763650	312	24	"fac"	
"597"	566100	6763290	325	57	"s1"	C3
"597"	566100	6763290	317	67	"s1b"	C3
"597"	566100	6763290	326	02	"fa"	
"597"	566100	6763290	117	39	"fab"	
"597"	566100	6763290	326	19	"fac"	
"598"	566030	6763000	322	47	"s1"	C3
"598"	566030	6763000	318	54	"s1b"	C3
"598"	566030	6763000	324	02	"fa"	
"598"	566030	6763000	137	02	"fab"	
"598"	566030	6763000	106	36	"fac"	
"599"	566130	6762760	282	89	"apc"	
"599"	566130	6762760	310	60	"s1"	C3
"599"	566130	6762760	295	49	"s1b"	C3
"599"	566130	6762760	280	80	"apcb"	
"599"	566130	6762760	310	59	"s1c"	C3
"599"	566130	6762760	331	31	"l1"	C3
"599"	566130	6762760	124	10	"fa"	
"599"	566130	6762760	328	32	"l1b"	C3
"599"	566130	6762760	296	15	"fab"	
"600"	566220	6762570	300	43	"s1"	C3
"600"	566220	6762570	305	43	"s1b"	C3
"600"	566220	6762570	308	49	"s1c"	C3

Station	Location (UTM)		Strike/ Trend	Dip/ Plunge	Structure	Domain
	Easting	Northing				
"600"	566220	6762570	357	38	"l1"	C3
"600"	566220	6762570	344	30	"l1b"	C3
"600"	566220	6762570	358	42	"l1c"	C3
"600"	566220	6762570	311	10	"fa"	
"601"	566380	6762170	288	55	"s1"	C3
"601"	566380	6762170	300	55	"s1b"	C3
"601"	566380	6762170	290	62	"s1c"	C3
"601"	566380	6762170	296	05	"s1d"	C3
"601"	566380	6762170	105	04	"fa"	
"601"	566380	6762170	290	02	"fab"	
"601"	566380	6762170	321	27	"l1"	C3
"601"	566380	6762170	309	32	"l1b"	C3
"602"	566550	6761800	291	45	"s1"	C3
"603"	566570	6761560	297	65	"s1"	C3
"603"	566570	6761560	144	06	"fa"	
"604"	566540	6761310	297	70	"s1"	C3
"604"	566540	6761310	155	30	"fa"	
"605"	566290	6761260	262	78	"s1"	C3
"605"	566290	6761260	100	24	"s1b"	C3
"605"	566290	6761260	077	45	"s1c"	C3
"605"	566290	6761260	124	36	"l1"	C3
"605"	566290	6761260	068	49	"l1b"	C3
"605"	566290	6761260	142	17	"l1c"	C3
"606"	566200	6761010	117	76	"s1"	C5
"606"	566200	6761010	298	77	"s1b"	C5
"606"	566200	6761010	136	53	"l1"	C5
"607"	566250	6760670	290	71	"s1"	C5
"607"	566250	6760670	306	61	"s1b"	C5
"607"	566250	6760670	094	39	"l1"	C5
"607"	566250	6760670	100	38	"l1b"	C5
"608"	563350	6756900	045	62	"s1"	C6
"608"	563350	6756900	269	72	"s1b"	C6
"608"	563350	6756900	072	62	"s1c"	C6
"608"	563350	6756900	045	46	"s1d"	C6
"608"	563350	6756900	053	37	"s1e"	C6
"608"	563350	6756900	047	86	"s1f"	C6
"608"	563350	6756900	061	70	"s1g"	C6
"608"	563350	6756900	088	04	"l1"	C6
"608"	563350	6756900	082	18	"l1b"	C6
"608"	563350	6756900	196	24	"l1c"	C6
"608"	563350	6756900	047	00	"l1d"	C6
"608"	563350	6756900	233	21	"l1e"	C6
"609"	563290	6756650	045	46	"s1"	C6
"609"	563290	6756650	053	37	"s1b"	C6
"609"	563290	6756650	047	86	"s1c"	C6

Station	Location (UTM)		Strike/ Trend	Dip/ Plunge	Structure	Domain
	Easting	Northing				
"609"	563290	6756650	061	70	"s1d"	C6
"609"	563290	6756650	196	24	"l1"	C6
"609"	563290	6756650	047	00	"l1b"	C6
"609"	563290	6756650	233	21	"l1c"	C6
"610"	563290	6756460	020	78	"s1"	C6
"610"	563290	6756460	045	47	"s1b"	C6
"610"	563290	6756460	060	16	"l1"	C6
"611"	563250	6756260	047	68	"s1"	C6
"611"	563250	6756260	212	22	"l1"	C6
"612"	563070	6755960	023	47	"s1"	C6
"612"	563070	6755960	115	37	"s1b"	C6
"612"	563070	6755960	192	11	"l1"	C6
"612"	563070	6755960	199	37	"l1b"	C6
"613"	562880	6755970	055	37	"s1"	C6
"613"	562880	6755970	030	59	"s1b"	C6
"613"	562880	6755970	218	12	"l1"	C6
"613"	562880	6755970	235	12	"fa"	
"614"	562730	6755920	048	60	"s1"	C6
"614"	562730	6755920	112	72	"s1b"	C6
"614"	562730	6755920	212	26	"l1"	C6
"614"	562730	6755920	258	60	"l1b"	C6
"615"	562590	6755930	070	65	"s1"	C6
"615"	562590	6755930	050	71	"s1b"	C6
"615"	562590	6755930	210	54	"l1"	C6
"615"	562590	6755930	214	37	"l1b"	C6
"616"	562310	6755990	152	67	"s1"	C7
"616"	562310	6755990	145	57	"s1b"	C7
"616"	562310	6755990	150	49	"s1c"	C7
"617"	562130	6755890	164	60	"s1"	C7
"617"	562130	6755890	155	74	"s1b"	C7
"617"	562130	6755890	133	79	"s1c"	C7
"617"	562130	6755890	303	41	"l1"	C7
"618"	561970	6755860	163	44	"s1"	C7
"618"	561970	6755860	105	72	"s1b"	C7
"618"	561970	6755860	112	57	"s1c"	C7
"618"	561970	6755860	167	44	"s1d"	C7
"618"	561970	6755860	176	55	"s1e"	C7
"618"	561970	6755860	256	48	"l1"	C7
"618"	561970	6755860	269	40	"l1b"	C7
"618"	561970	6755860	264	36	"l1c"	C7
"618"	561970	6755860	257	44	"l1d"	C7
"618"	561970	6755860	299	50	"l1e"	C7
"619"	561660	6755580	162	48	"s1"	C7
"619"	561660	6755580	152	71	"s1b"	C7
"619"	561660	6755580	310	30	"l1"	C7

Station	Location (UTM) Easting	 Northing	Strike/ Trend	Dip/ Plunge	Structure	Domain
"620"	561430	6755510	107	68	"s1"	C7
"621"	561020	6755420	120	66	"s1"	C7
"622"	596020	6713700	060	33	"s1"	
"623"	596150	6713520	018	75	"s1"	
"624"	603420	6738320	007	63	"s1b"	
"624"	603420	6738320	030	57	"s1c"	
"624"	603420	6738320	022	82	"s1d"	
"624"	603420	6738320	038	13	"l1"	
"624"	603420	6738320	026	24	"l1b"	
"625"	602540	6738030	007	70	"s1"	
"626"	601140	6739450	350	60	"s1"	
"626"	601140	6739450	340	57	"s1b"	
"626"	601140	6739450	105	31	"fa"	
"626"	601140	6739450	080	27	"fab"	
"627"	600260	6739960	306	39	"s1"	
"628"	599360	6740300	317	45	"s1"	
"628"	599360	6740300	321	58	"s1b"	
"628"	599360	674030 0	121	29	"l1"	